EARTHQUAKE INDUCED FISSURING IN BANKS PENINSULA LOESSIAL SOILS: A GEOTECHNICAL INVESTIGATION OF THE RAMAHANA ROAD FISSURE TRACE

A thesis submitted in partial fulfilment

of the requirements for the Degree of

Master of Science in Engineering Geology

In the Department of Geological Sciences

University of Canterbury

by

Christopher Stuart White

University of Canterbury

2016

Acknowledgements

Firstly I would like to thank my supervisory team of David Bell and Clark Fenton for making this thesis possible. Your guidance and help in organisation has made my work go a lot smoother than it could have otherwise, and your challenges to my ideas has helped to develop my knowledge and understanding of soil mechanics.

Secondly I would like to thank Samuel and Amy Hampton for allowing me to riddle your property with holes and flatten your hill slope for geophysical testing. Most of the information for this thesis has been gathered from your property and I simply could not have done this thesis without your tolerance and help.

Thank you to Matt Cockcroft for the organising and lending technical knowledge for the geophysical testing. Thank you also to Southern Geophysical Ltd.

An immense thank you must go out to Coffey Geotechnics NZ Ltd, and in particular John Fenwick and James Davidson, for conducting the CPT free of charge. Thank you also to Josh Pillage for conducting the service locations as well.

Thank you to the all of the university technical staff who helped me at various stages in this thesis: Chris Grimshaw, Cathy Higgens, Sarah Pope, Rob Spiers, Sacha Baldwin-Cunningham, and John Southward.

Finally I would like to thank my family, my friends and my girlfriend for offering guidance and supporting me throughout this process.

Abstract

One of the less understood geotechnical responses to the cyclic loading from the M_W6.2 Christchurch Earthquake, on the 22nd of February 2011, is the fissuring in the loessial soil-mantled, footslope positions of the north-facing valleys of the Port Hills. The fissures are characterized by mostly horizontal offset (≤500mm), with minor vertical displacement (≤300mm), and they extend along both sides of valleys for several hundred metres in an approximately contour-parallel orientation. The fissure traces correspond to extensional features mapped in other studies.

Previous studies have suggested that the fissures are the headscarps of incipient landslides, but the surface and subsurface features are not typical of landslide movement. Whilst there are some features that correlate with landslide movement, there are many features that contradict the landslide movement hypothesis. Of critical importance to this investigation was the fact that there are no landslide flanks, there has been no basal shear surface found, there is little deformation in the so-called 'landslide body', and there have been no recorded zones of low shear strength in the soil deposit that are indicative of a basal shear surface.

This thesis is a detailed geotechnical study on the fissures along part of Ramahana Road in the Hillsborough Valley, Christchurch. Shallow and deep investigation methods found that the predominant soil is loess-colluvium, to depths of ~20m, and this soil has variable geotechnical characteristics depending on the layer sampled. The factor that has the most influence on shear strength was found to be the moisture content. Direct shear-box testing of disturbed, recompacted loess-colluvium found that the soil had a cohesion of 35-65kPa and a friction angle of 38-43° when the soil moisture content was at 8-10%. However when the moisture content was at 19-20% the soil's cohesion decreased to 3-5kPa and its friction angle decreased to 33-38°, this moisture content is at or slightly above the plastic limit.

An electrical resistivity geophysical survey was conducted perpendicular to multiple fissure traces and through the compressional zone at 17 Ramahana Road. The electrical resistivity line found that there was an area of high resistivity at the toe of the slope, and an area of high conductivity downslope of this and at greater depths. This area correlated to the compressional zone recorded by previous studies. Moisture content testing of the soil in these locations showed that the soil in the resistive area was relatively dry (9%) compared to the surrounding soil (13%), whilst the soil in the conductive area was relatively wet (22%)

compared to the surrounding soil (19%). Density tests of the soil in the compressional zone recorded that the resistive area had a higher dry density than the surrounding soil (~1790 kg/m^3 compared to ~1650 kg/m^3). New springs arose downslope of the compressional zone contemporaneously with the fissures, and it is interpreted that these have arisen from increased hydraulic head in the Banks Peninsula bedrock aquifer system, and earthquake induced-bedrock fracturing.

A test pit was dug across an infilled fissure trace at 17 Ramahana Road to a depth of 3m. The fissure trace had an aperture of 450-470mm at the ground surface, but it gradually lost aperture with depth until 2.0-2.1m where it became a segmented fissure trace with 1-2mm aperture. A mixed-colluvium layer was intercepted by the fissure trace at 2.4m depth, and there was no observable vertical offset of this layer. The fissure trace was at an angle of 78° at the ground surface, but it also flattened with depth, which gave it a slightly curved appearance. The fissure trace was at an assumed angle of 40-50° near the base of the test pit.

Rotational slide, translational slide and lateral spread landslide movement types were compared and contrasted as possibilities for landslide movement types, whilst an alternative hypothesis was offered that the fissures are tensile failures with a quasi-toppling motion involving a cohesive block of loessial soil moving outwards from the slope, with an accommodating compressional strain in the lower less cohesive soil. The mechanisms behind this movement are suggested to be the horizontal earthquake inertia forces from the Christchurch Earthquake, the static shear stress of the slope, and bedrock uplift of the Port Hills in relation to the subsidence of the Christchurch city flatlands. Extremely high PGA is considered to be a prerequisite to the fissure trace development, and these can only be induced in the Hillsborough Valley from a Port Hills Fault rupture, which has a recurrence interval of ~10,000 years.

The current understanding of how the loess-colluvium soil would behave under cyclic loading is limited, and the mechanisms behind the suggested movement type are not completely understood. Further research is needed to confirm the proposed mechanism of the fissure traces. Laboratory tests such as the cyclic triaxial and cyclic shear test would be beneficial in future research to quantitatively test how the soil behaves under cyclic loading at various moisture contents and clay contents, and centrifuge experiments would be of great use to qualitatively test the suggested mode of movement in the loessial soil.

Table of Contents

1. Introduction

1.1. Research Background

The M_W 6.2 Christchurch earthquake on the 22nd of February, 2011 caused widespread land damage to Christchurch city and the greater Christchurch area. Ground shaking was the direct cause of much of the damage to buildings and infrastructure, but indirectly the ground shaking caused much more of the damage through liquefaction of the Springston Formation and Christchurch Formation silts and sands on the Christchurch city flatlands, and through rockfall, cliff collapse, and landslide movement on the Port Hills (Kaiser et al. 2012). Of the widespread and well documented geotechnical damage caused by the Christchurch Earthquake, the fissure traces that formed in the loessial-soil mantled, foot-slope positions of the Port Hills are of current significance. Figure 1.1 is a photo of the fissure traces running through Ramahana Road in the Hillsborough Valley.

Figure 1.1: Fissure traces running through Ramahana Road. Photo looking North towards Centaurus Road. Photo after Stephen-Brownie (2012).

The fissure traces are openings in the ground surface that are characterized by mostly horizontal displacements with minor vertical offsets. According to investigations done by Stephen-Brownie (2012), the fissures mostly have <0.2m crack apertures and they can extend

segmentally for several hundred metres. Dellow et al. (2011) explains that 1m of accumulative displacement is rarely exceeded. The extensional movement at the fissure traces is often accompanied by compressional features near the base of the slope (Stephen-Brownie 2012; Massey et al. 2013). This combination of features has led many authors to interpret the fissures as the head-scarps of incipient landslides (e.g. Dellow et al. 2011; Hancox et al. 2011; Kaiser et al. 2012; Massey et al. 2013); however, as yet there has been no catastrophic failure of soil related to the fissures.

The fissures are present on both sides of most of the north-facing valleys of the Port Hills at the toe of the slope. They generally follow a roughly contour-parallel orientation, but there can be multiple fissures at any one location. Most of these valleys have been developed for residential subdivisions, with the highest concentration of buildings located in the toe-slope positions. Many of these hillside properties were severely damaged by the opening of the fissures directly underneath or closely adjacent to the dwelling.

The movement and mechanisms that led to the fissure traces are significant, not only because of the fissure proximity to residential households and infrastructure, but also because they have behaved in a very complex and poorly understood way. The fissures appear to be a result of earthquake-induced stress that has exceeded the soils internal strength; however the mechanism behind this movement, the mode of movement, and the boundaries of movement are still incompletely understood.

The most detailed studies to date on the fissure traces can be found in the GNS stage 1 report compiled by Massey et al. (2013) and the unpublished thesis by Stephen-Brownie (2012). Loess slumping, which is a rotational slide mass failure following the classification of Cruden & Varnes (1996), is deemed to be the most likely mode of failure in the work of Massey et al. (2013), and their loess slump hypothesis has since been widely accepted by various parties, including the Christchurch City Council (CCC) and many engineering consultancies. Figure 1.2 is the loess toe slump model from the GNS stage 1 report. Within the stage 1 report, however, it is recognised that the mechanisms of movement are poorly understood, and considerable geotechnical investigations are needed to gain greater understanding of the fissure trace movement. At this stage it would seem presumptuous to nominate the fissure traces as slide or slump landslide movement types.

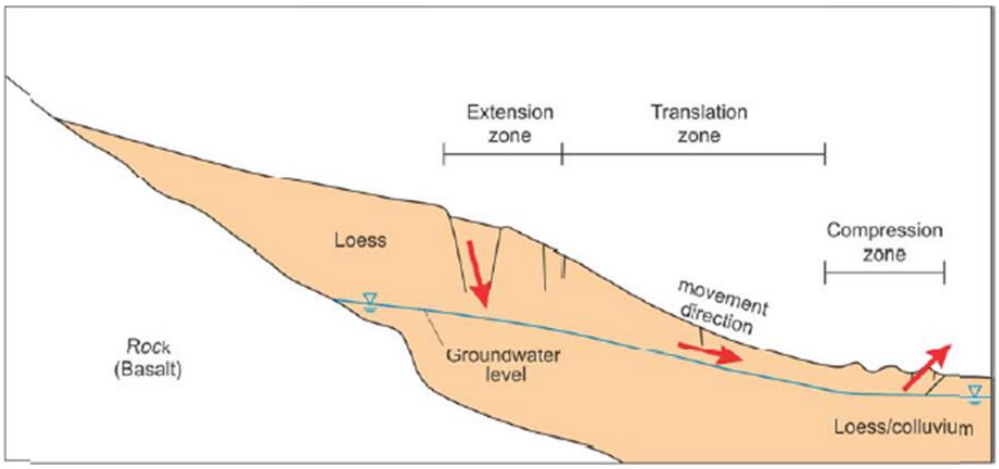

Figure 1.2: The loess toe slump model. From Massey et al. (2013).

Stephen-Brownie (2012) offered an alternative hypothesis to the fissure trace mode of movement, in which a combination of bedrock fracturing of the up-thrusted Port Hills volcanics propagated stress into the overlying loessial deposits, while the 'trampoline effect' (where strong downward acceleration during an earthquake causes dilatational strains that make the near surface material reach their bulk tensile strain, causing the soil and rocks to lose their cohesion (Aoi et al. 2008)) temporarily removed lateral strength of the slope, causing an imbalance of stresses, and resulting in lateral spreading similar to the fissures that formed parallel to river banks on the flatlands. It was thought that the fissures formed along internal sub-vertical fractures that are inherent in the loess deposits of the Port Hills, and therefore could be defined as a quasi-toppling movement following the classification of Cruden & Varnes (1996). Figure 1.3 provides for a model of the quasi-toppling movement.

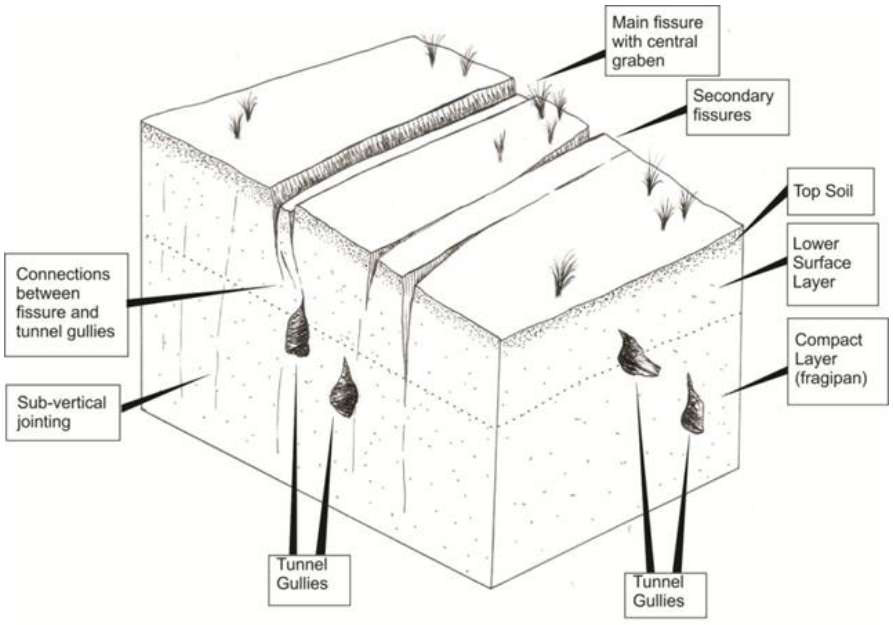

Figure 1.3: The quasi-toppling model. From Stephen-Brownie (2012).

This current study is focussed on one such area where the fissure traces formed: downslope of Ramahana Road, which, for the purposes of this thesis shall henceforth be called the Ramahana Road fissure trace. The term fissure trace is used in this context because it is defined as simply a crack or opening, which avoids any potential presumptions. Figure 1.4 provides a map showing the location of the study area.

Figure 1.4: The two main study areas for this thesis: 17 Ramahana Road and Centaurus Park in the Hillsborough Valley.

1.2. Statement of the Problem

The problem can be summed up as a lack of understanding of the mechanisms and movement type of the fissure traces. The aforementioned hypothesis of Massey et al (2013) does not correlate well with surface features, geotechnical field investigations and laboratory analysis of samples taken from the site. Rotational slide failures are a common form of mass movement in loessial soils following earthquakes in overseas deposits of loess; however New Zealand loessial soils are generally more compact, have a lower permeability, are non-homogeneous, and non-calcareous compared to loess from other parts of the world (Raeside 1964; Ives 1972; Pye 1995). This makes it very difficult to correlate the fissure trace movement to the movements of other loess deposits around the world.

Whilst it is not unusual for landslides to develop in the loess-colluvium of Banks Peninsula, particularly of the translational slide failure, flow type failure, or a combination of both, these predominantly occur following prolonged or intense rainfall (Bell & Trangmar 1987). Earthquakes do not generally cause extensive slope stability issues in the loessial soils of Banks Peninsula due to their general absence of saturation, their relative compactness, and their distance from most earthquake epicentres. Earthquakes of a lesser intensity than the 22nd of February 2011 Christchurch Earthquake have occurred within the vicinity of Banks Peninsula before, however no extensive instability issues in the loessial soils have been recorded following these events, including after the 4th of September 2010 Darfield Earthquake. The fissure traces are then potentially the result of unprecedented behaviour in Banks Peninsula loess, at least for within the recorded history timeframe of New Zealand, and this means that there are no applicable case studies to draw from.

In contrast to the loess toe slump hypothesis, the quasi-toppling hypothesis offered by Stephen-Brownie (2012) offers a good correlation to the geotechnical properties and features of the soil at Ramahana Road; however some of the mechanisms are not applicable. More research is needed to gain a better understanding of the potential mechanisms for this mode of movement.

The mechanisms and mode of movement that are accepted for the fissure traces have far-reaching implications: they will not only determine the Christchurch City Council's building requirements for future construction in these areas, they will also aid in the understanding of loessial soil behaviour during an earthquake for the academic and infrastructure consultancy

fields. New Zealand is a tectonically active region and loessial soils embrace a significant proportion of surface soils in the South Island and lower North Island. It is critical that the correct mechanisms and mode of movement are determined so that accurate decisions on land use and construction requirements can be made in the future on Banks Peninsula and farther afield in New Zealand.

Figure 1.5 is a schematic model from the 'Build it Right Canterbury' report by the Ministry of Business Innovation and Employment, which depicts the toe slump model. If this model is accepted as the mode of movement for the fissure traces, then it will have to be assumed that any construction built within the zone of movement will be adding loading to the slide surface and all geotechnical constraints that accompany this assumption will need to be considered. In contrast there are no loading implications for construction under the quasi-toppling model assumption.

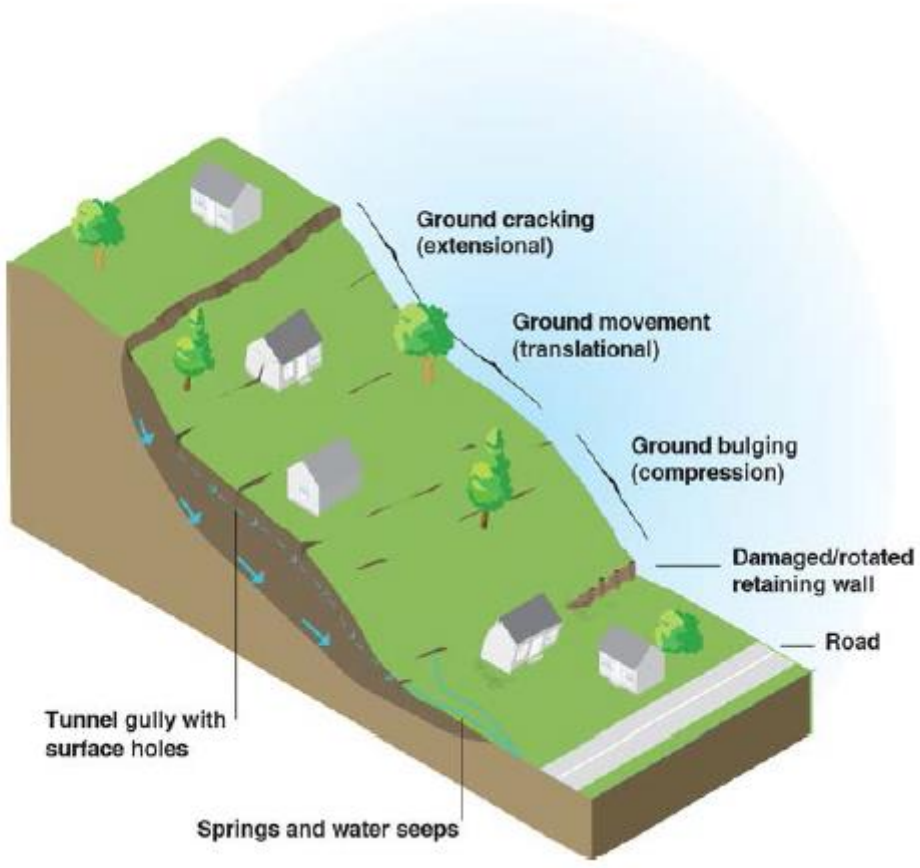

Figure 1.5: A schematic model of the toe slump hypothesis sourced from 'Build it Right Canterbury' report, after the Ministry of Business Innovation and Employment (2013).

1.3. Research Objectives

1.3.1. Main Goal

The main goal of this research is to gain a better understanding of the mechanisms that caused the fissure traces to occur during the 22nd of February 2011 Christchurch Earthquake.

1.3.2. Hypothesis

The hypothesis examined in this research is that the fissure trace mode of movement is not a slide or slump landslide type, but a tensional stress/strain movement caused by the unique behavioural characteristics of Banks Peninsula loessial soils and the unique characteristics of the Christchurch Earthquake.

1.3.3. Specific Objectives

To achieve the main research goal, the following objectives were identified:

- **Objective 1**: Identify key features of fissure trace expression using subsurface investigations to explore any potential landslide movement types and mechanisms that could have led to the creation of the Ramahana Road fissure trace.

- **Objective 2:** Identify why the fissures formed at the locations they did, and put the soil in context with other loessial soils of the Port Hills using laboratory analysis of samples.

- **Objective 3**: Visually portray the interpreted subsurface geology, and create more accurate models depicting the failure below ground surface than are currently available.

- **Objective 4**: Determine the most likely landslide movement type and the mechanism behind this failure.

1.4. Geological and Geomorphological Setting

The Ramahana Road fissure traces are located in the city of Christchurch in the South Island of New Zealand. Appendix 1.1 provides more detail on Christchurch city. New Zealand is located on the boundary of the Pacific and Australian Plates, which makes it a tectonically active land mass. Figure 1.6 shows the current tectonic system of New Zealand. Bradley & Cubrinovski (2011) explain that in the North Island the current tectonics are governed by oblique subduction of the Pacific Plate beneath the Australian Plate along the Hikurangi trough; in the South Island the current tectonics are governed by oblique, right-lateral strike-slip along numerous crustal faults, but largely through the Alpine Fault, which extends for 650km up almost the entire western side of the South Island; in the sea to the west of Stewart Island the movement is once again governed by oblique subduction, but this time it is along the Puysegur trench, where the Australian Plate is subducting beneath the Pacific Plate.

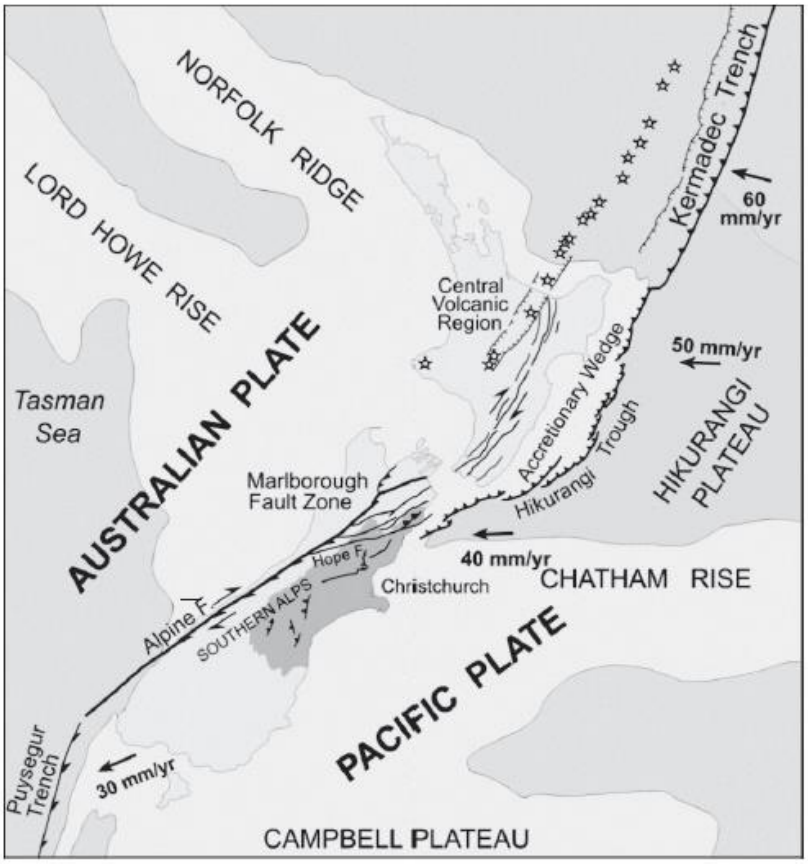

Figure 1.6: New Zealand tectonic system, after Bradley and Cubrinovski (2011)

The Canterbury area has a complex geological history, which in recent times has been largely governed by the Kaikoura Orogeny which is uplifting the Southern Alps to the west of Christchurch city (Kingma 1974). The Southern Alps is the sediment source for the

Canterbury Plains, which connects the mainland to the eroded remains of the Miocene volcanic complex known geographically as Banks Peninsula (Brown et al. 1995), Appendix 1.2 provides details on the evolution of the Canterbury Plains. The volcanic rocks of Banks Peninsula are extensively mantled by loess and loessial soil. This sediment was most likely sourced from the Southern Alps during periods of glaciation, and transferred to Banks Peninsula by the predominant easterly winds (Ives 1972; Griffiths 1973). The northernmost hills of Banks Peninsula are known as the Port Hills, and it is here that the fissure traces formed. Figure 1.7 shows a geological map of the northern Canterbury Plains.

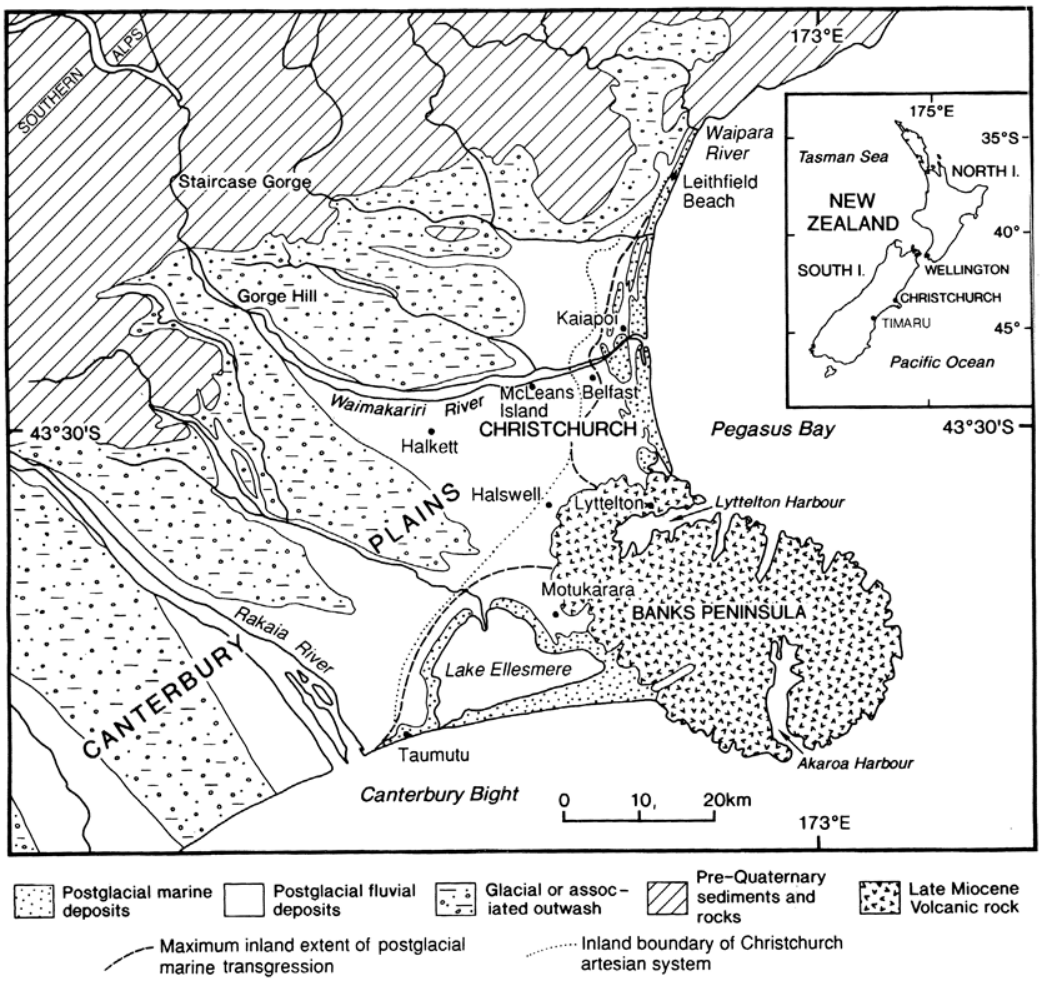

Figure 1.7: General Geology of the Northern Canterbury Plains. From Brown et al. (1995)

The 1:25,000 scale *Geological Map of New Zealand: Part Sheets M35 & M36: Christchurch Urban Area* map by Brown and Weeber (1992) displays Ramahana Road as underlain by 'Valley fill and slope wash of loess-volcanic derived colluvium', within the valley floor and 'Loess (*in-situ*) and loess-colluvium and mixed loess-volcanic derived colluvium overlying volcanic rock', on the Huntsbury spur. According to Bell and Trangmar (1987) loessial soil deposits of the Port Hills exhibit variable characteristics, but generally they are: coloured

yellow-brown or buff, composed predominantly of quartz (50% +) and feldspars (20% +), and dominantly consist of silt-sized particles (>50%), with fine sand and clay-size particles making up lesser fractions.

The study area is comprised of three suburbs in the Port Hills: Huntsbury, St Martins, and Hillsborough. For simplification purposes the area is termed 'Hillsborough Valley', as this suburb makes up the majority of the valley area. Refer to Figure 1.4 for a map of the location of the study area.

The slopes of the Hillsborough valley are generally gentle to moderately sloping <25°, but localized steeper gradients in the slope can be found, and these tend to be man-made features located on the upslope and downslope side of house platforms or roads/paths. Figure 1.8 is a photo of the area where the Ramahana Road fissure traces occurred. The top of the slope is composed of either exposed bedrock or shallow loessial soils (<1.5m), whilst the lower slopes are composed of loess-colluvium which thickens towards the base of the slope to over 25m. The valley floor is relatively flat (<3°) and is composed of interlayered deposits of silts, organic silts, sands, peat, and some gravels. The silt is of a loessial nature, and is derived from the slopes above, but it has been rewashed and remixed to a variable degree by surface water processes. The area is sparsely vegetated in wilding pines, gorse, grass and garden variety plants.

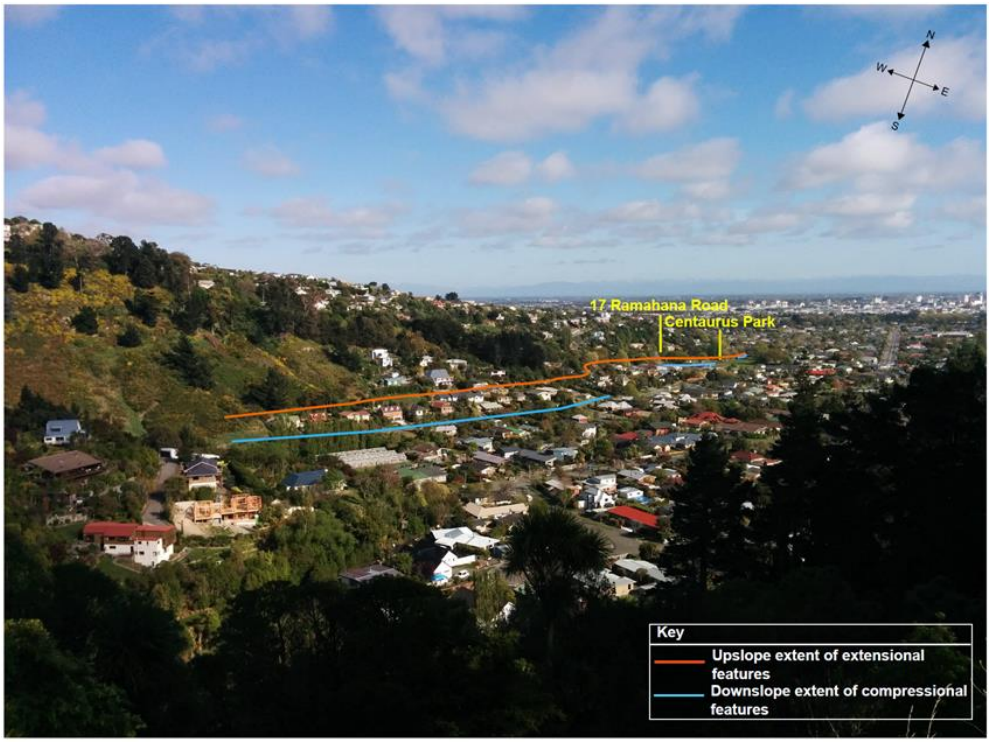

Figure 1.8: Photo of the Ramahana Road fissure trace area taken from the top of Rapaki Road facing North West. The area of fissuring had been overlaid to show the toe slope location and gentle slope where they occur.

There are two surface water drainage paths that meet at the southern end of the valley and flow near the centre of the valley out into the Heathcote River at the northern end. The drainage channel can be seen as the linear depression in Figure 1.9. This channel has been excavated and concrete-lined to form a confined drainage path. Figure 1.9 is a map of the valley topography in relation to the fissure trace expression.

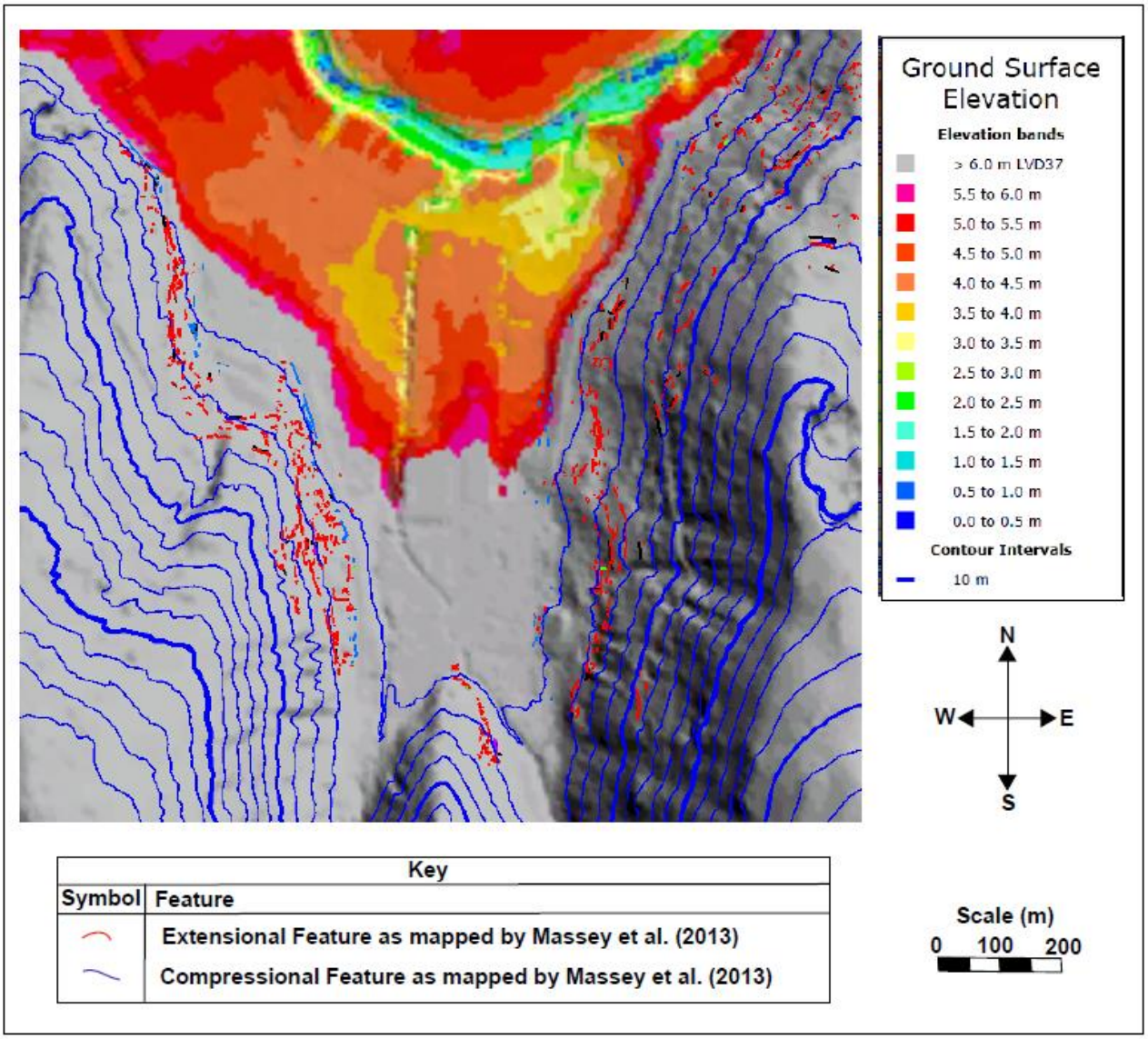

Figure 1.9: The Hillsborough valley topography in relation to the fissure trace expressions. The North-South orientated linear depression is a man-made drainage channel that flows into the Heathcote River, which is the depression to the north of the map.

1.5. Fissure Trace Characteristics

The Ramahana Road fissure trace is the primary concern of this thesis. At its northern end the Ramahana Road fissure trace originates up-slope of the intersection between Ramahana Road and Centaurus Road, and then it approximately follows Ramahana Road to the south before turning with the contour of the slope to follow up-slope of Albert Terrace. It terminates near the narrowest point of the western side of the Hillsborough Valley. Figures 1.8, 1.9 and 1.12 provide the location and orientation of the fissure traces. The Ramahana Road fissure trace is typical of the Christchurch Earthquake initiated loessial soil fissures across the Port Hills: it is generally in a North-South orientation at approximately toe-slope elevation, and it follows a roughly contour-parallel course.

Stephen-Brownie (2012) explains that whilst the fissures follow a roughly contour-parallel orientation, they tend to occur where there is a break in the slope, normally on a flatter piece of ground, and there can be multiple fissures in any one location. Their shape is roughly linear to rough undulating in plan view. They extend segmentally for nearly 1km across the entire western side of the Hillsborough valley. Figures 1.1 and 1.10 illustrate a typical fissure trace.

Figure 1.10: A fissure trace on the Vernon Terrace side of the Hillsborough valley showing a roughly linear orientation with mostly horizontal displacement in the downslope direction. Photo from Dellow et al. (2011).

The maximum accumulative displacements recorded by Massey et al. (2013) were 0.6m horizontal and vertical for the Ramahana Road section, and 0.8m horizontal and 0.4m vertical for the Albert Terrace section. The horizontal displacement is predominant, and this allows an open view into the trace; whereas the vertical displacement is not always evident.

The fissure traces along Ramahana Road are associated with compressional features downslope. The features are obviously compressional in some areas, but more subtle in others. For example, on the neighbouring Vernon Terrace fissure trace the compressional features are evident as buckles in fences, foundations, roads, and kerbs orientated parallel to the slope; whereas on the Ramahana Road fissure trace the compressional features can be as simple as a cracked step or tilted fence. This makes defining the boundary of movement on the Ramahana Road side more complicated than on the Vernon Terrace side. Figure 1.11 is a photo of a typical compressional feature downslope of Vernon Terrace.

Figure 1.11: Buckling in a curb in the compressional zone downslope of Vernon Terrace. Photo from Dellow et al. (2011).

Between the compressional features and the extensional features there is a zone with no obvious deformation, which has been interpreted as a translational zone by Massey et al. (2013). Figure 1.12 illustrates the extensional, compressional, and translational zones as interpreted by Massey et al. (2013). Houses that were located within the translational zone during the 22nd of February 2011 Christchurch Earthquake are without significant damage to foundations.

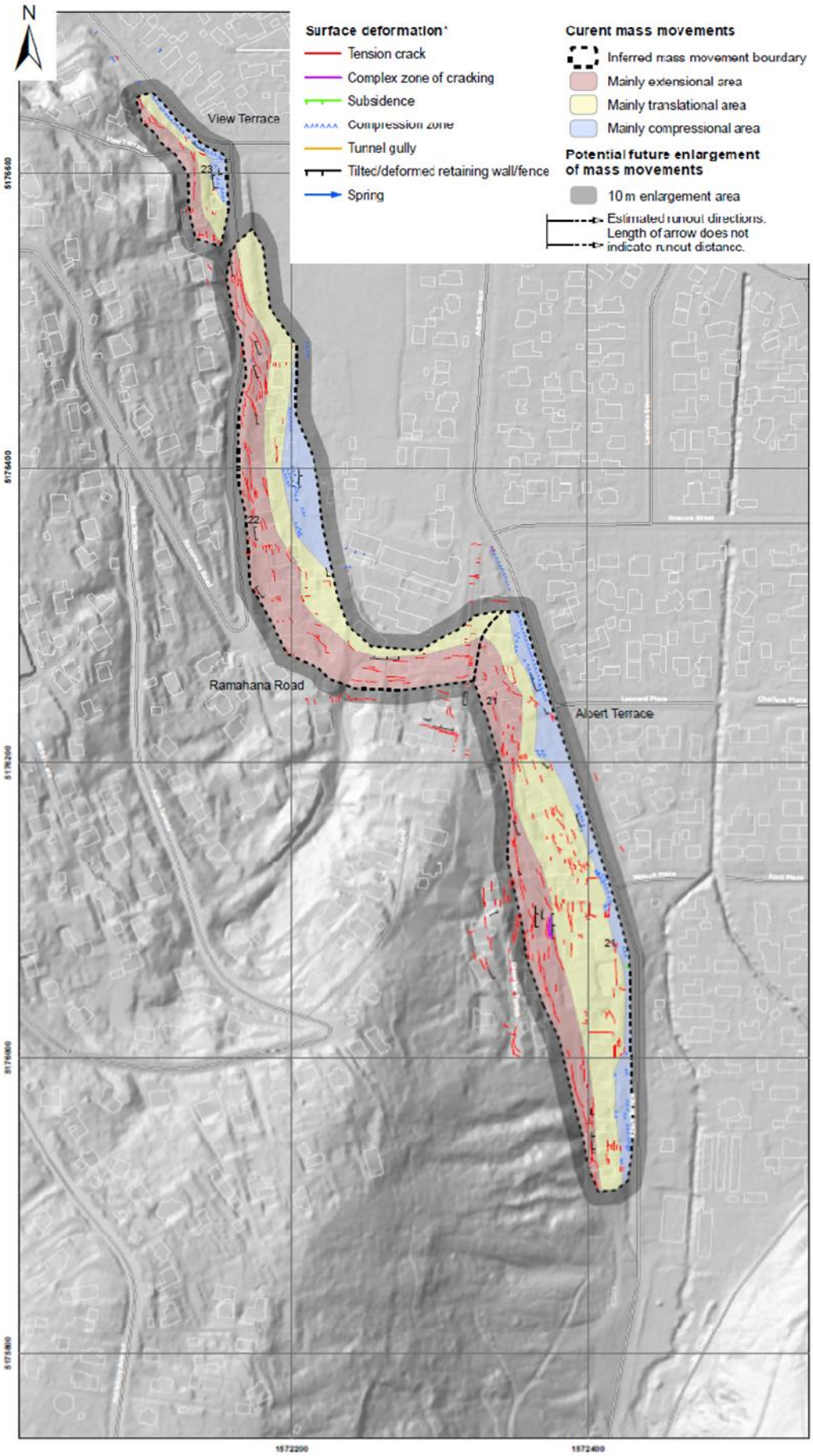

Figure 1.12: The Ramahana Road Fissure Trace, modified after Massey et al (2013).

The fissure traces opened during the Christchurch Earthquake induced shaking, but no movements were observed following the cessation of ground movement. In fact only the Vernon Terrace fissure trace was observed to have any possible creep movement after ground shaking had ceased, and this was only recorded during large magnitude earthquake aftershocks (Massey et al. 2013). These aftershocks caused no recorded movement in any other fissure traces. There has been no movement observed following periods of increased rainfall or individual occurrences of intense rainfall.

A feature of the Christchurch Earthquake that coincided with the occurrence and location of the fissure traces is the development of new springs and groundwater seepages at the base of slopes. Hydraulic changes were also noted following the Darfield Earthquake, but the springs and seepages that occurred following the Christchurch Earthquake were much more significant in volume and number (Cox et al. 2012). Whilst the springs do not occur at every area of fissuring, they are prevalent in the Hillsborough Valley, particularly in the northernmost point of the valley. Figure 1.13 is a photo of a typical spring induced by the Christchurch Earthquake.

Figure 1.13: A spring within the compressional zone of Centaurus Park as of the 4th of August 2015. The water bottle is 30cm to the right of where the spring is seeping water to the ground surface. Around the seepage point there is stagnant water and a build-up of loose mud up to 5cm deep. The longer grass indicates the area affected by the spring.

1.6. Research Methodology

This research conducted for this thesis follows on from the previous work of Stephen-Brownie (2012). This earlier thesis was an overarching regional study of the fissure traces that focussed on their locations and characteristics of occurrence. The current study is a more detailed geotechnical study which focusses on a smaller area of fissuring. There were two main sites where this study was conducted, both of which were downslope of Ramahana Road: 17 Ramahana Road and Centaurus Park.

There were multiple fissures at the top of the slope at 17 Ramahana Road, and there was evidence for compression at the base of the slope. This allowed for testing of both extensional and compressional features. The residential building that was on the site during the Christchurch Earthquake had been seriously damaged by multiple fissure traces opening up underneath it, and it had subsequently been demolished. At the time this study began the site was largely empty apart from two small newly-built huts at the base of the slope and remnant structures in sheds, retaining walls, fences, and paths from before the earthquake.

Prior to the investigations of this thesis Tonkin & Taylor Ltd had drilled 3 boreholes at the site to determine the extent of damage to the site. These were located above the extensional area, within the extensional area, and below the compressional area. From the top of the slope to the bottom of the slope these were called BH-RMH-01, BH-RMH-02, and BH-RMH-03. Appendix 2.7 provides the borehole logs. Piezometers had been installed in BH-RMH-02 and BH-RMH-03, and these were used for groundwater observations. Figure 3.2 illustrates where the boreholes were located on the site.

A range of geotechnical testing methods were conducted on this site as part of the thesis study that included: hand augers, Scala penetrometer tests, a test pit (excavated to 3m depth and conducted across a fissure trace), and a cone penetration test with pore-pressure dissipation tests at varying depths. Geophysical testing methods were also conducted on this site that included: ground penetrating radar, electrical resistivity geophysical survey, and seismic reflection survey. These testing methods were chosen due to their accessibility, relatively low cost, and low disturbance to the site. Efforts were made to excavate another test pit in the compressional zone and through another fissure; however due to access restrictions these were unable to be conducted. A desktop study of previous geotechnical tests

in the wider area of the Hillsborough Valley was also undertaken to gain a greater understanding of the geological model of the site.

20 samples were taken from the hand augers within the compressional zone and 10 from the test pit (extensional zone). These were later tested in the laboratory for particle-size analysis, Atterberg Limits, natural moisture contents, density tests, and direct shear-box testing. These testing methods were chosen to classify the soil so that estimations of behavioural characteristics under cyclic loading could be made. These methods were also accessible due to the testing equipment being available at the University of Canterbury. Efforts were made to get soil samples tested by cyclic triaxial tests and cyclic shear tests, but the necessary equipment was unavailable.

The other site was Centaurus Park. The fissure traces were present upslope of Centaurus Park on Ramahana Road, but these had been repaired prior to the investigations in this thesis. Centaurus Park is assumed to be the downslope compressional area for the fissure traces on Ramahana Road at this location. Centaurus Park is largely devoid of any structures and there was very little evidence of compression at the ground surface.

Stephen-Brownie (2012) had used Centaurus Park to conduct an electrical resistivity geophysical survey, which crossed diagonally through the park and crossed through a newly formed spring at the base of the slope and this was correlated to the resistivity survey from 17 Ramahana Road. SCIRT conducted 5 boreholes in Centaurus Park, and just upslope of Centaurus Park on Ramahana Road in 2012. The core was donated to the University of Canterbury for logging and testing in this thesis. 18 samples were taken from the SCIRT borehole core and these were tested by the same methods as for the 17 Ramahana Road samples. Due to this land being owned by the Christchurch City Council and due to its close proximity to St Martins Primary School, this site was not as extensively tested as 17 Ramahana Road. However the electrical resistivity geophysical survey results in Centaurus Park, conducted by Stephen-Brownie (2012), and the survey results in 17 Ramahana Road were very similar. The borehole core also proved to be invaluable for laboratory testing and understanding the nature of the soil profile.

1.7. Thesis Format

The format of this thesis is as follows:

Chapter 1-Introduction: this chapter introduces the background of the fissure traces, what the problem is, and it introduces the site area tested. It covers the basic geology and geomorphology of the site area, the characteristics of the fissure traces, and the methodology for the testing methods.

Chapter 2-Literature Review: a review on previous studies of the geological and geotechnical properties of the different soil and bedrock units in the Hillsborough Valley. It covers the common slope stability issues on Banks Peninsula, the characteristics of the Canterbury Earthquake Sequence, and the hydrogeological setting of the site.

Chapter 3-Qualitative Assessment: Subsurface Investigations: an in-depth recording of results and interpretations of the various geotechnical and geophysical testing methods.

Chapter 4-Quantitative Assessment: Laboratory and Computational Investigations: an in-depth recording of results and interpretations of the various laboratory tests that were conducted on samples taken from 17 Ramahana Road and the borehole core from Centaurus Park. Also includes a computational slope stability analysis for 17 Ramahana Road.

Chapter 5-Potential Movement Types and Mechanisms: this chapter is a discussion about the potential movement types and mechanisms of the fissure traces. It covers four potential scenarios including rotational slide movement, translational slide movement, lateral spread movement, and quasi-toppling movement. Other factors involved in the movement are also discussed.

Chapter 6-Conclusions: a summary of the main points of discussion from the previous chapters and a relation of the results to the project objectives. Recommendations for future land use along the Ramahana Road fissure trace are made, as well as future research for testing the interpretations in this thesis.

2. Literature Review

2.1. Introduction

The focus of this research is to gain a better understanding of the mechanisms behind the soil movement that caused the fissure traces by a detailed investigation of a small segment of the Ramahana Road fissure trace. A comprehensive investigation cannot be completed without an accurate geological model which encompasses previous studies on the geological units present within the site area. This literature review investigates the geological and geotechnical properties of the different soil and rock units on the Port Hills, and it covers the common causes of slope instability on the Port Hills in order to compare and contrast the characteristics of these movement types to the fissure trace characteristics. The characteristics of the Canterbury Earthquake Sequence are explored and the changes to the hydrogeology of the site are introduced. This section provides necessary background to the geological model of the site.

Loessial soil and the volcanic rock of the Lyttelton Volcanic Group are the main geological units in the Hillsborough Valley. The loessial soil deposits overlie the Lyttelton Volcanic Group, but there has been mixing of eroded volcanic rock with eroded loessial soil to form the colluvial deposits that flank the ridges of the valley. The colluvial material has been further mixed at the valley floor by surface water processes, and localized blockages in drainage have formed interlayered deposits of loessial soil, peat, and organic silt. Figure 2.1 shows the geological units of the north facing valleys of the Port Hills and the Christchurch city flatlands in relation to the location of the fissure traces

2.2. Lyttelton Volcanic Group

The Lyttelton Volcanic Group (LVG) forms the bedrock of the Port Hills, but the basement rock is the late Triassic Torlesse Supergroup, which is found beneath it at a depth of around 1km (Brown & Weeber 1992). According to Read and Richards (2007) the Torlesse Supergroup (more commonly known as greywacke), is composed of inter-bedded indurated muddy sandstones and mudstones. The sandstone component consists of coarse to medium grain-sized, poorly sorted, angular quartz and feldspar, and to a lesser extent metamorphic and igneous rock fragments indurated within a clay mineral matrix, whilst the mudstone consists of indurated layers of dark grey to black claystone, siltstone, or mudstone (Read & Richards 2007). It forms the basement rock of a large portion of New Zealand and the

majority of the Southern Alps (Read & Richards 2007), but it has little surface expression on the Port Hills. The Christchurch Earthquake was sourced on the Port Hills fault, which is located within this geological unit (Beavan et al. 2011). Figure 2.2 shows the Port Hills fault and the epicentre of the Christchurch Earthquake in relation to the fissure traces.

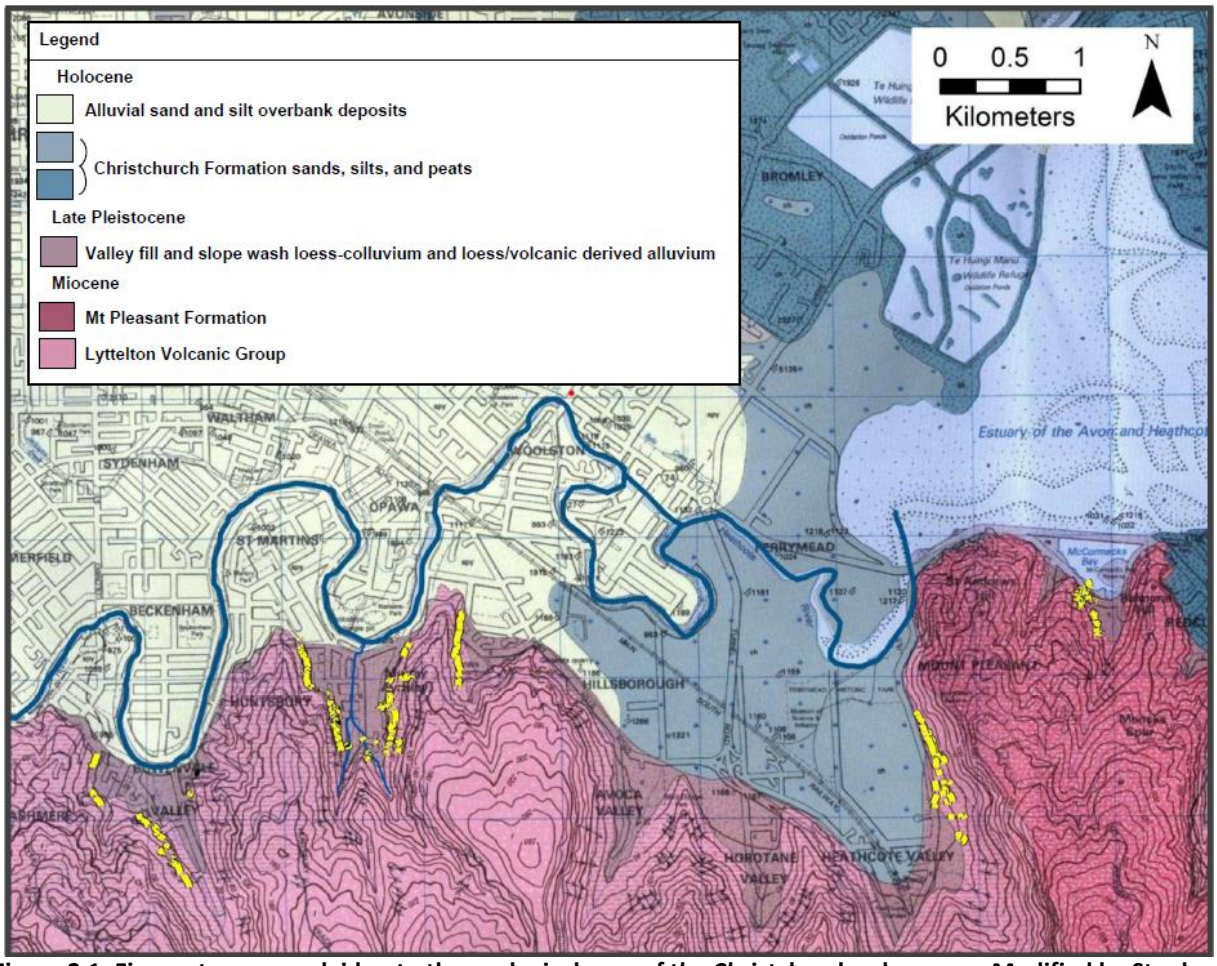

Figure 2.1: Fissure traces overlaid onto the geological map of the Christchurch urban area. Modified by Stephen-Brownie (2013) after Brown and Webber (1992). Scale = 1:25 000. Institute of Geological and Nuclear Sciences geological map by Brown and Weeber (1992).

The Lyttelton Volcanic Group was formed during a period of volcanic activity during the Miocene east of the former coastline of New Zealand. Two main composite cone volcanoes were active during this period: known as Lyttelton and Akaroa, and their eroded remnants are what form the outline of the present-day Banks Peninsula (Hampton 2010). The Lyttelton Volcanic Group was formed by the Lyttelton Volcano, which is the older of the two. This volcano was active 11.0-9.7Ma; whereas the Akaroa volcano was active 9.1-8.0Ma (Sewell et al. 1992). Shelly (1987) hypothesised that the Lyttelton volcano had two main eruptive centres, one at the head of Lyttelton Harbour, and one in Charteris Bay. Figure 2.3 shows the two eruptive centres in the Lyttelton Harbour. Appendix 1.2 provides further information on the joining of Banks Peninsula to the Canterbury Plains.

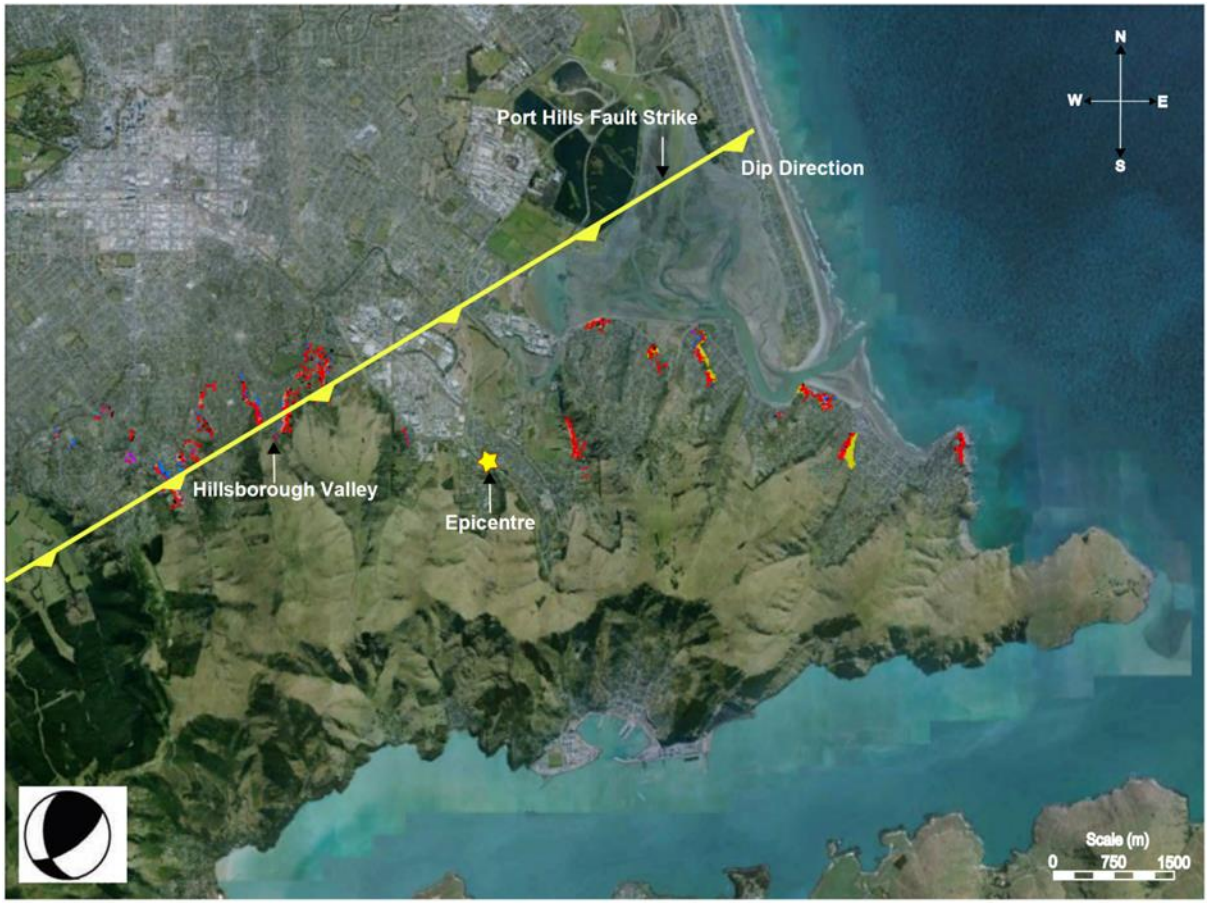

Figure 2.2: Fissure traces in relation to earthquake epicentre and Port Hills fault. Fissure traces mapped by Massey et al. (2013), map modified from Project Orbit. Fault orientation and location after Kaiser et al. (2011).

The successive eruptive phases of the volcanoes have left rocks of indurated ash beds and laharic deposits; and of basaltic and andesitic lavas of rubbly and massive aa-type (Bell & Trangmar 1987). The Lyttelton Volcanic Group is described by Brown & Weeber (1992) as 'Dark grey to black, plagioclase-pyroxene-olivine phyric basalt through to grey-green trachyte interbedded with pyroclastic deposits'.

The original height of these composite cone volcanoes would have been much larger than today, estimations vary from 1500m (Weaver & Smith 1987, cited in Hampton 2010) to >3000m (Speight 1917, cited in Hampton 2010), but at the completion of the volcanic activity, with no addition of volcanic material, erosion worked at bringing their peaks down. Figure 2.3 shows two estimates of the original heights of the volcanoes compared to the current outline of Banks Peninsula. The erosion of the two cones is estimated to have reached a maximum during the late Miocene or early Pliocene (Bell & Trangmar 1987). Today the highest point on the Port Hills is ~500m a.s.l. and the highest point on Banks Peninsula is 920m a.s.l. at Mount Herbert. The continued sea level fluctuations during the Quaternary

helped to erode the drainage channels through the Lyttelton Volcanic Group into steep sided valleys during glacial periods, and the flooding of these deep valleys during inter-glacial periods led to the deposition of fine-grained sands, silts, and muds.

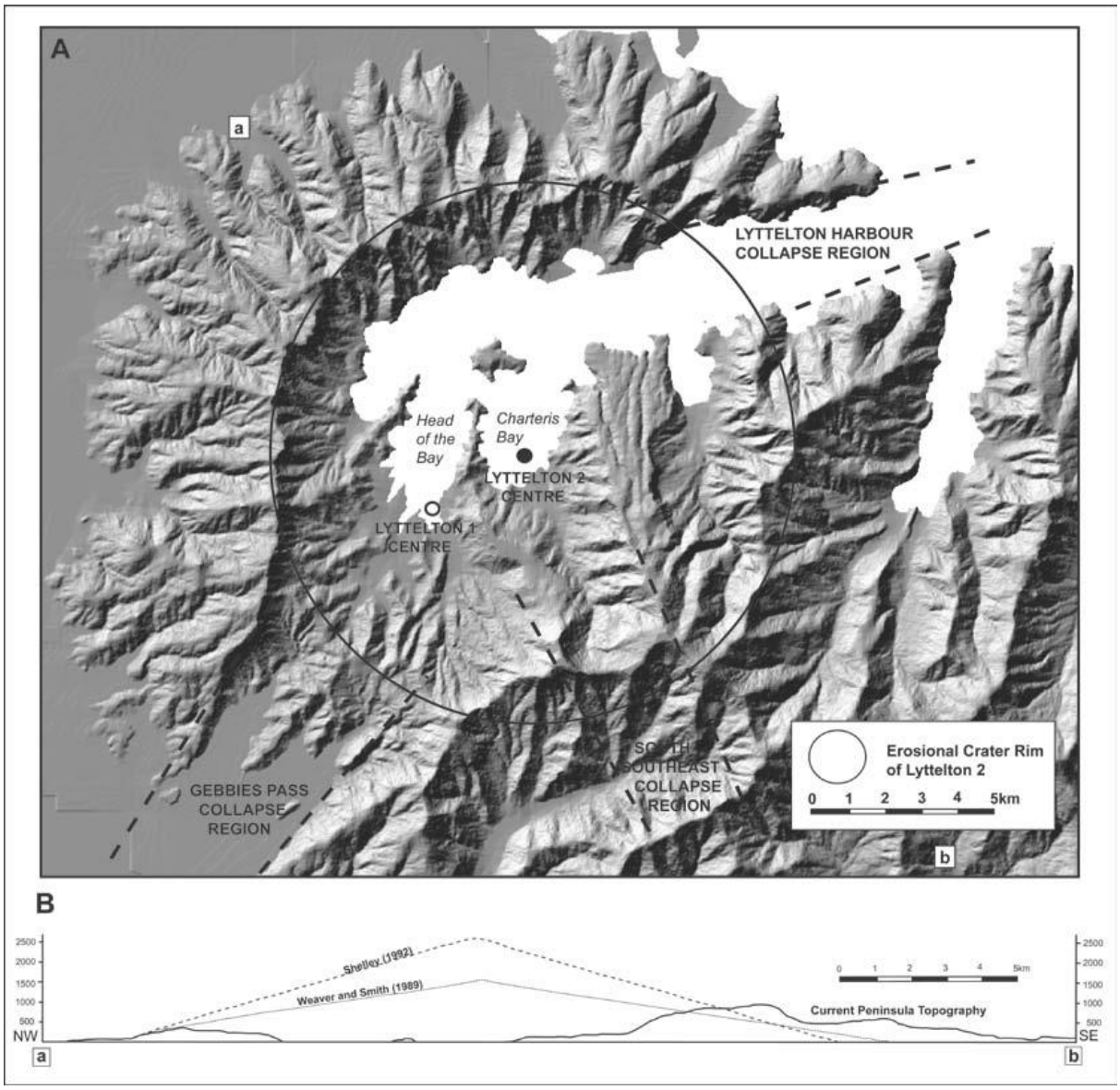

Figure 2.3: The Lyttelton volcano eruptive centres and estimates of original height. A shows the two eruptive centres of the Lyttelton Volcano, as hypothesised by Shelley (1992), and three collapse regions which are not mentioned in this thesis. B shows the projected heights of the Lyttelton Volcano after Shelley (1992) and Weaver and Smith (1989). From Hampton (2010).

2.3. General Properties of Loess

According to Kirchenheimer (1969) as cited by Pye (1995) the term "loess" is a derivation from the German word for loose, "löss". It was first coined in 1823-1824 by the geologist Karl Caesar von Leonhard, to describe the silty and friable soil deposited along the Rhine

Valley in Germany. Loess can primarily be understood to be a fine-grained deposit of aeolian origin; although, Pecsi (1990) would rightly argue that this is an over-simplification. In the interest of not giving an overly prescriptive definition, Pye (1995) states that:

> *'The only essential criteria for a sediment to qualify as loess are that (a) the deposit consists principally of wind-deposited silt and (b) accumulation occurred sub-aerially. Sediments consisting largely of wind-blown dust which accumulate sub-aqueously in oceans and lakes can be referred to as aeolo-marine and aeolo-lacustrine deposits respectively.'* (p. 654)

Under this definition, the predominantly silt-sized particle deposits of aeolian origin in the South Island, New Zealand can be classified as loess; however, there are numerous examples of loess definitions that exclude certain properties of New Zealand deposits from this classification. Pecsi (1990), for example, argues that carbonate-free loess should be classified as 'loam', with similar properties to loess. This would exclude the majority of New Zealand loess, as most contain little to no carbonate (Pye 1995). Raeside (1964), in identifying a discrepancy in an earlier loess definition states that:

> *'The definition proposed by Russel (1944), which requires that 50% of the particle size distribution should fall between 0.01 mm and 0.05 mm, and that the deposit should be porous, calcareous, unstratified, and homogeneous, would also exclude New Zealand deposits, which are not only compact and of low permeability, but also non-homogeneous, and non-calcareous.'* (p. 812)

The variable sources of loess material and the different depositional processes across the world are the reasons for the variability in the properties of loess. These variances can cause confusion when attempts are made to correlate the behaviour of New Zealand loess to the behaviour of Chinese loess for example, because New Zealand loess is generally compact and of low permeability, whereas Chinese loess is generally loose and porous. In spite of the discrepancies in definition, aeolian deposits across the world, of predominantly silt-sized particle distribution, that accumulated sub-aerially, are most commonly termed loess, and as such, the deposits of wind-blown silt in New Zealand are termed loess.

According to Pye (1995), the accumulation of thick sequences of loess requires a large and relatively continuous supply of suitably sized sediment, such as a tectonically active mountain belt with streams to transport and sort the sediment, and a sediment trap downwind

of the source, which is normally a well vegetated topographic barrier, such as a forested hill. This deposition style creates primary loess, otherwise known as *in-situ* loess or airfall loess. The distinction between primary loess, which is of the original aeolian deposition, and secondary loess, which is primary loess that has undergone redepositional processes, or sufficient alteration/degradation *in-situ* was originally emphasized by Obruchev (1945). Secondary loess deposits are generally present as colluvium. They can have a variable amount of mixing with other local geological deposits due to their formation by slope instability processes. Appendix 1.3 provides for further detail on loess classification.

According to Pye (1995), quartz is generally the greatest constituent of typical loess, as it comprises 45-55% of the material, and the rest consists of feldspars, heavy minerals, carbonates, volcanic glass shards, and clay minerals. The clay minerals consist mainly of mixed-layer smectite/illite, illite, kaolinite, and chlorite (Derbyshire & Mellors 1986; Grabowska-Olszewska 1989).

2.3.1. General Geotechnical Properties of Loess

Grabowska-Olszewska (1989) explains that the framework of loess is typified by loose silt to fine sand-sized, sub-angular to sub-rounded particles that are connected by bonds, buttresses, and bridges of clay-sized particles. Figures 2.4 and 2.5 show the microstructure of loess. The framework lacks orientation and the pore spaces are of an open, isometric configuration (Grabowska-Olszewska 1989). The silt to fine sand-sized particles do not touch, or connect with one another, and therefore loess' mechanical behaviour is completely directed by its framework and the bonds between grains (Tan 1986).

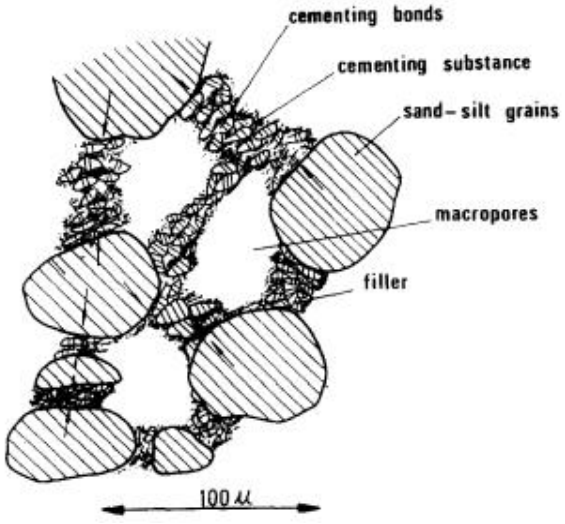

Figure 2.4: Loess microstructure, sourced from Tan (1986)

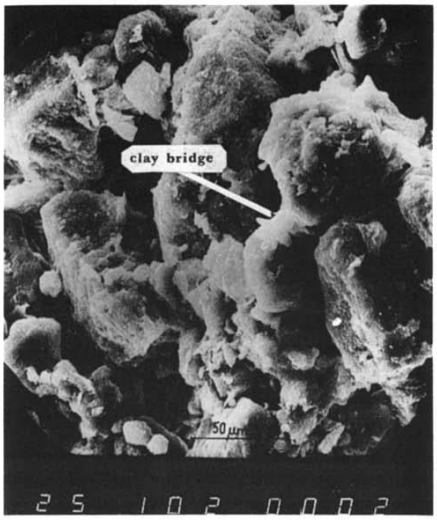

Figure 2.5: Loess microstructure, sourced from Grabowska-Olszewska (1989)

The buttresses can be visualised as silt-sized aggregations of clay that are syngenetic (i.e. they were deposited in this way), whilst the bridges can be visualised as accumulations of clay-sized minerals at points of contact between silt-sized particles that are post-depositional in origin (Derbyshire & Mellors 1986). After deposition the clay-sized particles flocculate non-uniformly on the surface of the silt to fine sand-sized particles, leading to the larger-sized particles being coated in clay-sized particles. The non-uniformity of the flocculation leads to the building of 'bridges' to other larger-sized grains (Grabowska-Olszewska 1989).

The clay bridges are sensitive to wetting. For this reason the moisture content has a major influence on the mechanical properties of loess. Loess generally has a high shearing resistance, which allows it a high bearing capacity with little resultant settlement, if its moisture content is low; if the moisture content is high the shearing resistance and bearing capacity are appreciably lowered. The shearing resistance and bearing capacity are, however, mainly influenced by the density of the loess deposit (Bell 1993). This correlates with the work of Higgins and Modeer (1996) who state that North American loess can have cohesion values of >400 kPa when it is dry, and of high clay content and density; whereas cohesion values of 0 kPa have been found in laboratory tests of samples of low clay content, low density, and high moisture contents.

2.4. Banks Peninsula Loess

The sediment source for Banks Peninsula loess was the uplifting Southern Alps during periods of Pleistocene glaciation (Ives 1972; Griffiths 1973). The grinding power of glacial movement across mountain gullies eroded and transported vast quantities of sediment to the foothills. The transport of the sediment from the foothills towards the Pacific Ocean was accommodated by movement of eastward-flowing meltwater streams and rivers, such as the Waimakariri and Rakaia Rivers (Brown et al. 1995). The flow of these rivers over the Canterbury Plains sorted the sediment, and the finer sediment settled on outwash fans (Bell & Trangmar 1987). This finer sediment was subsequently entrained by the predominantly north-westerly wind and successively deposited onto the topographical barrier of the eroded remains of the Banks Peninsula volcanoes (Ives 1972; Griffiths 1973). Figure 2.6 illustrates the movement and deposition of primary loess from the foothills of the Southern Alps to Banks Peninsula.

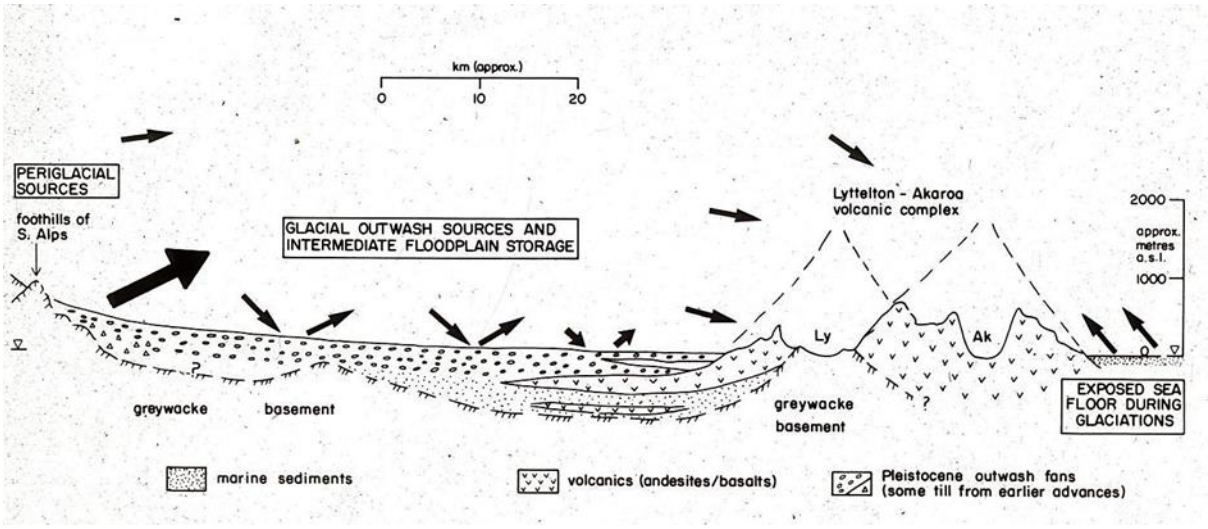

Figure 2.6: Likely conditions under loess deposition on Banks Peninsula. From Bell and Trangmar (1987).

The deposits of loess on the Port Hills were originally more extensive, laterally and vertically across Banks Peninsula; however, *in-situ* loess deposited in the Pleistocene were immediately exposed to erosion that continues to the present day. The primary loess material that was eroded from its original position was often reworked and re-deposited downslope as colluvium, or transported into a marine setting. Griffiths (1973) estimates that much of this erosion was a consequence of freezing and thawing of the loess deposits during the Pleistocene, but it is now understood that erosion rates have since been accelerated by the removal of forests and the subsequent development for agricultural and urban practices (Bell and Trangmar 1987).

Bell and Trangmar (1987) identify five primary regolith materials of the Port Hills. One is primary loess, one is residual soil, and the other three deposits can be classified as colluvium with varying amounts of loessial content. The three colluvium deposits are defined below:

- Loess-colluvium: all loessial material that has been eroded downslope since its primary deposition. It may contain up to 10% volcanically derived gravel to boulder sized fragments. The volcanic material is mixed into the loess during movement downslope and may be present as distinct layers or spread throughout the colluvium deposit. The variable history behind each successive phase of colluvium deposition has a great influence on the characteristics of loess-colluvium; this results in layers within the deposit having variable characteristics.
- Volcanic-colluvium: all colluvium of dominantly volcanically derived material of gravel to boulder sized rock fragments set within a matrix of volcanically derived

fines mixed with less than 10 % loess-colluvium. It generally occurs overlying slightly to highly weathered volcanic bedrock material.

- Mixed loess/volcanic colluvium: all loess-colluvium that has been sufficiently mixed with volcanic-colluvium, derived from the erosion of volcanic outcrops upslope. It may contain 10-90% volcanic-colluvium to loess-colluvium.

2.4.1. Composition of Banks Peninsula Loess

In the Port Hills loessial deposits the silt to fine sand-sized particles are predominantly composed of quartz (≥50 %) and feldspars (≤20 %); while the clay-sized particles are composed of clay minerals, clay-sized quartz and feldspar minerals, and rarely calcite (Bell & Trangmar 1987). Bell (1978) explains that the clay minerals consist of illite, hydrous mica, and kaolinite, which are non to low swelling minerals. Shrink/swell clay minerals of montmorillonite and vermiculite are formed by subsequent weathering of the deposit, and result in an increase in plasticity.

Calcite can also be classified as a secondary mineral: secondary minerals form from the aggregation of colloids in cavities, microfissures, worm channels, and along roots, and they include montmorillonised volcanic glass shards (Raeside 1964). According to Raeside (1964), secondary minerals along with volcanic glass, sponge spicules, plant opal, charcoal, and diatoms make up the light mineral fraction of Canterbury loess (<2 % of total mineral fraction).

2.4.2. Geotechnical Properties of Banks Peninsula Loess

A typical primary loess profile on Banks Peninsula shows vertical variations in colour, plasticity, erodibility, density, and swelling characteristics, as recorded by Yetton (1990). A typical profile of primary loess can be viewed in Figure 2.7. The different layers show distinct geological and geotechnical properties that are attributed to pedogenic processes. The compact layer is generally clayey silt with minor sand and low plasticity (PI = 6-12), whilst the layers above and below this are silt with some sand and minor clay with non to slight plasticity (P1<7) (Yetton 1990). Griffiths (1973) explains how vertical cracks can be displayed within the compact layer, with mottling and gammation occurring as a result. The compact layer is also called the fragipan, and it is hypothesised by Selby (1976) to arise from summer drying, and consequential cracking of the soil, which results in infilling by loose material. The following winter brings wetting, which causes the soil to swell and compact.

Bell & Trangmar (1987) state that the compact layer adds to the susceptibility of the primary loess to subsurface erosion, and Goldwater (1990) explains that it also can affect slope stability.

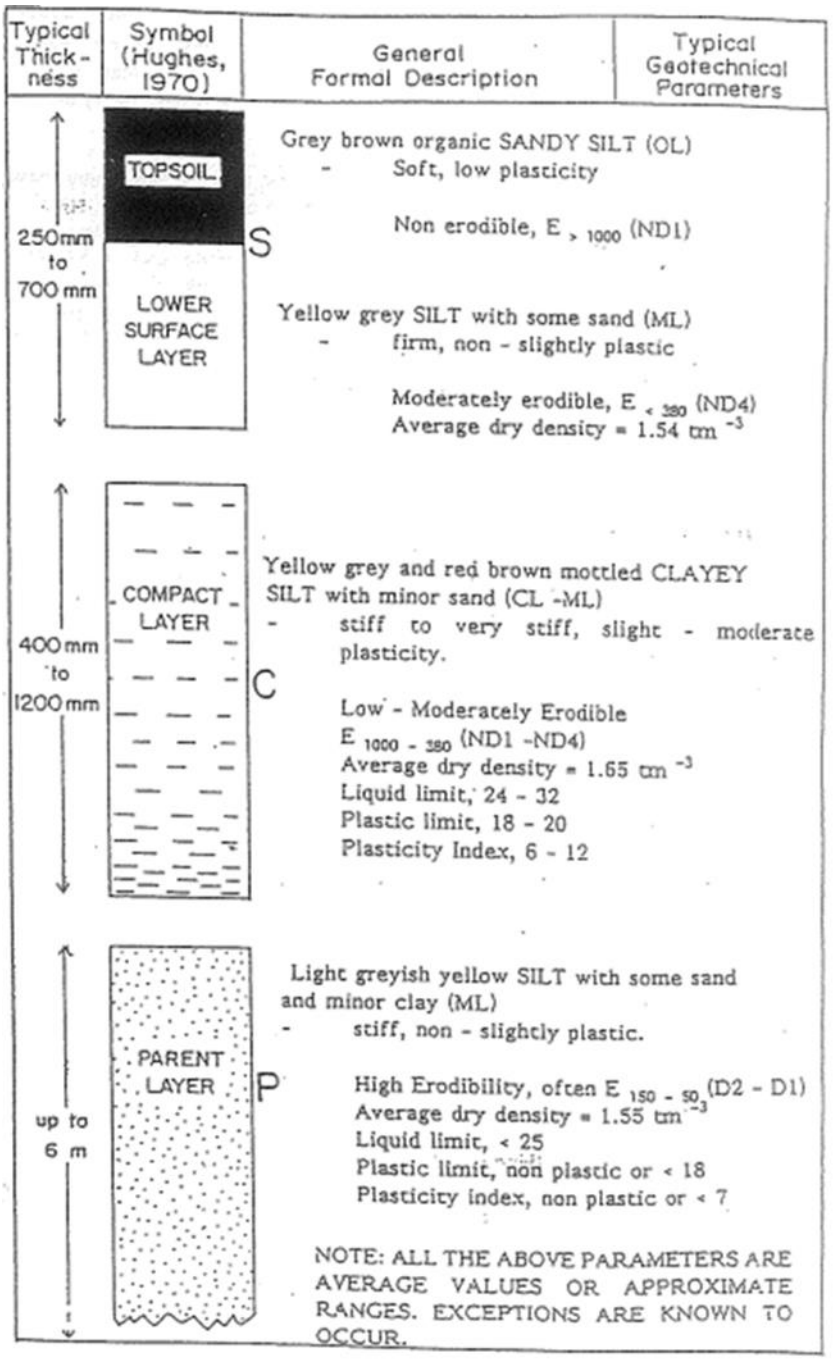

Figure 2.7: Typical vertical variations in loess due to pedogenic layering. From Yetton (1990).

A table of typical geotechnical properties of Banks Peninsula loess is shown in Appendix 1.4 and details on construction considerations in Banks Peninsula loess are provided for in Appendix 1.5

2.4.3. Loessial Soils in the Hillsborough Valley

Within the steep sided valleys of the Hillsborough Valley the primary loess was eroded and transported from the ridges and hill tops to be deposited on the lower slopes, and within the low-gradient valley floor. This has left the ridges and hill tops with bedrock exposed or with very thin deposits of loessial soils; whereas the lower slopes and valley floors have loessial deposits of extensive depths (>25m). The loessial soil deposits on the flanks of the valley ridges are loess-colluvium and the deposits on the valley floor are known as valley alluvium. Figure 2.8 shows the exposed bedrock and thin loessial cover on the ridges at the head of the Hillsborough Valley and Figure 2.9 shows the low-gradient valley floor, which has been in-filled by the material from the ridges above.

Figure 2.8: Exposed bedrock to thin loessial soil cover seen on the ridgeline above Rapaki Road on the eastern side of the Hillsborough Valley. Photo taken from Huntsbury Avenue.

Figure 2.9: The low-gradient Hillsborough Valley floor, in-filled with sediment sourced from the ridgeline above. Photo taken from Huntsbury Avenue.

Loess-colluvium deposits often display discrete layering that follows the slope angle (Wu 1996); however the layering in the loess-colluvium deposits of the Hillsborough Valley are not easily identified: the different layers tend to grade into each other, rather than forming discrete boundaries. Layers can have colouring differences, but the main differences in a geotechnical sense are the grain-size distribution changes, density variations, and consequent moisture content differences (Bell & Trangmar 1987). Differences in grain-size distribution in different layers of colluvium can be caused by changes in climate and changes in the source material (Leopold & Volkel 2006). Due to the complex nature and history of deposition, loess-colluvium can have variable geotechnical properties throughout the deposit, which makes it very difficult to gather representative samples for testing.

The valley floor has been influenced by both sides of the valley, and the small streams flowing through the valley floor have reworked the loessial material overtime. The deposition of loessial material in the valley floor probably led to a flattening of the valley floor, and a blockage of drainage. This would have led to the creation of swamps and still water which would be a trap to organic material. Over time this led to the formation of peat deposits up to 3m in thickness. The peat deposits are generally black and fibrous with a high moisture content. The Hillsborough Valley was still largely swamp land when Europeans first arrived, but it was subsequently drained to accommodate new subdivisions. Figure 2.10 shows a section of the 1856 'black map', which outlined the wetland areas in Christchurch.

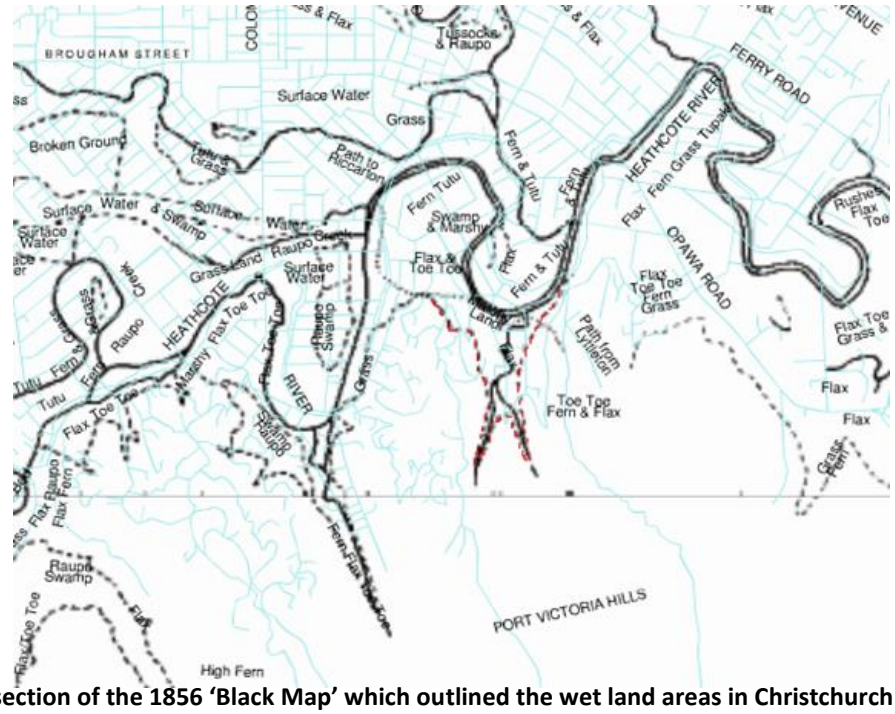

Figure 2.10: A section of the 1856 'Black Map' which outlined the wet land areas in Christchurch. The relevant wet land area for the Hillsborough valley is marked in red. Sourced from Lucas Associates, historical maps of Christchurch.

2.5. Slope Stability Issues in Bedrock and Loessial Soils of Banks Peninsula

2.5.1. Principal Types of Instability in Banks Peninsula Loessial Soils

Loess is considered very stable in vertical slopes 15-20m high, albeit at low moisture contents of around 8-10% (Dijkstra et al. 1994). Moisture is generally the cause of slope instability in loessial soils, but there are many erosional processes that have shaped the current landscape of Banks Peninsula. These processes were described by Bell and Trangmar (1987), and they include:

- Rock and debris falls;
- Soil creep;
- Sheet and rill erosion;
- Tunnel-gully erosion;
- Wind erosion;
- Slide-avalanche-flow mass movements.

Artesian slides are another form of mass movement in Banks Peninsula loessial soils that were not considered by Bell and Trangmar (1987), but they were considered to be of sufficient difference and importance for Yetton (1992) to distinguish them.

The principal stability issues are briefly described in the following sections. Appendix 1.6 provides information on historical fissures in Banks Peninsula loessial soils.

2.5.2. Rock and Debris Falls

These are a form of mass movement where material dislodges from a cliff face and free-falls under gravity (Cruden & Varnes 1996). Rockfalls occur in the volcanic bedrock of the area; whereas debris falls occur in any of the soil types aforementioned. It can occur anywhere where there is a steep face, such as a cliff, and it is caused by a loss of cohesion and loss of contact with adjacent materials (Varnes 1978). This failure occurs in loessial material when shallow deposits of loessial material are located overlying bedrock near a cliff face. Falls of loess occurred during the Christchurch Earthquake due to brittle fracturing induced by the earthquake-induced shaking. Figure 2.11 illustrates the process of rock and debris falls on the Port Hills during the Christchurch Earthquake.

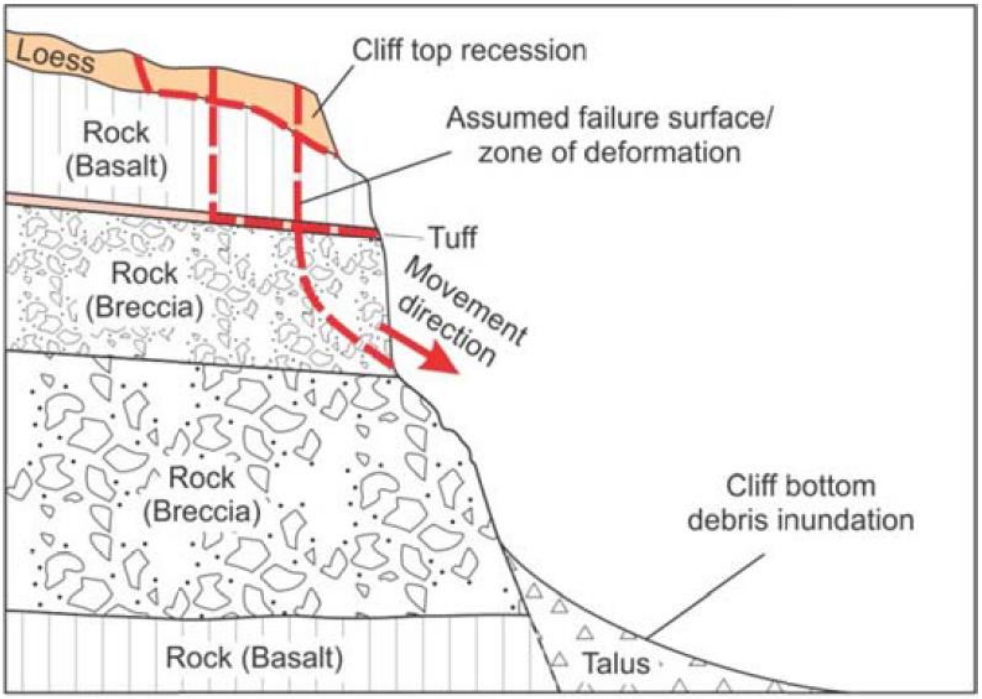

Figure 2.11: Rock and debris falls in the Port Hills during the Christchurch Earthquake. From Massey et al. (2012).

2.5.3. Soil Creep

Soil creep is a form mass movement, and is typified by imperceptibly slow downslope movement of surface material, generally caused by seasonal fluctuations in temperature and water (Bell 1999). According to Bell and Trangmar (1987), creep on Banks Peninsula generally occurs on slopes >15° in *in-situ* loess, loess-colluvium, mixed-colluvium, or volcanic-colluvium.

The occurrence of creep is generally confined to the surface 1.5m of the soil in zones of high water content, and this is generally restricted above a relatively low permeability layer such as the compact layer, at a contact layer between two colluvium layers, or at a contact between two deposits of different geology. The low permeability layer may act as a poorly defined basal shear surface, and may progress into a rapid mass movement failure if stresses increase, but the dominant features that form from this process are terracettes, parallel to the contour of the slope, and larger wavelength mounds or hummocks (Bell & Trangmar 1987). Figure 2.12 shows the central ridge at the head of the Hillsborough Valley with evidence of soil creep.

Figure 2.12: The central ridge at the head of the Hillsborough Valley showing signs of creep. The small terracettes and hummocks are visible on the shaded slope below the ridge top. Photo taken from the end of Albert Terrace.

2.5.4. Sheet and Rill Erosion

Zhungu (1980) explains that sheet erosion occurs through detachment of soil particles caused by the impact of raindrops, and the associated downslope movement by sheet water flow. It occurs on gentle slopes, and results in a more or less uniform denudation of the entire surface area. Rill erosion occurs where surface water flow erodes the surface soil, and forms a channel in a 'U' or 'V' shape (Zhungu 1980). This usually occurs on moderately sloping to steeply sloping soils. These processes can occur relatively quickly on cut loess faces or denuded slopes, and the resultant erosion can be significant if the upslope catchment is of sufficient area. Bell & Trangmar (1987) state that sheet and rill erosion is confined to areas with depleted vegetation cover, where the soil surface is exposed. Figure 2.13 shows rill erosion on an exposed slope in a former quarry in Hillsborough.

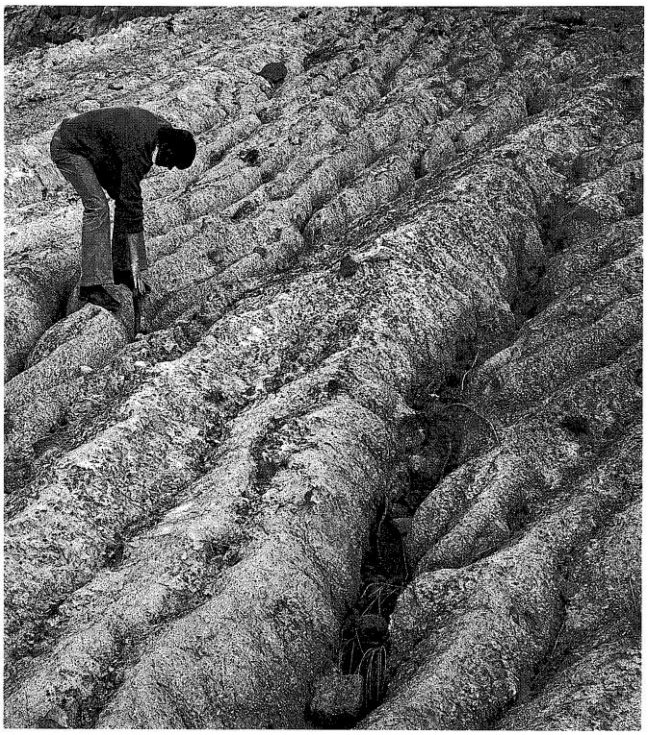

Figure 2.13: A slope of loess-colluvium in a former quarry in Hillsborough showing rill erosion. Photo from Brown & Weeber (1995).

2.5.5. Tunnel-Gully Erosion

Tunnel-gully erosion is caused by the progression of subsurface piping erosion. Bell & Trangmar (1987) explain that subsurface piping erosion occurs where infiltrating water entrains soil particles and carries them downslope. Infiltrating water is aided by soil desiccation and shrinkage cracks on de-vegetated slopes that develop from seasonal drying and wetting. Clay mineral dispersion and slaking occurs due to the presence of the infiltrating water, and the eroded sediment is entrained in the water, which moves downslope. Overtime the voids are enlarged. The water is confined to movement above or below the compact layer due to the relative difference in permeability of the surface/parent and compact layer.

The piping progresses into an underground tunnel as the enlargement of the voids continues. Further water coursing over the compact layer erodes this layer, and when the highly erodible parent material is exposed the rate of erosion increases. Lateral erosion of the side walls eventually causes the overburden to collapse into the eroded space, forming a gully. The gullies can be up to 4m deep, 10m wide, and 100m long (Bell & Trangmar 1987). Figure 2.14 shows extensive erosion problems in a loessial slope, and a large tunnel-gully running up the centre of the photo.

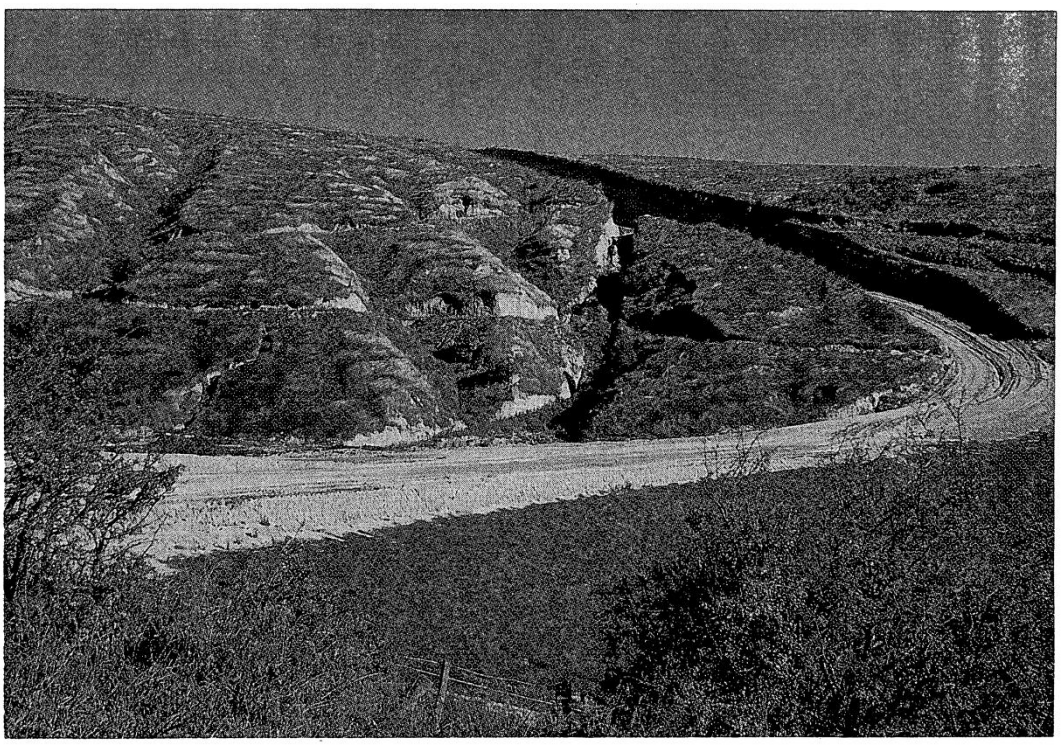

Figure 2.14: Extensive erosive issues on a slope of loessial soil. A tunnel-gully is visible as the darker area running up the slope near the centre of the photo. Photo from Brown & Weeber (1995)

2.5.6. Wind Erosion

Wind Erosion involves the detachment of soil particles from the ground surface by strong wind. Loessial soils are particularly prone to wind erosion during dry periods, and where the subsoils are exposed (Zhungu 1980). Wind erosion is restricted to areas where depletion of vegetation has caused the soil to be exposed.

2.5.7. Slide-Avalanche-Flow Mass Movements

This is a combination of landslide classification types to describe the complex failure mode observed in loessial soils. These failures result from saturation of the loess during prolonged rainfall events or, less frequently, during individual high intensity rainfall events. Top down saturation causes increased pore-water pressures and a corresponding decrease in effective normal stress acting along a potential basal shear surface. This normally occurs at a boundary between geological layers of different permeability. Bell & Trangmar (1987) state that the boundaries are typically between the surface and compact layers in primary loess, at a contact between different colluvium layers at 0.9-2.0m depth, at a contact between an erosive surface underlying a younger colluvium deposit at 1.2-2.5m depth, or at a contact between volcanic bedrock and a colluvium layer at 1.0-1.9m depth.

A block of loess originally moves downslope across a basal shear surface, and due to the saturation and low liquid limit of the loess there is a resultant remoulding of the block into a mobile fluid as it moves downslope. The avalanche part is related to the rapid velocity of movement. The critical slope angle for these failures is about 28°, which also happens to be a typical friction angle of loess (Yetton 1992). As noted, the cohesion of loess is diminished upon saturation. Mass movement failures are mostly relatively shallow, generally occurring within the top <1.5m of soil. Figure 2.15 shows a slide-avalanche-flow of loess that has seriously damaged a house on the Port Hills.

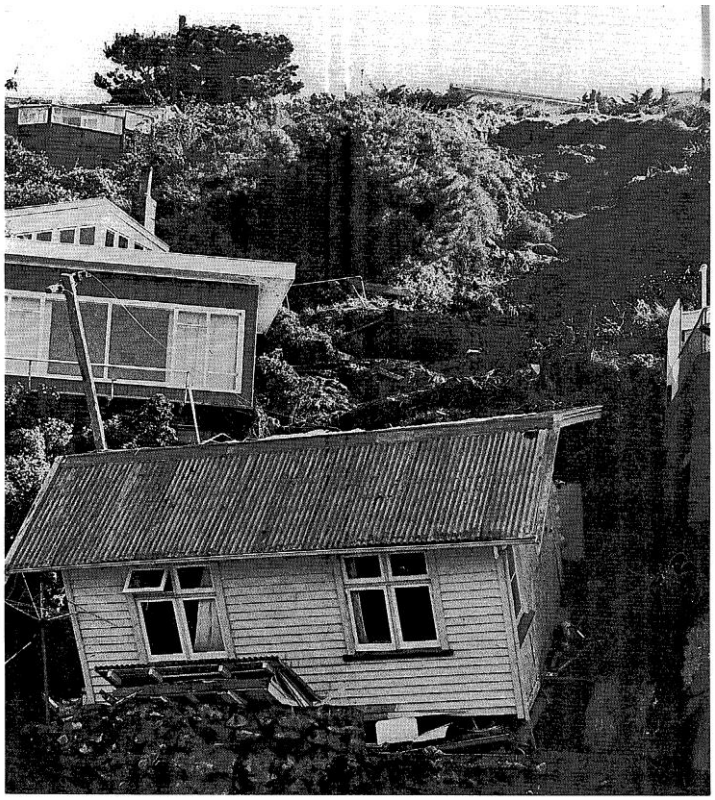

Figure 2.15: A slide-avalanche-flow in loess-colluvium at Taylors Mistake in 1975. Photo from Brown & Weeber (1995).

Most of the historical damage caused by slide-avalanche-flow failures in loessial soils of Banks Peninsula has resulted from the inundation of buildings from debris material sourced on steep slopes, upslope of the subdivision or building. A good example of this type of failure is the Anchorage Bay slide in Wainui, where 343mm of rain fell over 3 days, saturating the surficial loessial soils and causing multiple slide-avalanche-flow failures which destroyed one property, damaged another, and blocked Mt Bossu Road. Yetton (1992) explains that buildings are rarely affected by these types of movements occurring underneath them, due to the reluctance for endorsement of subdivisions on slopes greater than 25°.

2.5.8. Artesian Slides

In contrast to the slide-avalanche-flow mass movements, where the saturation and corresponding loss of cohesion, and increased pore-water pressure are associated with rainfall infiltration; in artesian slides the pore-water pressures and loss of cohesion are related to artesian pore-water pressure from below. The artesian pressure can be caused by either spring flow from the underlying volcanic bedrock, or from a blocked erosion tunnel. These failures are of the slide type classification, and are related to deep-seated movement. The basal shear surface can be either completely within the loessial deposit, or along the weathered bedrock contact. These slides can occur on gentle slope angles due to the build-up of artesian pressure and corresponding decrease in effective normal stress. Their movement can be episodic, and most movement is associated with periods of prolonged rainfall rather than individual intense rainfall events. They most frequently occur in gullies, and can also result in gully formation due to the large area of displaced soil.

La Clare landslide in Akaroa is an example of one of the rare cases on Banks Peninsula where a mass movement occurred beneath a subdivision. Yetton (1992) explains that it was an artesian slide, which was caused by increased pore-water pressure within the slope from the placement and compaction of fill over active springs (one with a seepage rate of 25-50 l/min), with no drainage provided. The lack of importance put into the discharge of groundwater led to multiple ‘blow-outs’ of saturated soils on the sides of the fill embankment and small surficial debris slides further down the slope. These surficial failures were soon followed by slow deep-seated movement of the slope, which was identified by foundation damage and cracks in the roads and pavement. The slow movement ultimately led to a 2m high landslide headscarp being formed, and the subdivision subsequently abandoned. Later engineering geological assessments of the slide by Hill (1985) cited in Yetton (1992) would show that the basal shear surface was actually an old surface that was reactivated by the increased pore-water pressure due to the placement of fill.

Whilst artesian slides offer the best correlation to the surface features of the fissure trace movement from the typical erosional processes in Banks Peninsula loessial soils, the La Clare landslide is an example of bad engineering, and artesian slides rarely occur naturally. The increased artesian pressure below the ground surface has to be brought on by a change in hydrogeology, otherwise the slope would have already moved.

2.6. Canterbury Earthquake Sequence

2.6.1. Christchurch Earthquake

The M_W6.2 Christchurch Earthquake on the 22nd of February 2011 caused wide-spread damage to Christchurch city and the surrounding area. It was just one of many aftershocks in a series of seismic events initiated on the 4th of September 2010 by the Mw7.1 rupture of the Greendale Fault (Hancox et al. 2011), but its effects were the most devastating. Peak ground accelerations (PGA) of 2.2g vertical and 1.7g horizontal were recorded near the epicentre during the Christchurch Earthquake (Kaiser et al. 2012). For an earthquake of Mw6.2 these PGA values were extraordinary, and they rank as the highest ground accelerations ever recorded during a New Zealand earthquake (Hancox et al. 2011).

The Canterbury Earthquake Sequence of 2010-2011 generated over 8700 earthquakes of larger than M_L2 (Sibson et al. 2011). The original Darfield Earthquake caused up to 5.3 ± 0.5m of dextral strike-slip displacement along a well-defined 29.5 ± 0.5km long surface rupture in low relief agricultural land west of Christchurch (Quigley et al. 2010). Bannister & Gledhill (2012) explain that the initial sequence progressed to the southwest from the hypocentre of the Darfield Earthquake along a blind thrust fault called the Charing Cross Fault. After intersection with the Greendale Fault, shallow (upper c. 5km) earthquakes were initiated east and west along the Greendale Fault, but predominantly to the east (Bannister & Gledhill 2012). Five and a half months after the Darfield Earthquake the Christchurch Earthquake occurred after redistribution of stress along the Greendale Fault progressed to the Port Hills Fault. Figure 2.16 is a diagram illustrating the Darfield aftershock sequence.

The Port Hills Fault was a previously unrecognized fault beneath the Port Hills to the southeast of Christchurch city centre. There was no surface expression of the fault prior to or since the earthquake due to its location within Mesozoic basement rock, buried beneath 1km of Tertiary volcanic rock (Bradley & Cubrinovski 2011). The Port Hills Fault has since been modelled as a planar feature with a strike of 059° and a dip of 69° to the southeast (Beavan et al. 2011).

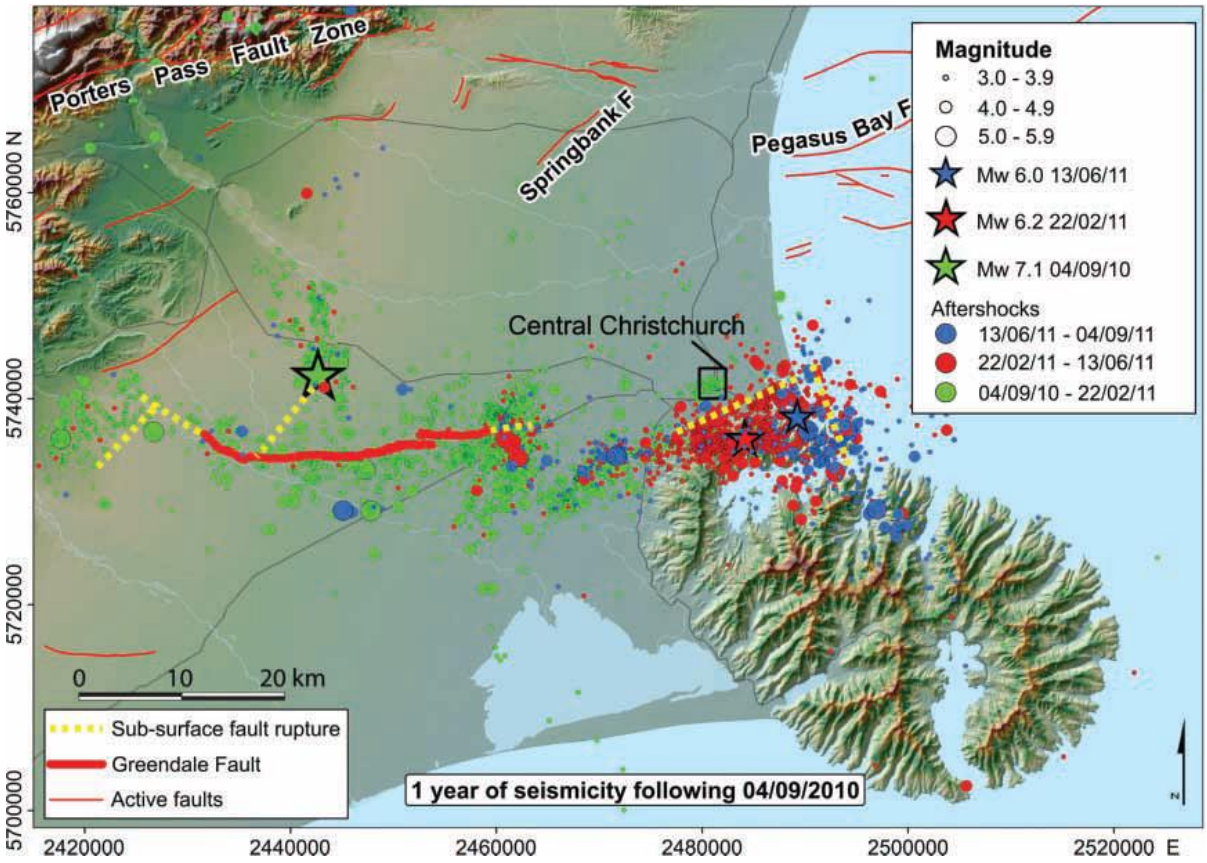

Figure 2.16: The Darfield earthquake (green star) and its aftershock sequence, generally trending from west to the east. The Christchurch earthquake is the red star and the June aftershock is the blue star. The Greendale fault, identified after the Darfield earthquake, is shown as the red lines. From Kaiser et al (2012).

The oblique-thrust fault rupture had an epicentre underneath the Heathcote Valley (Kaiser et al. 2012), and a shallow hypocentre of ~4km (Beavan et al. 2011). There were peak slip measurements of 2.5-3m at the hypocentre and slip measurements of 1m within 1km of the ground surface (Beavan et al. 2011). At the ground surface, this movement was accommodated by uplift of the Port Hills by up to 1m in certain areas relative to the Christchurch city flat lands (Beavan et al. 2011). Beavan et al. (2011) used geodetic ground-displacement data from nearly 200 GPS sites and synthetic aperture radar data to record the ground deformation due to the Christchurch Earthquake and subsequent aftershocks. This information was used to model the recorded ground deformation against predicted ground deformations using the estimated orientation and characteristics of the Port Hills Fault. Figure 2.17 shows the actual (blue) and modelled (red) uplift of the Port Hills in relation to the subsidence of the Christchurch city flatlands.

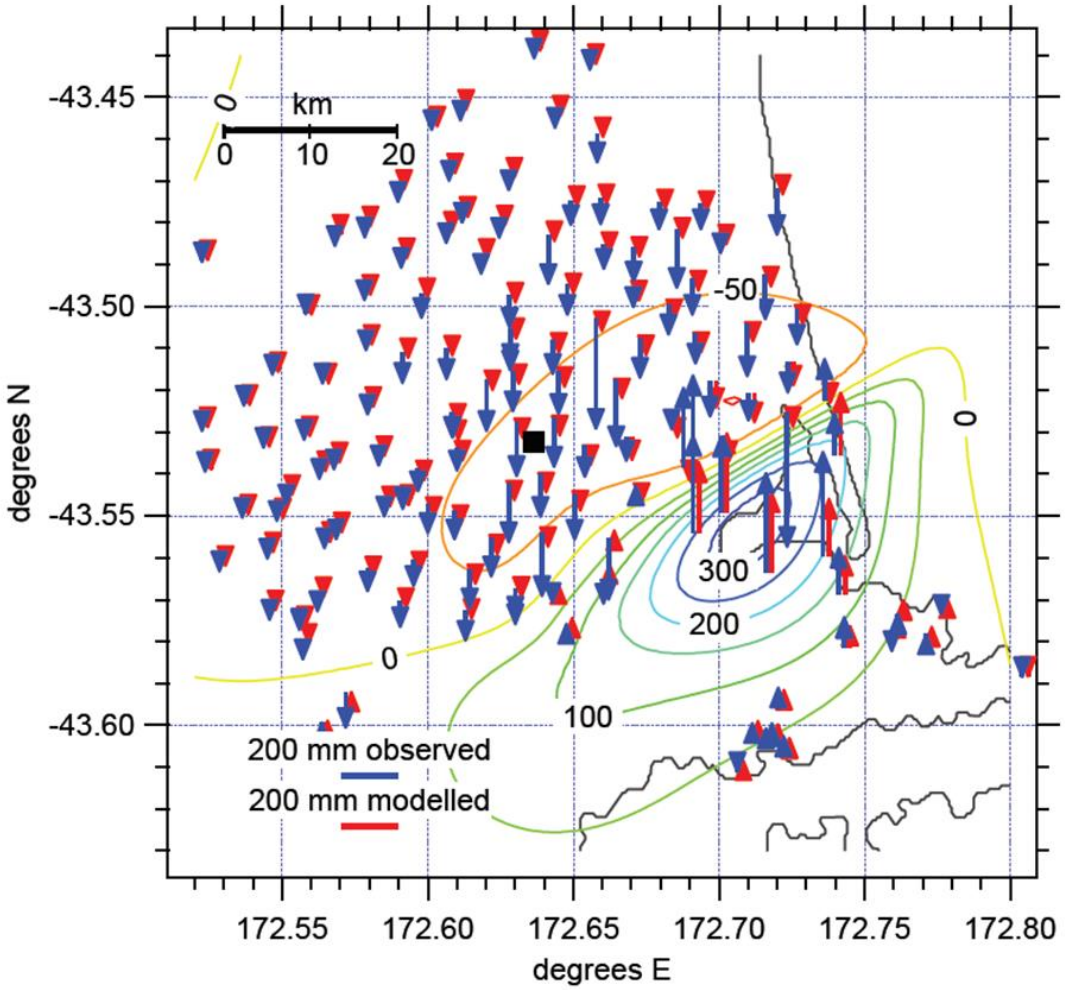

Figure 2.17: Observed and modelled uplift and subsidence around Christchurch following the Christchurch earthquake. Blue is for observed and red is for modelled. Central Christchurch is depicted as the black square in the centre of the model and the outline of the east coast is the black lines on the right side. The contours are predicted displacements with 50 mm contours. From Beavan et al. (2011).

Kaiser et al. (2011) summarized the reasons for the extraordinarily high PGA values experienced in Christchurch city during the Christchurch Earthquake, these included: the proximity of the city to the fault plane, the high apparent stress, the high rupture velocity and directivity of rupture, and site effects such as the 'trampoline effect'. These factors combined to make the Christchurch Earthquake one of the most damaging earthquakes in New Zealand's history:

- socially - 185 deceased (NZ Police 2011);
- financially - NZ $15-20 billion (English 2011);
- environmentally - wastewater overflows of raw effluent into Avon & Heathcote Rivers (Barr et al. 2012) & hydrological effects (Cox et al. 2012).

2.6.2. Earthquake Effects on the Port Hills

The Port Hills were affected by rockfall, cliff collapse, retaining wall and fill failures, and the fissure traces, which were originally identified by some as incipient landslides. Figure 2.18 is a diagram of the various forms of landslides that developed on the Port Hills as a consequence of the Christchurch Earthquake. The fissures traces are part of the tension cracks/rents, shallow slides, and deep-seated landsliding on the north side of the Port Hills.

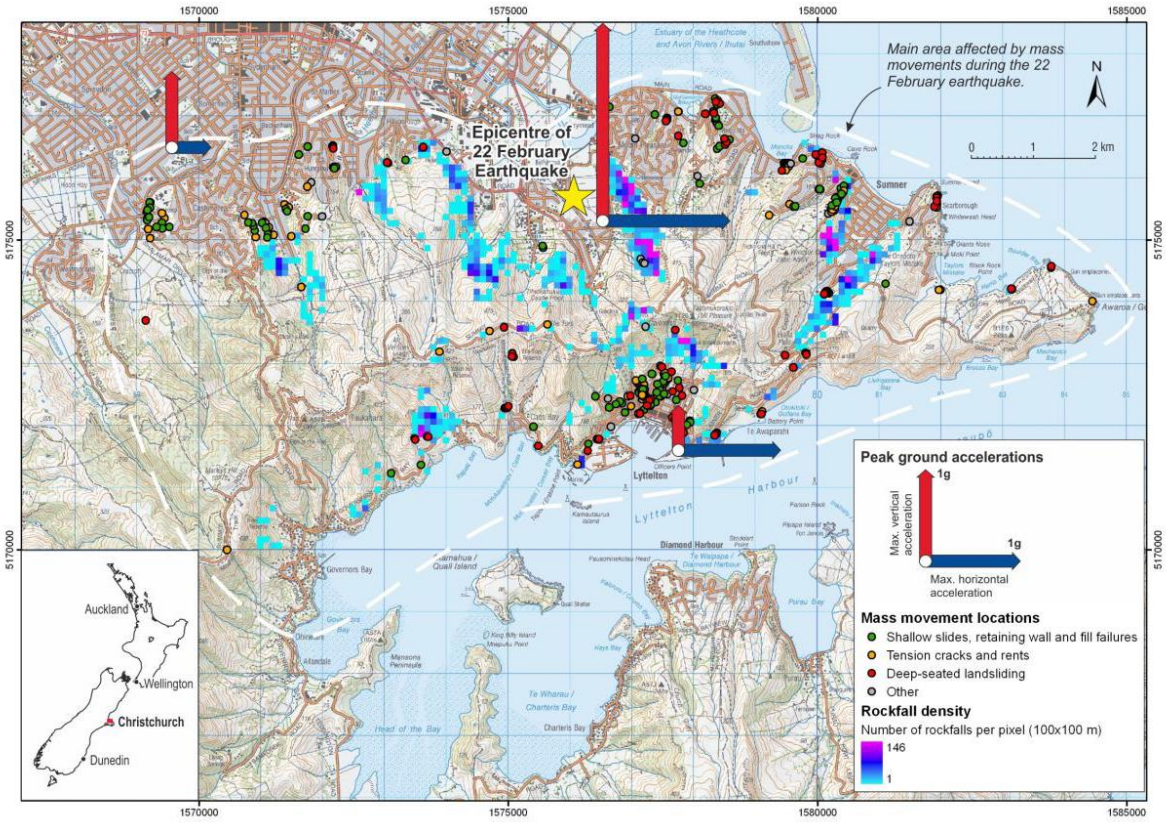

Figure 2.18: Landslide damage in the Port Hills caused by the Christchurch Earthquake. From Dellow et al. (2011).

Dellow et al. (2011) explain that the cases of cliff collapse were few, but they were of volumes in the order of thousands of cubic metres of soil and rock. These occurred on old Holocene sea cliffs on the north-eastern side of the Port Hills, on former quarry faces, and on steep bluffs. Many buildings were destroyed by cliff collapse occurring underneath them, or falling onto them. The urban areas affected by cliff collapse were Peacocks Gallop, Sumner, Whitewash Head, and Redcliffs (Dellow et al. 2011).

The cases of rockfall were many and spread across the entire Port Hills. There was potential for rockfall to occur anywhere where there was an exposed outcrop of rock. Many buildings were damaged or destroyed by rockfall, due to their location on the lower slopes of valleys underneath rock outcrops. Dellow et al. (2011) states that the worst affected areas by rockfall

were Sumner and Lyttelton. The worst affected valleys of the Port Hills were Heathcote Valley, Bowenvale Valley, Horotane Valley, Avoca Valley, and Morgans Valley. Sumner Road, Summit Road, Rapaki Road, and Governers Bay Road were the worst affected roads.

2.6.3. Earthquake Effects in the Hillsborough Valley

17 Ramahana Road is ~4.5km to the west of the Heathcote Valley Primary School GeoNet station, which recorded the highest peak ground accelerations of the Christchurch Earthquake. The nearest GeoNet station to 17 Ramahana Road was ~2.5km to the west at Cashmere High School where 0.85g vertical peak acceleration and 0.35 and 0.40g peak orthogonal horizontal components were recorded (Kaiser et al. 2012).

There was no cliff collapse in the Hillsborough Valley, but there were many cases of rockfall, particularly in the southernmost point of the valley where the slopes are steeper and more bedrock is exposed. Rapaki Road on the eastern side of the valley was the worst affected area by rockfall in the Hillsborough Valley. The insert in Figure 2.11 shows the sites where rockfall occurred in the Hillsborough Valley, as recorded by Vick (2015). The western side of the valley had no recorded observations of rockfall, but there is a walking track at the end of Albert Terrace that leads to a rock climbing area that is still closed due to damage by rockfall.

The Huntsbury reservoir, which is situated on the ridgeline above Albert Terrace, was severely damaged by the Christchurch Earthquake. Beca Infrastructure Ltd (2011) studied the damage and found that a series of fractures in the floor of the reservoir had caused the stored 36,000,000 L of water to drain into the Lyttelton Volcanic Group rock below. These fractures had an average strike of 290-315° and a dip of 65-85° ± 10° SW, which does not correspond with the Port Hills Fault. Slickenside surfaces and soft clay gouge in the inlet/outlet pipe led to the conclusion that this was an old feature that had become reactivated by the Christchurch Earthquake. Figure 2.19 shows the Huntsbury Reservoir and the orientation of the shear zone.

The main form of damage to the houses and infrastructure in the Hillsborough Valley came from the opening of fissure traces or the compression of soil, directly beneath or closely adjacent to the dwelling. Massey et al. (2013) explain that the fissure traces occurred within seconds to several minutes after the Christchurch Earthquake initiated. Other damage was caused by new springs interfering with foundations, and minor differential settlement of the valley floor material in localised areas.

Figure 2.19: The Huntsbury Reservoir and shear zone orientation. Albert Terrace and Rapaki Road are shown for locations of rockfall. The insert on the right is a section of a rockfall map sourced in Vick (2015) showing the locations of rockfall in the Hillsborough Valley.

2.7. Hydrogeological Setting and Earthquake Induced Flow Alterations

2.7.1. Groundwater Systems

Two aquifer systems meet near the base of the Port Hills: the northern Canterbury Plains aquifer system and the Banks Peninsula volcanics aquifer system (Brown & Weeber 1994).

The northern Canterbury Plains aquifer system is mostly recharged by seepage of the Waimakariri River through its bed, and by rainfall over the Canterbury Plains and foothills of the Southern Alps. This is a mostly confined aquifer system with the upper Springston Formation aquifer unconfined. The aquifers are composed of fluvial-derived greywacke gravel of late quaternary age (Brown & Weeber 1994). The groundwater generally flows from the west to the east towards the sea.

According to Brown & Weeber (1994) the Banks Peninsula bedrock aquifers are recharged through rainfall and stream flow over the outcrops of Banks Peninsula volcanics. It is an unconfined aquifer system, and water is held within fractures, fissures, and joints in the

volcanic rock. Bell et al (1988) explain that the volcanic bedrock is composed of a complex interlayering of gently dipping (<10°), low permeability pyroclastics and basaltic lava flows with a brecciated upper and lower margin, and a more massive central portion with significant vertical and sub-horizontal joints (30mm apertures and 300mm spacings). The thicknesses of each layer ranges up to 20m for the basaltic lava flows and <5m for the pyroclastic units (Bell et al. 1988). This creates an aquifer which has good vertical and horizontal permeability through the joints within the central portion of the lava flows, but poor vertical and good horizontal permeability through the brecciated margins. The pyroclastic layers of scoria, tuff, and red ash also restrict vertical movement, semi-confining the water to lateral flow movement along the upper brecciated margins of lava flows.

Bell et al. (1988) explains that in the summer and autumn seasons the spring flow is generally low with ≤ 2.5 L/min; however fluctuations are common and flow rates of 1000 L/min have been recorded following wet periods. Deep seated faults also bring thermal water to the ground surface of the peninsula at Ferrymead, Cass Bay, and Motukarara (Yetton 1992). The springs from colluvial material generally have a shallow infiltration component, but the majority of water is sourced from deep subsurface flow paths through volcanic rock (Bell et al. 1988).

2.7.2. Development of New Springs

No surface springs were evident near Ramahana Road prior to the Christchurch Earthquake, but it is one of the peculiar features of the fissure traces that new springs began seeping water to the ground surface at the base of the slopes within a few days of the Christchurch Earthquake, and in some places even following the Darfield Earthquake. Stephen-Brownie (2013) explains that the Hillsborough Valley was affected by at least 24 new springs following the Christchurch Earthquake, and that these were still flowing in August 2013. It can now be confirmed that the springs were still flowing in December 2015, although the flow rates have dropped in some springs. Figure 2.20 indicates the locations of new springs following the Christchurch Earthquake.

The springs are generally located to the downslope side of the compressional zones of the fissure traces, but they can also be found within the fissure traces themselves (e.g. at 211 Centaurus Road). Figure 2.20 shows the location of the fissure traces. Flat ground affected by spring flow at the base of Hillsborough Valley, such as in household gardens and in Centaurus Park, has essentially been turned back into their pre-suburban state of swamp land.

Green (2015) states that the water table in the valley floor is generally shallow at <1m b.g.l. and the water table slightly curves upwards at the ridges.

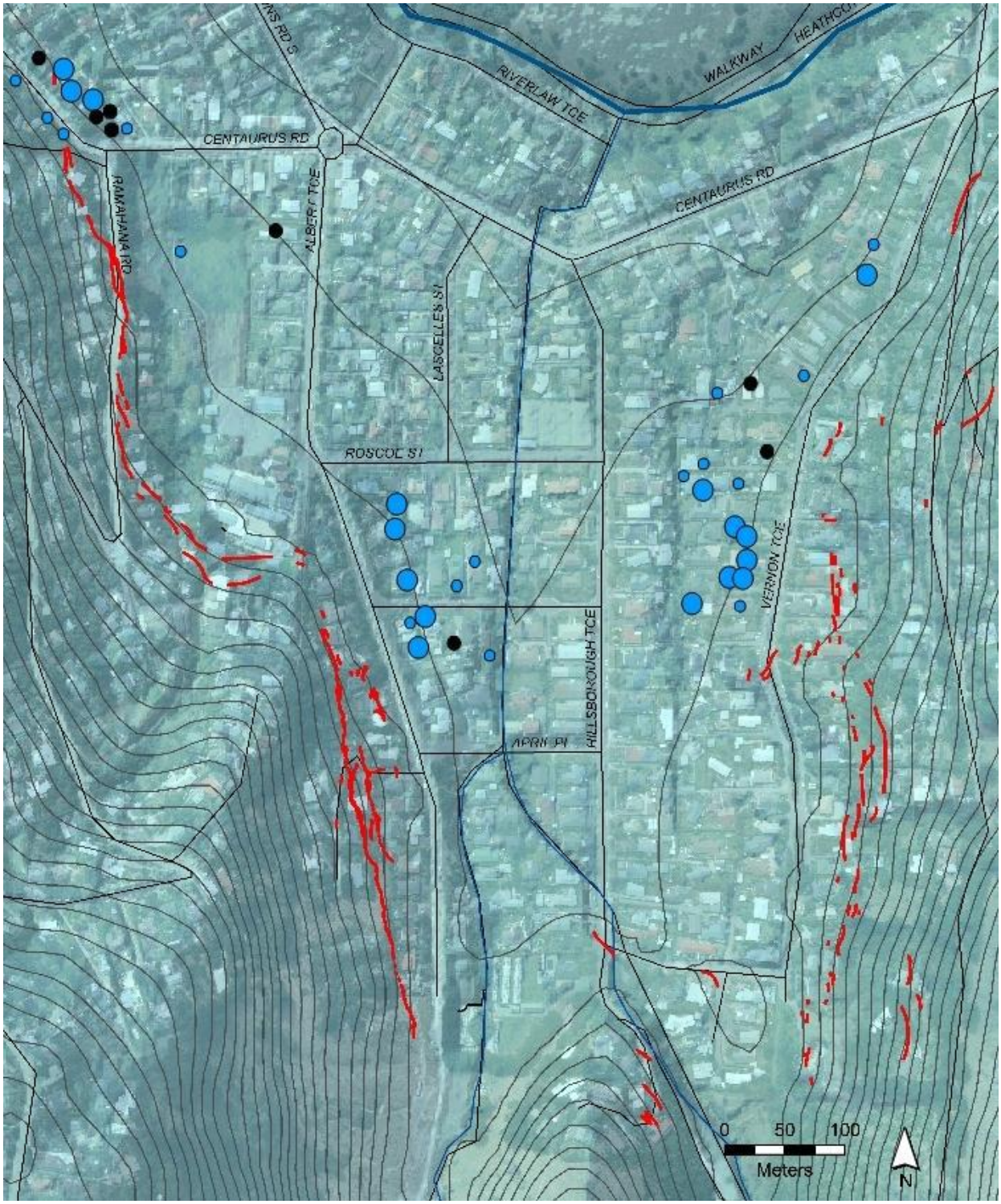

Figure 2.20: Location of new springs in the Hillsborough Valley. From Stephen-Brownie (2012).

The spring flow out of some springs is significant with 9000 litres/day discharged from 211 Centaurus Road (Stephen-Brownie 2012), whilst in others it is merely seen as a dampness on

the ground. In areas of high spring flow, the water has caused significant damage to buildings, and health issues due to mould (Cox et al. 2011).

Stephen-Brownie (2012) explains that seasonal changes and individual rainfall events do not greatly alter the springs flow. However, some alteration in flow rates has since been recorded following significant rainfall events by Green (2015) who observed between 4.2 and 14.4L/min variability in spring flow over a four day period following cyclone Lusi in 2015. Green (2015) suggests that rainfall increases the groundwater potentiometric surface of the Banks Peninsula aquifer system which leads to increasing spring flow. The ponding of water on the flat ground at the base of Hillsborough Valley becomes more significant in wetter periods, but this can be attributed to lower infiltration rates due to the higher groundwater table and saturation of near surface valley alluvium soils.

Changes to the hydrogeology at Centaurus Park was noted in subsurface testing by Pro-Drill, who drilled five boreholes at Centaurus Park for SCIRT in 2012. In the drilling logs it was noted that BH-01 had artesian pressures of 0.75m head above the ground surface at 15.00m depth. BH-01 was the closest borehole to the most prominent spring in Centaurus Park.

2.7.3. Spring Characteristics

Chemistry testing of the spring water from these areas shows that they have a closer chemical composition to water from the Banks Peninsula unconfined aquifer system than the Canterbury Plains confined aquifer system. Figure 2.21 is a comparison of the chemical compositions of four spring waters in the Hillsborough Valley, and two tap sourced waters from the Canterbury Plains confined aquifer system. The two-tap sourced waters are an obvious cluster to the left side of each diagram, whilst the spring waters trend towards the right of the diagram. The spring water from 211 Centaurus Road can almost be put on its own as an outlier from the other spring waters, making this site unique in chemical composition, rate of spring flow, location (flows from within a fissure trace rather than from the compressional zone), and date of occurrence (flowed following the Darfield Earthquake rather than the Christchurch Earthquake).

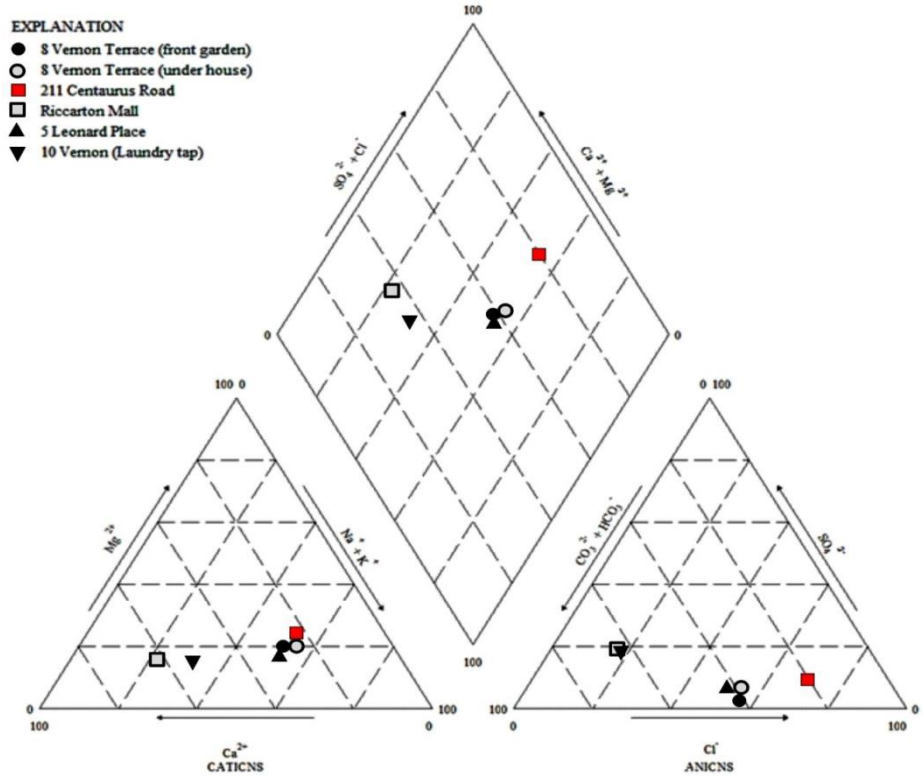

Figure 2.21: Chemical composition comparison of groundwater and Christchurch aquifer waters. The two tap-sourced waters are the Riccarton Mall water and 10 Vernon Terrace. From H. Rutter, Aqualinc Research Ltd, pers. comm. 2012, cited in Stephen-Brownie 2012).

The source and causation of the new springs is still in debate and considerable research is needed to reach a conclusion. One potential source of water is the Huntsbury reservoir which cracked during the Christchurch Earthquake and leaked its entire 36,000,000 L of water into the subsurface material below the site. It is currently unknown where all the water leaked to, but the water must have infiltrated into the bedrock below the site, and from there it either flowed to the west side of the ridge or to the east side, and if it flowed east then it likely at least added to the hydraulic head of the groundwater table.

Another potential source is from bedrock fracturing due to violent shaking during the Christchurch Earthquake which would have allowed groundwater that was semi-confined at positive artesian pressure below a pyroclastic layer to come to the surface, or simply through increased permeability. Settlement of the valley floor material through consolidation of peat layers would also have resulted in surplus groundwater (Green 2015). A final source is from leakage between the volcanic rock aquifers and Quaternary sediment aquifers, resulting in a rise in shallow groundwater levels (Cox et al. 2012). A combination of all four sources is also a possibility and could explain the significant quantity of water that has been brought to the ground surface through spring flow.

The occurrence of new springs and changes to groundwater levels following an earthquake are not unusual. Cox et al. (2012) measured the responses in boreholes from around New Zealand following the original Darfield Earthquake, and found that there were groundwater level increases of over 20m in areas near to the Greendale Fault and over 5m in areas within 20km of the fault, although most of these were temporary increases which returned to their pre-earthquake state within 24 hours. What makes the springs in the Hillsborough Valley unique is their contemporaneous occurrence with the fissure traces and the length of time they have been active for. They have been flowing for nearly 5 years which suggests that they reflect permanent changes in hydrogeology.

2.8. Synthesis

This chapter has introduced concepts about the geology of the site, typical erosional processes at the site, the characteristics of the Christchurch Earthquake, and hydrogeological alterations associated with the fissure traces. The purposes of introducing previous studies on these topics were to gain a better understanding of the geological model of the site, to compare the movement of the Ramahana Road fissure trace to the typical erosive processes on Banks Peninsula, to understand the characteristics and processes of the Christchurch Earthquake and Canterbury Earthquake Sequence, and to introduce the hydrogeological alterations induced by the earthquakes.

The bedrock and cover soils have unique geotechnical properties and behavioural characteristics. Loessial soils of Banks Peninsula are particularly difficult to correlate with overseas deposits of similar material due to their relative compactness and low permeability. The consistent behavioural characteristics in loessial soils from across the world are that increasing moisture contents diminish cohesion values, but low moisture content loessial soil has a relatively high bearing capacity and is relatively stable in near vertical cut faces.

The typical erosional processes on Banks Peninsula include: rockfall/debris fall, soil creep, sheet and rill erosion, tunnel-gully erosion, wind erosion, slide-avalanche-flow mass movement, and artesian slides. These typical erosional processes do not correlate with the features of the fissure traces. Artesian slides have the best correlation to the fissure traces, but these do not normally occur naturally. The fissure traces appear to be related to an unprecedented form of movement on Banks Peninsula.

The Christchurch Earthquake also displayed highly unique characteristics. The peak ground accelerations were the highest ever recorded for a New Zealand earthquake. Widespread landslide damage was caused by the earthquake on Banks Peninsula, including cliff collapse, rockfall, tilting and failure of retaining walls, and the occurrence of fissure traces. Uplift of the Port Hills in relation to subsidence of the Christchurch city flat lands was observed and this could have caused tensional strain at the boundary of different movement directions.

High intensity earthquake induced ground shaking is hypothesized by some authors to have caused bedrock fracturing in the Lyttelton Volcanic Group beneath the site. This combined with compression of joints, fractures, and fissures in this unit would have caused an increase in the hydraulic head of the groundwater table within the Hillsborough Valley, resulting in the springs that formed contemporaneously with the fissure traces. The spring water and groundwater has a chemical composition that is more similar to the Banks Peninsula aquifer system than the Canterbury Plains aquifer system.

3. Qualitative Assessment: Subsurface Investigations

3.1. Introduction

The objective of this chapter is to gain an understanding of the site specific models at 17 Ramahana Road and Centaurus Park and to identify any features that may help to determine the mode of ground movement and the mechanisms that led to formation of the fissure traces. To achieve these objectives shallow and deep subsurface investigation methods were used. Shallow investigation methods (≤4m) included engineering geological mapping, test pitting, shear vane tests, hand augers, and Scala penetrometer tests. Deep investigation methods (>4m) included geophysical survey methods of ground penetrating radar, electrical resistivity geophysical survey, and seismic reflection survey, all conducted by Southern Geophysical Ltd. Other deep investigations included groundwater investigations, a cone penetration test with pore-pressure dissipation tests drilled by Coffey Geotechnics Ltd, interpretation of Tonkin & Taylor Ltd borehole logs from 17 Ramahana Road, and logging of borehole core from Centaurus Park that was donated to the University of Canterbury by SCIRT.

This chapter is divided into six subheadings. Following the introduction, the subheadings include: mapped geology of the Hillsborough Valley, which presents the general geology of the area where the subsurface investigation methods were conducted; shallow investigations at 17 Ramahana Road; deep investigations at 17 Ramahana Road; investigations at Centaurus Park; and Ramahana Road Fissure Trace, which synthesizes the investigation results and discusses the key conclusions of this chapter.

3.2. Mapped Geology of the Hillsborough Valley

Figure 3.1 shows part of the 1:250,000 Christchurch geological map produced by Forsyth et al. (2008), specifically covering the greater Christchurch area.

Figure 3.2 shows part of the 1:25,000 Christchurch geological map produced by Brown & Weeber (1992), specifically covering the geology of the north-facing valleys of the Port Hills with the fissure traces, as mapped by Stephen-Brownie (2012), overlaid.

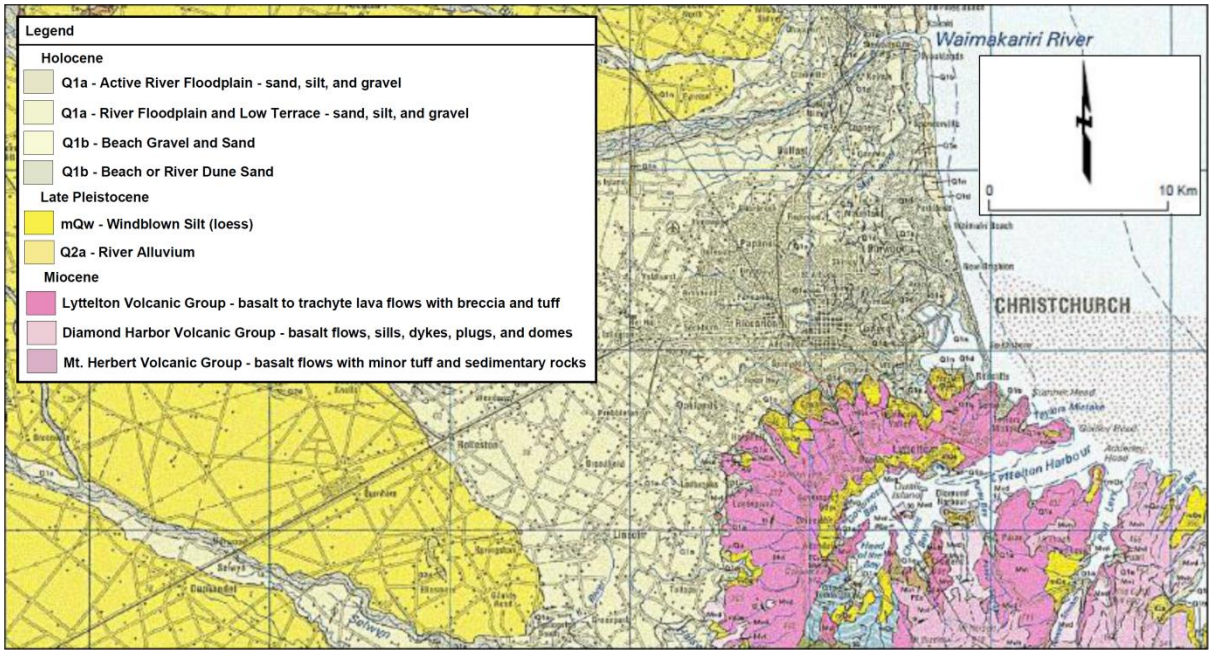

Figure 3.1: Part of the 1:250,000 Christchurch geological map produced by Forsyth et al. (2008).

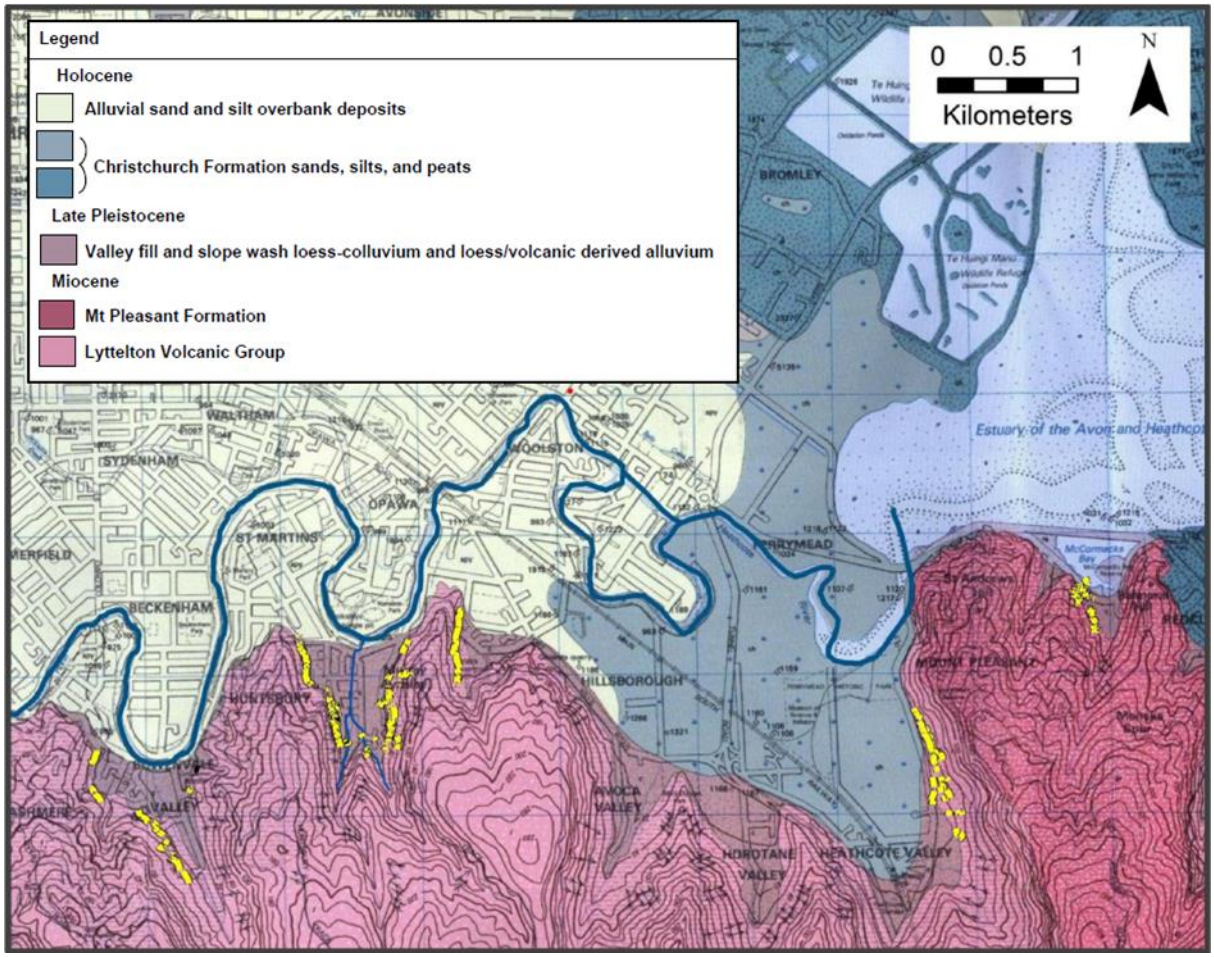

Figure 3.2: Part of the 1:25,000 geological map of the Christchurch urban area produced by Brown & Weeber (1992), with fissure traces, as mapped by Stephen-Brownie (2012), overlaid.

Figure 3.3 shows geological units recognised in the Hillsborough Valley. The mapping was conducted on 14th of October 2015. It involved walking around the boundaries of the valley and noting where the bedrock could be seen. The bedrock was generally firstly identified in road cuttings at <1m depth below a loess-colluvium cover, and then upslope of this the bedrock could be viewed breaching the ground surface in certain locations. The bedrock was only exposed as outcrop in very limited spatial areas, where it was generally observed as scattered outcrops with a shallow loess-colluvium and topsoil covering.

The valley fill was defined by the steepness of the slopes. The gentle valley floor (<5°) was deemed to be valley fill, whilst the more inclined toe of the slope was deemed to be loess-colluvium. The valley fill is a mixture of eroded loessial material and eroded volcanic rock with layers of gravel, sand, silt, and peat up to 3m thick. The alluvial sand and silt overbank deposit location was determined by its boundary on the map of the Christchurch urban area by Brown & Weeber (1992).

The Hillsborough Valley cross-section is shown in Figure 3.4, without vertical exaggeration. The valley alluvium in this instance has been simply joined with the loess-colluvium, because there is little difference between these geological units in terms of particle-size analysis and the boundaries between them are ambiguous. The main purpose of this cross-section is to show the thickness of the loess-colluvium/valley-alluvium in relation to its position in the valley, and also the bedrock profile beneath the ground surface.

Whether the bedrock is as deep as shown on the cross-section is debatable because there are no boreholes that have been drilled to the bedrock in the middle of the valley. The reason it is assumed that the bedrock is at this depth is because the Lyttelton Volcanic Group was met at 17.8m below ground level in BH-VRN-04, whilst in the nearby downslope BH-VRN-07 it was met at 53.0m. If the bedrock continued at this steepness it would have reached a greater depth than the 90.0m in this cross-section, but it is assumed that the steep drop between the two boreholes reflects a localized area of greater erosion prior to valley filling.

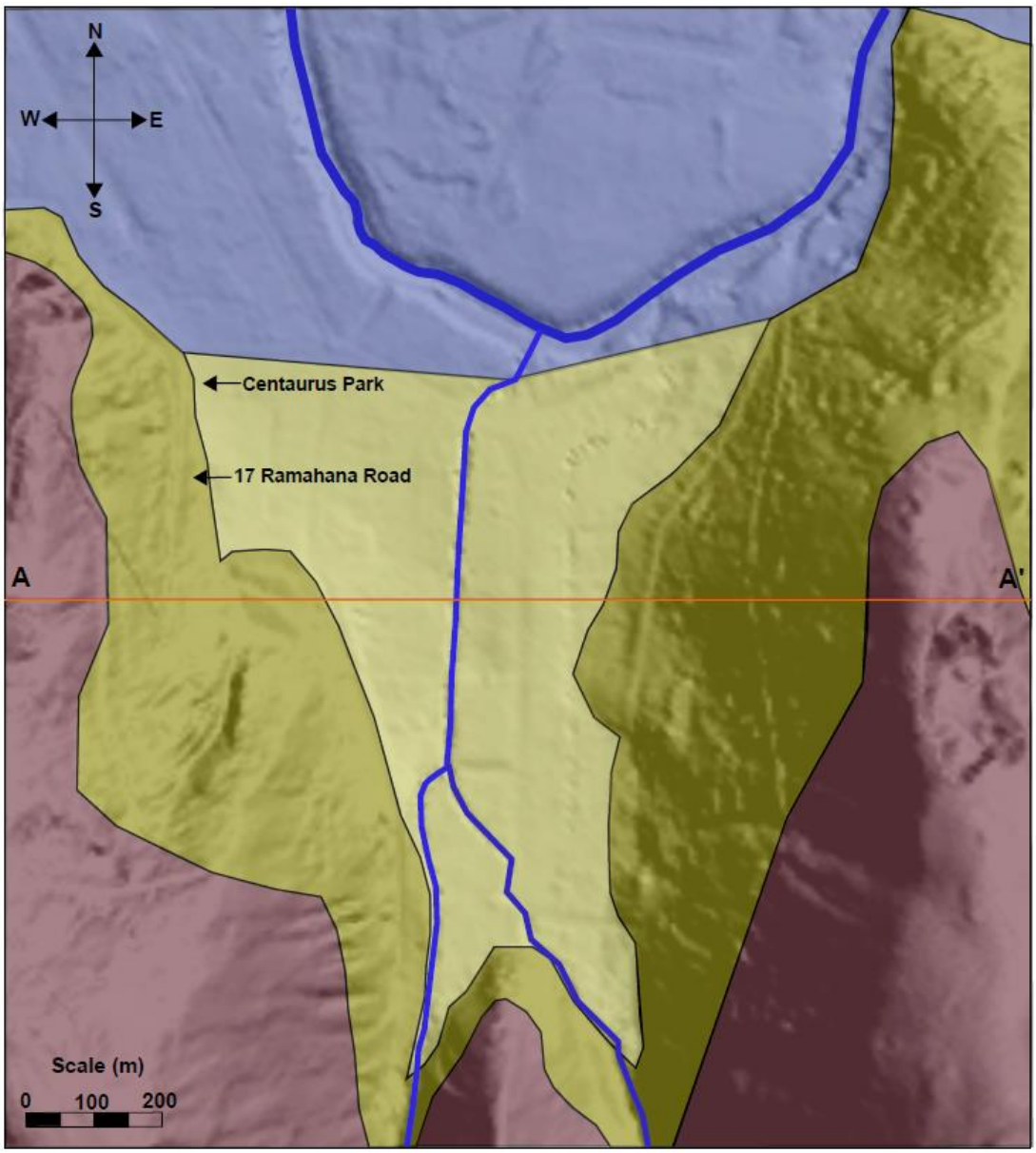

Legend	
	Alluvial sand and silt overbank deposits: As mapped by Brown & Weeber (1992)
	Valley fill: mixture of eroded loessial and volcanic bedrock material with interbedded peat layers <3m thick
	Loess-colluvium: mixture of eroded loess and up to 10% volcanic bedrock material
	Lyttelton Volcanic Group outcrop/shallow (<1.5m) loessial soil cover over Lyttelton Volcanic Group
	Drainage channels.

Figure 3.3: Engineering geological units within the Hillsborough valley. Refer to Figure 3.4 for cross-section A-A'.

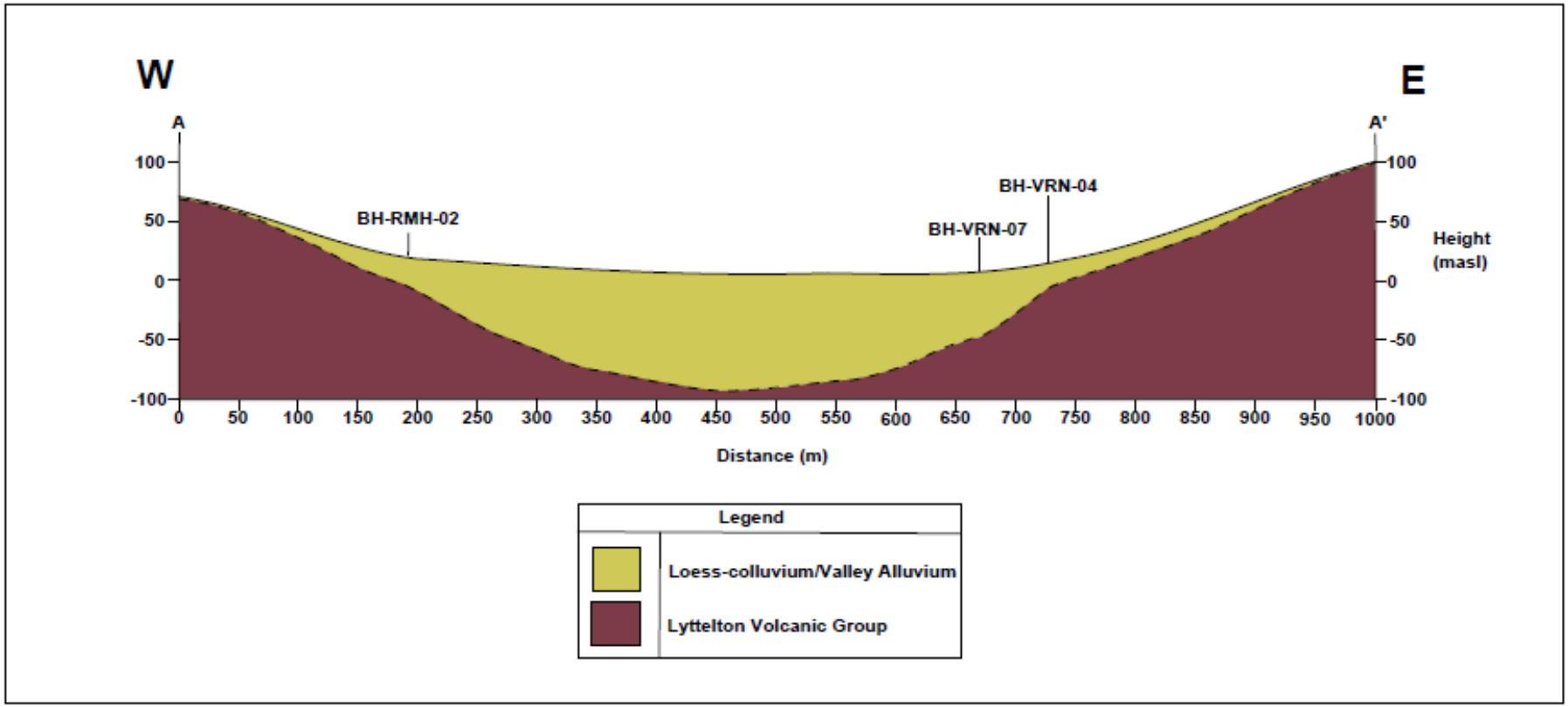

Figure 3.4: Interpreted Hillsborough Valley cross-section. Note: This cross-section is an assumption of the subsurface geological conditions at the site based on the borehole logs identified in the section, and on other borehole logs viewed from Project Orbit that did not reach bedrock. The actual conditions may vary. Refer to Figure 3.3 for cross-section line.

3.3. Shallow Investigation Methods at 17 Ramahana Road

3.3.1. Engineering Geological Mapping

The engineering geological map of 17 Ramahana Road is presented in Figure 3.5. The old house that had been destroyed during the earthquake had been demolished, and the conditions of the fissure traces had been highly disturbed by rain water coursing and infill material. This map represents the site conditions at the time of mapping. The surface conditions at the site changed considerably over the course of this thesis as construction of the new building began.

The site has an undulating slope, it generally has a relatively gentle gradient of <20°, but it varies from 2° at the valley floor to 36° at localized steeper gradients near the top of the slope. There is mixture of old structures that were present before the earthquake and ones that have been built since. The new structures include temporary accommodation at the base of the slope and the wooden retaining wall at the top of the site. The old structures include a concrete pad that was damaged by a fissure opening beneath it; a concrete path with a cracked step at the base of the slope, and a displaced side path at the valley floor; two sheds at either side of the temporary accommodation; and a tilted fence, pergola, and garden retaining wall. The old structures on the site help to identify the boundaries of the extensional and compressional zone. The damage to the neighbouring houses corresponds with these zones of deformation.

The fissure traces are present at the top of the site. Only two traces were clearly visible and easily identified as fissure traces, whilst three potential traces were observed as shallow undulations in the ground. The demolition of the old house, building of the new retaining wall, and clearance of vegetation is likely to have in-filled these features, and in-filling was evident in the two more obvious fissure traces. A small crack (5-10mm wide) that ran approximately NWW-SEE was also identified downslope from the compressional zone.

The location of the boreholes logged by Tonkin & Taylor Ltd, the CPT conducted by Coffey Geotechnics Ltd, and the test pit are shown on the map. The test pit location is also shown. The cross-section line that runs from the top of the site to the bottom of the site was also the line used for the geophysical investigations.

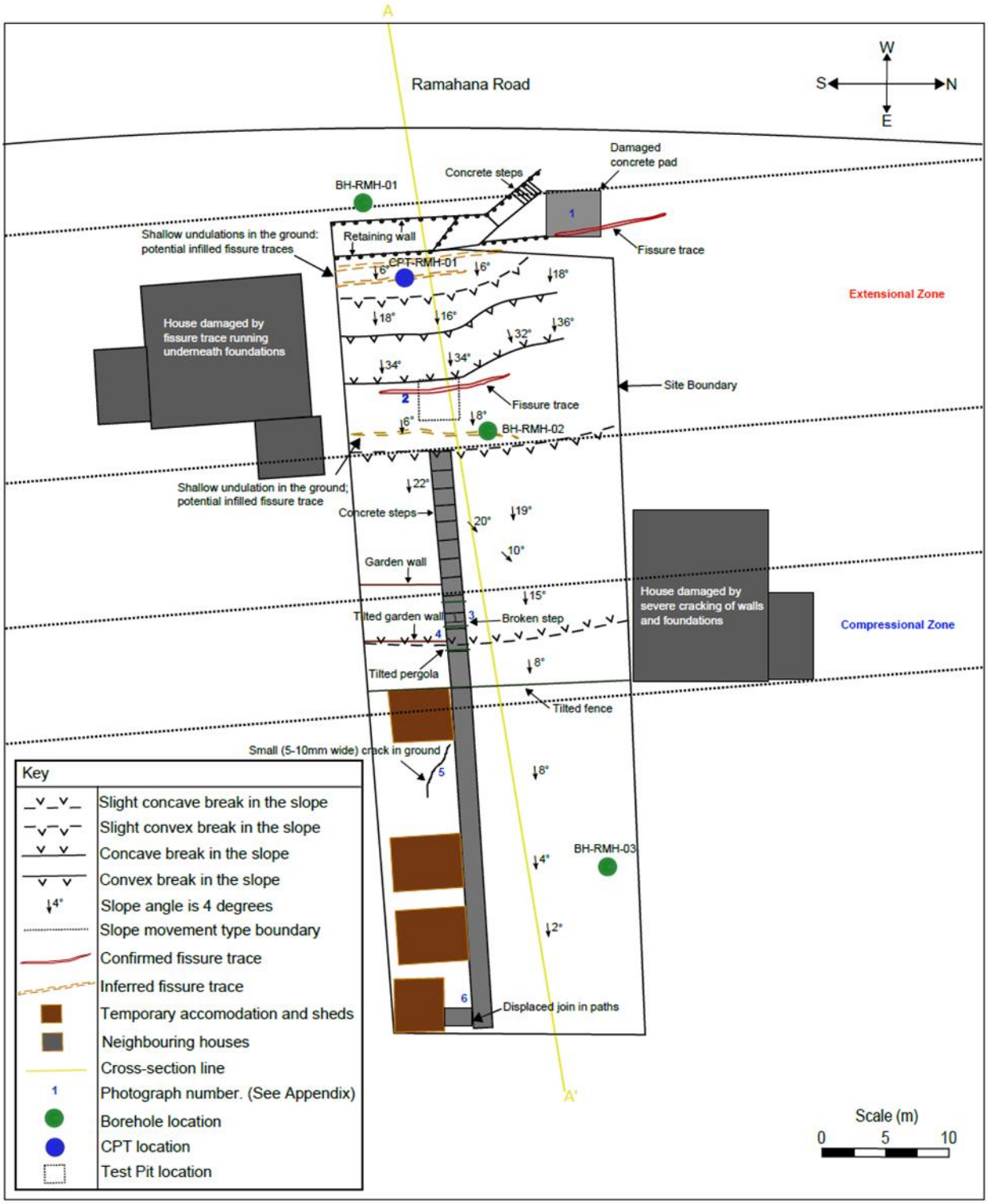

Figure 3.5: 17 Engineering geological map of 17 Ramahana Road. Refer to Figure 5.4 for cross-section. Appendix 2.1 presents mapping photos, and Appendix 2.8 shows the borehole logs from Tonkin & Taylor Ltd.

3.3.2. Test Pitting

A test pit was dug perpendicular to the un-remediated and partially in-filled trace at 17 Ramahana Road on the 20th of April 2015. The test pit was dug to a depth of 3m, a width of 2.1m, and a length of 3.3m. Due to the depth of 3m it meant that the sides of the test pit would need to be benched to allow safe access. The benches were dug to a depth of 1.5m and a width of 0.7m, the middle section (the deepest section) was dug to a depth of 3.0m and a width of 0.7m. Photos of the test pit are presented in Figures 3.6-3.9 and the test pit location is shown in Figure 3.5.

The test pit was logged in accordance with the NZGS (2005) guidelines. It was an overcast day with some passing showers that potentially had an effect on the *in-situ* moisture contents and consistencies of the soil, particularly on top of the cut benches. Samples were taken every 0.5m vertically down the test pit; one was taken from the puggy infill material on each wall of the test pit; one from the drier infill material on the north wall; and one from the mixed-colluvium layer on the north wall. These were sampled by pushing a metal pipe into the test pit wall and then removing it carefully so as to keep the material in as undisturbed a condition as possible. These samples were later tested for particle-size distribution, natural moisture content, and Atterberg Limits. The results are discussed in Chapter 4.

The fissure trace was clearly visible in the top 1.5m bench but it became less defined with depth. Figure 3.6 is a photo of the south wall of the test pit with the fissure trace features overlaid. Appendix 2.2 presents a photo of the fissure trace at the ground surface, and logs of the test pit. The fissure trace had already been largely in-filled following disturbance of the surrounding soil since the Christchurch Earthquake; demolition of the old house; and further in-filling following excavation of the test pit.

Because the infill was the same material as the surrounding soil, the boundaries of the fissure trace cavity were relatively difficult to define. An interesting feature of the fissure trace was that only one side of the opening was visible at any depth in the test pit, and the side that was visible could alternate across the cut bench. The cavity associated with the fissure trace was, however, visible from the ground surface, and following this line downwards parallel to the visible trace allowed interpretation of where the boundary was.

Figure 3.6: Photo of the south wall of the test pit perpendicular to the fissure trace at 17 Ramahana Road. A is without interpretation, B is with interpretation of fissure trace features.

The fissure trace had an aperture of ~450mm at the ground surface, but it gradually reduced with depth. Following the visible fissure trace line to where it met the inferred boundary of infill material gave an estimation of the fissure cavity depth, which was determined to be at 2.0m. Below 2.0m the fissure trace was visible as a segmented semi-curved feature that extended to the base of the test pit. The segmented fissure trace below 2.0m had an aperture of 1-2mm, and continued to an unknown depth below the base of the test pit at 3.0m.

The visible fissure trace was at an angle of 78° from horizontal near the ground surface, but it gradually flattened with depth, which gives it a slightly curved appearance. At 1.8m depth the angle is at 72°, and although accurate readings were not able to be recorded where the fissure trace became segmented, it was estimated at 40-50°. The angle appears steeper in the photo of Figure 3.6 due the camera being turned slightly towards the west. The undulating path of the infill material is probably misleading, as both sides of the fissure trace were likely to be relatively linear when the fissure traces originally opened, but there are no photos available of the original state of this fissure trace to confirm this.

The boundary of the infill material was defined by interpretation of the infill material compared to the natural material. The infill material was softer and more easily eroded than the surrounding natural soil. There were also pieces of debris from the demolition of the house, a coffee cup lid, and a milk capsule (dated 13th November 2011) within the infill material which aided its identification. Pieces of fibre cement were located at a depth of 1.9m on the south wall, whilst the coffee cup lid and milk capsule were found within the infill material at 1.5m depth on the south wall.

A softer and wetter section of the infill material was found at a depth of 0.5m on both sides of the test pit. This material was slightly gleyed on the south wall. These areas are thought to correlate to the depth of infill prior to excavation of the test pit, because it was noticed in an earlier site walkover that the fissure trace was filled with stagnant water from rainfall and/or tap water from a tap that was leaking upslope of the fissure trace. The depth of 0.5m is about the depth to the top of the infill material within the fissure trace prior to excavation.

Figure 3.7 is a photo of the north wall of the test pit with the features of the fissure trace overlaid. On the north side the fissure trace had an aperture of 470mm at the ground surface and gradually reduced with depth to 2.1m, where it became a segmented fissure trace with 1-2mm aperture. An inferred boundary of disturbed material has been drawn to the right of the inferred boundary of infill material because there was some uncertainty about the exact depth

Figure 3.7: Photo of the north wall of the test pit perpendicular to the fissure trace at 17 Ramahana Road. A is without interpretation, B is with interpretation of fissure trace features.

of closure of the fissure trace. 2.1m correlates more accurately with the other side of the test pit, but the soil is relatively soft to the right of this boundary down to a depth of 2.5m, and there appears to be disturbance within the mixed-colluvium layer at 2.4m.There is a layer of mixed-colluvium that extends across both sides of the test pit. On the south wall of the test pit there are two layers separated vertically by ~100mm of loess-colluvium, both of which extend for less than 1m before petering out. On the north wall there is only one layer, which extends the entire length of the test pit, and slopes slightly downslope. It intersects the path of the fissure trace at 2.4m depth near the middle of the wall, but it has caused no visible offset of this layer.

Figure 3.8 is a photo of the mixed-colluvium layer with interpretations of the fissure trace intersecting it. Below where the fissure trace meets the mixed-colluvium layer there is a softer area where there is more gravel than in the surrounding material. This feature could have been deposited in this way, or it could be excavator induced, or perhaps it the result of the earthquake and subsequent fissuring. It looks as if the colluvium layer has bulged downwards, or perhaps the fissure trace opened the colluvium layer before some of its gravel subsequently fell into the opening. Because this potentially disturbed material is located where the fissure trace crosses the mixed-colluvium layer, the preferred interpretation is that it was caused at the time of fissuring.

Figure 3.9 is a photo looking down into the test pit from the west wall. The fissure traces have been overlaid, and connected across the north and south wall and at the base of the pit. This photo is useful to see that how fissure traces on each wall line up, and it is a good angle to visualize the orientation of the fissure traces in 3D. The photo makes it clear that the test pit does not line up perfectly perpendicular to the fissure trace. The fissure trace was evident at the base of the test pit, but it was not as visible on the benches of the test pit, probably due to rainwater and human disturbance.

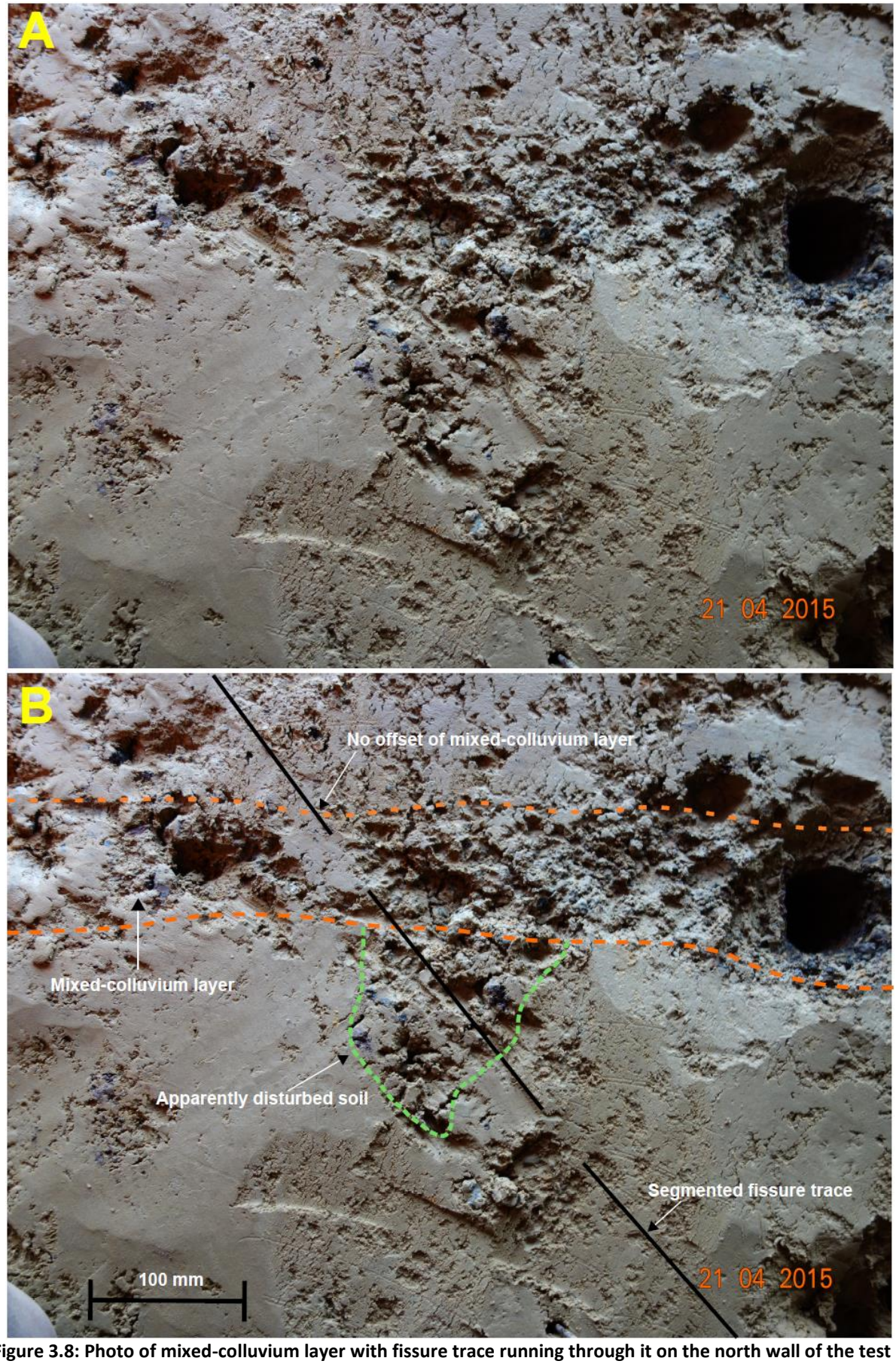

Figure 3.8: Photo of mixed-colluvium layer with fissure trace running through it on the north wall of the test pit. A is without interpretation, and B is with interpretation of fissure trace features.

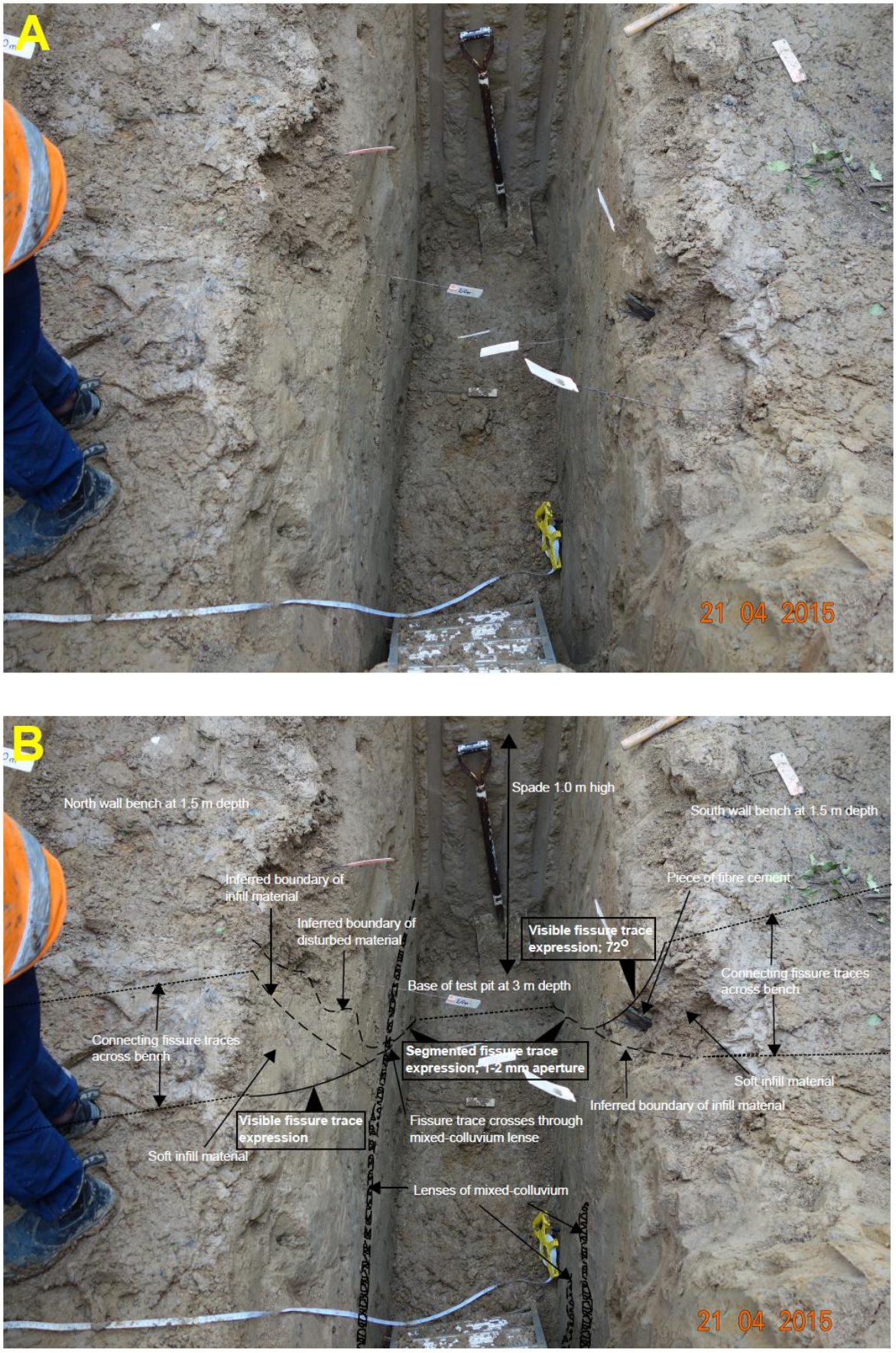

Figure 3.9: Photo of test pit through fissure trace at 17 Ramahana Road looking down into test pit from the western side. A is without interpretation, and B is with interpretation of fissure trace features.

3.3.3. Shear Vane Results

Hand held shear vane tests were taken at 0.5m intervals in the test pit on the upslope side of the fissure trace, on the downslope side of the fissure trace, and within the fissure trace. A standard Pilcon brand shear vane was used with a 19mm blade. The blade was inserted 70mm into the cut face and rotated at one revolution per minute as per NZGS (2001) guidelines. The recorded undisturbed and remoulded undrained shear strength results were recorded from the dial reading on the vane and then adjusted to BS1377 calculation. Table 3.1 & 3.2 present the vane shear strength/remoulded vane shear strength values obtained from the test pit.

As would be expected the lowest values were found within the fissure trace (i.e. in the infill material), whilst the upslope and downslope values are similar. The highest shear strength value was found on the north wall at 0.5m depth, upslope of the fissure trace with a value of 194 kPa. The lowest values outside of the fissure trace were found at a depth of 3.0m on both walls, on both sides of the fissure trace. The values recorded within the fissure trace at 3.0m depth approach the values of the undisturbed soil, probably due to the 1-2mm aperture at this depth. On the south wall the shear strength is higher within the fissure trace than on the uphill side.

The shear strength of the loess-colluvium generally decreases with depth in the 3.0m profile; however there are some notable exceptions, including: at 1.5m depth on each wall, on each side of the fissure trace, at 2.5m on the north wall downhill of the trace, and at 2.0m and 3.0m within the trace.

South Wall			
Depth	Vane Shear Strength/Remoulded Vane Shear Strength (kPa)		
	Uphill of Trace	Downhill of Trace	Within Trace
0.5	126/63	137/31	48/15
1.0	73/33	82/34	24/15
1.5	117/49	164/82	19/6.
2.0	129/63	60/31	27/13
2.5	103/48	58/33	43/18
3.0	45/18	58/22	54/25

Table 3.1: Vane shear strength/remoulded vane shear strength results at 0.5m spacing from the south wall of test pit.

North Wall			
Depth	Vane Shear Strength/Remoulded Vane Shear Strength (kPa)		
	Uphill of Trace	Downhill of Trace	Within Trace
0.5	194/78	82/36	72/24
1.0	73/28	99/46	37/12
1.5	151/67	184/72	33/9
2.0	143/33	78/30	49/9
2.5	105/46	99/54	36/13
3.0	63/27	60/21	52/27

Table 3.2: Vane shear strength/remoulded vane shear strength results at 0.5m spacing from the north wall of test pit.

3.3.4. Hand Augers/Scala Penetrometer Testing

Six hand augers were conducted in conjunction with Scala penetrometer tests, otherwise known as dynamic cone penetrometer tests or DCPs, to a depth of 4-4.2m at 17 Ramahana Road on 10th February, 2015. The DCPs were conducted by Aurecon NZ Ltd prior to this investigation in 2012. The hand augers and DCPs were done as part of a geotechnical appraisal report for the construction of a new residential building on the site. They were spaced around the surface expression of the fissure trace at the boundaries of the future building envelope to assess the near-surface material properties, and the bearing capacity of the soil. The location plan and logs of the hand augers and DCPs are shown in Figure 3.10. The hand auger and DCP logs are presented in Appendix 2.3

Another five hand augers in conjunction with DCP tests were conducted to a depth of 4-4.2m and 2.9m respectively at 17 Ramahana Road on the 20th of May, 2015. The hand augers and DCPs were conducted to explore the areas of relatively high resistivity and relatively low resistivity identified in the electrical resistivity geophysical survey. The hand augers were spaced at 2m apart in a straight line along the electrical resistivity geophysical survey line, with the middle auger located at the mid-point of the high/low resistivity anomaly. The location plan of the hand augers and DCPs are shown in Figure 3.10. The hand auger and DCP logs are presented in Appendix 2.3. Four samples of 200mm length were taken from each hand auger core, spaced one metre apart from 0.8m depth for laboratory testing.

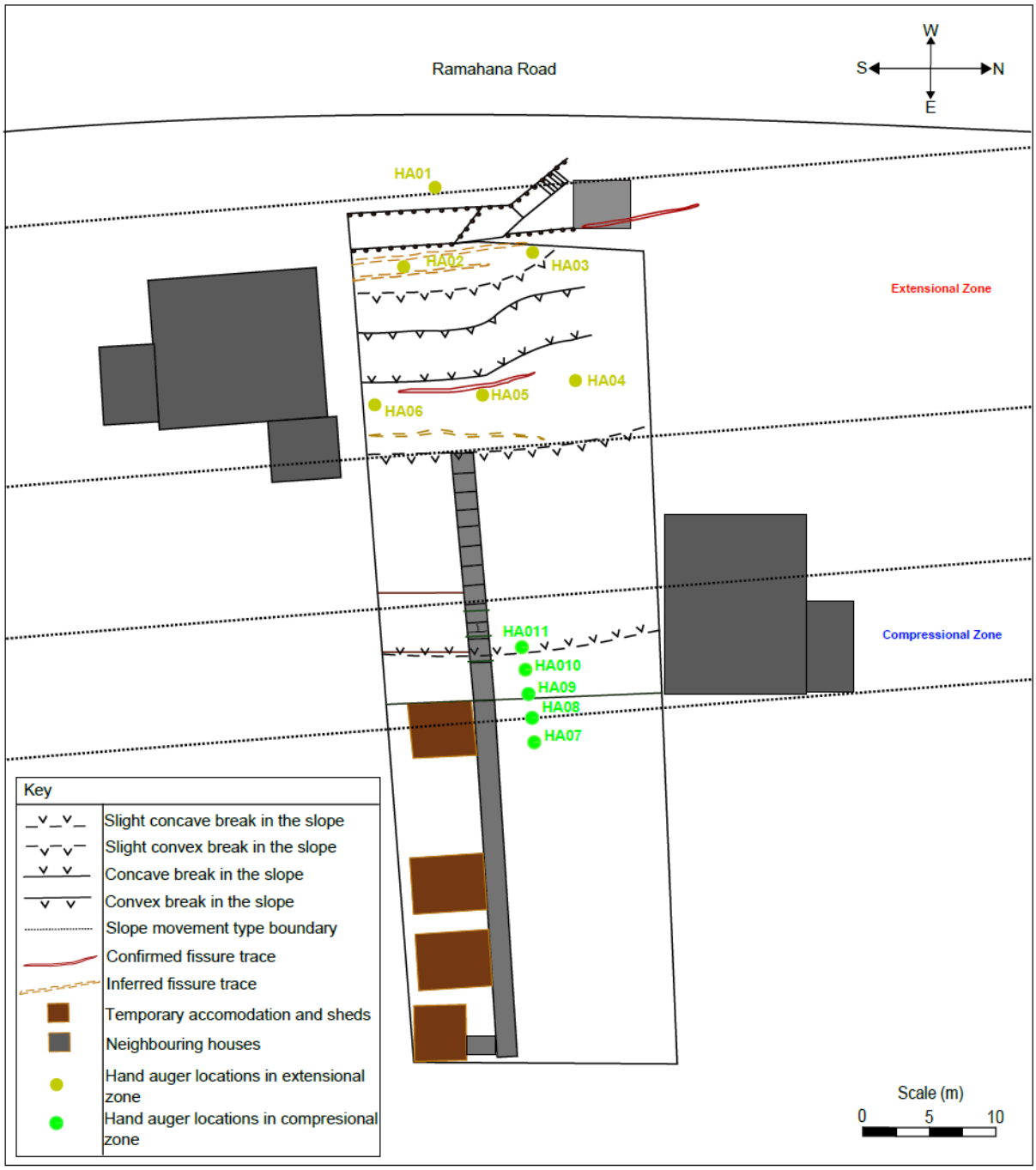

Figure 3.10: Hand auger and DCP locations at 17 Ramahana Road as part of geotechnical appraisal and testing the compressional zone at the site.

The soil logged from the six hand augers in the extensional zone generally had an engineering geological description of SILT with some clay and minor sand, trace gravel; yellowish brown. Firm to stiff, moist, low plasticity; sand, fine; gravel, fine, basalt. The moisture content generally increased with depth, but there were pockets of higher moisture contents within a generally low moisture content soil mass, and a particular section of high saturation near the ground surface in HA3. The DCPs identified that an ultimate bearing

capacity of ≥300kPa (required for foundations) is found at a depth of 0.8-1.2m below the ground surface across the building envelope.

The soil logged from the five hand augers in the compressional zone was similar to the soil from the top of the site; however there was less gravel content and a higher moisture content. The soil generally had an engineering geological description of SILT with some clay and minor sand; yellowish brown. Firm, moist to wet, low plasticity; sand, fine. The moisture content tended to increase with depth, and standing water was found within HA9 at a depth of 4.2m. The DCP's identified that an ultimate bearing capacity of ≥300kPa was found at a 0.9-1.1m depth, which shows consistency with the upslope tests.

Figure 3.11 is a comparison of the DCP results for HA07-HA011 located in the compressional zone. HA09 is located closest to where the most compression is thought to have occurred. It was hypothesized that this soil would have more resistance to penetration due to its compressed, and therefore, denser state than the surrounding soil. What actually was recorded was gradual increase in number of blows/100mm depth in all of the DCP's, but there was generally less resistance in the downslope DCP tests than in the upslope ones. This could be more due to the moisture content being higher at the base of the slope than further up the slope than due to any changes in density in the soil, so density tests of *in-situ* samples were also conducted. The density tests are presented in Chapter 4.

3.3.5. Shallow Site Model for 17 Ramahana Road

Figure 3.12 is the shallow site model for 17 Ramahana Road determined from the shallow subsurface investigation results. The soil description is based on the general engineering geological descriptions determined from the hand auger and test pit logs. The soil strength estimates in the soil description are based on the DCP and shear vane results.

The profile of the fissure trace was generalized from the logged profile of the north and south wall of the test pit. The key features of the fissure trace are displayed, which include: the flattening off of the fissure trace with depth, the loss of aperture of the fissure trace with depth to 1-2mm thickness at 2m depth, the segmentation of the fissure trace below 2m depth, and the absence of offset in the mixed-colluvium layer that intersected the fissure trace at 2.4m depth.

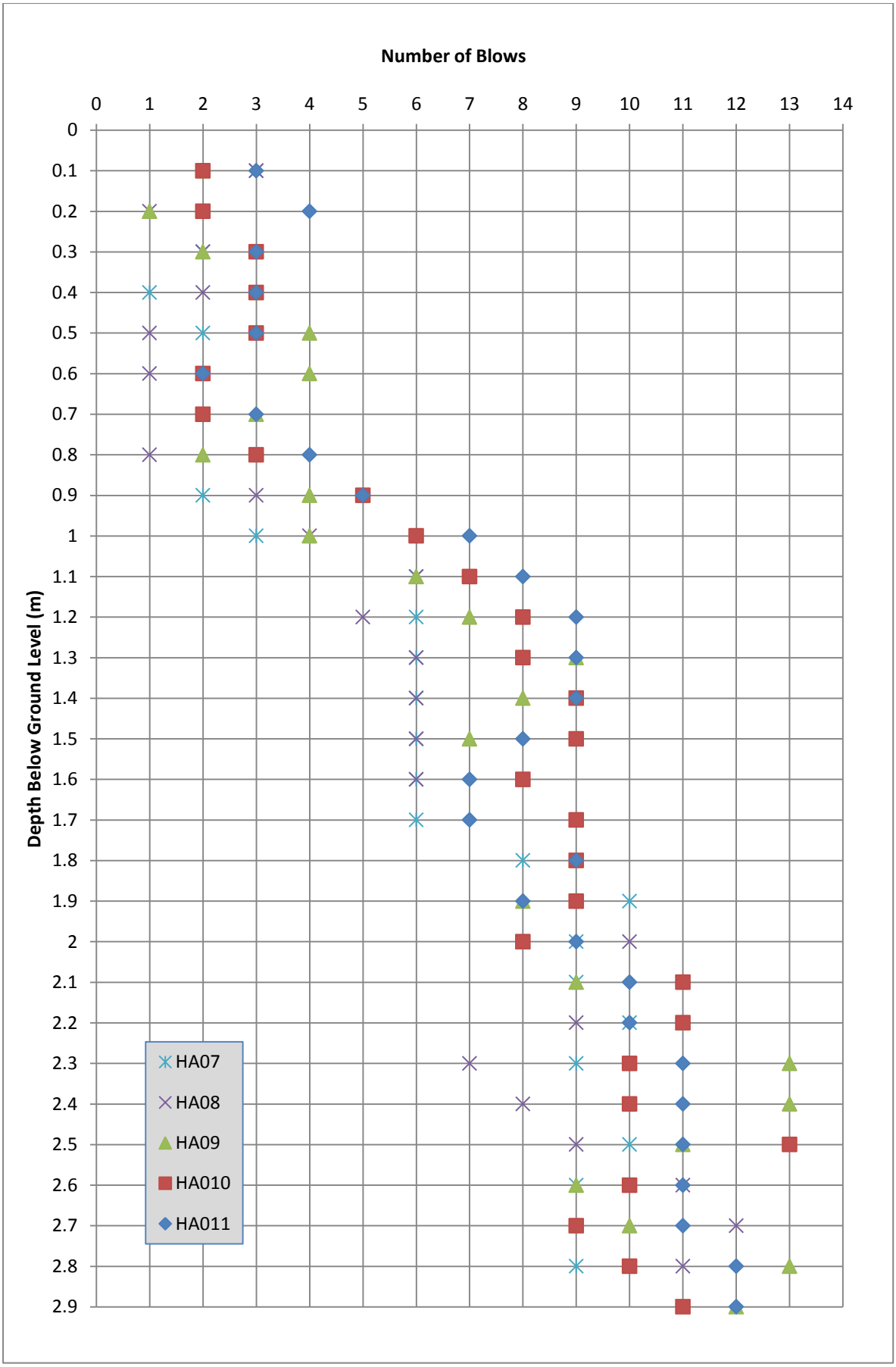

Figure 3.11: Comparison of the DCP results for HA07-HA011 in the compressional zone at 17 Ramahana Road.

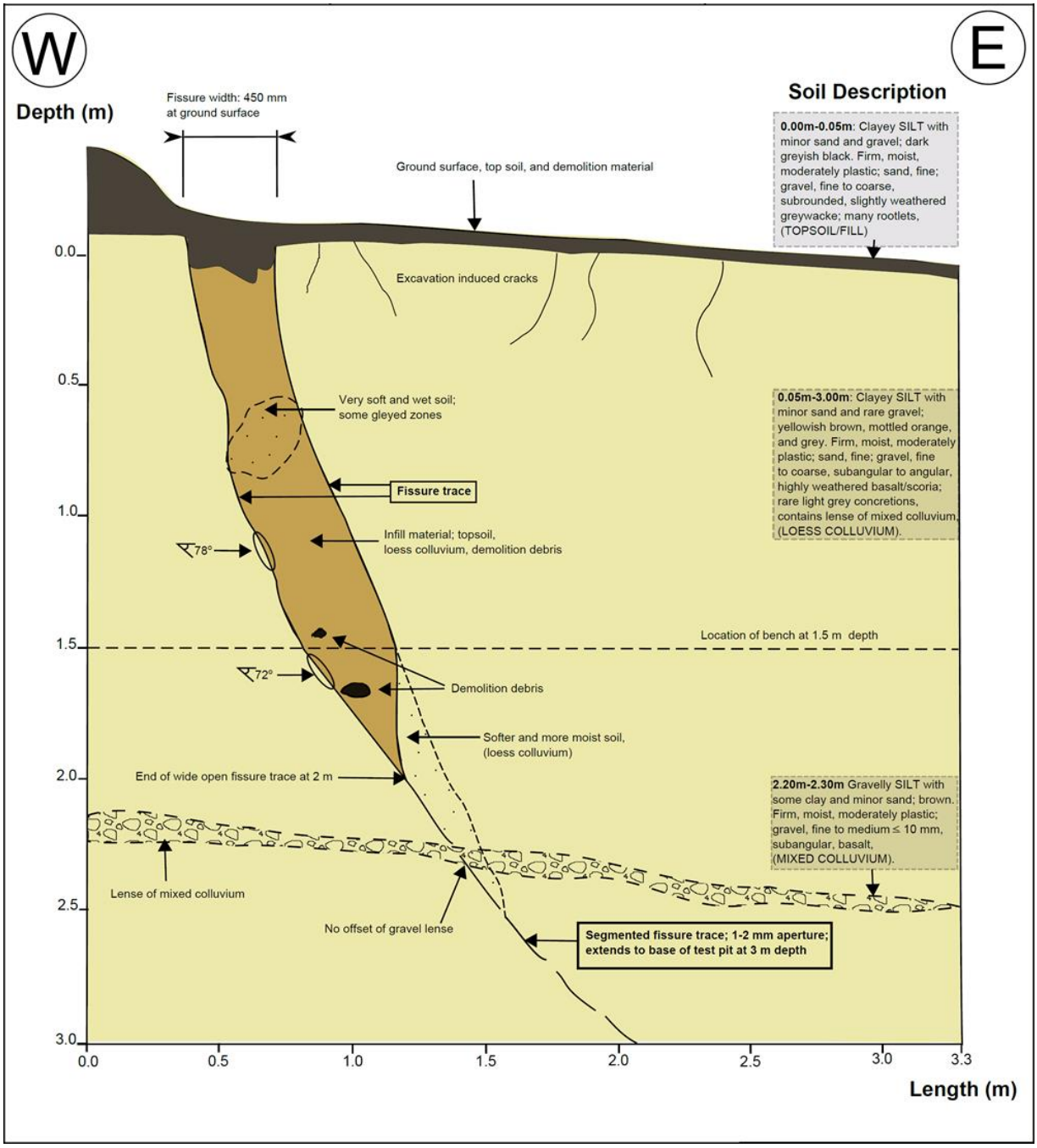

Figure 3.12: Shallow site model for 17 Ramahana Road.

3.4. Deep Investigations at 17 Ramahana Road

3.4.1. Ground Penetrating Radar

The purpose of the ground penetrating radar (GPR) was to gather information on the depths and variations in material properties. It was also used to detect whether the fissure traces connect to a basal shear surface, as suggested by Massey et al. (2013). The GPR was conducted on the 17th of March, 2015 at 17 Ramahana Road on a clear day. The path of the GPR was cleared of debris and loose organic matter, and smoothed where it was possible; however the surface was still rough in places, and the sharp changes in slope gradient did not offer good grounding for the GPR for the entire length of survey. Appendix 2.4 provides a photo of the GPR line.

The data acquired from the GPR survey was of adequate resolution for the first 1.2m, but it quickly lost resolution with depth after this point. This loss of resolution is attributed to the conductivity of the clay fraction in the loess-colluvium, and the increasing moisture content with depth, both of which would have attenuated the radar signal. The data acquired from this survey was not added to this thesis due to the lack of depth of penetration: a depth of 1.2m does not reach the base of fissure trace opening, and therefore it does not allow interpretation of any base of shear movement as suggested by Massey et al. (2013).

3.4.2. Electrical Resistivity Geophysical Survey

The electrical resistivity geophysical survey (ERGS) was conducted on the 24th of March 2015 on a clear day. The electrodes were spaced at a distance of 1m for 63m in a straight line, from the easternmost boundary of the property at the bottom of the slope to the westernmost boundary at the top of the slope. This resistivity line was chosen because it crossed roughly perpendicular to the extensional zone, the compressional zone, and beyond into the valley floor alluvium.

The objective of the ERGS was to determine the changes in the moisture content at depth, the changes in soil properties, and potentially whether there was a basal shear surface. The raw data was assessed by Southern Geophysical Ltd, and then provided interpreted figures. The results of the ERGS are displayed in Figure 3.13, which are two interpretations of the same data to show the potential variations. Figure 3.5 shows the survey line, and Appendix 2.4 includes a photo looking down the survey line.

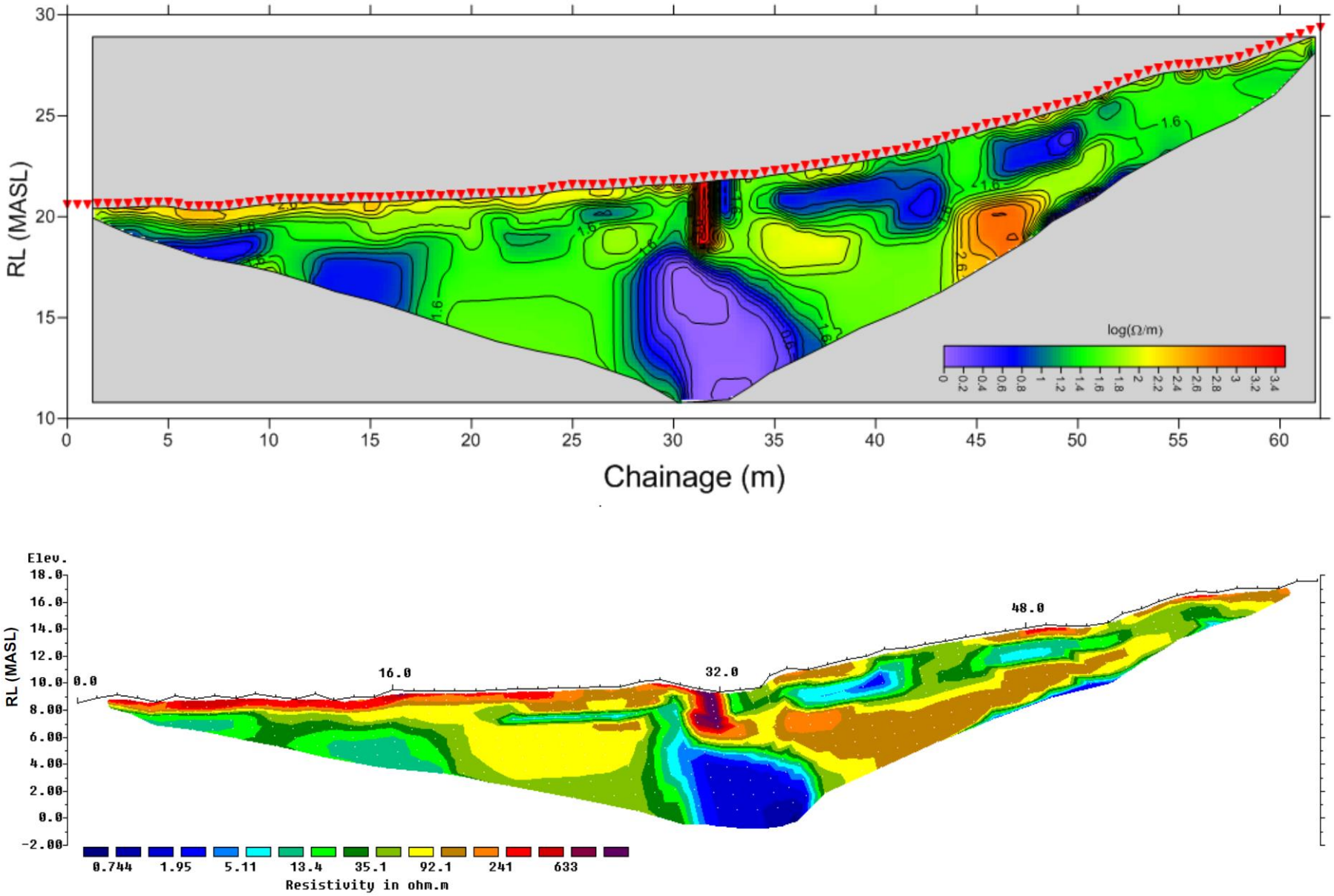

Figure 3.13: Comparison of different electrical resistivity geophysical models for the same survey at 17 Ramahana Road. The resistivity anomaly in the centre is consistent in both models. Refer to Figure 3.5 for survey line.

The most striking features of the resistivity survey are in the center of the diagram where there is a large area of relatively conductive soil below and to the east of a relatively resistive area of soil. The highly conductive area is at its highest conductivity (0 log Ω/m) at the chainage of 37m near the extent of survey depth. The highly resistive area is at its highest resistivity (3.4 log Ω/m) at the chainage of 33m from the soil surface to a depth of 4m below ground level. This high resistivity area continues westward at depth into the slope, although the resistivity reduces to the west.

There are localized areas of high conductivity near the ground surface at chainage 5m, 25m, 3m, 39m, 49m, and 59m, and near the base of data penetration at chainage 14m and 50m. The near-ground surface is largely characterized by high resistivity that is more pronounced on the flatter slope, and this was unexpected due to it being topsoil which should be more conductive due to the organic content. The rest of the diagram is relatively consistent in resistivity at about 1.2-1.8 log Ω/m.

Samouelian et al. (2005) explain that many soil properties can affect the electrical resistivity of the soil, including: the nature of solid constituents, the volume and arrangement of voids, the amount of saturation by water, the chemical composition of the fluid, and the soil temperature. The moisture content of the soil shows a particularly strong correlation to increased soil conductivity. According to Samouelian et al (2005) the increase in moisture content will cause a rapid increase in electrical conductivity up to a moisture content of 15%, but it will begin levelling off after this point, and there is little response after 20%.

The changes in conductivity across the slope profile are most likely to be related to moisture content changes. The relatively high resistivity value (~2.2 log Ω/m) of the near-surface material in the valley floor adds to this assumption, because this material should be more conductive than the surrounding soil when its organic content is considered, but its low moisture content of ~9% gives it relatively high resistivity.

3.4.3. Seismic Reflection Survey

The seismic reflection survey was conducted for the purposes of 1) finding a basal shear surface, and 2) analyzing the thickness and orientation of various layers in the deposit. It was assumed that a basal shear surface would be indicated by a lower seismic velocity area through the deposit, if it was of sufficient thickness. The seismic survey was conducted on 13th April, 2015 at 17 Ramahana Road and can be viewed in Figure 3.14. It followed the

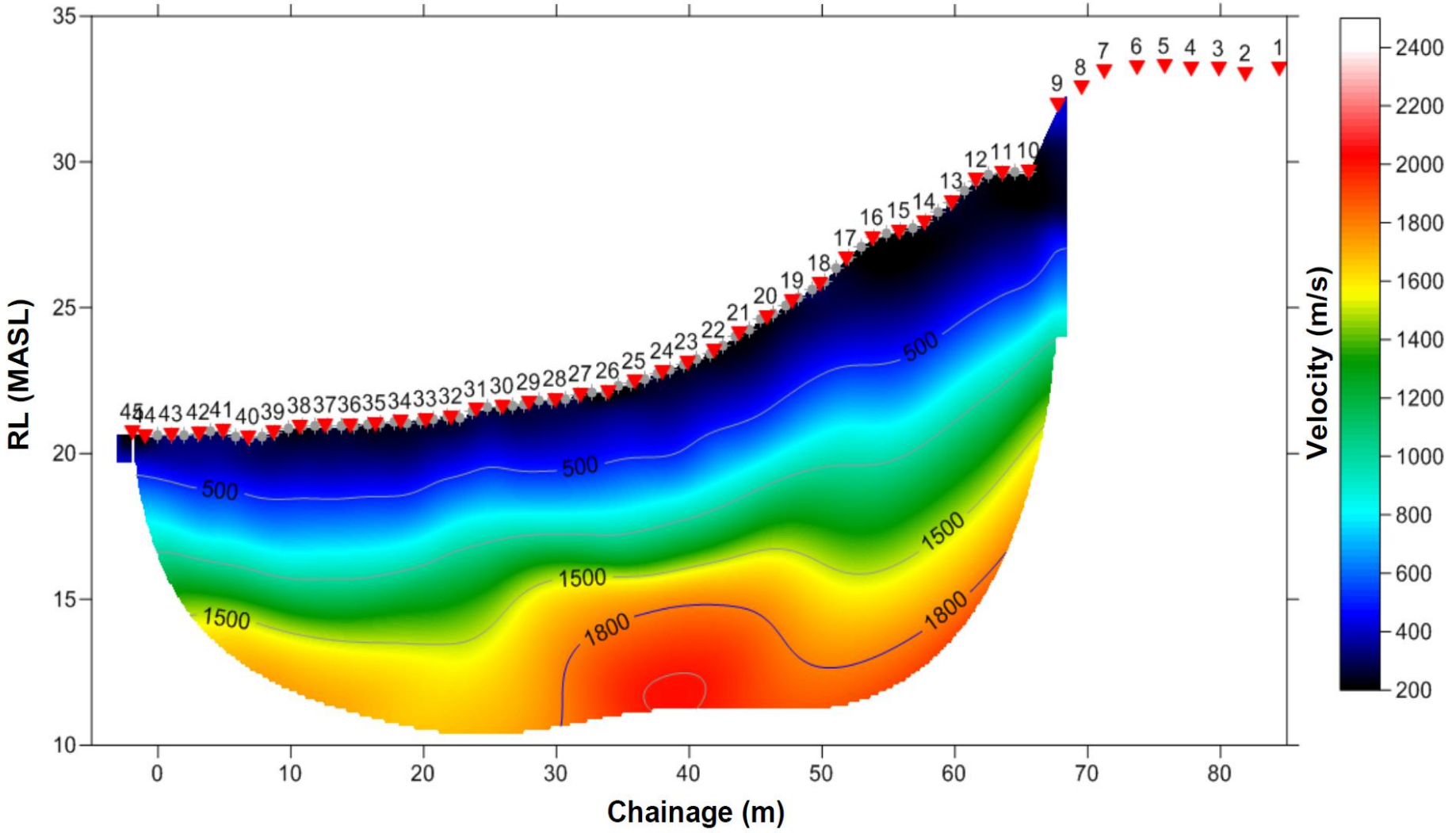

Figure 3.14: Final interpreted model of the seismic reflection survey for 17 Ramahana Road with topography at 2 x vertical exaggeration. Note that the blue contour = water velocity.

same line as the electrical resistivity geophysical survey. Figure 3.5 shows the survey line, and Appendix 2.4 presents a photo looking down the line. The raw data was assessed by Southern Geophysical Ltd, and developed into interpreted figures.

The geophones were spaced at 1m from the upper westernmost point of the property on the far side of Ramahana Road to below the easternmost point on the property within St Martins School. Appendix 2.5 shows the initial model and raypath model. The final model can be viewed in Figure 3.14, and it shows increasing density with depth, which is what is expected considering the soil profile identified in the borehole logs from the site. There is 2x vertical exaggeration in this model.

It is important to note that the model makes more assumptions with depth and the seismic velocity contours could be flatter than what the model suggests. The bulge in the centre of the diagram is likely to be a limitation of the model because there are more raypaths that cross the centre of the survey than at the edges. The survey shows that the loess-colluvium is layered on the same angle as the slope, and that the soil increases in density with depth. There are no weak spots or low density areas identified in the deposit and there is nothing to suggest that there is a basal shear surface in the survey profile. This does not mean that there is no basal shear surface; it simply means that if there is one, the survey has not made it readily identifiable.

3.4.4. Cone Penetration Test

The purpose of the Cone Penetration Test (CPT) profiling was to assess the deep soil conditions at the site and determine if there were any weaker layers within the deposit. The CPT rig was placed within the extensional zone, on a flat bench at the base of the driveway. Figure 3.5 shows the location of the CPT profile. It would have been beneficial to conduct another CPT at the base of the slope within the compressional zone to assess how the soil behaviour changes across the resistivity anomaly identified by the electrical resistivity geophysical survey, but this was not possible due to the slope being exposed and wet, and at a relatively steep angle for machinery.

The CPT profile was conducted on the 20th of July 2015. It penetrated to a depth of 25.15m where it is assumed to have reached bedrock due to the rapid increase in cone resistance. The raw data from this survey was uploaded into the computer software system CLiq v.1.7.6.49 to assess the soil behavior type variation with depth, and the potential response of the site to

cyclic loading. A water level of 9.0m was determined for the profile, due the water levels in BH-RMH-01 and BH-RMH-02, and from the depth in the CPT profile where the pore-pressure begins to increase. The CPT logs are presented in Appendix 2.6.

The main spikes in pore-pressure can be seen at a depth of 23m, where according to the nearby BH-RMH-02 the soil is within volcanic-colluvium, at 19m where it is within saturated sand, and at 13.5m which is around the boundary between a silt with minor clay and a clayey silt. There is an interesting anomaly at 15.5m where the friction ratio increases dramatically whilst the pore-pressure drops to zero, which could be where the cone has passed through a highly weathered volcanic cobble. There are three other locations where there is a sudden drop in pore-pressure: at 10.75m, 12.75m, and 14.75m. These locations correspond with small spikes in the friction ratio and could simply represent drier areas in the loess-colluvium profile.

There is good cone resistance throughout the soil profile until the cone reaches bedrock at 25.15m. There is an average of 3.95MPa throughout the entire soil profile, a mode of 1.38MPa, and a minimum of 0.14MPa. The lowest cone resistance of 0.14MPa is found in the top 0.05m of soil. The cone resistance then increases steadily before dropping below 1Mpa to as low as 0.74MPa at a depth of 1.63-1.86m. The rest of the soil profile has a cone resistance greater than 1MPa.

The liquefaction potential of the soil was calculated by assessing the soil under SLS and ULS conditions. 8mm of settlement over the entire soil profile was determined under SLS conditions, and 60mm of settlement over the entire soil profile under ULS conditions. There is no lateral displacement in either scenario. Appendix 2.6 shows the liquefaction potential logs. The Christchurch Earthquake data was also inputted into the Cliq software to see what potential for liquefaction there was under this scenario (i.e. M_W6.2 earthquake with 0.85g peak ground accelerations, as recorded at the nearest seismograph to 17 Ramahana Road: at Cashmere High School). This recorded 60mm of settlement over the entire soil profile and zero lateral displacement.

The cyclic resistance ratio to cyclic stress ratio plot in Appendix 2.5 shows that liquefaction potential occurs within distinct layers of the loess-colluvium; however the soil behaviour types, calculated by the equations of Robertson et al. (1986), do not correlate with the nearby borehole logs and laboratory tests conducted on samples of this soil. The deposit is known to

be predominantly silt throughout the entire soil profile, until near the base of the deposit where sand can be more prominent. In contrast the soil behavioural type plots the soil as being predominantly clay and sand in various layers throughout the profile. This would create an unrealistic behavioural response to cyclic loading because the sand layers close to the ground surface, which are not actually present in the deposit, would be deemed as layers with potential for liquefaction.

Another noteworthy factor in the liquefaction assessment is that the groundwater level was assumed to be at 9.0m, but this could vary from actual site conditions. The borehole logs show that the soil is wet in certain layers below 9.0m, but it is largely moist throughout the entire logged soil profile. The water level of 9.0m might be misleading to the calculations because the soil is not completely saturated from this level until 25.15m at the base of the CPT. The as-built for the piezometer in BH-RMH-02 is not available, so the screen depth is unknown. 9.0m could represent a perched water level or artesian water pressures from groundwater within the Lyttelton Volcanic Group at depth.

There are many discrepancies between the soil behaviour type and what was recorded in the borehole logs, and this can be attributed to the factors that are assessed in the calculations defined by Robertson et al (1986). The soil behaviour type is defined by plotting normalized cone resistance vs. normalized friction ratio as seen on the graph in Figure 3.15 and 3.16, but the mechanical behaviour of loess is governed by its moisture content. The same sample of loess with different moisture contents could be plotted on a different section of the graph, for example: a section of dry loess could be determined to be sand due to its high cone resistance relative to its sleeve friction, whereas a saturated loess could be determined to be clay due to its low cone resistance relative to its sleeve friction. Robertson (2009) explains that saturated, soft, low plasticity silt can have the behavioural response of a clay, as they tend to have low undrained shear strength, whilst very stiff, overconsolidated, fine-grained soils, (i.e. silts), can have the behavioural response of a sand, as they tend to dilate under shear and have a high undrained shear strength relative to their drained shear strength.

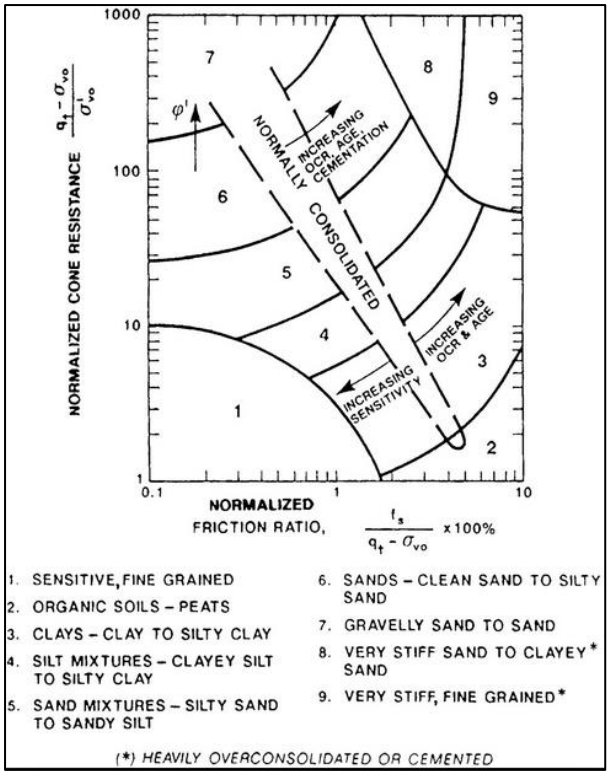

Figure 3.15: Soil behavioural type based on the normalized cone resistance and the normalized friction ratio. After Rogers (2006).

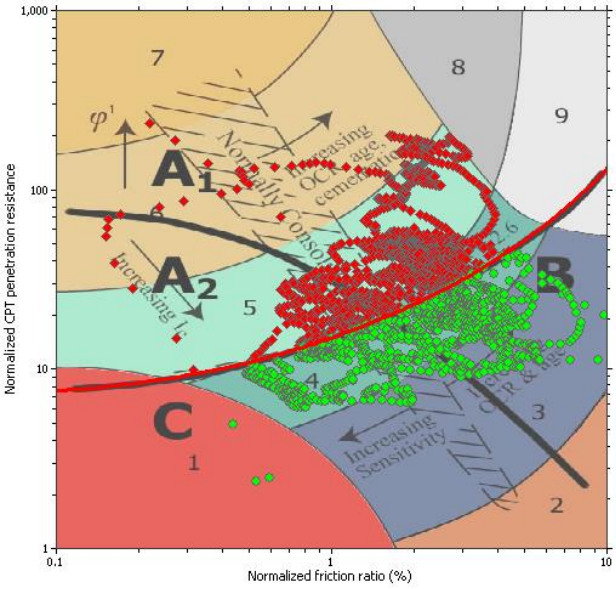

Figure 3.16: Soil behavioural classification based on the normalized cone resistance and the normalized friction ratio with data points from the CPT and liquefaction analysis. Model taken from CLiq.

3.4.5. Pore Pressure Dissipation Tests

The purpose of the pore pressure dissipation test was to test whether the soil was dilatant or contractive under static shear stress conditions, and to determine the *in-situ* coefficient of consolidation and coefficient of permeability. A pore pressure dissipation test uses the cone of a CPT to induce *in-situ* monotonic loading to a section of soil, which will either cause an increase, decrease, or no change in pore pressure. Robertson (1992) explains that an increase in pore pressure indicates that the soil is contractive under monotonic loading, and this normally occurs in clays; a decrease in pore pressure indicates that the soil is dilative under monotonic loading, and this occurs in dilative silts, overconsolidated clays, and dense sands; when there is no change in pore pressure it indicates high porosity, and this is usually associated with sands. The permeability of the deposit is able to be calculated using the time it takes for pore pressures to return to equilibrium values. Appendix 2.7 provides the coefficient of consolidation and coefficient of permeability calculations.

The pore pressure dissipation tests were conducted on the 20th of July, 2015 in conjunction with the CPT test. They were conducted at 9m, 11m, and 13m. These depths were chosen

because they were below the 9.0m groundwater level determined from the water level in BH-RMH-02. The results of the test are presented in Table 3.3.

Depth	Coefficient of Consolidation (Robertson et al. 1992)	Coefficient of Permeability (Robertson et al. 1992)	Hydraulic Conductivity (Lunne et al. 1997)
9.0m	5.33×10^{-6} m^2/s	9.50×10^{-10} m/s	5.21×10^{-7} m/s
11.0m	1.50×10^{-4} m^2/s	5.03×10^{-8} m/s	2.23×10^{-8} m/s
13.0m	1.34×10^{-5} m^2/s	3.98×10^{-9} m/s	5.21×10^{-7} m/s

Table 3.3: Coefficients of consolidation and permeability from equations defined by Robertson et al. (1992) using the pore pressure dissipation test results and hydraulic conductivity from equations defined by Lunne et al. (1997).

Figures 3.17-3.19 show the pore pressure dissipation tests at 9.00m-13.0m. The pore pressure reached its highest point at 13m where it reached a value of 536KPa; this is 7 times greater than its hydrostatic pressure of 76.1 KPa. The second highest pore-water pressure was found at 11m where it reached 486.3 KPa; however this value dropped to 263.8 KPa within 1 second of the cone reaching a static state. The hydrostatic pressure was 22.9 KPa, which means the pore-water pressure reached 22.2 times its hydrostatic pressure when subjected to monotonic loading, but dropped to only 11.5 times its hydrostatic pressure within 1 second. The lowest pressures were found at 9m where the pressure reached 94.6 KPa, which was 5.3 times its hydrostatic pressure of 17.8 KPa. All of the pore pressure dissipation tests reached their equilibrium pressure within 25 minutes regardless of how high the pore-water pressure reached in the first instance.

These results show that there is potential for pore pressure increase in the loess-colluvium at 17 Ramahana Road under monotonic loading. The potential increase varies depending on the coefficient of consolidation, natural moisture content, and permeability of the soil. It is currently unknown what effect cyclic loading would have on pore pressures, but it is hypothesized that the pore pressure increase would be more substantial than under monotonic loading. Because the pore pressures in the loess-colluvium at 17 Ramahana Road increase under monotonic loading, then if liquefaction were to occur in the deposit during an earthquake, it should present itself as flow liquefaction rather than cyclic mobility.

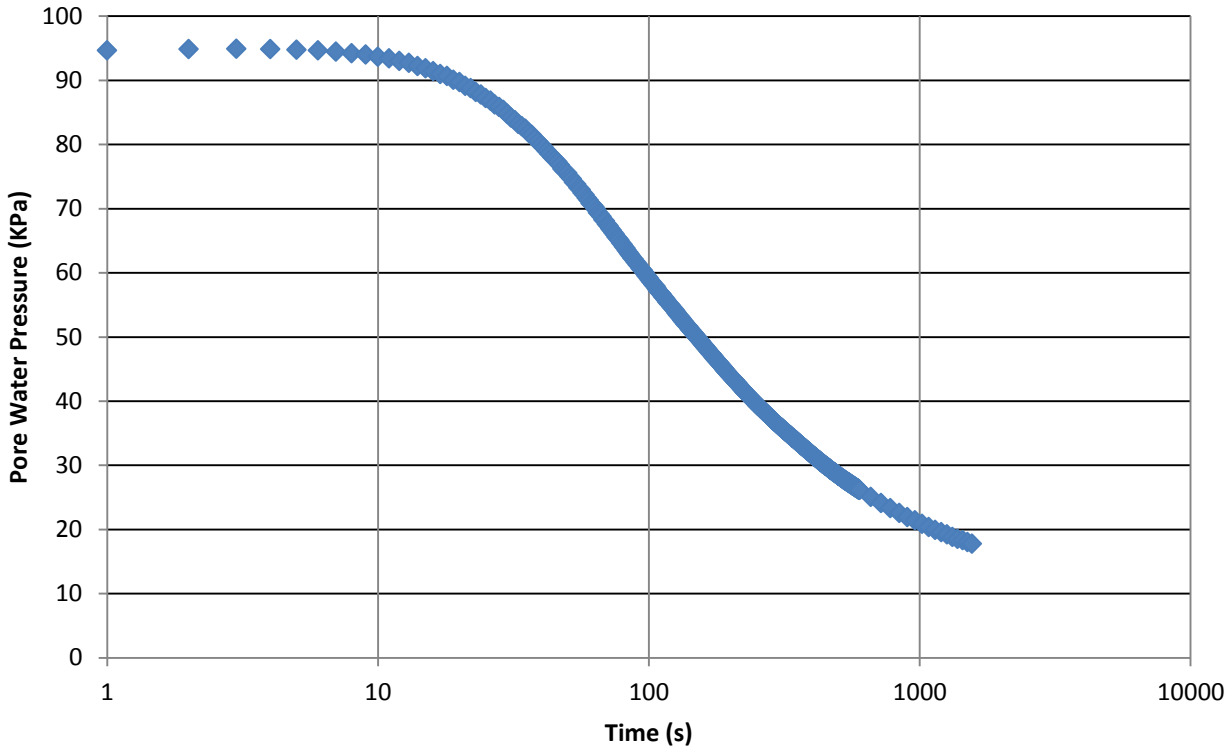

Figure 3.17: Pore pressure dissipation test at 9.00 m depth in CPT-17RMH-01.

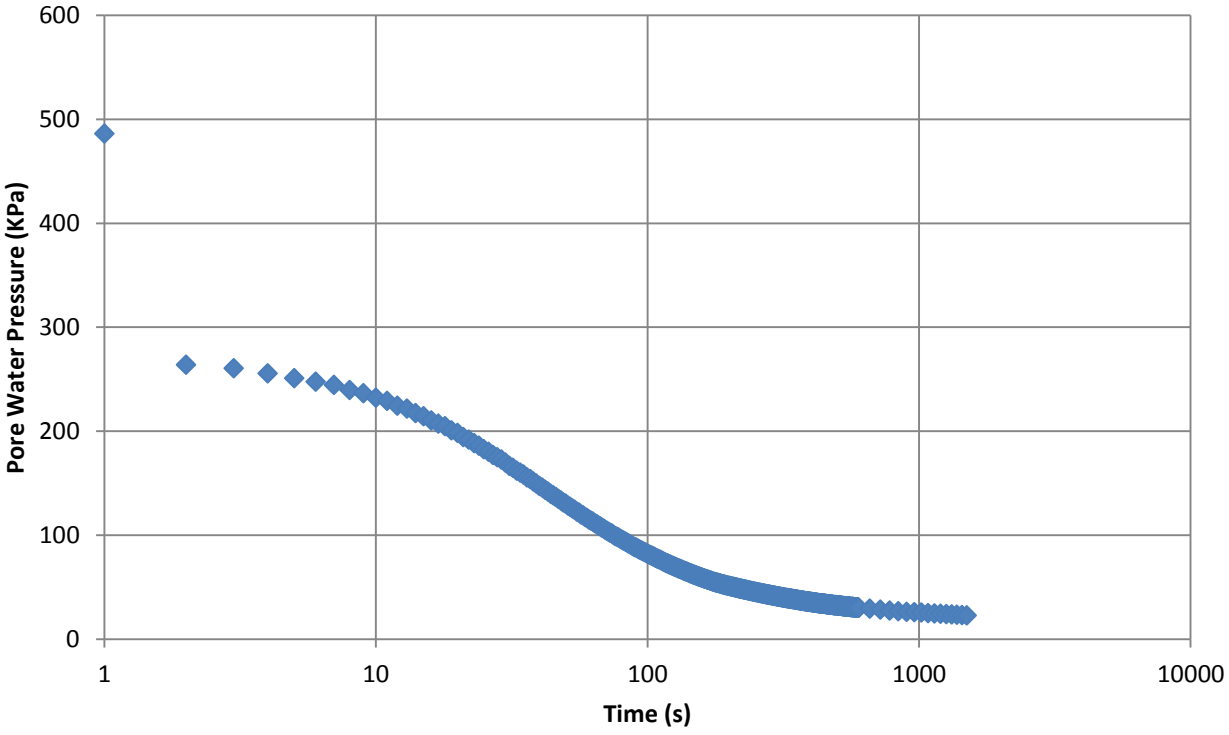

Figure 3.18: Pore pressure dissipation test at 11.00 m depth in CPT-17RMH-01.

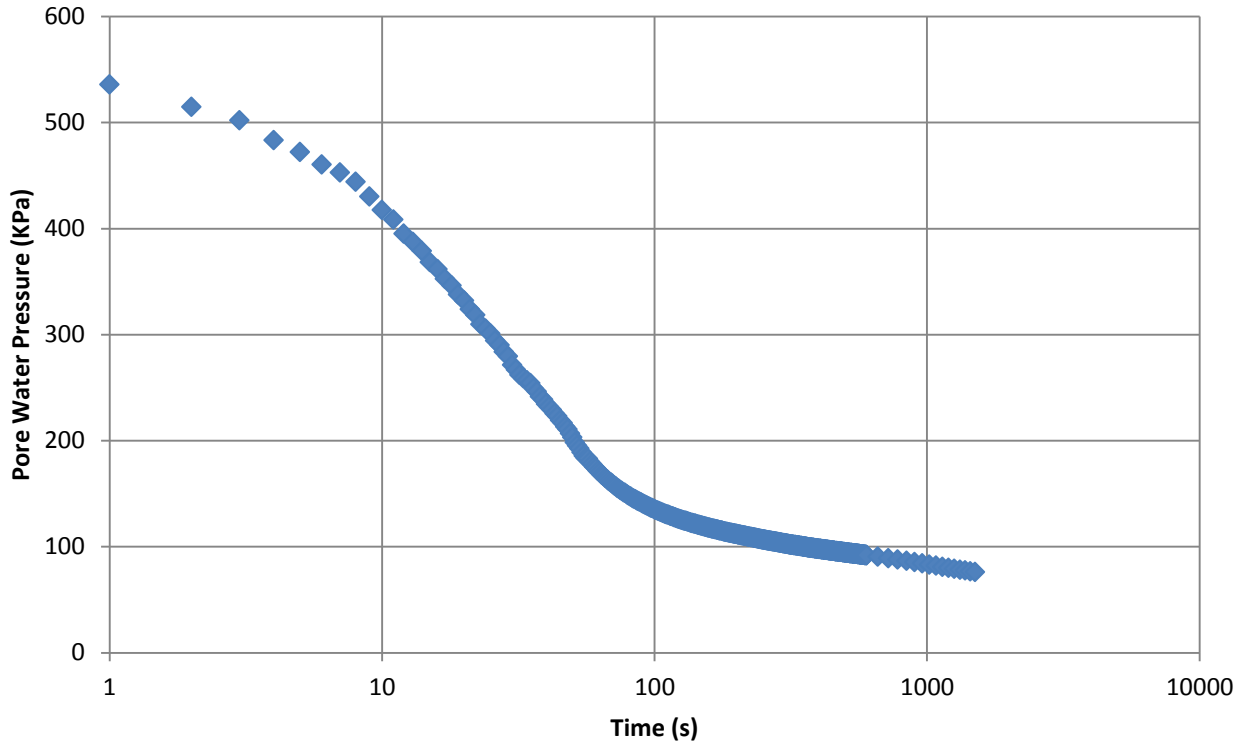

Figure 3.19: Pore pressure dissipation test at 13.00 m depth in CPT-17RMH-01.

Comparisons between the equations by Lunne et al (1997) that use the soil behavioural type or $I_{c,}$ and the equations by Robertson et al (1992), show large differences. The best correlation is seen at a depth of 11.0m where the I_c is 2.9 and the normalized soil behavioural type is 3, which denotes a clay/silty clay. At 9.0m and 13.0m the correlations are poor. An I_c of 2.4 and a normalized soil behavioural type of 5 is calculated at a depth of 9.0m, denoting a silty sand/sandy silt. An I_c of 2.6 and a normalized soil behavioural type of 4 is calculated at a depth of 13.0m, which indicates a clayey silt/silty clay. The significance of these comparisons is that the soil behaviour type is not a good indicator of soil permeability for the loess-colluvium at 17 Ramahana Road because the soil is generally a silt with some clay to a clayey silt, but its permeability has a closer resemblance to a compacted clay.

What these comparisons indicate is that the soil behaviour type is not a good indication of what the actual soil material really is, or even what the actual soil behaviour will be: whilst the SBT denotes a silty sand/sandy silt and a clayey silt/silty clay, the *in-situ* coefficient of permeability is more closely correlated to a compacted silt or clay. These findings back up the statements by Been & Jefferies (2006): '…the CPT cannot be used in isolation and requires an appropriate program of sampling and laboratory or related testing to confirm the selected soil parameters'. Because the loess-colluvium at the site is predominantly silt, it does

not follow the idealized behaviours of a sand or a clay, and could then be an example of where traditional CPT methodologies are not sufficient for the type of soils encountered.

3.4.6. Groundwater Investigation

The springs that formed following the Christchurch and Darfield Earthquakes are generally present within the compressional zone of the fissures at the toe of the slope, but there are some cases where the springs have come up through the fissure traces, as at 211 Centaurus Road. It should be noted that in this case the fissure trace is within the valley floor, rather than at the toe of the slope where most are located. Groundwater conditions of acidity, electrical conductivity, total dissolved solids, and temperature were tested at four sites: 211 Centaurus Road, 17 Ramahana Road, 10 Vernon Terrace, and 62 Vernon Terrace.

The four groundwater locations were tested on 17th July, 2015. The four test locations cover a variety of conditions: the groundwater at 17 Ramahana Road, and 10 Vernon Terrace were sourced from installed piezometers, the groundwater at 211 Centaurus Road was sourced from spring flow through a fissure, and the groundwater from 62 Vernon Terrace was sourced from spring flow through the compressional zone. Table 3.4 shows the variation in groundwater characteristics between these different sources.

Location	Depth	pH	EC	TDS	Temperature
211 Centaurus Road	Surface	7.15	1017	508	15.0
17 Ramahana Road BH-RMH-03	1.71 m	7.24	1682	841	10.9
10 Vernon Terrace	0.71 m	7.20	1102	552	9.5
62 Vernon Terrace	Surface	7.25	1090	545	10.1

Table 3.4: Groundwater characteristics from Hillsborough Valley springs and piezometers.

The groundwater from 211 Centaurus Road has the highest temperature, and this could imply that it has the deepest source, or it could signify that there is little meteoric mixing with the groundwater at this location. The meteoric water would be expected to be colder than the deeper sourced water, and if the groundwater mixes with the meteoric water then this will reduce the temperature. The other three locations are either from a shallower source, or there is more mixing with meteoric water in these locations.

The groundwater of the springs that formed following the Darfield Earthquake and the Christchurch Earthquake have a chemical composition that is closer to the Banks Peninsula unconfined aquifer system than the Christchurch confined aquifer system. The relatively high temperatures of the groundwater and spring water also suggest that they have been sourced from depth within the bedrock.

3.4.7. Deep Site Model for 17 Ramahana Road

The cross-section line for the 17 Ramahana Road cross-section is shown in Figure 3.20. This diagram has no vertical exaggeration and was created by interpretation of the three boreholes logged by Tonkin and Taylor Ltd: BH-RMH-01, BH-RMH-02, and BH-RMH-03, the CPT profile, the test pit, the geophysical surveys, and surface engineering geological mapping.

There are some gaps in information in this cross-section, for example the bedrock was only reached in BH-RMH-02 and in the upslope adjacent CPT-RMH-01. This left the slope and location of the bedrock above and below these points up to interpretation, and so the bedrock profile was determined by the seismic reflection survey. The volcanic-colluvium and the loess-colluvium were assumed to be thinner at the upslope end and thicker at the downslope end, due to the nature of typical colluvium. The locations of the different facies within the loess-colluvium were identified by interpretation of the borehole logs, and the notes on the behavioural characteristics at various depths in the logs. A similar pattern to the logs from Centaurus Park was observed. (Refer to section 3.5).

The water level was determined by dip test in the piezometers installed in BH-RMH-02 and BH-RMH-03, and by the moisture content of the soil in BH-RMH-01. It needs to be stressed that these are only considered to be water level readings and not necessarily indicative of the water table: they could simply represent perched water, a layer of particularly saturated loess-colluvium, or artesian pressure from the bedrock, because the screen depths are unknown.

The extensional zone and compressional zone have been assessed from the mapping done by Massey et al. (2013), and from the engineering geological mapping done in this study. The translational zone has been omitted due to its presumption that the fissures are the head-scarps of landslides, when there is not sufficient evidence to suggest that this is so at this stage.

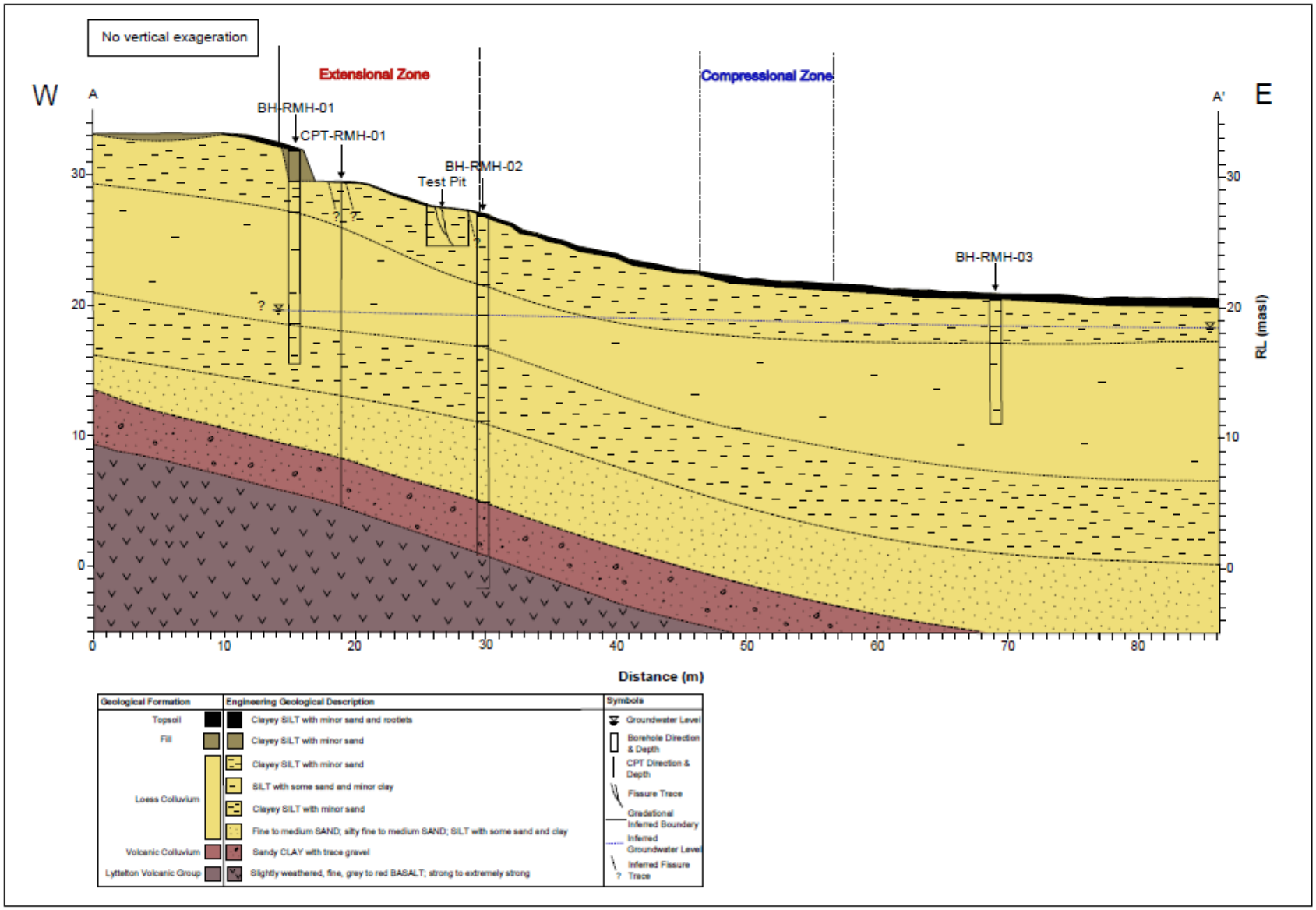

Figure 3.20: 17 Ramahana Road deep site model. Note that the water level line may not be indicative of the water table, because the depth of screen for BH-RMH-02 and BH-RMH-03 are unknown. Refer to Figure 3.5 for cross-section line and Appendix 2.8 for the borehole logs.

3.5. Investigations at Centaurus Park

3.5.1. Engineering Geological Mapping

The engineering geological map of Centaurus Park is presented in Figure 3.21. This was mapped on the 4th of August 2015, during winter, so the mapped boggy areas may have been larger than the average extent of surface saturation. There are three main areas of boggy ground on the park, but only the central one, near the path, has observable spring flow. The spring flow is bringing fine sediment to the ground surface which is slowly building a small mound of loose sediment near the path. The boggy areas have shallow stagnant water up to 30mm deep in localized hollows. There had not been significant rainfall in the time prior to the mapping.

The fissure traces and compressional features on the map follow the mapping of Massey et al. (2013), as these features have since been remediated and could not be mapped for this study. The fissure traces were all located on the flattened areas for Ramahana Road, driveways, and house platforms. There is a gentle slope of ~20° below the flattened areas that flattens to <5° at the valley floor. The compressional features, springs, and boggy ground are located on the valley floor.

The spring identified by Stephen-Brownie (2012) was no longer identifiable. The current spring was not observed by Stephen-Brownie (2012), which means that the spring has either moved, or the original spring ceased flowing and a new one began flowing since 2012. The line of the electrical resistivity geophysical survey conducted by Stephen-Brownie (2012) is outlined as the cross-section line on the map. The electrical resistivity geophysical survey is presented and discussed in section 3.5.3, and the cross-section in 3.5.4.

The locations of the borehole drilled by SCIRT in 2012 are shown on the map. These were drilled on Ramahana Road (BH-03, BH-04, and BH-05), and below the road at the base of the slope in Centaurus Park (BH-02 and BH-01). The borehole logs are discussed in section 3.5.2.

3.5.2. Borehole Logs

Borehole core was received from SCIRT for the purposes of this study. Five boreholes had been drilled in Centaurus Park and up slope from the park on Ramahana Road in 2012. The boreholes were drilled to depths ranging from 13.95m in BH3 to 25.08m in BH4. The

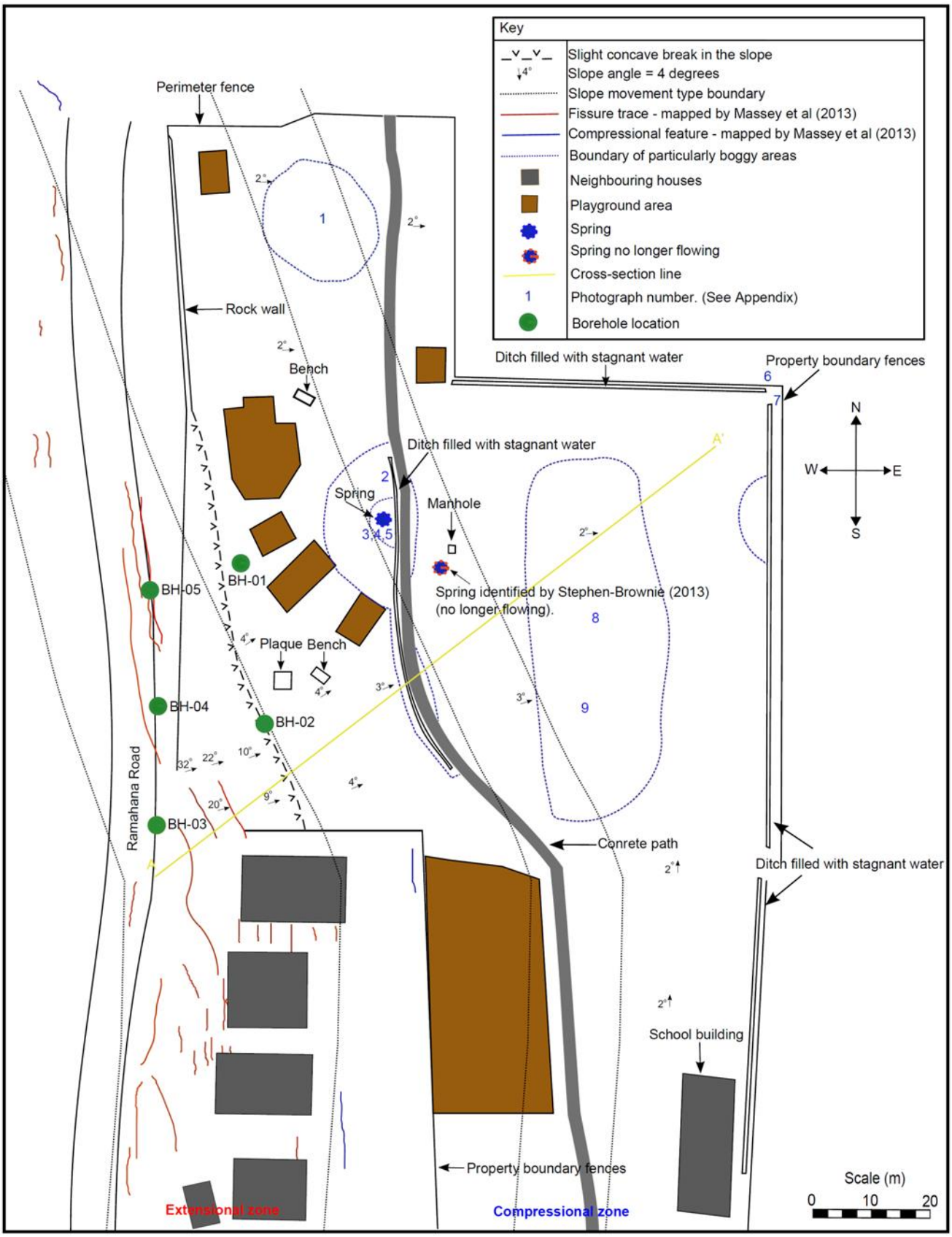

Figure 3.21: Centaurus Park engineering geological map. Refer to Figure 3.23 for cross-section, Appendix 2.9 for mapping photos, and Appendix 2.10 for borehole logs.

locations of the boreholes are shown in Figure 3.21 and the borehole logs are presented in Appendix 2.10.

It was noted in the drilling notes of BH-01 that artesian pressures were encountered at 15.00m depth below ground level. The artesian pressures had 0.75m head above ground level. BH-01 is the closest borehole to the spring in Centaurus Park and the artesian pressure encountered here is probably related to the spring flow.

The core was re-logged for the purposes of this study due to disagreement with the engineering geological soil descriptions given in the original borehole logs. Particle-size analysis was later done on samples taken from the borehole core, which confirmed the engineering geological descriptions given in the updated borehole logs. There were four generalized layers of loess-colluvium that overlaid a layer of volcanic-colluvium and basalt rock from the Lyttelton Volcanic Group at greater depths. The layers of loess-colluvium differed in particle-size distribution and consequentially in behaviour. The engineering geological descriptions of the different loess-colluvium layers, volcanic-colluvium, and the basalt of the Lyttelton Volcanic Group can be viewed in Figure 4.2. The generalized engineering geological description for the entire loess-colluvium profile is SILT with some clay, minor sand and trace gravel; yellowish brown. Firm to stiff, moist to wet, low plasticity; sand, fine; gravel, fine to medium, angular, highly weathered basalt.

3.5.3. Electrical Resistivity Geophysical Survey

Figure 3.22 displays the electrical resistivity geophysical survey done by Stephen-Brownie (2012) at Centaurus Park, and the results are remarkably similar to the results at 17 Ramahana Road. There is the same high conductivity area in the centre of the survey, with a high resistivity area above and upslope. The high resistivity area continues at 2-12m below the ground surface westward into the slope and there are perched high moisture content areas above this. The high conductivity area also appears to bend around the compressed area towards the ground surface.

There was no compressional zone identified in Centaurus Park in the mapping done by Massey et al. (2013), but there were springs identified by Stephen-Brownie (2012). It was interpreted that the high conductivity area in the centre of the survey was related to saturation from the newly formed spring system and the high resistivity area was related to a colluvium layer within the loess; however it is now understood that the soil is loess-colluvium.

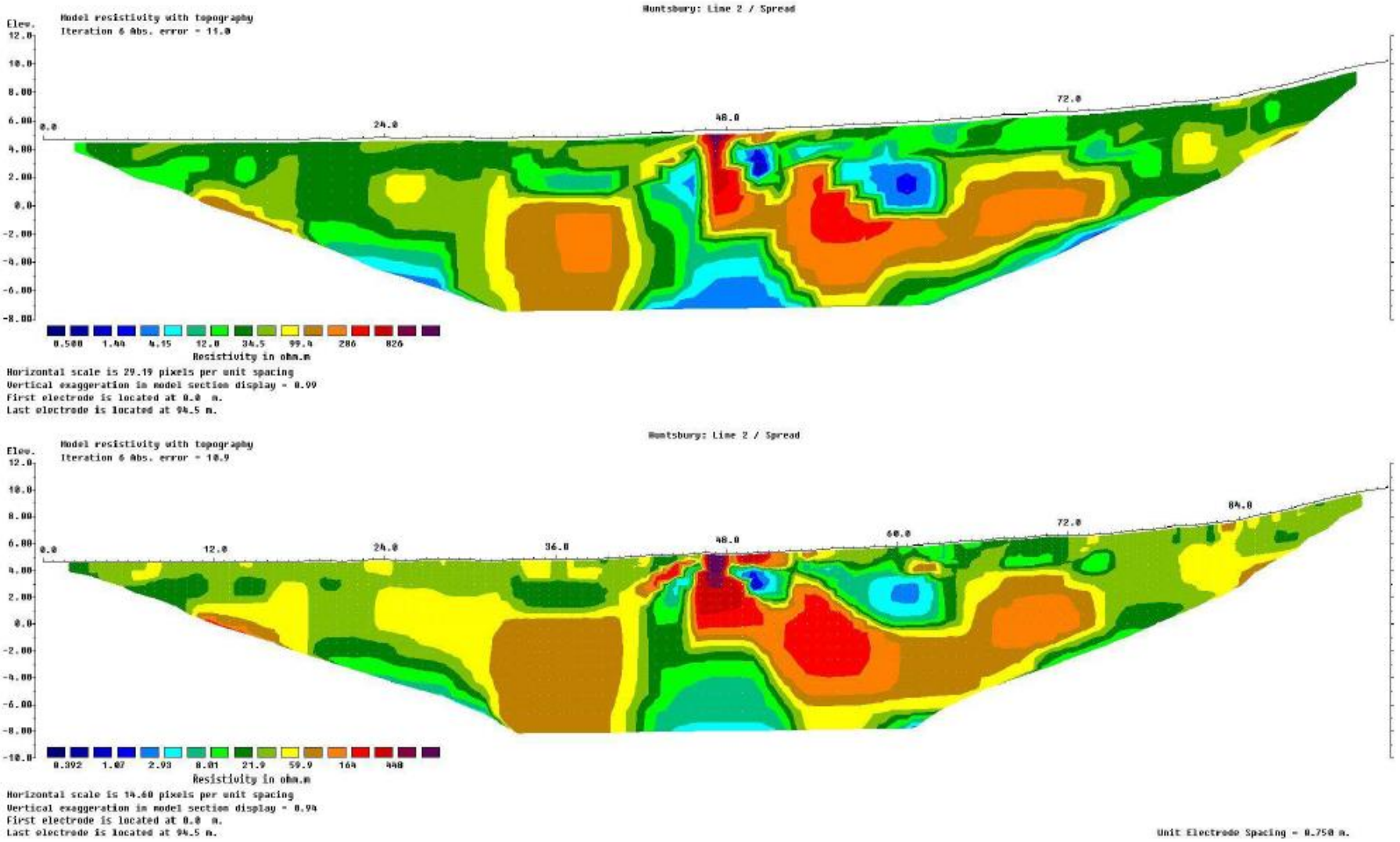

Figure 3.22: Comparison of models from the electrical resistivity geophysical survey for Centaurus Park, from Stephen-Brownie (2012). The resistivity anomaly in the centre is consistent for both models. Refer to Figure 3.22 for survey line.

The high resistivity area in the centre of the diagram is hypothesized to be related to compression of the soil, but this compression may not have been observable at the ground surface in Centaurus Park. Most of the compressional features on this side of the valley have been observable through cracks in concrete and tilted infrastructure, but because Centaurus Park is largely an open area, the compression of the soil may not have been observable at the ground surface.

3.5.4. Centaurus Park Model

Figure 3.23 is the Centaurus Park cross-section with no vertical exaggeration. This cross-section was created from the topography line of the electrical resistivity geophysical survey of Stephen-Brownie (2012) and interpretation of the core delivered to the University of Canterbury by SCIRT. BH-03 and BH-02 were the closest boreholes to the cross-section line. Refer to Figure 3.21 for the cross-section line.

Like the 17 Ramahana Road deep site model there are gaps in the information for this cross-section and the bedrock was only reached in BH-03, which gave little information to infer the bedrock profile further downslope. The bedrock profile was interpreted from the profile of the overlying loess-colluvium facies, and the bedrock profile of the 17 Ramahana Road cross-section.

The groundwater level was interpreted from the groundwater levels recorded in BH-03 and BH-02, and from engineering geological mapping of the ground surface where there was surface water. The water levels in the boreholes may not represent the groundwater table, and instead may represent more saturated layers of loess-colluvium because the water content decreases in the clayey silt layer at depth. There were also artesian pressures encountered in BH-01, and the rise in the water level, as depicted in the model at BH-02, probably reflects groundwater pressure from depth. The water level at the ground surface in the valley floor could represent perched saturation of the surface soils, and might not indicate that the groundwater table is at the ground surface.

The extensional zone and compressional zones were located by correlation with the mapping done by Massey et al. (2013), and by the mapping done in the present study. The translational zone has been omitted because this presumes there has been a translational slide movement when there is little evidence to suggest that there has.

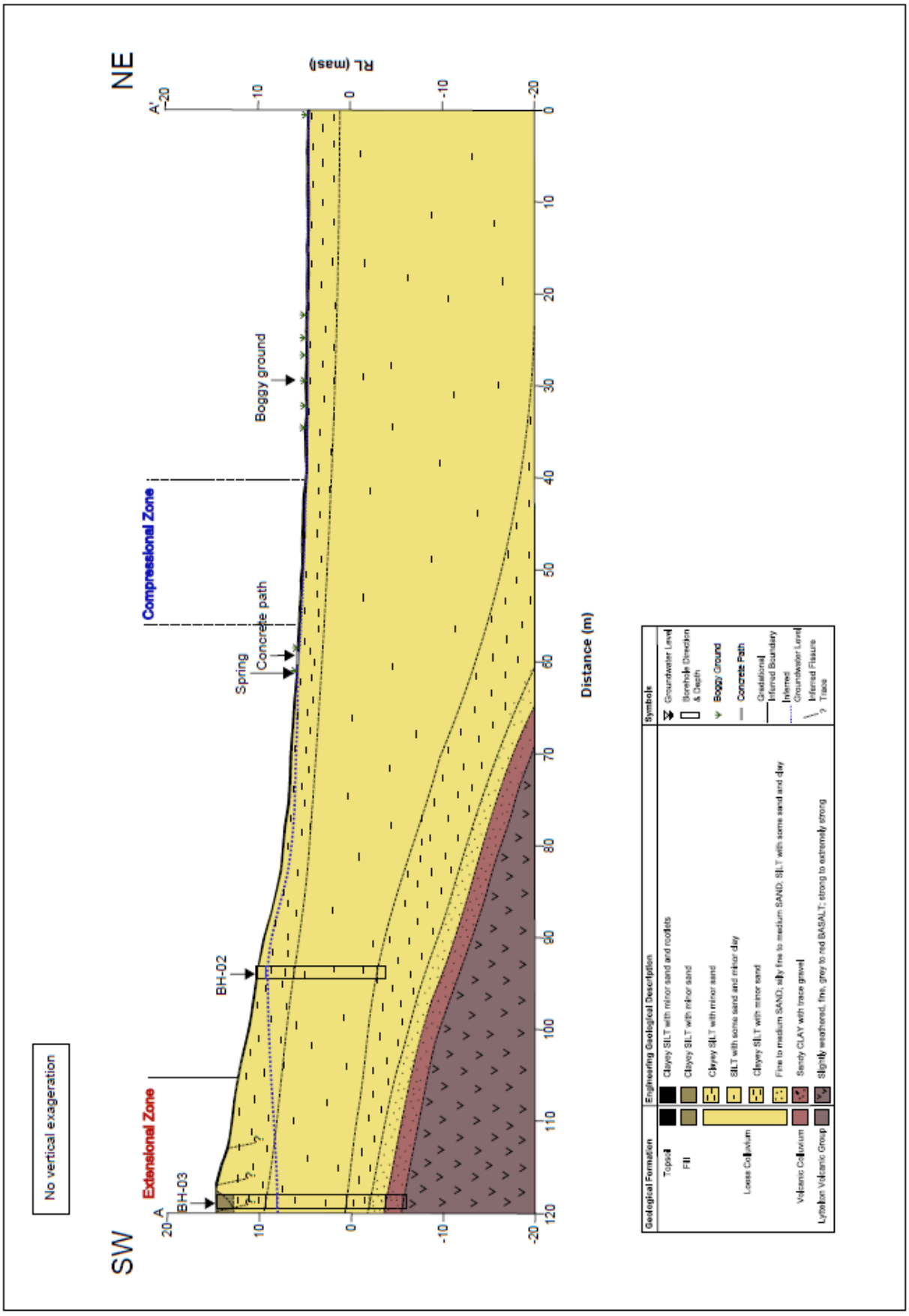

Figure 3.23: Centaurus Park cross-section. Refer to Figure 3.22 for cross-section line.

3.6. Ramahana Road Fissure Trace

3.6.1. Discussion and Synthesis

The test pit at 17 Ramahana Road showed that the fissure trace had an opening of 0.45-0.47m near the ground surface, and slowly reduced in aperture with depth until it closed to 1-2mm at 2.0-2.1m depth. At this depth the fissure trace became segmented, meaning that it was no longer a continuous trace and it had areas of undisturbed soil between observable trace lines. The segmented fissure trace continued to a greater depth than 3.0m. Near to the ground surface the fissure trace was steeply dipping at 78°, but it flattened off with depth, and is ~40-50° when it is segmented at ~2.1m depth.

The segmentation of the fissure trace could be for two reasons. The first, and more compelling reason, is because the fissure trace had flattened off at this point, and so the lateral extension of the soil mass downslope was not transferred as a purely tensile stress, rather it was transferred as tensile and shear stress, but less tensile and more shear with flattening. This also offers a reason as to why the aperture of the fissure trace became thinner with depth, because the tensile stress along the fissure plane was transferred into shear stress as it flattened off. Loess is not as resistant to tensile stress as it is to shear stress, so tensile stress would pull segments of the fissure trace apart, but where the stress was orientated as a shear stress the loess would be strong enough to resist deformation. The 1-2mm aperture reflects that the tensile stress was not as great at this depth due to the curvature of the fissure trace. An alternative reason for the segmentation of the fissure trace is that the tensile stress was greater at the ground surface than at greater depths. Mechanisms behind the induction of tensile stress are discussed in Chapter 5.

The segmented nature of the fissure trace at depth suggests that it would peter out at greater depths than the 3m excavated. The shear vane results conform to this assumption, with the shear strength values within the fissure trace approaching the values outside the trace at 3m depth. The lack of offset on the mixed-colluvium layer on the north wall also shows that the horizontal displacement was greater than the vertical displacement in this fissure. The area of disturbance in the mixed-colluvium layer suggests that there was considerable force in the movement of the fissure trace.

The electrical resistivity geophysical survey showed a resistivity anomaly in the centre of the diagram, and its location corresponds with the compressional area identified by Massey et al.

(2013) and by site walkovers prior to testing. The highly resistive area in the centre could then relate to compression of the slope toe material, and a corresponding loss of void space, which would leave this soil with less moisture. The compression may have continued into the slope and dissipated with distance from the toe, as suggested by the electrical resistivity geophysical survey.

The other areas of high resistivity near the ground surface on the flatter sections of the slope are probably related to surface evaporation, as the flatter ground is exposed to the sun for longer periods of the day, and at a more direct angle, especially during the summer which had just passed when the test was conducted.

The highly conductive area in the centre is probably related to groundwater movement. There were many new springs that formed following the Christchurch Earthquake, and most were formed within the compressional zone. Perhaps this is an area where the groundwater pressure is not high enough to breach the ground surface, but sufficient enough to saturate the soil within 4m of the ground surface. It appears that the groundwater flows upwards and bends around the compacted section, following an easier path.

The groundwater tests indicate that the water is derived from depth within the Banks Peninsula aquifer system, which correlates with the work of Green (2015). The ground shaking brought on by the Christchurch Earthquake is likely to have caused fracturing in the Lyttelton Volcanic Group, which would have allowed new pathways for groundwater to come to the ground surface, as suggested by Stephen-Brownie (2012). It also could have caused a pore-water pressure increase due to collapse and compression of fractures, joints, and fissures in the volcanic rock, which would cause the groundwater to drain to new areas. This would cause an overall rise in hydraulic head within the groundwater system and cause the groundwater level to rise. It could take many years for the groundwater pressure to re-equilibrate due to the vast network of joints within the Lyttelton Volcanic Group, and the 1km distance from the base of the Lyttelton Volcanic Group to the ground surface.

The other high conductivity areas near the ground surface could be perched water above the compacted material that continues into the slope. This water would probably be sourced from meteoric water infiltration. The resistivity within the valley floor material is much more consistent than within the slope and this reinforces the assumption that the resistivity anomaly is related to earthquake induced changes.

The CPT and associated liquefaction anlysis shows that there is potential for 60mm of vertical settlement over the entire soil profile under ULS conditions; however the lack of accuracy of the soil behaviour type casts doubt on the accuracy of this analysis. The groundwater level input for this analysis was 9.0m, although this depth does not correlate with continuous soil saturation and therefore casts further doubt on the liquefaction analysis.

The pore-pressure dissipation tests show that excess pore-pressures are generated in the *in-situ* soil under monotonic loading. This indicates that under static shear stress conditions there is not a dilatory response to monotonic loading. The significance of this result is that if liquefaction were to occur in the saturated layers of the loess-colluvium, then the loss of shear strength would result in a contractive response rather than a dilative response. The macro-behaviour of this would be flow liquefaction and a consequential flow type landslide failure, rather than cyclic mobility and a lateral spread type failure. This will be explained in greater detail in Chapter 5.

3.6.2. Key Conclusions

The shallow and deep subsurface investigation methods for 17 Ramahana Road and Centaurus Park have allowed a good interpretation of the geological model for the Ramahana Road fissure trace. The key findings from Chapter 3 are as follows:

- The fissure trace at 17 Ramahana Road had an opening of 0.45-0.47m near the ground surface, and generally slowly reduced in aperture with depth until it closed to 1-2mm at 2.0-2.1m depth.
- The fissure trace became segmented at ~2.1m depth, but it continued to a greater depth than 3.0m.
- The shear strength values within the fissure trace approach the values outside the trace at 3.0m depth.
- A mixed-colluvium layer that was intercepted by the fissure trace showed no observable vertical offset.
- The fissure trace is steeply dipping at 78°, but it flattens off with depth, and becomes ~40-50° when it becomes segmented at 2.1m depth.
- The resistivity survey showed an anomaly in the centre of the diagram, and its location corresponds with the compressional area. The anomaly shows a relatively

high conductivity area that appears to curve around a relatively high resistivity area towards the ground surface.

- Assessment of groundwater and spring water from various areas in the Hillsborough Valley show a chemical composition similar to the Banks Peninsula aquifer system and relatively high temperatures reflect a deep source.
- The seismic reflection survey shows that the depositional layers follow the same orientation as the slope angle. There are no observable weak spots in the model.
- The CPT did not find any noticeable weak layers.
- The soil behaviour type calculated by the CPT data was shown to be inaccurate when compared to the adjacent borehole logs, which indicates that the loess-colluvium at the site cannot be assessed by traditional CPT methods alone.
- Liquefaction analysis under ULS conditions determined that 60mm of settlement could be possible over the entire soil profile; however the inaccuracy of the soil behaviour type and lack of saturation in the soil profile casts doubt on the accuracy of this analysis.
- Pore pressure dissipation tests recorded an increase in pore-pressure under monotonic loading which indicates that if liquefaction were to occur it would be flow liquefaction and a consequential flow type landslide would occur, rather than cyclic mobility and a lateral spread type landslide.
- Coefficients of permeability values were more analogous to compacted clay than silt with some clay, which is what the soil is largely composed of.

4. Quantitative Assessment: Laboratory and Computational Investigations

4.1. Introduction

The objectives of this chapter are to gain a quantitative understanding of the strength, classification, and slope stability of the soils at 17 Ramahana Road and Centaurus Park to reinforce the qualitative assessment conducted in Chapter 3. To achieve these objectives soil classification tests were conducted on the soil to determine particle-size, Atterberg Limits, and natural moisture contents. These tests were done to assess how the soil profile changes with depth, and what behavioural characteristics would be expected in various sections of the soil profile. Other tests included:

- Natural moisture content tests on samples from the compressional zone at 17 Ramahana Road to test whether the relatively high conductivity and high resistivity area identified in the electrical resistivity geophysical survey reflect relatively higher and lower moisture contents respectively.
- Density tests were conducted on soil obtained from the compressional zone at 17 Ramahana Road to assess whether the soil in the relatively high resistivity area identified in the electrical resistivity geophysical survey showed measurably higher dry density in relation to the soil upslope and downslope.
- Direct shear-box strength testing was conducted on samples of various clay and moisture contents from 17 Ramahana Road and Centaurus Park to test what affect each of these properties had on the shear strength of the soil.
- A slope stability analysis was conducted on two models of 17 Ramahana Road to assess how stable and resistant to shear movement the slope was in its static condition. One model considered the loess-colluvium as a homogeneous deposit, whilst the other split it into four different facies that were reflected in the classification tests. Both models were tested for rotational and translational slide failure.

4.2. Sampling Methodology

Samples were taken from the test pit at 17 Ramahana Road, the hand augers in the compressional zone at 17 Ramahana Road, and the SCIRT borehole core from Centaurus

Park. This allowed testing of samples from the extensional zone (test pit), compressional zone (hand augers), and at greater depths (borehole core).

The test pit samples were taken at every 0.5m depth on the north wall, from undisturbed ground, to understand the vertical changes in the soil profile. Samples were also taken from the puggy infill on both sides of the test pit, and one form within the mixed-colluvium layer. The samples from the puggy infill were taken to quantify the differences between the infill and undisturbed ground. The sample from the mixed-colluvium layer was taken to quantify the difference between this layer and the loess-colluvium around it. A metal cylinder was penetrated into the walls of the test pit and then carefully dug out to obtain the soil samples. The samples taken from the test pit are indicative of the soil properties within the extensional zone at 17 Ramahana Road.

The hand auger samples were taken at every 1.0m depth from 1m to 4m at the end of the auger hole. These samples were taken to quantify the soil properties and test if there were any changes in the properties with depth that correlate to the changes in the resistivity, as recorded by the electrical resistivity geophysical survey. The samples were disturbed due to the nature of retrieval, and were taken by removing ~20cm of hand auger core from each 1m depth. The results of the tests conducted on the samples taken from the hand augers are indicative of the soil properties within the compressional zone at 17 Ramahana Road.

The location of the samples from the SCIRT boreholes were chosen after logging of the soil revealed general behavioural differences between five layers in the soil profile. These five layers from the soil surface to bedrock are described here: a moist to dry top layer that held its shape in the core boxes; a wet to saturated layer that had deformed and spread out in the core box; a section that held its shape and was very stiff to hard, with dry to moist water conditions; a saturated sand to silty sand layer that was completely deformed; and a hard reddish layer with a higher clay and gravel content.

BH-01 and BH-02 did not reach the fourth layer and basalt rock was found below the fifth layer of soil. The fifth layer was determined to be volcanic-colluvium, and no tests were done on this layer because it was very unlikely that this layer was the source of movement due to its low moisture, high density, and great depth. The samples were all taken from the first to fourth layers of loess-colluvium to better determine what made these layers behave differently.

Samples were taken by removing 5cm of borehole core from each depth. The depths of the samples taken are presented in Table 4.1. The results of the tests conducted on samples taken from the SCIRT boreholes are indicative of the soil properties at Centaurus Park from the extensional zone (BH-03, BH-04, BH-05) and upslope from the compressional zone (BH-01, BH-02) and at greater depths than what was tested in the extensional and compressional zones at 17 Ramahana Road.

Sample	Borehole No.	Depth (m)
S1	BH1	1.10-1.15
S2	BH1	4.00-4.05
S3	BH1	7.00-7.05
S4	BH1	13.40-13.45
S5	BH1	14.90-14.95
S6	BH2	5.00-5.05
S7	BH2	8.00-8.05
S8	BH2	12.50-12.55
S9	BH3	2.90-2.95
S10	BH3	8.50-8.55
S11	BH3	14.00-14.05
S12	BH3	17.00-17.05
S13	BH4	12.50-12.55
S14	BH4	15.00-15.05
S15	BH4	21.00-21.05
S16	BH5	1.00-1.05
S17	BH5	3.00-3.05
S18	BH5	14.00-14.05

Table 4.1: Depths of samples taken from SCIRT borehole core.

4.3. Soil Classification

4.3.1. Particle-Size Analysis

Particle size analysis was conducted on the 20th of March 2015 by the method of laser diffraction. The tests were conducted on eighteen samples from various depths within the SCIRT borehole core of BH01-BH05 from Centaurus Park. This method was determined to unsatisfactorily represent the clay fraction of the loess-colluvium, which corresponds to the results of Di Stefano et al. (2010). Figure 4.1 shows the particle-size analysis results for S18 from the laser diffraction method, whilst Figure 4.2 shows the particle-size analysis results for S18 from the pipette analysis. The laser diffraction method determined that there was 10.9% finer than 2μm (i.e. 10.9% clay-sized material); whereas the pipette analysis

determined that there was 18.8% finer than 2µm. It was therefore decided that the pipette method would be used in preference of the laser diffraction method, and to follow NZS 4402:1986 guidelines for particle-size analysis.

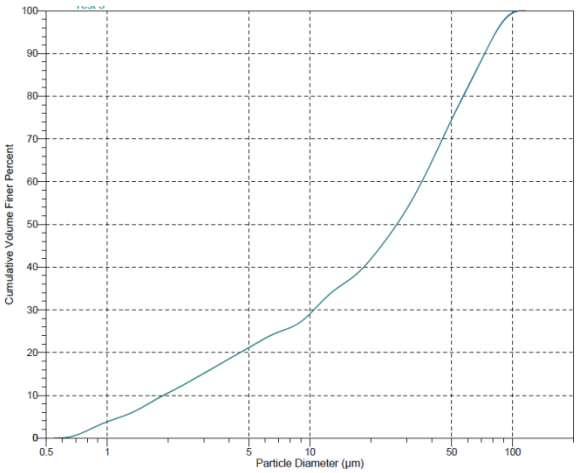

Figure 4.1: Laser diffraction particle-size analysis results for S18 from the SCIRT borehole core.

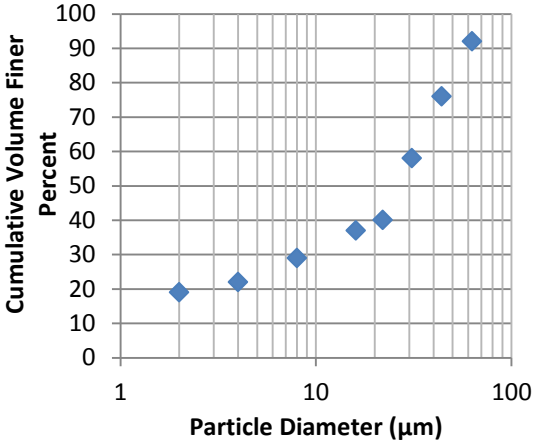

Figure 4.2: Pipette analysis particle-size analysis results for S18 from the SCIRT borehole core.

Particle size analysis was conducted on the same samples from BH1-BH5 by pipette analysis in accordance with NZS 4402: 1986, on the 14th of April 2015. Nine samples from various depths in the test pit were later tested, followed by twenty samples from the hand augers in the compressional zone. Figures 4.3-4.8 show the average particle-size analysis results for the four layers of loess-colluvium identified in the SCIRT borehole core from Centaurus Park, the samples from the test pit within the extensional zone at 17 Ramahana Road, and the samples from the hand augers within the compressional zone at 17 Ramahana Road.

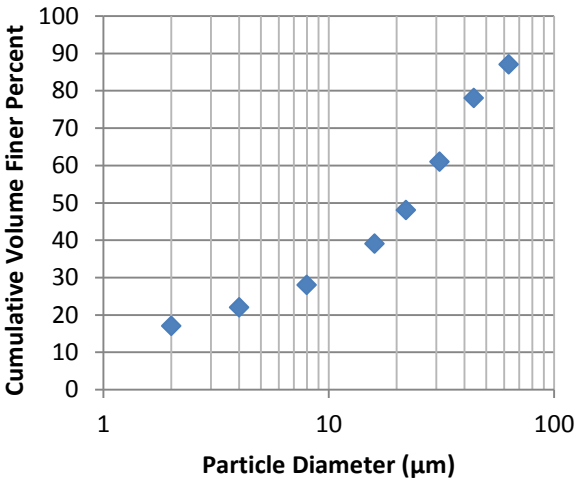

Figure 4.3: Average particle-size analysis results for first layer of loess-colluvium from the SCIRT borehole core.

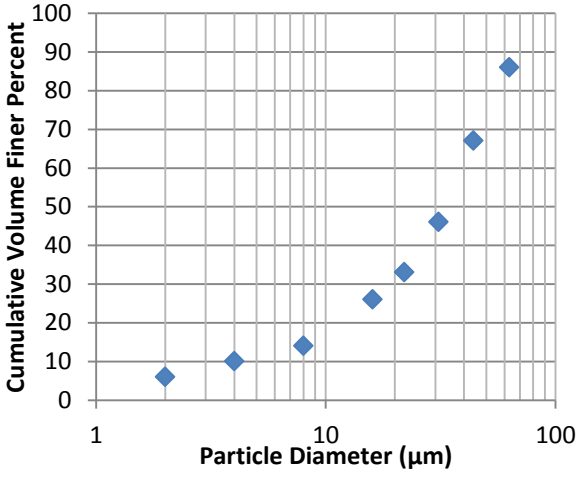

Figure 4.4: Average particle-size analysis results for second layer of loess-colluvium from the SCIRT borehole core.

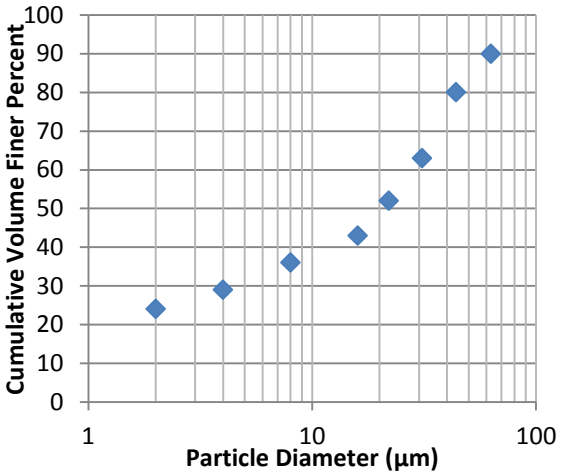

Figure 4.5: Average particle-size analysis results for third layer of loess-colluvium from the SCIRT borehole core.

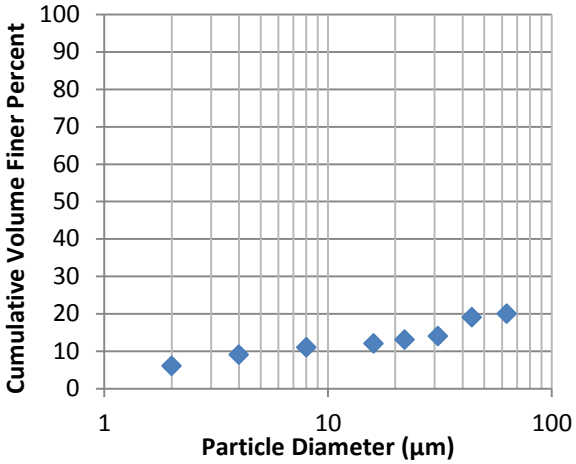

Figure 4.6: Average particle-size analysis results for fourth layer of loess-colluvium from the SCIRT borehole core.

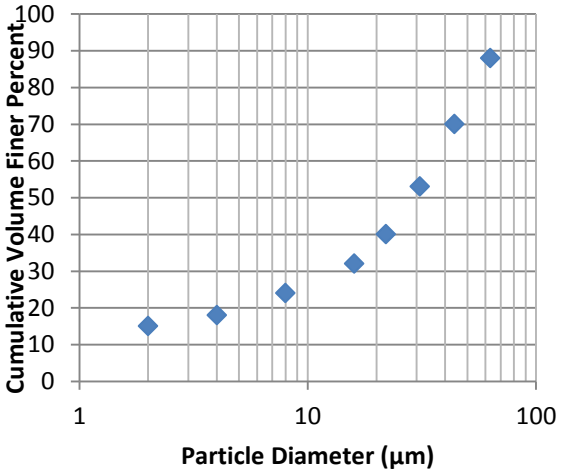

Figure 4.7: Average particle-size analysis results for test pit samples of loess-colluvium from the extensional zone at 17 Ramahana Road.

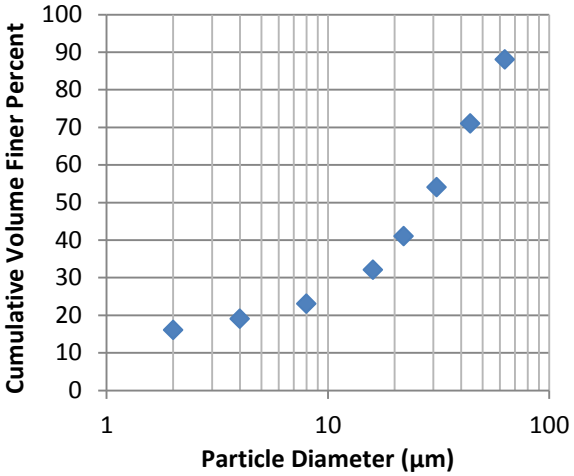

Figure 4.8: Average particle-size analysis results for test pit samples of loess-colluvium from the compressional zone at 17 Ramahana Road.

The particle-size analysis results show similar trends within the surface soils from 17 Ramahana Road and Centaurus Park. There is variance in the results with greater depth: the second layer of loess-colluvium has less of the finer fraction, the third layer has more of the finer fraction, and the fourth layer is predominantly sand. These trends will be discussed in greater detail in section 4.3.4. The results of the particle-size analysis are presented in Appendix 3.1. All of the samples tested by particle-size analysis were also tested for Atterberg Limits and natural moisture contents.

4.3.2. Atterberg Limits

Atterberg Limits tests were conducted on the same soil samples as that were tested for particle-size distribution. These tests were conducted in accordance with NZS 4402:1986. The results of the Atterberg Limits tests are presented in Appendix 3.1.

Banks Peninsula loess generally has a plasticity index of <12, and this is what was found for the loess-colluvium in the first layer near the ground surface, but the plasticity index was shown to decrease to <5 in the second layer, and increase to <15 in the third layer. The samples from the test pit show decreasing plasticity index with depth and all are <6 except for the puggy infill material in the south wall fissure trace which has a plasticity index of 10-11. The samples from the hand augers in the compressional zone had a plasticity index of <12, there was a spread of 3-11 and there were no obvious patterns, the mean and mode were 7.

Figure 4.9 shows that all of the samples can be plotted from CL, OL, or ML on the USCS chart in Figure 4.10, these represent inorganic clays of low to medium plasticity, organic silt and organic silt-clays of low plasticity, and inorganic silts and very fine sands with slight plasticity respectively. Because all of the samples are primarily silt, the most relevant group symbol is ML.

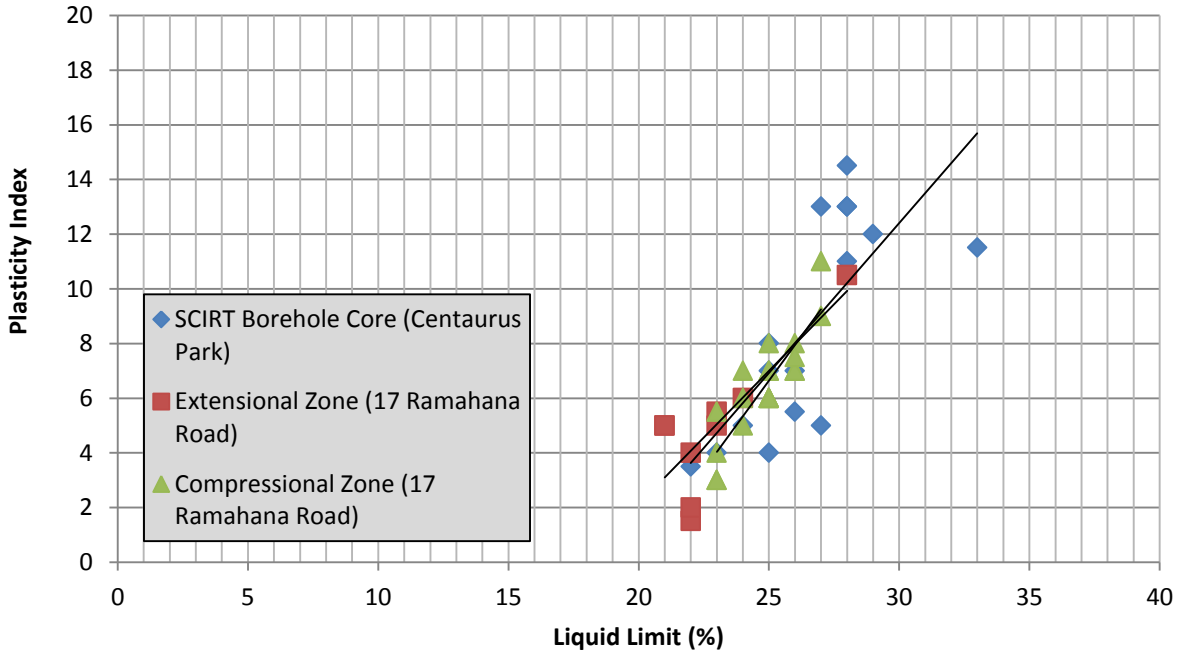

Figure 4.9: Plasticity Index vs Liquid Limit for all samples tested.

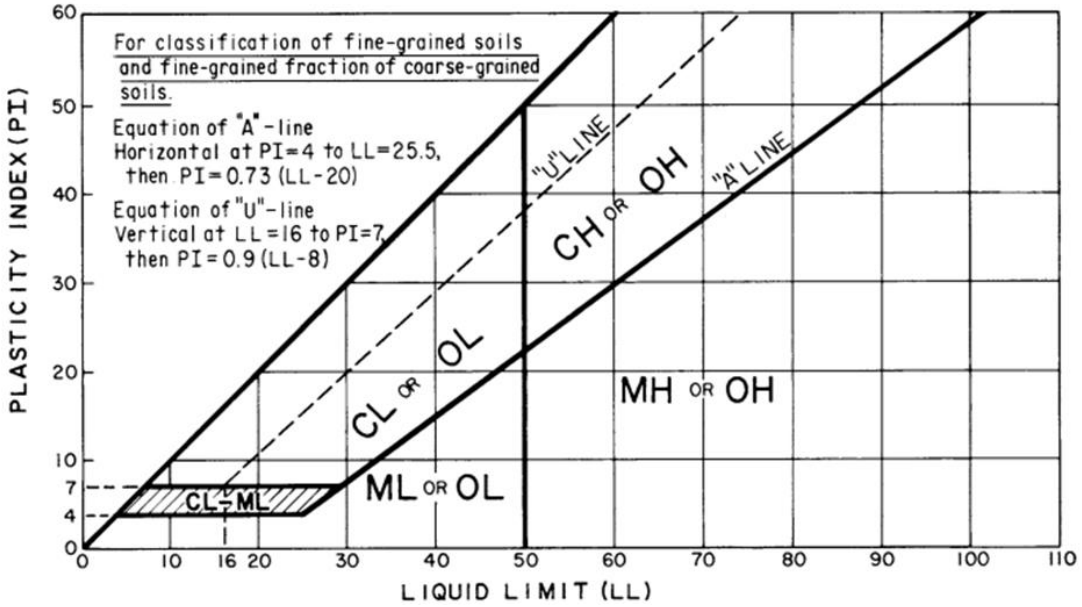

Figure 4.10: Plasticity Index vs Liquid Limit for the Classification of Soil for Engineering Purposes under the Unified Soil Classification System (USCS). Sourced from ASTM (2011).

In all of the samples tested, generally as the clay content increases the plasticity index increases as well. Figure 4.11 shows that this is not a perfect relationship, and this could be for a number of reasons: firstly there are potential human and mechanical testing errors involved, secondly there are different kinds of clays within the loess-colluvium samples that will have different effects on plasticity, and thirdly the pipette analysis determines clay-sized grains, and not exactly clay minerals: a clay-sized grain is any grain under 2µm and this can include clay minerals and any quartz and feldspars of this size which do not necessarily increase plasticity.

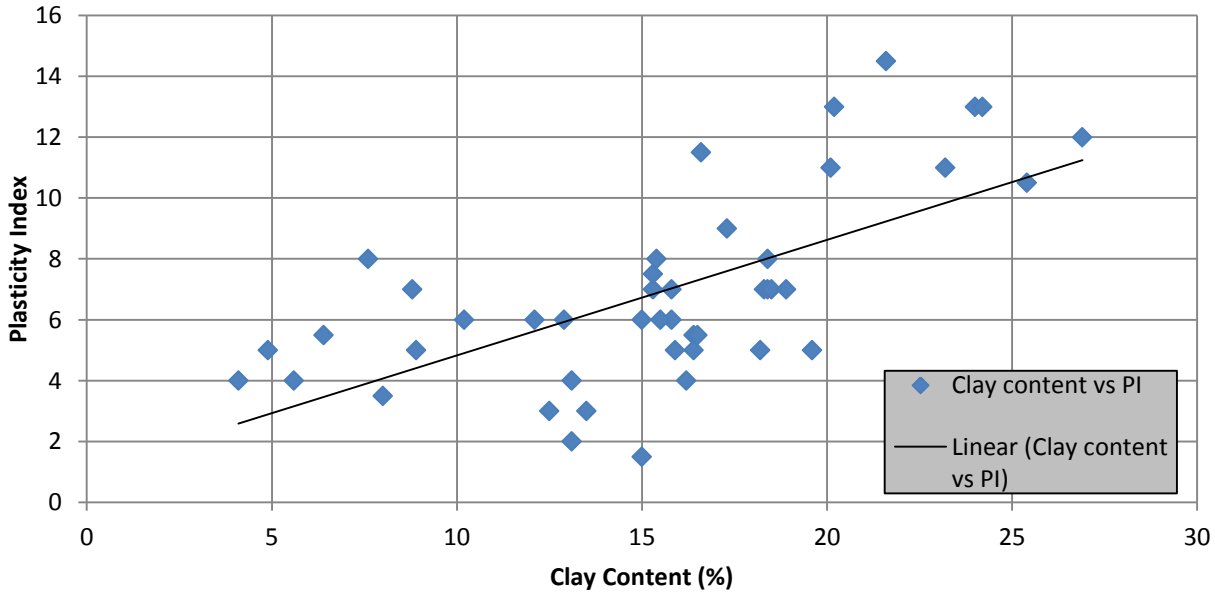

Figure 4.11: Clay content and plasticity index relationships in the loess-colluvium samples tested by pipette analysis.

Bell (1978) explains that a proportion of the clay-sized minerals in Banks Peninsula loess are finely ice-ground quartzo-feldspathic materials, which offer little cohesion and plasticity. Montmorillonite and vermiculite offer more plasticity than the low to non-swelling clay minerals of illite or kaolinite, however these are secondary minerals formed by weathering, and they can be present in differing quantities depending on the climatological history of the site (Bell 1978).

4.3.3. Natural Moisture Contents

Natural moisture content tests were conducted on the same soil samples as that were tested for particle-size distribution and Atterberg's limits. These tests were conducted in accordance with NZS 4402:1986. The results of these tests are presented in Appendix 3.1.

The natural moisture contents generally increased with depth in the surface soil: the test pit samples from the extensional zone at 17 Ramahana Road, the hand auger samples from the compressional zone at 17 Ramahana Road, and the samples from the first layer in the SCIRT boreholes all generally increased in moisture content with depth. Table 4.2 shows the increasing moisture content with depth in the compressional zone at 17 Ramahana Road, refer to Figure 3.10 for the location of the hand augers. Table 4.3 shows the general increase in moisture content in the extensional zone at 17 Ramahana Road, refer to Figure 3.5 for the location of the test pit.

Depth (m)	HA7: MC (%)	HA8: MC (%)	HA9: MC (%)	HA10: MC (%)	HA11: MC (%)
1.0	13	13	12	9	9
2.0	17	17	17	17	17
3.0	18	21	21	21	20
4.0	22	22	22	19	19

Table 4.2: The general increasing moisture contents with depth in the compressional zone at 17 Ramahana Road.

Depth (m)	MC (%)	Depth (m)	MC (%)
0.5	12	2.0	17
1.0	16	2.5	21
1.5	20	3.0	18

Table 4.3: The general increasing moisture contents with depth in the extensional zone at 17 Ramahana Road.

The second layer in the SCIRT boreholes also showed increasing moisture content with depth (16 to 23%) until the soil began to grade into the third layer where it began to decrease in moisture content to 8-10%. The moisture content was recorded to increase again as the third layer graded into the fourth layer where the moisture content reached 20%.

The reason the moisture content tests are significant is because many previous studies on loessial soils have shown that their mechanical behaviour is governed by their moisture content. At low moisture contents (<10%) loessial soil has a relatively high shearing resistance, but this is lowered at increasing moisture contents. The deformation style also changes at different moisture contents: the deformation will be brittle when the moisture content is under the plastic limit, but it will become plastic as the moisture content approaches the plastic limit (PL is ~15-20% for all of the samples tested). This means that where the moisture content is >15% the expected deformation style would be plastic, and at moisture contents of <15% the expected deformation style would be brittle. Hughes (2002) records a brittle-ductile change in loessial soils of Canterbury at moisture contents of 10-15%. The liquid limit for all of the samples tested is ~22-28%, and this is the moisture content at which the soil would be expected to behave more like a fluid under deformation. A moisture content of 23% was only reached in S17 from the SCIRT borehole core, which was located in the second layer.

4.4. Classification Test Trends

The generalized soil profile for the area below Ramahana Road is presented in Figure 4.12. This should only be considered a general guide to the area's subsurface properties, and variations from what has been recorded are possible because the extent of sampling is limited in relation to the area that this soil profile represents. Factors to note in this soil profile are that the silty sand to sandy silt layer can be present as interbedded silts and sands that grade into each other and that all boundaries within the loess-colluvium are gradational. There are no distinct boundaries to be found in any of the core logs (except for where there are mixed-colluvium layers within the loess-colluvium), but there are sharper boundaries between the topsoil and loess-colluvium, the loess-colluvium and volcanic-colluvium, and the volcanic-colluvium and the Lyttelton Volcanic Group.

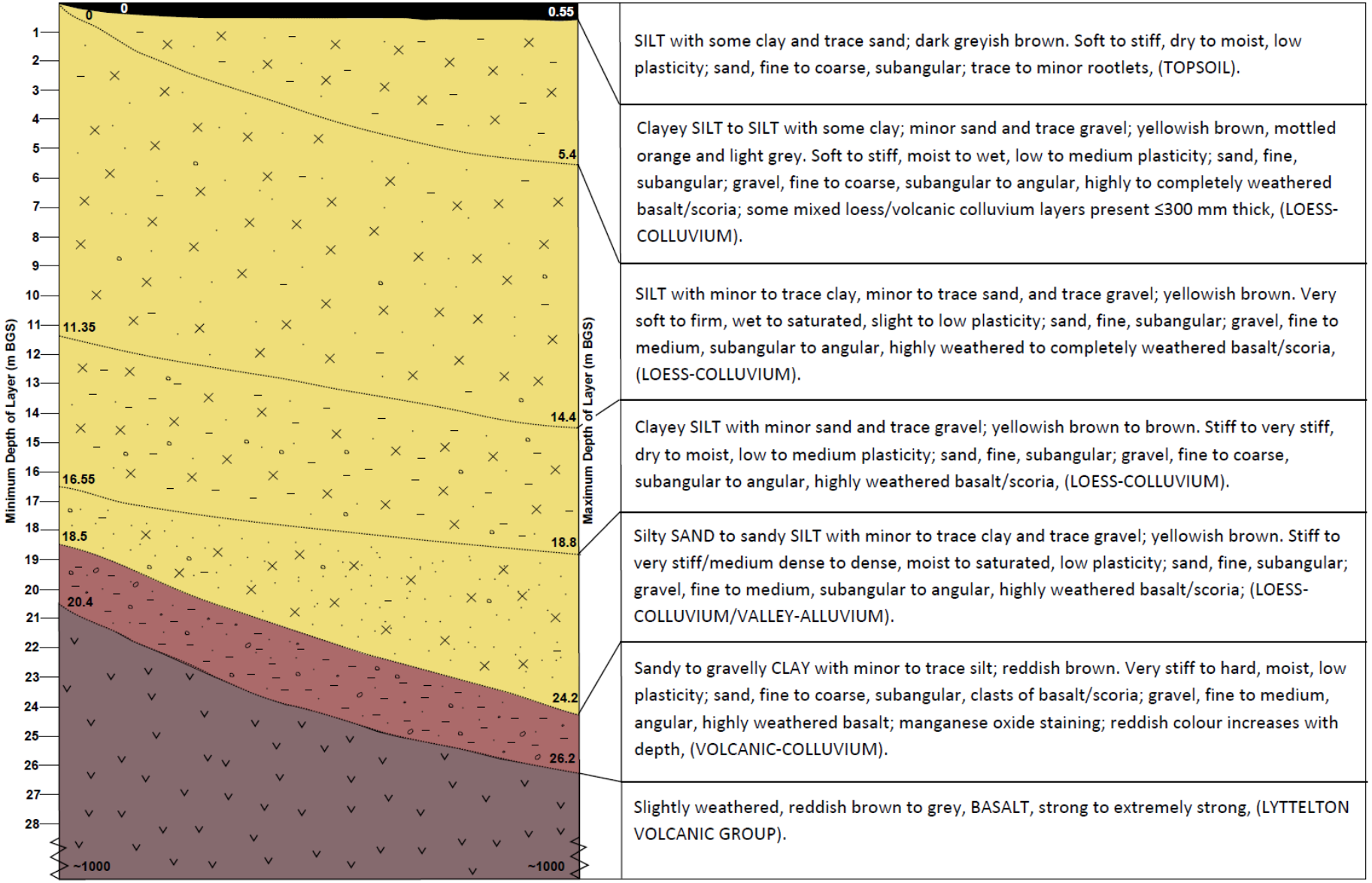

Figure 4.12: Soil profile for the area around Ramahana Road. The four layers of loess-colluvium are nominated as first layer, second layer, third layer, and fourth layer from below the topsoil layer to the volcanic-colluvium layer.

The Lyttelton Volcanic Group is found at a depth of 20.4m at Centaurus Park to 26.2m at 17 Ramahana Road. The joints in the basalt were recorded as subhorizontal, undulating-smooth, and closely spaced. The rock was also moderately to highly weathered and moderately strong, but because this is the surface of the Lyttelton Volcanic Group it is likely to have been more affected by weathering alterations than in deeper sections of the rock.

The Lyttelton Volcanic Group is overlaid by volcanic-colluvium. This layer contains a high proportion of weathered volcanic material mixed with some loess-colluvium, which becomes less prominent with depth. It is generally hard and moist. This layer was formed by the erosion of an upslope outcrop of volcanic rock and its subsequent downslope deposition.

The fourth layer of loess-colluvium is a sandy silt to silty sand. This facies can have layers of silty sand within it up to 3m thick, and interlayered deposits of silty sand and sandy silt ≤1m thick. According to laboratory assessments the silty sand layers within this layer have a clay content of 3.4-8.6%, and a moisture content of 20%. This layer represents a period where the energy behind erosion/deposition was higher. The loessial material must have been reworked to a great extent in order to wash out most of the fine material.

According to laboratory assessments the third layer of loess-colluvium has a clay content of 16.6-26.9%, a moisture content of 8-10%, and a plasticity index of 12-15. Volcanic gravels are located in bands or spread throughout the deposit and they can be from fine to coarse sizing, but they tend to be of similar size in any particular area. This layer is dry to moist, and of generally fine particle-size distribution. The source of the loess may have been from a compact layer of primary loess, which is known to be of higher plasticity than the surface layer or parent layer.

The second layer of loess-colluvium possibly represents a change in the source of loess and climate of the area. It could represent a period when the source of primary loess was down to the parent layer which has high erodibility and tends to be composed of silt with some sand and minor clay with no to slight plasticity. If this layer was deposited during a wetter climate then much of the fine fraction could have been washed out on deposition and deposited farther down the slope. According to laboratory assessments the second layer has a clay content of 4.1-8.9%, a moisture content of 16-23%, and a plasticity index of 3-5.

Because this layer is coarser than the layers above and below it, it has a higher moisture content. The higher moisture content is probably exacerbated by the relative impermeability

of the clayey silt layer below it and above it. Drainage channels through this layer could have resulted in a further loss of clay in a vertical direction towards the clayey silt layer below, and this could have added to the differences in clay fraction between the two layers.

The first layer of loess-colluvium is similar to the third layer except it is not as dense and it has a slightly lower clay content and corresponding plasticity index. According to laboratory assessments this layer has a clay content of 7.6-20.1%, a moisture content of 8-19%, and a plasticity index of 8-12. It also can have a higher moisture content than the deeper clayey silt which reinforces that it has a lower density. The first layer is the ground surface material just below the topsoil, and it is largely above the groundwater level on the slope, but the groundwater level is within it on the valley floor. This layer could represent a period when the climate became drier and therefore the fines were not washed out to the same extent on deposition.

4.4.1. SCIRT Borehole Core from Centaurus Park Sample Trends

The classification tests for the SCIRT borehole core samples from Centaurus Park showed variability, but there were good trends found between the four layers identified previously. Table 4.4 shows the trends found in the four layers.

The soil from the test pit only reached a depth of 3m which is still within the first layer, and therefore the observed trends between the layers at Centaurus Park could not be correlated with 17 Ramahana Road. What was observed in the testing of the soil from the test pit was that with depth, generally the clay content decreased (19.6% at 0.5m to 13.1% at 3m), the moisture content increased (12% at 0.5m to 18% at 3m), and the plasticity index decreased (5 at 0.5m to 2 at 3m). If the soil continues in this manner with further depth then it would eventually become similar to the second layer at Centaurus Park.

4.4.2. Test Pit Samples from Extensional Zone at 17 Ramahana Road Trends

Samples within the test pit show what would be expected if the soil profile follows the same trend to Centaurus Park, but the plasticity indexes are much lower in the test pit samples than in the first layer from Centaurus Park. This implies lateral variation from Centaurus Park to 17 Ramahana Road, but the particle-size analysis results are similar to the first layer at Centaurus Park. The low plasticity index results can be put down to either testing error, alterations to the soil since fissuring and exposure, or most likely, changes in the source material and deposition of colluvium at this location. The particle-size analysis results show

decreasing clay content with depth (19.6% to 13.1%) and the corresponding plasticity index results show decreasing plasticity index with depth (5 to 2). Appendix 3.1 provides the classification test results for the test pit samples from the extensional zone at 17 Ramahana Road.

Layer	Clay Content (%)	Plasticity Index	Moisture Content (%)
First Layer (S1,S8,S9,S16)	7.6-20.1	8-12	8-19
Second Layer (S2,S3,S6,S10,S13,S17)	4.1-8.9	3-5	16-23
Gradational Boundary Between 2nd & 3rd layer (S7,S11)	8.8-18.3	7	18
Third Layer (S4,S5,S8,S14,S18)	16.6-26.9	12-15	8-10
Fourth Layer (S12,S15)	3.4-8.6	N/A	20

Table 4.4: The general trends found in clay content, plasticity index, and moisture content in the four layers of loess-colluvium identified in the SCIRT borehole core from Centaurus Park.

4.4.3. Hand Auger Samples from Compressional Zone at 17 Ramahana Road Trends

The soil from the hand augers HA07 to HA11 had highly variable results. The results from the compressional zone show the highly variable nature of colluvium, the intermixing and interlayering of the soil sourced from upslope and along the valley floor, and perhaps the compression and disturbance due to the movement of the slope and groundwater flow. There is also the potential of mixing of the soil by disturbance with the hand auger, which could have had some influence on the results. Perhaps if the hand augers could have reached a greater depth, then trends may have been observed.

It was expected that the samples from this zone would follow a similar pattern to the soil from further up the slope in the test pit and from Centaurus Park, but the soil profile in this location showed no observable pattern with depth in terms of clay content or plasticity index. Only the moisture content showed any trend with depth, and it generally increased with depth as in the test pit and first layer samples from Centaurus Park. The particle-size analysis results are similar to the first layer in Centaurus Park. Appendix 3.1 provides the

classification test results for the hand augers samples from the compressional zone at 17 Ramahana Road.

4.5. Density Tests in Compressional Zone

It was thought that if the soil from the compressional zone was found to have a greater dry density than the surrounding soil, then the observed compressional features would likely be a response to the underlying soil compacting during the Christchurch Earthquake. Figure 4.13 shows the electrical resistivity geophysical survey results that were introduced in Chapter 3. The area of high resistivity in the centre of the model is thought to represent an area of soil compression and a corresponding decrease in porosity, because its location correlates to the compressional zone at 17 Ramahana Road.

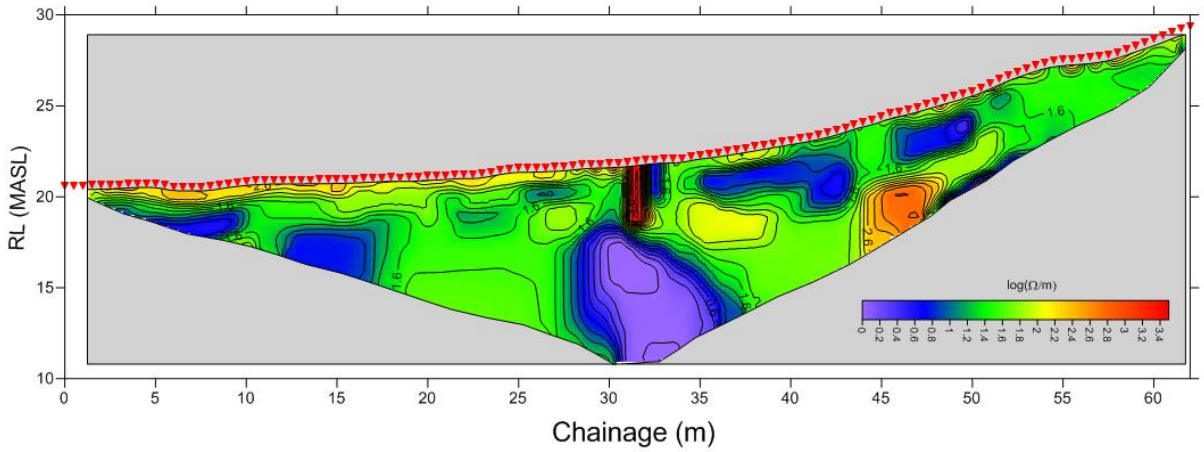

Figure 4.13: The electrical resistivity geophysical survey model for 17 Ramahana Road.

Five *in-situ* samples of loess-colluvium were taken from the compressional zone at 17 Ramahana Road on the 11th of November 2015. The samples were taken from the same locations as the hand auger and DCP locations in the compressional zone, refer to Figure 3.10 where S1-S5 correlates to HA07-HA11 respectively. The samples were obtained by digging to the base of the topsoil at ~0.55m depth and inserting a hollow metal cylinder into the top of the loess-colluvium. The cylinder was then carefully dug out of the soil to cause as little disturbance as possible. The samples were taken back to the lab for dry density testing.

It was assumed the soil would have the highest dry density at S3 because its location corresponds with chainage 33m on the electrical resistivity geophysical survey diagram in Figure 3.13. Table 4.5 shows that it is actually S4 that has the highest bulk and dry density at 2058.5 kg/m^3 and 1793.7 kg/m^3 respectively. This corresponds with chainage 35m which is

slightly upslope of the resistivity anomaly in the Figure 3.13, but there could be error in either the measurement of where the samples were taken from or error in the chainage of diagram, so the actual location of the resistivity anomaly could have been at S4 or between S3 and S4 at chainage 34m. The lowest bulk density was found in S1 at 1921.8 kg/m^3, and the lowest dry density was found in S2 at 1657.7 kg/m^3. The moisture content was lowest in S5 at 13% and highest in S2 at 18%. S5 is the highest point that any of the samples were taken from and S4 is the second highest, so these lower moisture contents probably reflect the increase in slope as well as the increase in dry density.

Sample	Moisture Content (%)	Bulk Density (Kg/m3)	Dry Density (Kg/m3)
S1	16	1921.8	1663.3
S2	18	1955.5	1657.7
S3	16	1944.8	1674.6
S4	15	2058.5	1793.7
S5	13	1937.7	1715.7

Table 4.5: Moisture content, bulk dry density, and dry density of samples taken from the compressional zone at 17 Ramahana Road. All samples taken from ~0.55m depth where it is below the topsoil layer.

It would have been beneficial to gain samples from deeper in the loess-colluvium deposit because, at 0.55m, these samples were located within the near surface soils. Considering that the highly resistive zone in the resistivity anomaly reaches the ground surface it was assumed that testing soil from the near surface would reflect whether the soil had compressed. If deeper samples could have been gained, these would have shown if there was any density variability with depth in the compressional zone. These samples would have had to be gained by excavating a test pit in the compressional zone which was not feasible for this study.

The moisture contents are significant because they reflect how the soil would be expected to compress. The moisture contents are all ≥15% except in S5 where it is 13%. At these moisture contents the soil's shear resistance would be lowered, and it would be expected to deform plastically.

4.6. Direct Shear-Box Strength Tests

Due to sampling constraints the soil samples had to be disturbed and reconsolidated. The only samples that could have been obtained to retain their relatively undisturbed *in-situ* conditions would have been in the test pit, but these would not have represented the entire range of soil

conditions that have been logged and tested from the loess-colluvium profile. Samples were taken from the hand augers done in the compressional zone at 17 Ramahana Road and the borehole core from Centaurus Park. These were chosen because they were representative, in a classification sense, of the soil material at various depths within the loess-colluvium profile, refer to the particle-size analysis results in Figures 4.3-4.8.

Samples were chosen at various clay contents and natural moisture contents to test what effect each of these properties had on the soil shear strength. Previous studies conducted on the shear strength of loess have shown that clay contents and natural moisture contents have the greatest effect on the shear strength of the soil e.g. Higgins & Modeer (1996); Hughes (2002). Bell (1993) explains that density is another property which has a great effect on the shear strength of loess; however the density in the loess-colluvium profile does not appear to show as much variability as the clay content and natural moisture content, and it generally increases with depth. The density of the samples would also have been very difficult to vary with any accuracy for the purposes of this test.

Clay contents of 18-19%, 15-16%, and 5-8% were chosen because they had a good spread and these samples had natural moisture contents below their plastic limit, near their plastic limit, and above their plastic limit. The plastic limits of the samples were 16-19%, and the moisture contents were 8-11%, 16-17%, and 19-22%. These moisture contents are significant because the soil was observed to behave substantially differently at natural moisture contents below, near, and above the plastic limit.

A sample of 10.2% clay was later tested at 10, 16, and 21% moisture content because of the gap of clay content between 15-16% and 5-8%, although it is to be noted that the natural moisture content of this soil was 21% and air drying was conducted on the sample to reach the required subsequent moisture contents. This was undesirable because there are many reasons as to why a soil has any particular natural moisture content and any effort to alter this moisture content can undermine the relevance of the test. Appendix 3.2 shows the method of sample reconsolidation and Appendix 3.3 shows the raw data of the direct shear box strength tests.

The samples were subjected to 20kg, 50kg, and 100kg applied weight and sheared at a constant rate. If the average density of the samples is used (1750kg/m^3), then these weights correspond to overburden depths of 1.45m, 3.64m, and 7.28m respectively. The results were uploaded into specialist software during shearing of the sample, and the raw data was later

analysed to create a failure envelope for the three tested samples at each clay content and moisture content.

4.6.1. Cohesion with Moisture Content and Clay Content

Figure 4.14 shows how the cohesion of the loess-colluvium decreases with increasing moisture content. The amount of clay has influence over the cohesion value at lower moisture contents, but at higher moisture contents its influence is reduced. At a moisture content of 8-10% the higher the clay content, the higher the cohesion; the same trend is seen at a moisture content of 16-17%; however this is to a lesser extent.

At moisture contents of 19-22% (i.e. above the plastic limit) the influence of clay content is unobservable, and the cohesion values are scattered at or below 5 kPa. This could be because the test is a drained test, which causes the moisture to drain from the sample during testing. The samples with less clay are coarser than the other samples tested, and therefore have a greater porosity and permeability. This would make these samples easier to drain when loaded, and it was noticed that more moisture was left in the shear-box test during testing of the coarser samples. The effects of drainage would have less of an effect on the samples with a finer grain-size, but all would have been affected to a certain degree. In hindsight moisture content tests should have been carried out on the samples post-test to quantify this loss of moisture.

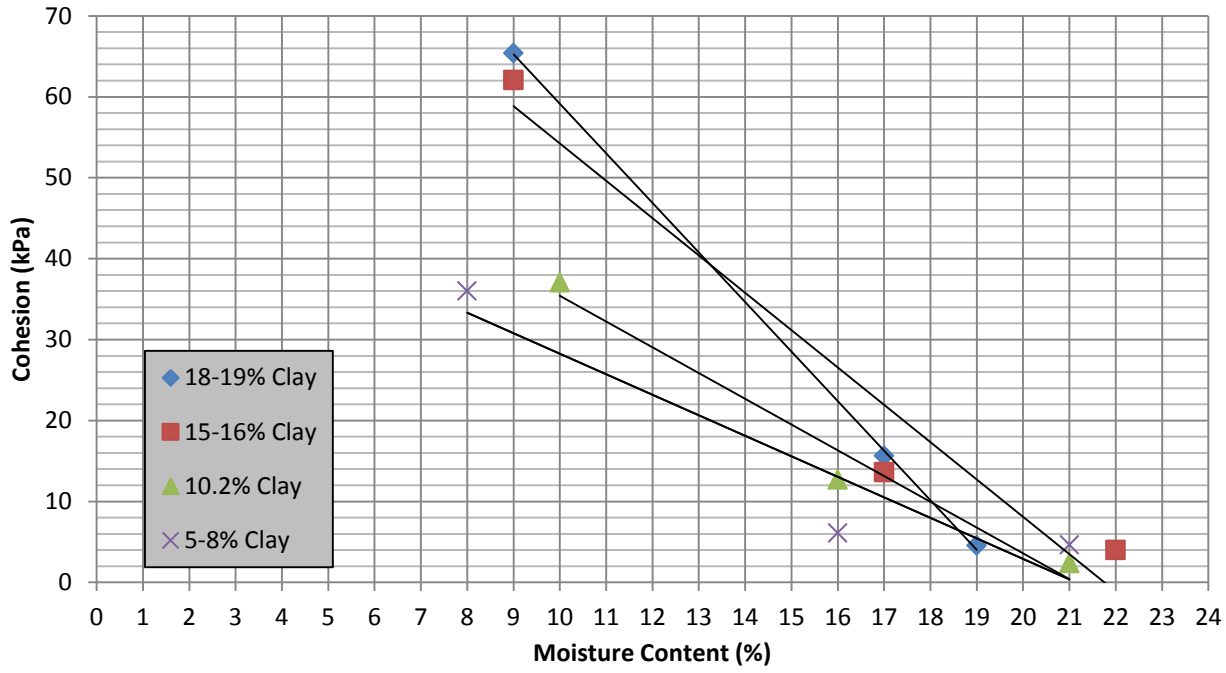

Figure 4.14: The cohesion with moisture content for soil samples of various clay contents as tested by the direct shear-box strength test. Trendlines are linear.

This relationship shows that the strength of the loess-colluvium samples in terms of cohesion is dependent on the moisture content. This suggests that where the soil profile has been found to be at a higher moisture content in natural moisture content tests is where the soil would be more likely to deform under cyclic loading. At higher moisture contents of >15% the deformation is likely to be of the ductile/plastic deformation style (following Hughes, 2012).

4.6.2. Friction Angle with Moisture Content and Clay Content

The friction angles of the sample were less clearly affected by the moisture content. Figure 4.15 shows the relationship between friction angle and moisture content for samples of varying clay contents. The friction angle has been recorded to decrease under increasing moisture contents until ~19% moisture content, and then increases at 21-23% moisture content. The reasons for this are unclear, but perhaps suction and capillary action have a greater effect on friction angle at higher moisture contents.

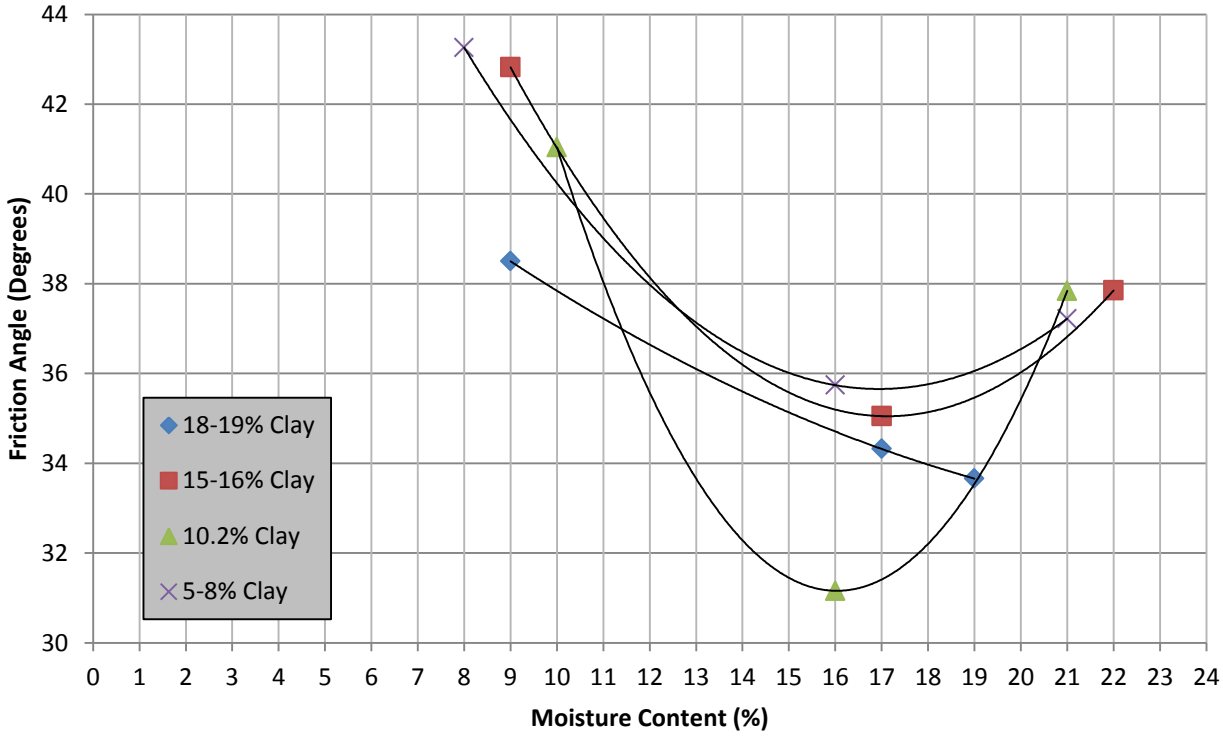

Figure 4.15: The friction angle with moisture content for soil samples of various clay contents as tested by the direct shear-box strength test. Trendlines are polynomial.

There is a considerable amount of scatter in this relationship, and the trends are not as obvious as in the relationship between cohesion and moisture content. The clay content does not appear to have a major effect on the friction angle, but the moisture content appears to have some affect. The scatter and variability can be attributed to the reconsolidated nature of

the samples, and to the differences in the soil samples that were tested. The only consistent properties in this test were the clay content, the density, and the general source area of the samples; however the friction angle is also governed by the contacts between grains, the particle-size distribution, and the void-space, among other factors. Further testing is needed to confirm whether the friction angle decreases with moisture content until 16-19% moisture content and then increases.

4.7. Computational Slope Stability Investigation

4.7.1. Model Inputs

This section calculates the stability of the slope at 17 Ramahana Road under static stress conditions. The purpose of the slope stability analysis is to show how stable the slope was in its pre-earthquake state, and find what factors its stability was most sensitive to. 17 Ramahana Road has been specifically used because this is where most of the information for this thesis has been obtained, and therefore where the most accurate site conditions are known. It must be noted that the soil profile at the site is complex, and the vast and interchangeable features cannot all be accounted for by a simplified computational model.

The factor of safety (FOS) for 17 Ramahana Road was calculated using Rocscience software Slide 5.0. Two models were created for the Slide 5.0 software: one considered the loess-colluvium as a homogeneous deposit with 34 kPa cohesion, 35° friction angle, and 17 kN/m^3 unit weight, and the other split the loess-colluvium into the four facies discussed previously; the data input is outlined in Table 4.2. These inputs are considered to be conservative values and are based on the values found in the shear-box strength tests up to unit 4. Unit 5 and 6 are volcanic-colluvium and the Lyttelton Volcanic Group bedrock respectively, and these values were determined from reviews of previous studies on the strength of these units.

Unit	Cohesion (kPa)	Friction Angle (°)	Unit Weight (kN/m^3)
1	65	39	14
2	5	37	15
3	16	34	16
4	0	39	17
5	300	45	19
6	3000	30	27

Table 4.6: Slide inputs for different geological units

The water levels found in BH-RMH-02 and BH-RMH-03 were also inputted as the water table, which may or may not be correct, as these water levels could be simply indicative of layers of higher saturation within the loess-colluvium deposit. The water level is also a conservative estimate. The layered model is more conservative than the homogeneous model because its layers are defined as discontinuities when in reality they are gradational boundaries between facies in a singular deposit. The translational slide failure planes were identified by adding a polygonal potential surface along the water table within the 2nd layer of loess-colluvium in the layered model, this was kept in the same location in the homogeneous model.

4.7.2. Model Outputs

Bishop modified method and Janbu's generalized procedure of slices methods of limit equilibrium were used to calculate the FOS for rotational and translational slide surfaces respectively. Both are presented because these limit equilibrium methods can be used interchangeably for rotational or translational failures, but the Janbu method is more applicable to non-circular slip surfaces. Table 4.7 outlines the lowest FOS slip surface calculated by the models.

Type of Failure Surface	Type of Model	Limit Equilibrium Method	
		Bishop	Janbu
Translational	Homogeneous	5.1	4.8
	Layered	6.8	6.5
Rotational	Homogeneous	3.9	3.4
	Layered	3.3	3.1

Table 4.7: FOS equated by Bishop and Janbu methods for translational and rotational failures in homogeneous and layered models of 17 Ramahana Road.

According to the stability analysis results in Table 4.7 the slope can be considered extremely stable under static stress conditions. The higher FOS recorded for the translational slide failure plane possibly reflects that the polygonal potential surface was not located in the right orientation and location to identify the lowest potential FOS. The polygonal potential surface was located where it would interact with the inputted water table and follow the location and orientation of the fissure traces if they are the head-scarps of slide failures, and the compressional zone is the toe of the slide.

4.7.3. Sensitivity Analysis

A sensitivity analysis was then conducted on the deposit to test which factor, out of cohesion decrease, or pore-pressure increase (i.e. unit weight decrease), would have the greatest effect on the stability of the slope. The cohesion was dropped to 0 kPa, and the unit weight was dropped to 12 kN/m^3. Both values are considered to be highly conservative. These changes were only brought on in the 1st and 2nd layer of the layered model, but it was applied over the entire loess-colluvium profile in the homogeneous model. The lowest FOS was often recorded as a failure of the retaining wall at the top of the slope, and these values were ignored because they had no reflection on the actual location of movement; these failures still had a FOS of ~1.5 however. Table 4.8 outlines the changes in the lowest FOS slip surface in response to changes in the strength of the loess-colluvium.

Loss of Either Cohesion or Unit Weight	Type of Model	Limit Equilibrium Method	
		Bishop	Janbu
Cohesionless - Rotational	Homogeneous	2.4	2.2
	Layered	2.3	2.2
Cohesionless - Translational	Homogeneous	2.6	2.4
	Layered	2.9	2.7
Loss of unit weight – Rotational	Homogeneous	3.7	3.3
	Layered	3.1	2.9
Loss of unit weight - Translational	Homogeneous	5.5	5.2
	Layered	7.4	7.0
Loss of unit weight and cohesion – rotational	Homogeneous	2.0	1.7
	Layered	2.1	1.9
Loss of unit weight and cohesion – translational	Homogeneous	2.5	2.3
	Layered	2.8	2.7

Table 4.8: Sensitivity analysis considering the soil in a cohesionless state and with a loss of unit weight.

The FOS of the slope is reduced by a decrease of cohesion and unit weight for rotational slide failures, but a decrease in unit weight increases the FOS for a translational slide. The increase in FOS due to unit weight decrease on the translational slide model indicates that there is less driving stress on the failure plane under this scenario. When there is a decrease in cohesion and a decrease in unit weight for a rotational slide the FOS reaches its lowest values of ~2. The decrease in cohesion and unit weight for a translational slide causes this model to reach

its lowest value of ~2.5. The slope did not become unstable (i.e. with a FOS of <1) in any scenario.

The actual failure conditions observed at 17 Ramahana Road were not replicated by any of the inputs. If the fissure traces are the head-scarps of incipient landslides, and the compressional features are the toe of the slide, then in every scenario the lowest FOS slip surface did not follow the slip planes of the fissure traces. This could be for several reasons, the first reason is the simplified nature of the models, the second is that the cyclic stress induced by the earthquake is not accounted for in this analysis, and the third is that the fissure traces are not slide type movements. Appendix 3.4 shows exported pictures from Slide 5.0 that show the 10 slip surfaces with the lowest FOS for a rotational slide failure on the layered model and the slip surfaces with FOS <2.66 for a translational slide failure on the homogeneous model respectively. The latter picture is to show a slide plane that follows the fissure traces if they are the head-scarps of landslides.

It should be noted that this analysis does not account for any loss of strength in the toe material, or stress induced by horizontal earthquake inertia forces. The sensitivity analysis only encompasses factors that can arise within the slope that decrease the strength of the slope material, and not factors that arise outside the slope.

4.8. Discussion and Synthesis

There were four layers identified in the loess-colluvium profile that have distinct geotechnical characteristics. The vertical changes observed in the profile are thought to be related to changes in the source material and climatological changes during the depositional history of the site. It is hypothesised that the different layers would behave differently under cyclic loading. The second layer would be most likely to deform plastically under cyclic loading due to the low clay content (4.1-8.9%) and high moisture content (16-23%), whilst the first layer would deform in a more brittle fashion due to its higher clay content (7.6-20.1%) and lower moisture content (8-19%).

The density tests in the compressional zone show that the soil dry density is similar at S1 to S3 (from 1657.7 kg/m^3 to 1674.6 kg/m^3), but it increases to 1793.67 kg/m^3 2m upslope at S4. 2m further upslope at S5 the dry density decreases to 1715.7 kg/m^3, which suggests that the dry density begins to decrease with farther distance upslope, and this is what would be expected from the electrical resistivity geophysical survey in Figure 4.13 and from the

location of the compressional features. These results suggest that the resistivity anomaly in the electrical resistivity geophysical survey diagram, and the compressional features in the valley floor, depicts compaction of the toe slope material as a result of the Christchurch Earthquake induced ground shaking.

The direct shear tests show that the cohesion rates of the loess-colluvium are greatly affected by the moisture content. Samples of 8-10% moisture content show good cohesion values of up to 65 kPa in samples of 18-19% clay, whilst a minimum cohesion value of 36 kPa was recorded in the samples with 5-8% clay. The cohesion values drop to $\leq$ 5 kPa, and as low as 2 kPa when the moisture content is 19-22% regardless of clay content. This large drop in cohesion upon wetting is consistent with past studies on the shear strength of loess. Judging from these tests, it is likely that if there was any deformation in the loess-colluvium deposit then this would be most likely to occur within layers of loess-colluvium with a higher moisture content, and to a lesser extent, a lower clay content.

The computational analysis shows that the site under static stress conditions should be considered very stable. The sensitivity analysis shows that the FOS is lowered by both a loss of cohesion and a loss of unit weight, except in the translational slide type failure where a decrease in unit weight increases the FOS. Both of these factors can be induced within the loess-colluvium deposit by a build-up of pore-water pressure due to cyclic stress. The lowest FOS of ~2 and ~2.5, for the rotational and translational slide failure types respectively, are found when there is a decrease in cohesion and a decrease in unit weight.

The decrease in cohesion and unit weight would be extremely unlikely to occur for several reasons: firstly the first layer or loess-colluvium does not have a high enough moisture content to be considered likely to become completely cohesionless under cyclic stress, secondly the slip planes developed by the computational analysis with the lowest FOS do not follow the fissure traces if they are the head-scarps of landslides, and thirdly the loss of normal stress to 12 kN/m^3 is highly conservative and would require a higher moisture content in the soil profile.

What the computational analysis indicates is that this slope should not be considered unstable under static stress conditions, and could only become unstable, in terms of slide type failure, under extreme circumstances that were not met in this analysis. Other slope stability analyses using different computer software that consider horizontal earthquake inertia forces and

cyclic stress would be beneficial in future research to test the results of this computational analysis.

4.9. Key Conclusions

The quantitative assessments in this chapter have reinforced some of the key conclusions and assumptions made in Chapter 3. The key findings from Chapter 4 are:

- There are four facies in the loess-colluvium deposit at the site, from ground surface to depth these are: clayey silt to silt with some clay, silt with minor to trace clay, clayey silt, and sandy silt to silty sand with trace clay. It is hypothesised that the four facies identified would display different behavioural characteristics to cyclic loading.
- Direct shear tests show that moisture content has a large effect on the shear strength of the loess-colluvium. Samples with a moisture content of 8-10% had cohesion of ≤65 kPa, whereas samples with a moisture content of 19-22% had cohesion of ≤5 kPa.
- The clay content was shown to affect the shear strength of the soil at low moisture contents, but it had no affect at high moisture contents (19-22%). The higher the clay content the higher the shear strength, at low moisture contents of 8-10% and to a lesser extent at 16-17% moisture content.
- Density tests in the compressional zone found that the sample taken from the relatively high resistivity area in the electrical resistivity geophysical survey was higher in dry density than the surrounding soil.
- Computational slope stability analysis determined that the slope can be considered very stable in static conditions with a FOS of ~3-7.
- The FOS did not drop below 1 in any of the models. The lowest FOS was ~2, which was found for the rotational slide, layered and homogenous model with a loss of cohesion and unit weight.
- None of the lowest FOS slip planes generated in the computational analysis followed the fissure trace as a head-scarp, and all were generated upslope. The slip planes that followed the fissure trace as a head-scarp had some of the highest FOS in every analysis.

5. Potential Mechanisms of Fissuring

5.1. Introduction

This chapter provides a discussion about possible landslide movement types in relation to the Ramahana Road fissure trace. It draws upon surface observations, subsurface information, and soil mechanics theory to suggest what movement type and mechanism is most likely to have led to the fissure development.

Before the possible interpretations are explored it would be prudent to first define what a landslide is. Cruden (1991) states that:

> *'One obstacle to a simple definition of "landslide" is the erroneous assumption that a landslide is, simply, a slide of land. A similar linguistic analysis would suggest that a cowboy is a male calf.'* (p.1)

The term landslide is not to be confused with a slide failure, which is a type of landslide that indicates movement along a basal shear or slide surface (Cruden and Varnes 1996). There are many types of landslides, and the most generally accepted classifications are those originally defined by Varnes (1978), and later expanded on by Cruden and Varnes (1996). The simplest and broadest definition of a landslide is offered by Cruden (1991), who describes it as 'the movement of a mass of rock, debris or earth down a slope'. While it would be presumptuous to define the Ramahana fissure trace as a slide failure without extensive subsurface investigations, the classification of the fissures as a consequence of landslide movement cannot be overlooked. Figure 5.1 is a diagram of the principal failure types as classified by Cruden and Varnes (1996).

Terzaghi (1950) divided the causes of landslides into two categories: external causes and internal causes. The former embraces any mechanism that arises outside of the mass that causes the mass to exceed its shear strength, whilst the latter arises within the mass, and reduces the shear strength to the extent where the external forces can overcome it. External causes include: an increase in weight of the slope material, by either removal of the slope toe or overloading the top of the slope; saturation by water; earthquake ground motion; and gravity. Gravity is a factor in every landslide case, and considered simplistically the steeper the slope, the greater the chance of landslide failure (Bell 1999). Internal causes are generally

related to subsurface water effects, including pore water pressure; subsurface piping; deflocculation of clay minerals; and swelling/shrinking effects.

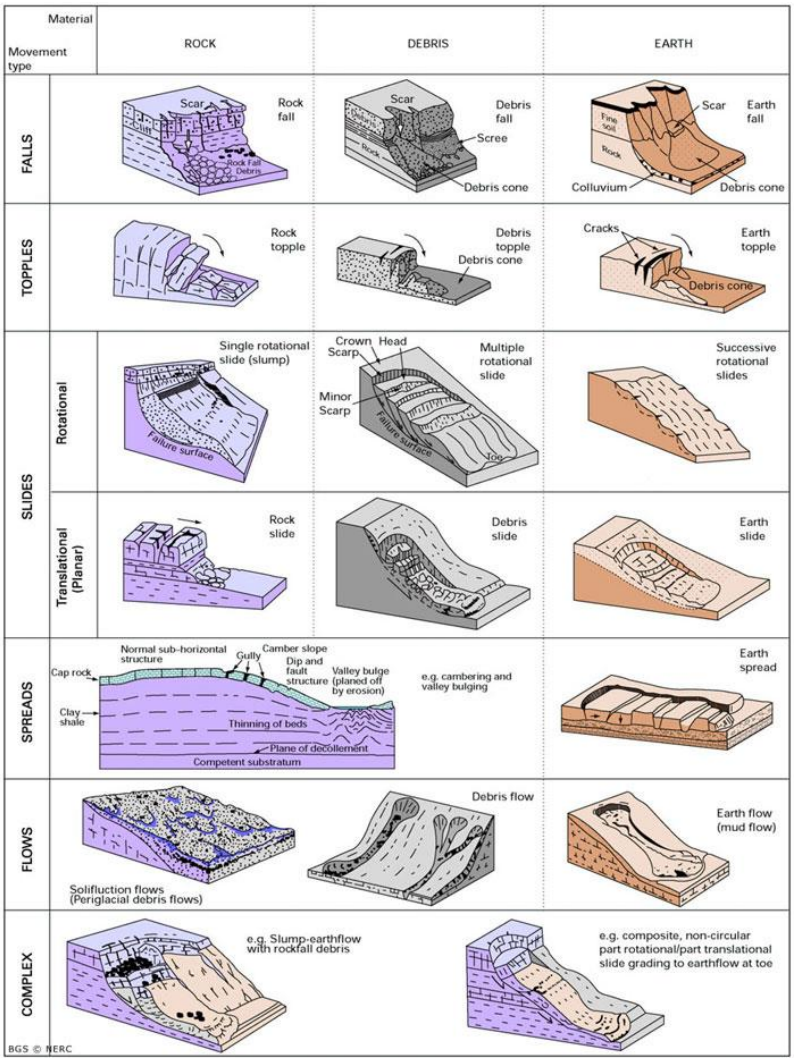

Figure 5.1: Landslide classifications. From Cruden and Varnes (1996). Note that movement in loessial soils comes under 'earth material'.

Landslides are primarily formed under the influence of water and gravity, although a number of other complex and interrelated processes will also affect landslide development. Normally there is a combination of processes that lead to a slope being unstable, but a principal triggering mechanism that sets the mass into motion (Bell 1999). In the case of the Ramahana Road fissure trace it can be said with confidence that the principal triggering mechanism was the Christchurch Earthquake.

5.2. Factors Involved in the Fissure Trace Movement

Bell (1999) describes how landslides are often associated with earthquakes, mostly within 40km of the earthquake epicentre, although the topography and the weather over the previous days have a great influence on their occurrence. Ambraseys and Srbulov (1994) explain that the likelihood of a landslide occurring on a given slope during an earthquake is dependent on the material strength, slope configuration, and ground motion. There are, however many factors other than earthquake magnitude that influence the observed ground motion at a given site, and therefore the likelihood of landslide occurrence. These include but are not limited to; distance from site, focal depth, duration, topography, and material type. Section 5.2 is an attempt to bring together all of the unique factors that may have played a part in where and why the fissure opened.

5.2.1. Earthquake Ground Shaking Intensity and Location of Port Hills Fault

0.85g vertical peak acceleration and 0.35 and 0.40 peak orthogonal horizontal components were recorded (Kaiser et al. 2012) at Cashmere High School, which was the nearest GeoNet station to 17 Ramahana Road (~2.5 km to the west). Figure 5.2 is a model of the orientation and location of the Port Hills Fault and epicentre of the 22 February, 2011 Christchurch Earthquake, in relation to the location of the fissure traces. The fissure traces are all located on the north facing valleys within 7km of the earthquake epicentre. This suggests that high ground shaking intensity was needed to induce the fissure trace movement.

It is also interesting to note that the fissure traces are all to the east of where the Port Hills Fault extends beneath the Port Hills, and to the west of this the occurrence of the fissure traces ceases. This suggests that a factor involved in the generation of the fissure traces could have been uplift of the Port Hills in relation to subsidence of the Christchurch city flat lands. The fissure traces roughly occur on the boundary of this difference in movement (see also Figure 2.17).

5.2.2. In-Filled Valleys

Nearly all of the fissures form upslope from Lyttelton Volcanic Group valleys which have been in-filled with loess-colluvium and valley alluvium, and there are two compelling reasons as to why this could be so. The first is that there is a greater thickness of loess-colluvium at the toe of the slopes which means there is more potential for the loessial soil to

accumulate strain, and simply more loessial soil that could be affected by cyclic stress. The second reason is that the in-filled valleys have a higher moisture content than on steeper slopes due to the effects of drainage. The higher moisture content in the valleys suggests that there is a greater potential for plastic deformation.

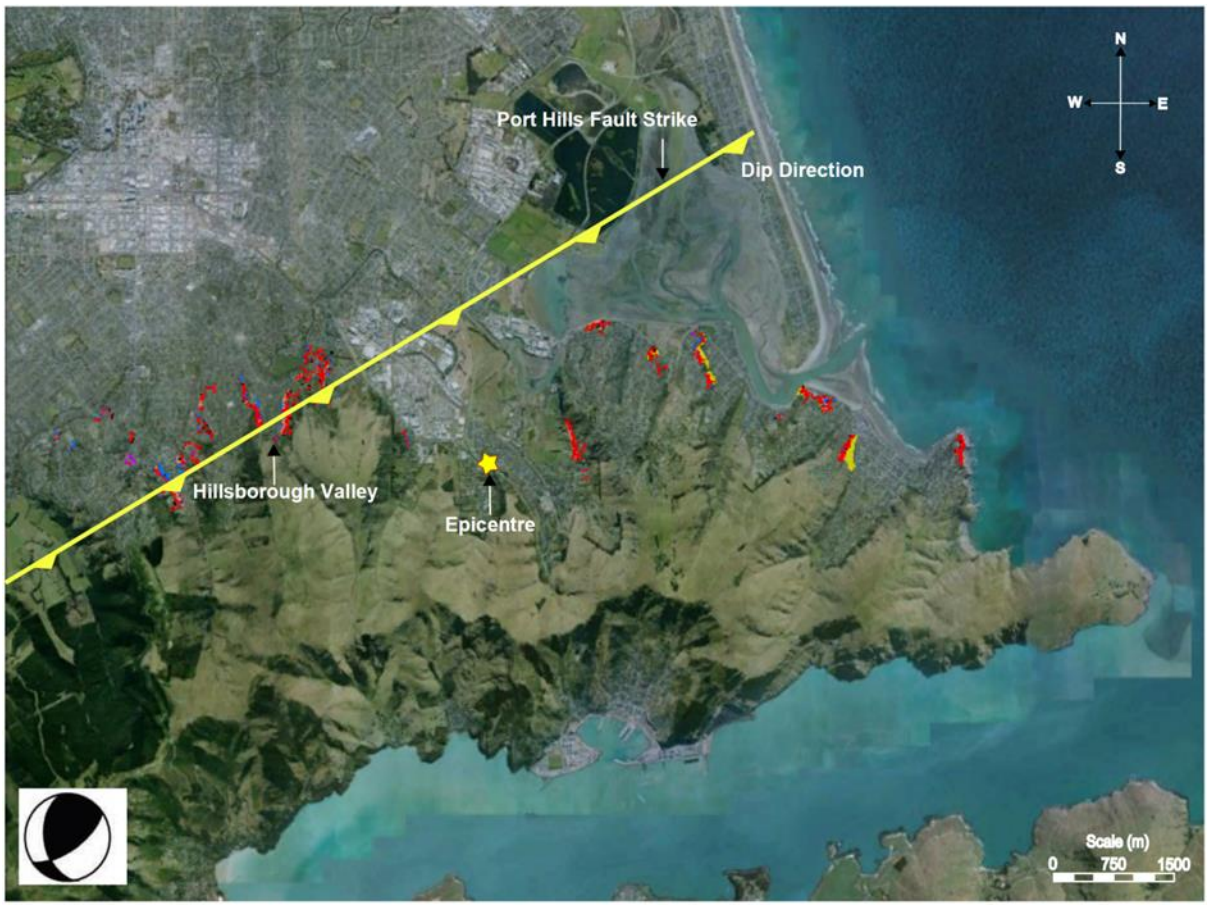

Figure 5.2: Fissure traces in relation to the 22nd of February 2011Christchurch Earthquake epicentre and Port Hills fault. Fissure traces mapped by Massey et al. (2013), map modified from Project Orbit. Fault orientation and location after Kaiser et al. (2011).

5.2.3. Steepness of Slope

All of the fissure traces occurred at the toe of the slope and not at steeper gradients upslope where the static driving forces on the slope should be higher. This suggests that static driving stress was not a major factor in the development of the fissures. A factor that adds to the resistance of the steeper slopes is that they have a lower natural moisture content due to the effects of gravitational drainage, which makes them have a higher cohesion. Another factor that adds to the resistance of the steeper slopes is that normal stress is more favourably orientated against horizontal earthquake inertia forces on steeper slopes.

5.3. Surface Features of the Fissure Traces

Before the potential landslide movement types are explored in detail, it is necessary to gather the strikingly similar observations at other sites where the fissure traces are present. Table 5.1 is a summary of the common features observed at all fissure trace sites.

Observations
The fissure traces occur in gently sloping, toe slope positions
They follow a roughly contour parallel orientation
They tend to have greater horizontal than vertical displacement, leaving open traces
They tend to occur near a convex break in the slope
The fissures are open near the ground surface and gradually lose aperture with depth to <5m
The fissure traces are long and linear and progress non-continuously for up to <1 km
Very little surface deformation is observed on the soil downslope of the fissures
Compressional features tend to be observed near the very base of slope
The fissures only occurred following the February 22nd 2011 Christchurch Earthquake
Subsequent movement has only been associated with moderate to strong earthquake ground motion
New springs arose contemporaneously with the fissuring following the February 22nd 2011 Christchurch Earthquake

Table 5.1: Observations of fissure trace features.

Two current hypotheses for the landslide type, as previously mentioned, are the toe slump failure in loess by Massey et al (2013), and the toppling failure along sub-vertical fractures in loess by Stephen-Brownie (2012). Papers by Wieczorek (1996) and Keefer (1984), are relevant, with the former explaining that the most common types of landslides triggered by earthquakes are rock falls and soil/rock slides on steep slopes of relatively shallow disaggregated material; and the latter explaining that earth spreads, earth slumps, earth block slides, and earth avalanches are very common on gentler slopes during earthquakes. The Ramahana Road fissure trace is more likely to be one of the types described by Keefer (1984) due to its gentle slope in earth material. The earth spread, slump, and block slide are particularly of interest, but the earth avalanche (a type of flow mass movement) does not fit the observations at Ramahana Road.

Some principal mass movement types will not be considered due to the nature of the observed features along the Ramahana Road fissure trace. Falls and flows are not considered, as the former are defined by a free fall motion off a shear face, whilst the latter are defined by strong internal deformation where the mass resembles a viscous fluid (following Cruden and Varnes 1996). Neither of these are applicable to the Ramahana Road fissure trace.

5.4. Earth Rotational Slide/Slump

5.4.1. Terminology

Slide movement is currently the generally accepted form of movement for the Ramahana Road fissure trace, largely due to the work of Massey et al. (2013) who classified the type of movement as a toe-slump in loess. Figure 1.2 is a diagram of how the loess toe-slump movement was visualised by the authors. A slump is a synonym for a rotational slide, and this implies that the loessial soil moved as a mass in an outwards and downwards direction, on a concave-upward basal shear surface (Cruden and Varnes, 1996).

Rotational slides generally occur in cohesive soils, as these often exhibit relatively uniform strength with increasing depth (Bell 1993). They also occur in homogeneous soils, such as fills (Cruden and Varnes 1996), and in highly weathered and extremely weak rock masses. The Ramahana Road fissure traces are within loess-colluvium, which is heterogeneous and any planes of weakness would be along the contacts between different depositional units parallel to the slope.

Cruden and Varnes (1996) describe how the head-scarp of a rotational slide may be almost vertical in profile, as the head of the displaced mass moves in an almost vertically downward direction, but the upper surface of the displaced material tilts backwards towards the head scarp, due to the concavity of the basal shear surface. A modified section of Rib and Liang's (1978) table of *features that aid recognition of common types of slope movements* is presented in Table 5.2, with a typical plan view of a rotational slide failure in Figure 5.3.

5.4.2. Mechanisms of Rotational Slide Movement

Figure 5.4 is a block model of 17 Ramahana Road interpreting the fissure traces as being caused by sliding on a circular basal shear surface. The mechanisms involved in this movement are theoretical liquefaction of the slope toe material, and pore-water pressure build-up along a potential curved basal shear surface. The mechanisms of rotational slide

Earth rotational slides			
Parts surrounding the slide			
Crown	Main Scarp	Flanks	
'Has numerous cracks that are mostly curved concave toward slide'	*'Is steep, bare, concave toward slide, and commonly high; may show striae and furrows on surface running from crown to head; may be vertical in upper part'*	*'Have striae with strong vertical component near head and strong horizontal component near foot; have scarp height that decreases toward foot; may be higher than original ground surface between foot and toe; have en echelon cracks that outline slide in early stages'*	
Parts that have moved			
Head	Body	Foot	Toe
'Has remnants of land surface flatter than original slope or even tilted into hill, creating at base of main scarp depressions in which perimeter ponds form; has transverse cracks, minor scarps, grabens, fault blocks, bedding attitude different from surrounding area, and trees that lean uphill'	*'Consists of original slump blocks generally broken into smaller masses; has longitudinal cracks, pressure ridges, and occasional overthrusting; commonly develops small pond just above foot'*	*'Commonly has transverse cracks developing over foot line and transverse pressure ridges developing below foot line; has zone of uplift. No large individual blocks, and tress that lean downhill'*	*'Is often a zone of earth flow of lobate form in which material is rolled over and buried; has trees that lie flat or at various angles and are mixed into toe material'*

Table 5.2: Surface features of earth rotational slides that aid in their recognition. After Rib & Liang (1978).

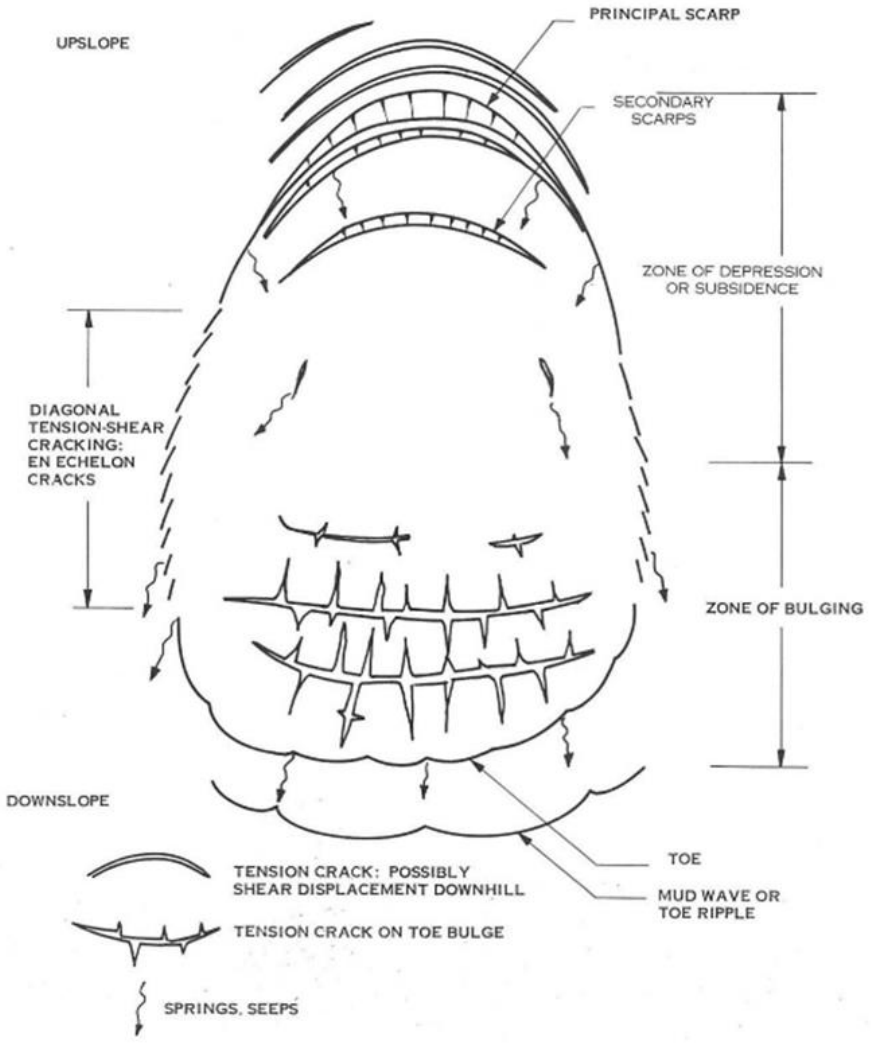

Figure 5.3: Plan view of a rotational slide failure showing typical features. After Sowers and Royster (1978).

movement are very similar to that of translational slide failure, but it is the movement of the soil mass that is distinctly different when comparing the two landslide movement types due to the different shapes of the basal shear surface. The basal shear surface and movement depicted in Figure 5.4 does not show a good correlation to the surface features observed. Because translational slide movement is considered to be much more likely than rotational slide movement, these mechanisms are covered in more detail in section 5.5.2.

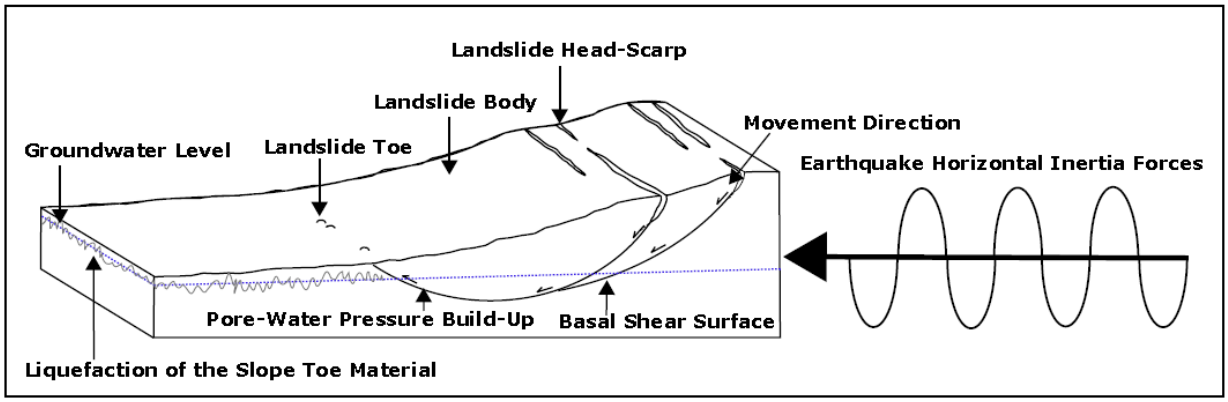

Figure 5.4: Rotational slide movement model. The slope, fissure traces, and compressional features are modelled from 17 Ramahana Road. The mechanisms of movement are hypothetical.

5.4.3. Interpretation of Rotational Slide Movement

The features that suggest rotational slide movement are the vertical displacement of the landslide head, and the compression at the toe, but these features can be explained by other landslide movement types which have a better correlation with the surface features. One of the most striking discrepancies between the features that aid recognition of a rotational slide movement, and the features of the Ramahana Road fissure trace, is that the cracks at the crown do not curve concavely toward the slide. In fact, they are fairly linear with only a slight downslope curve in some areas. Other notable features that are missing are: en echelon cracks on the flanks, a body that has been split into smaller masses, ponds above the toe or in main scarp depression, and a remnant of land surface flatter than original slope surface or back-tilted into the slope. The fissures are actually open at the ground surface, which makes rotational slide movement, where the displaced soil tilts backwards towards the slope, most unlikely.

Rotational slide movement does not match the surface features expressed by the Ramahana Road fissure traces, and the material that moved is not a homogeneous mass: it has varying geotechnical characteristics with depth, which reflects its depositional history. There was no

offset recorded in the mixed-colluvium layer that intersected the fissure trace in the test pit at 17 Ramahana Road, and this should be evident if the fissure traces are related to rotational slide movement. Rotational slide movement is considered to be the least likely landslide movement type, and the term 'toe-slump' is not appropriate for the fissures along Ramahana Road.

5.5. Earth Translational Slide

5.5.1. Terminology

A translational slide would imply that the mass has moved in a downslope direction, on a roughly planar basal shear surface (Cruden and Varnes 1996). Translational slides generally occur in course non-cohesive soils, at a shallow depth, because granular soil strength increases rapidly with depth (Bell 2007); or along a plane of weakness such as a bedding plane or fracture plane in rock or soil (Cruden and Varnes 1996).

According to Cruden and Varnes (1996) the surface of rupture of a translational slide is roughly shaped like a channel in cross section, which leaves it with less frictional resistance to sliding than in a rotational slide, and the movement can continue with less resistance if the separation at the head-scarp is steep. If the velocity of movement or the moisture content increases sufficiently, then the translational movement may turn into a flow slide. A modified section of Rib and Liang's (1978) table of *features that aid recognition of common types of slope movements* is given in Table 5.3 for translational slides, and Figure 5.5 shows features of a translational slide in cross-sectional view.

5.5.2. Mechanisms of Translational Slide Movement

Massey et al (2013) note that the loess-colluvium inter-fingers with the valley floor alluvium, which could be seen as a buttress to the slope toe, and it is known that the valley floor alluvium liquefied in localized areas of the Hillsborough Valley, which would theoretically remove an amount of toe support. Dellow et al (2011) suggested that liquefaction of the saturated marginal marine sediments, which buttress the Vernon Terrace landslide, could have led to loss of support in the slope toe, and consequently to the increase in shear stress needed for the slope to move. Dellow et al (2011) postulate that this could then explain why the Vernon Terrace landslide was observed to creep following the earthquake, as the strength of the marginal marine sediments would recover over days or weeks. This mechanism can

account for loss of support in the toe of the slope, and a consequential increase in shear stress in the soil mass.

Earth translational slides			
Parts surrounding the slide			
Crown	Main Scarp		Flanks
'Has cracks most of which are nearly vertical and tend to follow contour of slope'	*'Is nearly vertical in upper part and nearly plane and gently to steeply inclined in lower part'*		*'Have low scarps with vertical cracks that usually diverge downhill'*
Parts that have moved			
Head	Body	Foot	Toe
'Is relatively undisturbed and has no rotation'	*'Is usually composed of single or few units' is undisturbed except for common tension cracks that show little or no vertical displacement'*	*'Has none and no zone of uplift'*	*'Plows or overrides ground surface'*

Table 5.3: Surface features of earth translational slides that aid in their recognition. After Rib & Liang (1978).

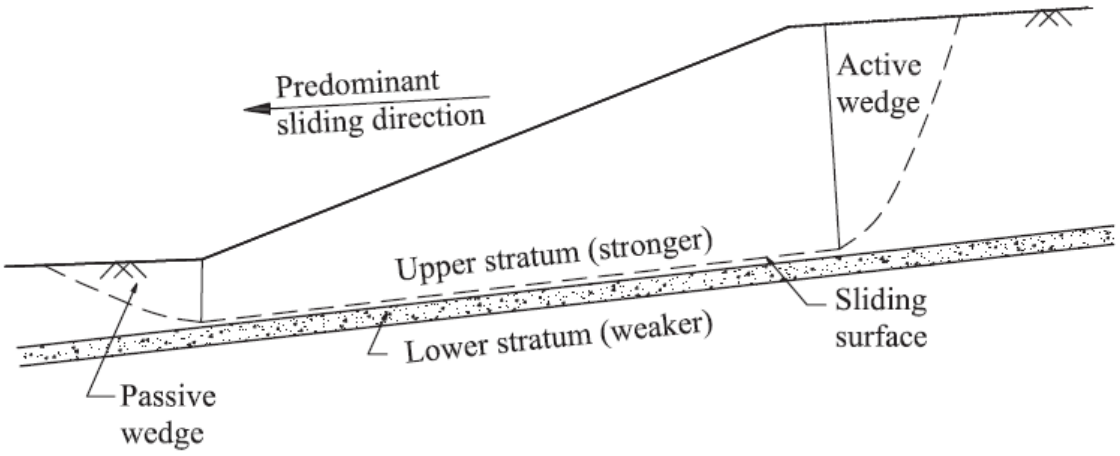

Figure 5.5: Cross-section through a translational slide, after Eid (2010).

Another translational slide mechanism that could have played a part in the generation of a basal shear surface is build-up of pore-water pressure within a distinct layer of saturated loess-colluvium. Pore-water pressures can increase within a soil medium during earthquakes by the contraction of the soil, and a corresponding loss of void space. This could lead to an artesian slide similar to the La Clare landslide (see Chapter 2), by the loss of normal stress acting on the potential shear surface in the saturated layer.

The translational slide model in Figure 5.6 incorporates the combined mechanisms of liquefaction of the slope toe (as suggested by Dellow et al. 2011) and pore-water pressure build-up along a potential basal shear surface. Under these combined mechanisms a basal

shear surface would form where the greatest increase in pore-water pressure was located, and where the greatest increase in shear stress was located. Horizontal earthquake inertia forces would also have been acting on the slope, and these would most likely have been the impetus needed to begin sliding on the basal shear surface.

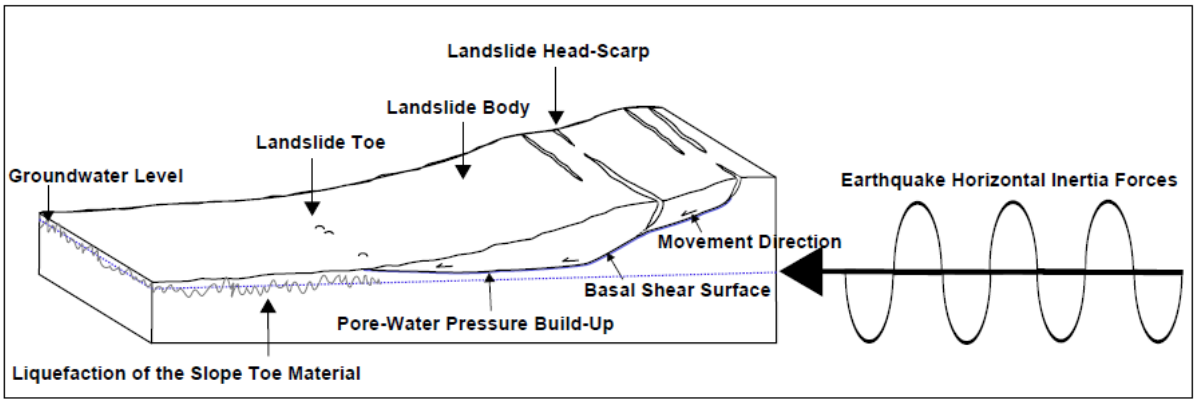

Figure 5.6: Translational slide model. The slope, fissure traces, and compressional features are modelled from 17 Ramahana Road. The mechanisms of movement are hypothetical.

Due to the relatively short movement that the soil below the fissure traces underwent and the lack of a basal shear surface, it could be argued that the landslides were actually progressive landslides, which had not fully developed their basal shear surface. The strain would have to have been concentrated at the toe of the slope where the compressional features developed, and upslope of this where the extensional features formed.

Appendix 4.1 provides for further details on the mechanisms of slide movement types in an earthquake.

5.5.3. Reasoning for Translational Slide Movement

Some of the features of the fissure traces correlate with translational slide movement: there is an open fissure trace at the landslide head which has more horizontal displacement than vertical; the fissures are sub-parallel to the contours of the slope; if there are any planes of weakness in the deposit they would likely be along the depositional layers parallel with the angle of the slope; and the compressional features can be explained by the basal shear surface not propagating out of the slope toe.

The descriptions in Table 5.3 of vertical cracks in the crown that follow the contour of the slope accurately fits that observed for the Ramahana Road fissure traces. The main scarp being nearly vertical in the upper part, and then becoming less inclined near the lower part, correlates with the observed nature of the fissure trace that was exposed in the test pit at 17

Ramahana Road. The head being undisturbed and showing no rotation also fits the relatively undisturbed nature of the soil that moved. If a principal headscarp is identified, then the fissures downslope of this could fit the description of the tension cracks with little or no vertical displacement in the body.

Because there hasn't been a basal shear surface identified and there are no landslide flanks to the movement, a form of progressive translational slide movement may appear to be a satisfactory explanation for the fissure traces. Under the translational slide movement scenario, when the earthquake ceased shaking, the movement ceased, because the pore-pressure immediately began to dissipate, and the theorized liquefied valley-floor alluvium regained its strength. This could make a convincing argument with the right subsurface data and analytical support.

5.5.4. Reasoning Against Translational Slide Movement

The observations that do not fit the translational slide movement features are the flanks and toe of movement. The Ramahana Road fissure traces have no observable flanks to their movement at the ground surface; whilst the compressional features observed at the toe of movement at Ramahana Road are not where the soil has ploughed over the ground surface. They are in fact simply a compression of the soil at this location.

Translational slide failures also occur most frequently in steep slopes with a main discontinuity angle that is less steep than the slope angle, making it 'daylight' the slope, but the depositional layers within the loess-colluvium tend to grade into each other, lie parallel to the slope angle, and extend into the valley floor. Landslides caused by movement along a basal shear surface generally occur where the slope is at a greater incline, where gravity causes a greater static driving shear stress.

Another problem with the translational slide movement hypothesis is that there is no readily identifiable main headscarp. The fissure traces follow the contour of the slope, but there are multiple fissures in any one location. If there was a basal shear surface between upslope and downslope fissure traces, then any movement of the upslope mass of soil should have worked to close the aperture of the downslope fissure trace. The translational slide movement hypothesis also does not give any explanation as to why there is vertical displacement at the fissure traces: translational slides are normally characterized by little to no vertical displacement.

The hypothesis that there was loss of toe support is not supported by evidence at 17 Ramahana Road or Centaurus Park. There has been very little subsidence identified in the valley floor. If there had been significant liquefaction of the valley floor alluvium, it would be unrealistic to assume that the settlement would be uniform across the valley floor: there should be evidence of differential settlement damage in the foundations of the valley floor buildings. There were only localized observations of liquefaction in the valley floor of the Hillsborough Valley, and if this mechanism is to be considered a main factor for fissure trace development, then it should have been observed downslope of all areas of fissuring.

The problem with the progressive slide hypothesis lies in how progressive slides occur. For a progressive slide to have occurred there needed to be sufficient stress build-up in the soil upslope of the loss of toe support, and a sufficient loss of normal stress on the potential basal shear surface due to pore-pressure increase. The loss of toe support would have needed to extend across all areas of fissuring, and it would need to have been for sufficient time for stress to build in the material upslope of the toe to overcome the normal stress acting on the potential basal shear surface, and the residual strength of the toe-slope material.

The highest shear stress would have been built in the slope-toe material just upslope of the liquefied valley floor, and the shear stress would have become progressively less with continuation upslope; therefore it must be assumed that the progressive slide would have started at the base of the slope, and progress upslope following the decrease in shear stress with distance from the slope toe (following Bjerrum 1966 and Skempton 1964). It should be noted that whilst the fissure traces are characterized by a contemporaneous compression at the slope toe, they are not always associated with this feature. The extensional features on the other hand are the most common feature, and they can occur without any downslope surface evidence of compression at the slope toe. This suggests that the shear stress build-up was more extensive at the landslide head (the fissure traces) than at the toe, and this is a direct contradiction to a progressive slide mechanism.

Another problem with the progressive translational slide hypothesis is that extensional movement at the slide head (i.e. the development of a landslide headscarp) is characteristic of a mature landslide. When the La Clare artesian landslide formed in Akaroa, it took 4 years from when the original movements were recorded for the landslide headscarp to form (Yetton 1992): in contrast the Ramahana Road fissure traces occurred during the period of the Christchurch Earthquake-induced ground shaking, which lasted <1 minute.

Following Skempton (1964) and Bjerrum (1966) a landslide head-scarp is indicative of a mature landslide, one with a near fully formed basal shear surface. The basal shear surface should have redistributed the stress from the toe of the slide, progressively up to the head of the slide. Once the headscarp has formed on a translational slide there is a loss of friction at the slide head, and this normally corresponds with an acceleration of movement (Varnes 1978; Cruden & Varnes 1996). If the fissures are the head-scarps of a progressive translational slide movement, then there should be a more clearly defined basal shear surface that would have been identified in subsurface investigations. It is also apparent that there would have been more downslope movement recorded for the landslide to progress enough for a head-scarp to form, and the flanks of the landslide should be evident (following Rib & Liang 1978).

5.6. Lateral Spread

5.6.1. Terminology

Cruden and Varnes (1996) define spread as a lateral movement of a cohesive soil or rock mass, with subsidence into the underlying softer material, normally by way of liquefaction or flow of the softer material. The extent of subsidence is dependent on the thickness of the softer or liquefied material; if it is thick then grabens may form, and upward flow can occur in the toe. There are no distinct shear surfaces in spread failures, and the displaced cohesive mass may subside, rotate, translate, liquefy, flow, or disintegrate in response to the movement (Varnes 1978; Cruden & Varnes 1996).

Figure 5.7 is a diagram of how the subsurface liquefaction can disturb the upper layers in a lateral spread failure. Spread movement is complex; it can involve elements of rotational and translational slide movement, and also flow (Varnes 1978). If the movement is largely translational, then the surface features of lateral spread type landslide will be similar to that of translational slides.

Rauch (1997) explains that liquefaction of subsurface layers beneath steep slopes can result in catastrophic flow slides of considerable volume, such as the one caused by the 1920 Haiyuan Great Earthquake in Kansu, China (Wang et al. 2004). However the term lateral spread is reserved for soil displacement on gentle slopes (0.3 to 5%) underlain by saturated liquefiable deposits (Rauch 1997). Upon liquefaction the unsaturated overburden can slide as a cohesive mass over the liquefied deposit, with the liquefied layer effectively acting as the

basal shear surface (Bell 1999). Solonenko (1977) expands on this, explaining that the soil that slides exhibits very little deformation, and structures are often moved without significant damage. However graben-like features can form at the slide head, and cause significant damage to buildings in this location by way of differential settlement.

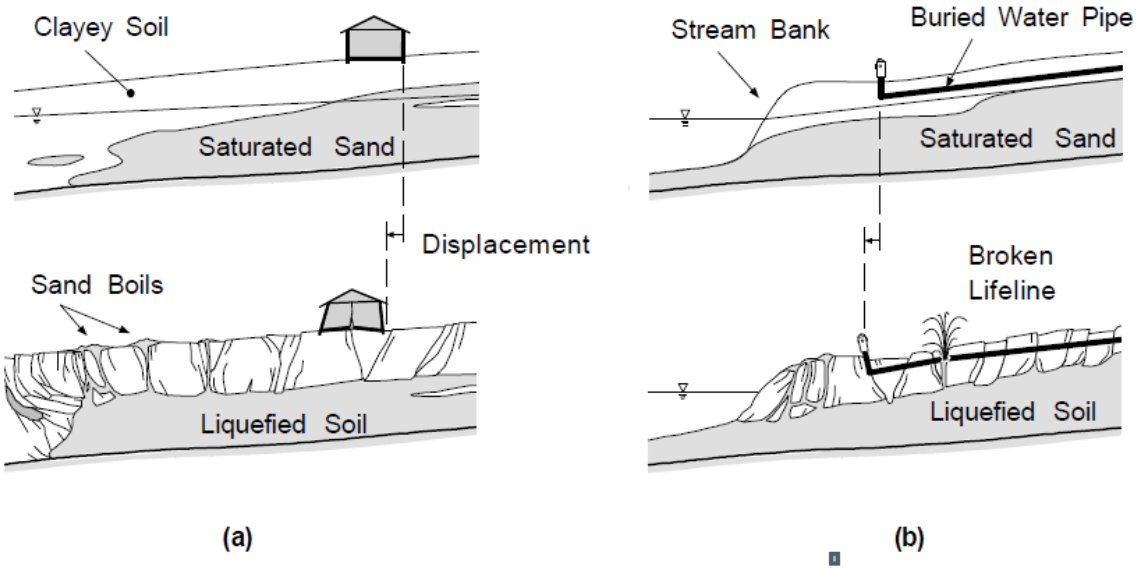

Figure 5.7: Lateral spreading induced by liquefaction below the ground surface on (a) gently sloping ground and (b) gently sloping ground behind a free face. After Rauch (1997).

This type of movement generally occurs along a stream bank or a shoreline where the groundwater table is high, the displacements move toward the steep face of the stream bank with fissures, and scarps and grabens forming at the head of the spread (Rauch 1997). Much of the damage in the Christchurch city flat lands was caused by lateral spreading along rivers and streams, such as the lower Avon River.

5.6.2. Mechanisms of Lateral Spread Movement

The lateral spread model in Figure 5.8 incorporates liquefaction of the loess-colluvium along the groundwater level. The base of displacement has been drawn as a definite line similar to the basal shear surface in the translational slide model. However, in a lateral spread type of movement the basal shear surface is poorly defined and occurs throughout the liquefied layer below, but this was not possible to draw. There are some elements of translational sliding in this model, but in contrast to the translational slide model it is purely the theoretical mechanism of liquefaction of the saturated material that causes a loss of shear strength in the soil. The earthquake horizontal inertia forces are the impetus needed to begin slope

movement by increasing the shear stress above the residual strength of the liquefied material. Due to the groundwater levels observed at 17 Ramahana Road extending into the slope rather than following the slope angle, the base of displacement becomes very deep at the upslope extent of fissuring.

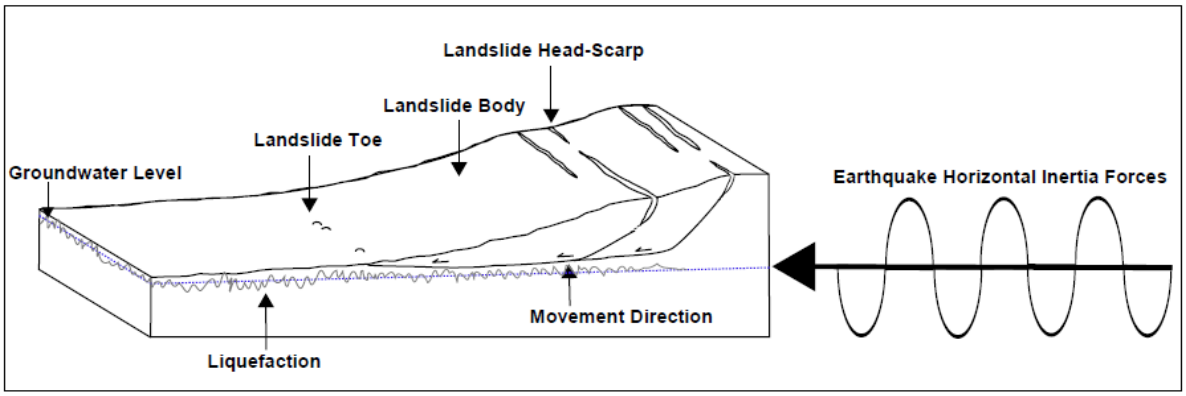

Figure 5.8: Lateral spread model. The slope, fissure traces, and compressional features are modelled from 17 Ramahana Road. The mechanisms of movement are hypothetical.

Appendix 4.2 provides for further details on lateral spread landslide movement type mechanisms in an earthquake.

5.6.3. Reasoning For Lateral Spread Movement

Many of the features of the fissure traces matched translational slide movement, but translational slide movement was rejected for reasons discussed in section 6.5. Lateral spreading can have elements of rotational and translational movement, and the soil that moves can sometimes move without significant deformation.

It has been established in previous studies on overseas deposits of loess that loess can be liquefiable under the right conditions (Wang et al. 2004), and due to the heterogeneous nature of the loess-colluvium at the site there may be potential for a depositional layer of loess-colluvium to meet these criteria. Some of the surface features of the fissure traces also match that of liquefaction-induced landslides, where the material upslope of the movement has become extensively fissured and cracked. Lateral spreading offers an answer as to why there were vertical displacements recorded at the fissure traces, because the cohesive ground surface material subsided into the theoretical liquefied deposit.

Laboratory investigations of the loess-colluvium found that there were four layers that could be distinguished in the deposit: a silt layer with some clay at the surface, which was underlain

by silt with minor to trace clay, underlain by a clayey silt deposit, and finally a section of interlayered deposits of sandy-silt and silty-sand. The surface silt with some clay was found to be the driest, whilst the silt with minor to trace clay was wet to saturated, the clayey silt was wet to moist, and the sandy-silt was wet to saturated. The differences in the clay fractions also reflected differing plasticity indexes, and the deposit generally became denser with depth. These observations suggest that the most likely layer to liquefy would be the silt with minor to trace clay layer. Direct shear-box testing of samples of loess-colluvium also found that the silt with minor to trace clay layer had low cohesion values (≤5kPa) at the natural moisture contents recorded, regardless of clay content or plasticity index.

Finally the resistivity survey shows a saturated layer at the base of the slope, coincident with the compressional zone that appears to be an injection feature. In lateral spreads the soil that moves can have little deformation, but the soil that liquefies flows downslope and there can be upwards flow at the toe. This could be an explanation for the saturated material, and the small cracks at the base of the slope could have been caused by upwards movement of liquefied material. The resistivity survey shows saturation of the material within the slope, upslope of the toe, and this could be the layer that liquefied.

5.6.4. Reasoning Against this Mode of Movement

The problem with the lateral spread hypothesis is that the slope angles where the fissure traces occurred are at a steeper angle than is expected for lateral spread failures. The steeper the slope, the greater the ratio of shear stress to normal stress, and this limits the liquefaction potential (Rauch 1997). Rauch (1997) explains that slopes above a 0.3 to 5% gradient are unlikely to have lateral spread failures, because the static driving shear stress is higher due to the higher confining pressure, and this would normally lead to a flow slide failure. If a distinct layer of loess-colluvium had liquefied at depth, then the cohesive soil above would probably have moved in the form of a slide-avalanche-flow style which is typical following top-down saturation of loess-colluvium in Banks Peninsula (following Bell & Trangmar 1987).

If the mechanism behind the fissure trace movement was liquefaction of a layer of loess-colluvium, then this layer would have to be laterally extensive across the entire side of the valley. If there is a more liquefiable layer that is continuous across the entire valley side then it should be expected that there would be signs of liquefaction at the ground surface. In the spread landslides of the 1964 Alaskan earthquake, the liquefaction of distinct sand layers led

to significant deformations of the slide material, deep graben formation, and obvious rotational aspects of movement (Seed 1967). Seed (1967) presents case-studies of other areas where lateral spread has occurred during an earthquake, which suggest that movement due to liquefaction is characterized by extensive displacements, mixing of soil material, and surface sand boils, none of which were identified at the site area.

Cyclic mobility occurs when the shear resistance is greater than the static shear stress, and the soil deforms only during each cycle of shear stress (Jefferies & Been 2006). The deformations are limited, and the soil immediately regains its strength upon cessation of cyclic stress, due to its tendency to dilate under monotonic loading. This mechanism at first appears to meet all criteria for the fissure traces; however cyclic mobility does not tend to occur on slopes above a 0.3 to 5 % gradient because the ratio of shear stress to normal stress is too great (Rauch 1997).

Rauch (1997) explains that cyclic mobility tends to occur on flat slopes (<5% gradient) or in deeper, denser deposits because this is where the shear resistance is greater due to the higher normal stress compared to shear stress. This problem was confirmed by the CPT pore-water dissipation tests, which recorded increased pore-pressure under monotonic loading in *in-situ* conditions; whereas if dilation were to occur it would be expected to decrease under monotonic loading. The lack of dilation under monotonic loading is contradictory to the potential for cyclic mobility.

5.7. Earth Quasi-Toppling

5.7.1. Terminology

Earth quasi-toppling failure was hypothesised by Stephen-Brownie (2012). It was thought that a form of toppling movement could have occurred in the loess along inherent sub-vertical fractures in response to the combined mechanisms of bedrock fracturing, lateral spreading, and the ‘trampoline effect’, with the presence of tunnel gullies as an exacerbating factor.

Toppling movement as defined by Cruden and Varnes (1996) can be considered as a special type of fall movement, where a cohesive block of earth rotates forward about a pivot point. Toppling generally occurs in rock masses on steep faces, such as the face of a cliff. The chance of toppling failure increases with increasing discontinuity angle and increasing slope angle (Bell 1999). Slopes most prone to toppling are steeply inclined, with a principal discontinuity at near vertical angles.

Rib and Liang (1978) describe the main features to identify toppling failures are a sub-vertical, fresh scarp with spalling on the surface and cracks behind the principal failure. Generally the parts that have moved are irregular in shape and consist of fallen material. Due to the geomorphology at the site, toppling failure as defined by Cruden and Varnes (1996) is not considered a possibility, however a quasi-toppling motion where cohesive blocks of loess-colluvium have rotated outwards from the slope, as suggested by Stephen-Brownie (2012) could be considered.

The quasi-toppling motion offers a very good correlation to the surface features at Ramahana Road. A quasi-toppling motion would cause a compression at the base of the slope as the cohesive block of soil rotated outwards from the slope. The rotation of the block would cause tensional stress in an orientation sub-parallel to the slope contour, and consequently cause fissuring in such an orientation. There would be no landslide flanks to this movement.

5.7.2. Mechanisms of Quasi-Toppling Movement

The Ramahana Road fissure trace occurs in loess-colluvium and not primary (airfall) loess. The sub-vertical fractures that are evident in primary loess are destroyed by movement and disturbance during colluvium deposition, and so there are no obvious vertical discontinuities; the main planes of weakness are expected to follow parallel to the slope along contacts between different colluvium layers and the contact with the Lyttelton Volcanic Group. Mechanisms that differ from Stephen-Brownie (2012) are required to explain how a quasi-toppling motion could occur in the soil along Ramahana Road.

For a cohesive mas of the surface soil to rotate outwards from the slope there needs to be an accommodating movement in either the soil that moves, or in the soil surrounding the soil that moves. If the soil that moves displays the accommodating movement, then this would have been observed as discrete vertical shear zones in the soil, which would have highly disturbed the soil mass. The fissure traces are characterized by very little deformation downslope of the extensional zone and so this mechanism is not likely. The alternative is that the soil surrounding the soil that moved accommodated the movement. Figure 5.9 shows the suggested mechanisms of movement for quasi-toppling. This would have to occur through compression in the soil downslope and underneath the soil that moved. The compression would have been magnified at the base of the slope and it would dissipate with distance upslope, and underneath the mass of soil that moved. This is what has been recorded in the compression at the base of the slope, which was evident in the density tests at 17 Ramahana

Road, and interpreted in the electrical resistivity geophysical surveys at 17 Ramahana Road and Centaurus Park.

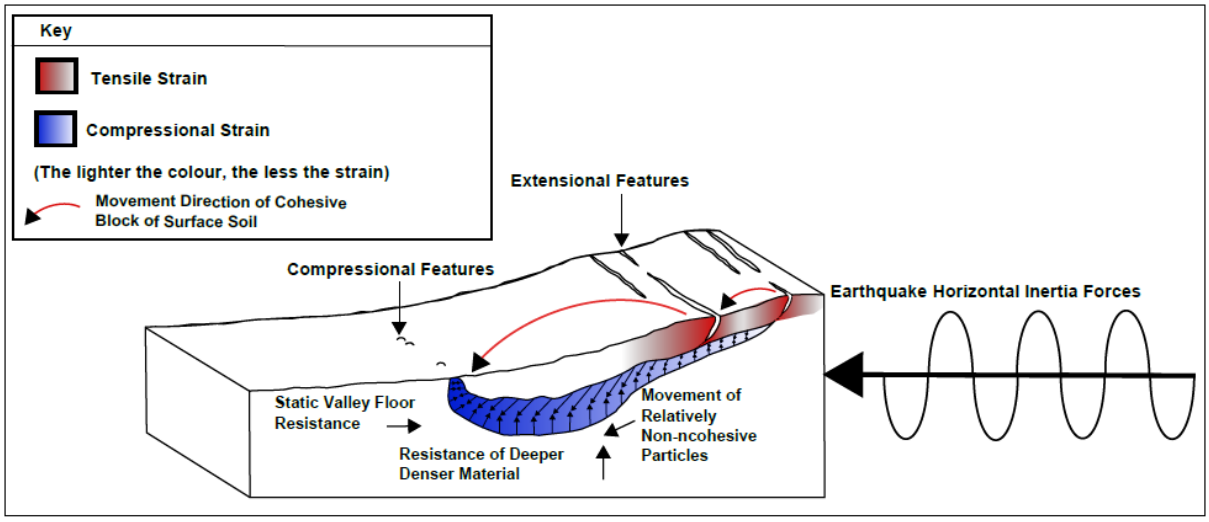

Figure 5.9: Tensile failure model. The slope, fissure traces, and compressional features are modelled from 17 Ramahana Road. The mechanisms of movement are hypothetical.

The tensile failure model in Figure 5.9 is an attempt to visually portray where the strain accumulated in the soil and how this dissipated upslope. In this model the earthquake horizontal inertia forces are the main mechanisms of movement because they lead to the compressional strain in the slope toe and tensile strain in the above material. Because this model is not portraying a typical landslide type movement, it does not use landslide terminology, and instead denominates the fissures as extensional features rather than landslide head-scarps. Likewise the compressional features are simply denominated as compressional features rather than the landslide toe. There is no translational zone in this model.

5.7.3. Tensile Strain

Fissures can be caused by a variety of factors, but in this case, due to their location and the factors involved, they would have to have been caused by horizontal earthquake inertia forces, the static shear stress from the weight of the slope material, and bedrock uplift.

As mentioned, the Christchurch Earthquake was sourced from the Port Hills oblique-thrust fault. Its epicentre was underneath the Heathcote Valley area (Kaiser et al. 2012) and its hypocentre was ~4 km below this (Beavan et al. 2011). There were peak slip measurements of 2.5-3m at the hypocentre, and slip measurements of 1m within 1km of the ground surface (Beavan et al. 2011). At the ground surface, this movement was accommodated by uplift of

the Port Hills by up to a metre in certain areas relative to the Christchurch City flat lands (Beavan et al. 2011). The uplift of the Port Hills in relation to the Christchurch city flat lands could have led to tensile strain in the loess-colluvium at the toe of the north facing valleys of the Port Hills.

The Christchurch Earthquake produced very high vertical accelerations that have already been mentioned, but what are more significant, in regards to the loessial soil fissuring at least, are the horizontal peak accelerations. Peak horizontal acceleration of 1.7g was recorded at the Heathcote Valley Primary School, and 0.4g at Cashmere High School, which is the nearest seismograph to Ramahana Road. These forces are significant, and when combined with static shear stress from the weight of the slope material, they could have caused an accumulation of tensile strain in the loess-colluvium at the toe of the slopes.

The tensile strain would accumulate at the toe of the slopes because this is where there are deeper deposits of loess-colluvium. The loess-colluvium also has a higher moisture content at these lower positions on the slope, which allows greater deformation. The shape of the Lyttelton Volcanic Group basin in relation to the loess-colluvium in-fill could also have aided the accumulation of tensile strain, because the fissures are located where the deposit becomes rapidly shallower with distance upslope (refer to Figure 3.4).

The tensile strain would have led to an outwards rotation of a cohesive block of soil from the slope where the tensile strain was greatest. The fact that there are multiple fissures at any location at the extensional zone of the slope shows that the strain accumulation was widespread across the toe of the slope.

One reason why the fissures could have occurred on breaks in the slope is because breaks in the slope are where the tensional strain would have been most pronounced: if the tensile strain developed perpendicular to slope contour orientation, then it would be greater at convex breaks in the slope. The horizontal earthquake inertia forces would also have a greater effect at the breaks in slope, because on the flatter sections of the slope the normal forces are orientated at a less favourable angle to the direction of applied earthquake force, whereas on the steeper slopes the normal forces are orientated closer to being against the horizontal earthquake inertia forces (see figure 5.10). The steeper the slope angle, the more favourably orientated the normal stress is to earthquake horizontal inertia forces.

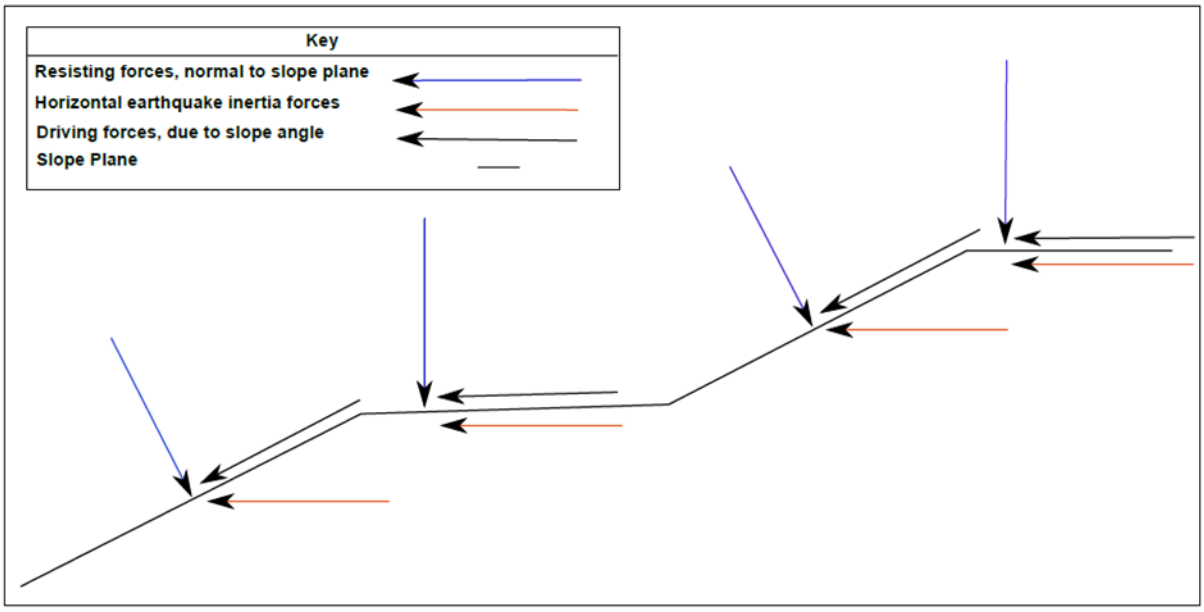

Figure 5.10: Forces on a slope face during an earthquake. Note: diagram not drawn to scale and forces are directional only; they are not indicative of magnitude.

5.7.4. Compressional Strain

The depth of the block that rotated would be defined by the cohesion and moisture content of the loess-colluvium deposit. It must be stressed that the mechanical behaviour of loess is completely governed by its water content. The four layers identified in the laboratory investigation had varying moisture contents, and the wetter loess-colluvium layers would have responded differently to the cyclic loading of the earthquake than the drier layers.

The third layer, which is a clayey silt, would be unlikely to significantly deform due to its higher density, its relatively low moisture content of 8-10%, and its relatively high clay content and corresponding plasticity index of 16.6-26.9% and 12-15, respectively. Any deformation would have been more likely to occur in the layers above this. The second layer is the most likely area where the soil could have deformed due to its lower density, its relatively high moisture content of 16-23%, and its relatively low clay content (4.1-8.9%) and corresponding low plasticity index of 3-5.

The second layer is unlikely to have rotated outwards from the slope as a cohesive block due to its low cohesion at natural moisture contents (see Chapter 4). It is only the first layer which is likely to have rotated outwards from the slope. The first layer is of 8-19% moisture content, 7.6-20.1% clay content, and has a plasticity index of 8-12. It has a higher cohesion than the second layer at its natural moisture contents, and a lower density than the lower layers. Near

the top of the second layer is where the compressional strain underneath the soil that moved is likely to have occurred. This reasoning is backed up by the depths where the compressional strain is evident in the resistivity survey, at around 2-8m, which is within the second layer.

The base of the slope is where the downslope extent of movement would occur. This is where the compressional strain is likely to have been greatest, and it would dissipate with distance upslope. This would be due to the higher moisture content in the soil at the base of the slope, and the resistance offered by the valley floor material, which is under little to no static shear stress in relation to the upslope material. The compressional strain would eventually peter out with distance upslope due to the soil becoming too dry and too shallow for compressional strain.

This compression may not always be visible at the ground surface, for example at Centaurus Park there were no compressional features mapped by Massey et al. (2013). However, the resistivity survey at Centaurus Park showed the same resistivity anomaly within the compressional zone as 17 Ramahana Road, and this suggests that the compression is not always evident at the ground surface. The compression should not be expected to be as great in all areas due to the differences in moisture content, slope material, and the changes in slope height/angle.

One feature of the compressional zone that suggests that it was caused by horizontal earthquake waves, rather than compression due to landsliding, can be seen on driveways of 48A and 54 Vernon Terrace. These driveways are orientated perpendicular to the slope contour and were damaged by compression during the earthquake. The damage can be seen in the form of small rises in the driveway that resemble ocean swell; they are similar in height, and are spaced evenly (about 4.5-5m) apart. Figure 5.11 is a diagram representing how compressional earthquake waves could cause this phenomenon

The movement of the upper cohesive soil would be in an outwards rotation from the slope face due to the compression being greatest at the base of the slope. This movement would largely be observed as a horizontal displacement at the fissure traces, but the compressional strain in the subsurface soil would cause the upper cohesive soil to subside slightly, and lead to the vertical displacement at the fissure traces.

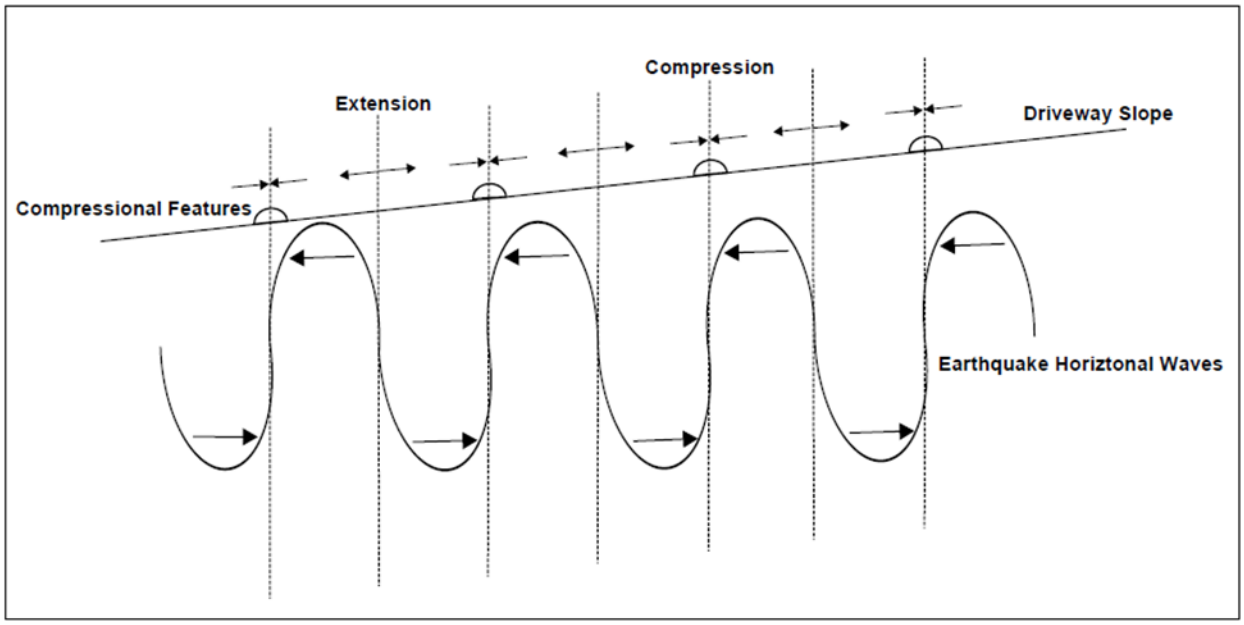

Figure 5.11: Earthquake horizontal waves and the evenly spaced compression they caused at the ground surface, (modified from Seed (1967).

5.7.5. Springs Within the Compressional Zone

The compression of the soil in the compressional zone is implied by the electrical resistivity geophyscial survey in Figure 3.13. The relative changes in resistivity are largely influenced by the moisture content of the soil, and the moisture content of the loess-colluvium profile is in turn influenced by its porosity and permeability. What the resistivity anomaly in the centre of the diagram could then be indicating is that there has been compression of the loess-colluvium at the base of the slope (where there are compressional features), and that this has caused a corresponding loss of moisture. The high conductivity area surrounding this would then be showing the drainage of the moisture from the compressed material to the surrounding soil.

The new springs that formed following the Christchurch Earthquake would be indicative of the newly formed preferential pathways that the groundwater can take to the ground surface due to the greater porosity and permeability in the soil surrounding the compressional zone, in contrast to the lesser porosity and permeability in the compressed soil. This can explain why nearly all of the springs formed within the compressional zone.

What could have aided the establishment of preferential pathways that would form into springs would be bedrock fracturing and compression of joints and fissures in the Lyttelton Volcanic Group. This would have released new groundwater from depth, and increased the

hydraulic head of the groundwater in the loess-colluvium, and the spring water has been recorded to have a chemical composition that is analogous to the Banks Peninsula aquifer system. If the groundwater rising from depth had met the compressed material upslope of the downslope extent of compression it would not be able to infiltrate the compressed material as easily, and therefore it would raise the hydraulic head of this water further. This could be why the drillers from Pro-Drill, who drilled BH-01 in Centaurus Park, met groundwater with artesian pressures having 0.75m head above the ground surface at 15m depth in the borehole.

The bedrock fracturing and changes to hydraulic head in the Port Hills unconfined aquifer system are likely to have been most pronounced at the north facing valleys of the Port Hills due to the orientation of the Port Hills fault. The Port Hills fault strikes in a NE-SW direction, and dips towards the SE (Kaiser et al. 2012). This is in a similar orientation to the Port Hills; although the fault is located underneath the Lyttelton Volcanic Group within the Torlesse Supergroup, 1km below the ground surface (Beavan et al. 2011) (see Figure 5.2). The compression of the fissures and joints that make up the Banks Peninsula bedrock aquifer system is likely to have been most pronounced at the north facing valleys of the Port Hills, due to the orientation and location of the Port Hills fault.

5.7.6. Questions Raised by the Quassi-Toppling Movement Hypothesis

Considering the suggested mechanisms of occurrence for the fissure traces, the first question is: why would the fissure trace flatten off at depth if it is a purely tensional feature? As was recorded in the test pit, described in Chapter 4 and shown in Figures 3.6 and 3.7. There is a relatively simple answer to this question, and that is because the normal resisting forces brought on by gravity and the weight of the soil overburden becomes greater with depth. Conversely, because of the slope angle, the normal forces become less with horizontal distance to the slope face. Putting this together, it is apparent that the tensional failure would be easiest to induce near the ground surface, but it would have become harder with depth, but easier with decreasing distance to the slope face. Figure 5.12 is a simple diagram explaining the forces acting on the slope that could have led to the fissure being curved with depth.

Because the fissure trace curved with depth, the tensional stress would have decreased with depth. As the fissure trace became flatter with depth, the stress would have become orientated as more of a shear stress rather than a tensional stress. Because loess is stronger in shear than in tension, this would have led to the fissure trace dissipating with depth, rather than continuing to greater depths. Figure 5.13 is a simple diagram of the fissure traces showing

how the horizontal forces became more shear than tension, as the angle between the horizontal forces and the fissure trace became more acute. This could explain why the fissure trace became segmented with depth, because the stress would be orientated as more of a shear stress with greater depth and curvature.

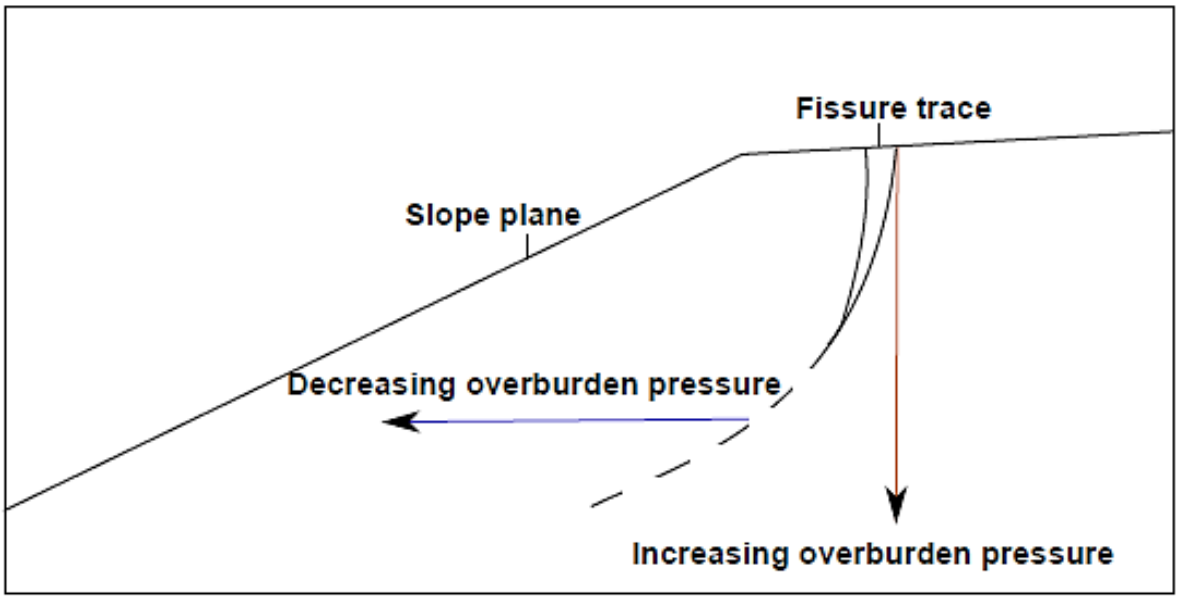

Figure 5.12: Forces on a slope during fissuring. Note: diagram not drawn to scale and forces are directional only; they are not indicative of magnitude.

There are other areas outside of the Hillsborough valley where the fissures occurred in soil that is relatively dry and shallow, and so the suggested mechanism of compressional strain in the second layer is not valid. In these cases it could simply be the horizontal earthquake forces and bedrock movement that induced the tensile force on the loessial soil and cause the fissuring, and indeed in the Hillsborough Valley there are some areas where this could also be true. These locations often do not have thick sequences of loess-colluvium to accommodate strain; however they tend to be located on a flatter surface with a steep or free-faced Lyttelton Volcanic Group outcrop downslope, and in these locations the loess can extend outwards without needing the accommodating compressional strain in the downslope material.

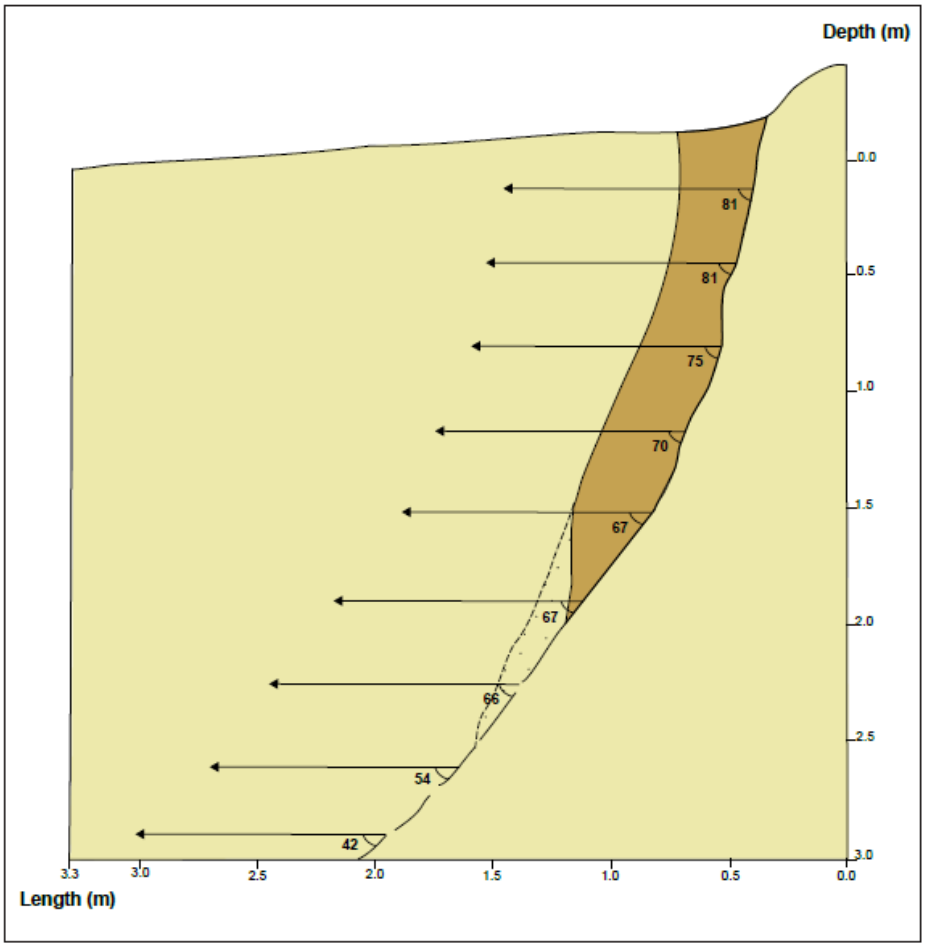

Figure 5.13: Scale diagram of the tensional vs shear forces acting on the fissure trace at 17 Ramahana Road as it curves with depth. Note: forces are directional only, they are not indicative of magnitude.

5.7.7. Quasi-Toppling Movement Model

A block model with the electrical resistivity geophysical survey overlaid is presented in Figure 5.14. This diagram has the interpreted features of the resistivity anomaly pointed out. An attempt to visually portray the suggested mechanisms and movement is displayed in Figure 5.15. This suggested mode of movement can be considered a quasi-toppling mode of movement similar to that suggested by Stephen-Brownie (2012), but with different mechanisms.

The quasi-toppling mode of movement offers an explanation for the observed compressional and extensional features; the resistivity anomaly recorded in 17 Ramahana Road and Centaurus Park; the springs in the compressional zone; the surface features of the fissure traces; the subsurface fissure trace characteristics uncovered in the test pit; and an answer as to why the fissure traces only occurred during the Christchurch Earthquake induced ground

motion. It is considered the most likely form of movement by the current author; however more research is needed to understand the mechanisms of this suggested form of movement.

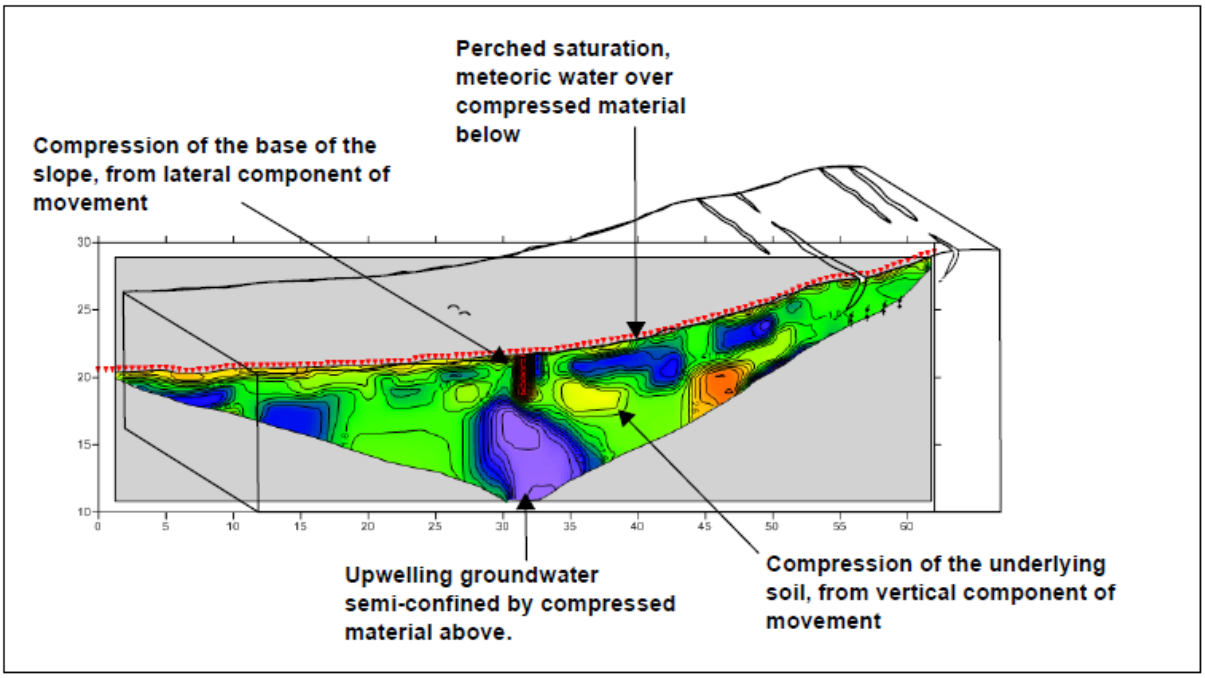

Figure 5.14: Tensile movement model with the electrical resistivity geophysical survey and interpretations overlaid. Modelled from 17 Ramahana Road.

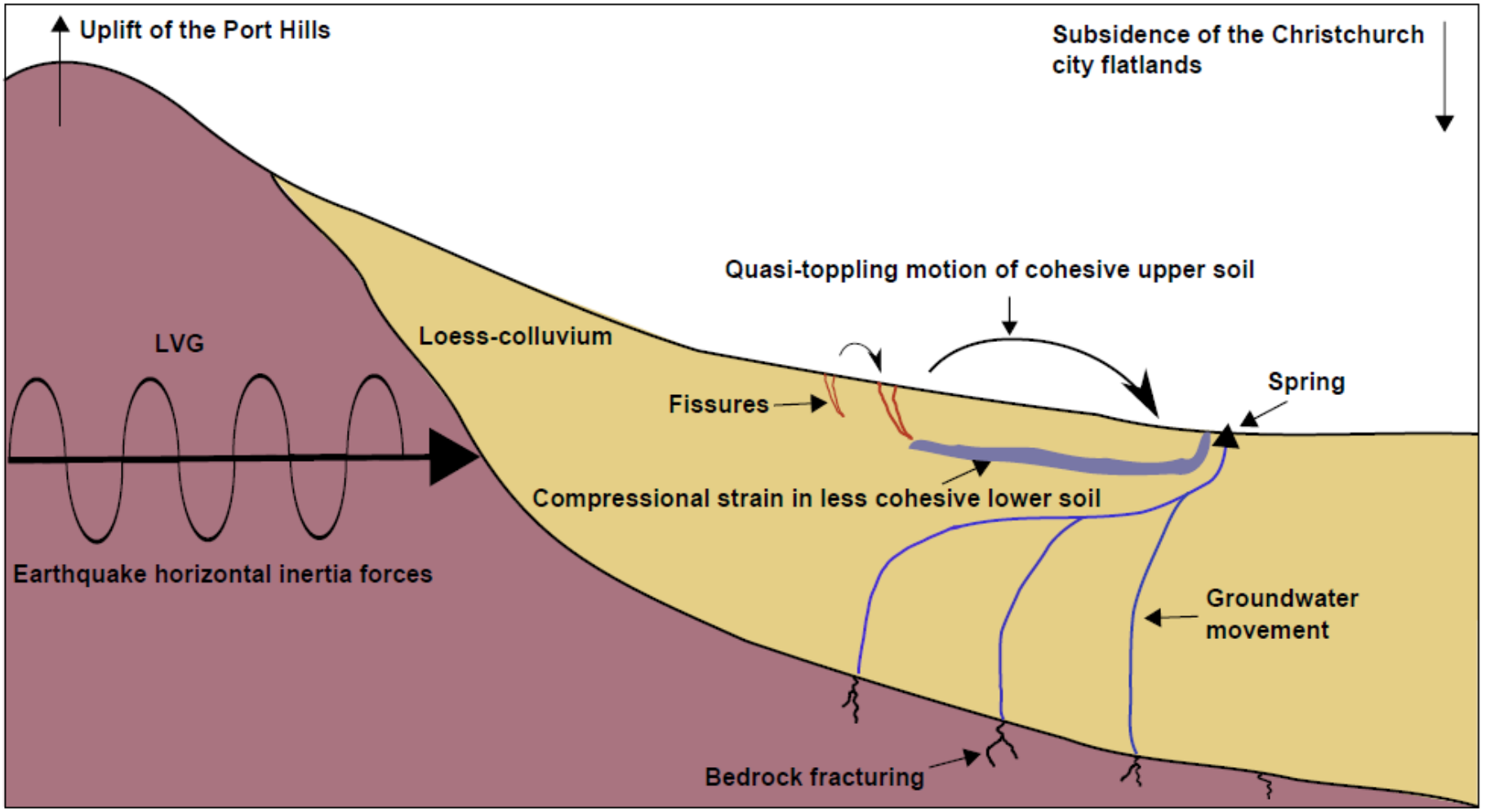

Figure 5.15: Diagram depicting the quasi-toppling motion of the surface soil and the compressional strain of the deeper soil, the horizontal earthquake inertia forces, the uplift of the Port Hills in relation to the Christchurch city flatlands, and the static shear stress from the slope. The generation of new springs at the base of the slope is from bedrock fracturing offering a new source of groundwater and an increased hydraulic head from compression of joints within the LVG. The springs form within the compressional zone due to the soil that has been under compressional strain retarding the upward movement of groundwater.

6. Summary and Conclusions

6.1. Project Objectives

The primary goal of this research has been to gain a better understanding of the mechanisms that caused fissure traces to occur during the February 22nd 2011 Christchurch Earthquake. The fissure traces correlate to the extensional features mapped by previous studies. It was hypothesised that the mode of movement was not a slide or slump landslide, but a tensional stress/strain movement caused by the unique behavioural characteristics of Banks Peninsula loessial soils and the unique characteristics of the Christchurch Earthquake.

Specific objectives were:

- **Objective 1**: Identify key features of fissure trace expression using subsurface investigations to explore any potential landslide movement types and mechanisms that could have led to the creation of the Ramahana Road fissure trace.

- **Objective 2:** Identify why the fissures formed at the locations they did, and put the soil in context with other loessial soils of the Port Hills using laboratory analysis of samples.

- **Objective 3**: Visually portray the interpreted subsurface geology, and create more accurate models depicting the failure below ground surface than are currently available.

- **Objective 4**: Determine the most likely landslide movement type and the mechanism behind this failure.

These objectives were met by qualitative assessment using subsurface investigations at 17 Ramahana Road and Centaurus Park, and quantitative assessment using laboratory analysis of samples from 17 Ramahana Road and Centaurus Park, and computational slope stability analysis for 17 Ramahana Road. The mechanical behaviour of loessial soils is known to be governed by its moisture content, and therefore methods such as the electrical resistivity geophysical survey, and natural moisture content tests of samples were of great importance to estimate the likely behaviour of the loessial soil under cyclic loading.

6.2. Fissure Trace Evaluation

6.2.1. Extensional and Compressional Features

The extensional features are the fissure trace openings in the ground surface. The fissure trace at 17 Ramahana Road had an aperture of ~450mm at the ground surface, and gradually reduced in aperture with depth. The fissure closed to 1-2mm aperture at ~2.1m depth, and from there it became segmented. The fissure became more curved with depth, varying from 78° near the ground surface to an assumed 40-50° at 3m depth. A mixed-colluvium layer was intercepted by the fissure traces at 2.4m depth and there was no observable vertical offset of this layer. It is assumed that the adjacent fissure traces have a similar geometry. The natural moisture content of the soil profile generally increases with depth from ~9% within 1m of the ground surface to ~20% at 3.0m, and this determines how the soil deforms under stress (i.e. brittle failure in the dry regions and plastic failure in the wetter regions).

The compressional features are characterized by lateral shortening of the ground surface in a downslope direction, and compression of the soil from the ground surface to ~8m depth. The compression is magnified near the ground surface at the toe of the slope, and it dissipates into the slope towards the extensional zone. As in the extensional zone, the natural moisture content of the soil generally increases with depth, and this determines how the soil deforms under stress. Near the ground surface there have been some brittle compressional features observed, but the compression is mostly observed as plastic deformation due to the generally higher moisture content of the soil at the toe of the slope (~13% compared to ~9% upslope).

6.2.2. Deep Soil Profile

The loess-colluvium profile was determined to have four layers, to a depth of ~20m that are distinct in clay content, plasticity index, and moisture content. The density of the deposit gradually increases with depth as shown in the seismic reflection survey. The moisture content generally increases in the first two layers of loess-colluvium, from ~9% to ≤23%, before it decreases in the third layer to ~9%, and then increases again in the fourth layer to ~20%. The changes in moisture content reflect density variations, clay content variations, the drainage of the slope, and upwelling of groundwater from depth. The fissure traces occur in the more cohesive, topmost layer of loess-colluvium, whilst the compressed soil is observed in the topmost layer at the toe of the slope, but into the less cohesive, second layer at greater depths where the compression dissipates into the slope towards the extensional zone. There

has been nothing to suggest movement in the third layer of loess-colluvium at ~12m, or at greater depths.

6.2.3. Spring Assessment

The springs that arose in the Hillsborough Valley after the Christchurch Earthquake are interpreted to represent increased hydraulic head in the Banks Peninsula unconfined bedrock aquifer system due to compression of inherent fractures and fissures in the bedrock, and earthquake-induced bedrock fracturing allowing new pathways of groundwater. The Port Hills fault is located 1km underneath the head of the Hillsborough Valley, and therefore the movement of the fault is likely to have caused the theorized bedrock fracturing and compression of inherent fractures and fissures in the bedrock at this location. The groundwater is relatively warm (~5° warmer than the Christchurch artesian aquifer system), and has a chemical composition that is closer to the Banks Peninsula aquifer system than the Christchurch artesian aquifer system, which confirms this assumption.

Artesian pressures would cause the groundwater to upwell in the loess-colluvium towards the ground surface. The groundwater would be semi-confined by the compressed material of the fissure traces, and this could cause the water to curve around the compressed material and rise to the ground surface downslope of the compressional zone. The greater void space around the compressed material would lead to preferential pathways for the groundwater to reach the surface. The springs would be expected to develop where there has been the greatest increase in artesian water pressure, and the greatest development of earthquake-induced fracturing of bedrock.

6.3. Preferred Engineering Geological Model

6.3.1. Rejected Models

The reasons that the Ramahana Road fissure traces are not considered likely to be the headscarps of rotational slide-type failures are as follows:

- The surface features do not match rotational slide movement geometry.
- The slope material is not homogeneous, and is in fact in a layered complex colluvial sequence with variable geotechnical characteristics.

The reasons that the Ramahana Road fissure traces are not considered likely to be the headscarps of translational slide-type failures are as follows:

- There are no distinct discontinuities within the loess-colluvium deposit that is continuous across the entire valley side, allowing a landslide of >500m in length across the slope.
- The presence of multiple fissure traces suggests that there is no principal single or main landslide headscarp.
- The loss of toe support from liquefaction is not applicable for the Ramahana Road fissure trace because of the absent evidence of liquefaction.
- When the headscarp of a progressive landslide develops it indicates that the landslide has a developed basal shear surface, but a basal shear surface has not been identified in any subsurface investigations in prior investigations, or in the current project.
- The fissures occur in toe-slope positions where the slope is gentle, whereas slide-type failures generally occur in steeper slopes where the static shear stress to normal stress ratio is greater.
- The fissures did not continue to move following the cessation of the Christchurch Earthquake induced cyclic stress, and have not been recorded to show any subsequent creep.

The reasons that the Ramahana Road fissure traces are not considered likely to be lateral spread-type failures are as follows:

- The slope is too steep for a typical lateral spread-type failure to occur.
- Flow liquefaction is not likely in Banks Peninsula loessial soils due to its low porosity and permeability, and general absence of saturation.
- Cyclic mobility is not likely or perhaps impossible due to the soils contractive response to monotonic stress.
- There is no evidence to suggest that liquefaction has occurred on the slope, despite the high PGAs and liquefaction on the adjacent flatlands.

6.3.2. Quasi-toppling Movement

The most likely slope movement type is considered to be a quasi-toppling motion similar to that suggested by Stephen-Brownie (2012), but with slightly different mechanisms. The movement model presented in Figure 6.1 is considered to be the most realistic representation of the mode of movement for the Ramahana Road fissure trace. This model depicts the movement occurring as a result of tensile stress/strain developed due to 1) bedrock uplift of

the Port Hills relative to the Christchurch city flatlands; 2) horizontal earthquake inertia forces; and 3) the static shear stress of the slope. The extensional outward movement of the upper more cohesive soil is considered to have been a quasi-toppling motion downslope, and this movement has been accommodated by compressional strain in the underlying less cohesive soil.

The quasi-toppling motion hypothesis offers a good correlation to the recorded surface and subsurface features of the fissure traces at 17 Ramahana Road and Centaurus Park. More research is needed to test and confirm the mechanisms suggested in this thesis, but there has been sufficient evidence from this research to indicate that the 'loess-slump' hypothesis is not applicable to the Ramahana Road fissure trace.

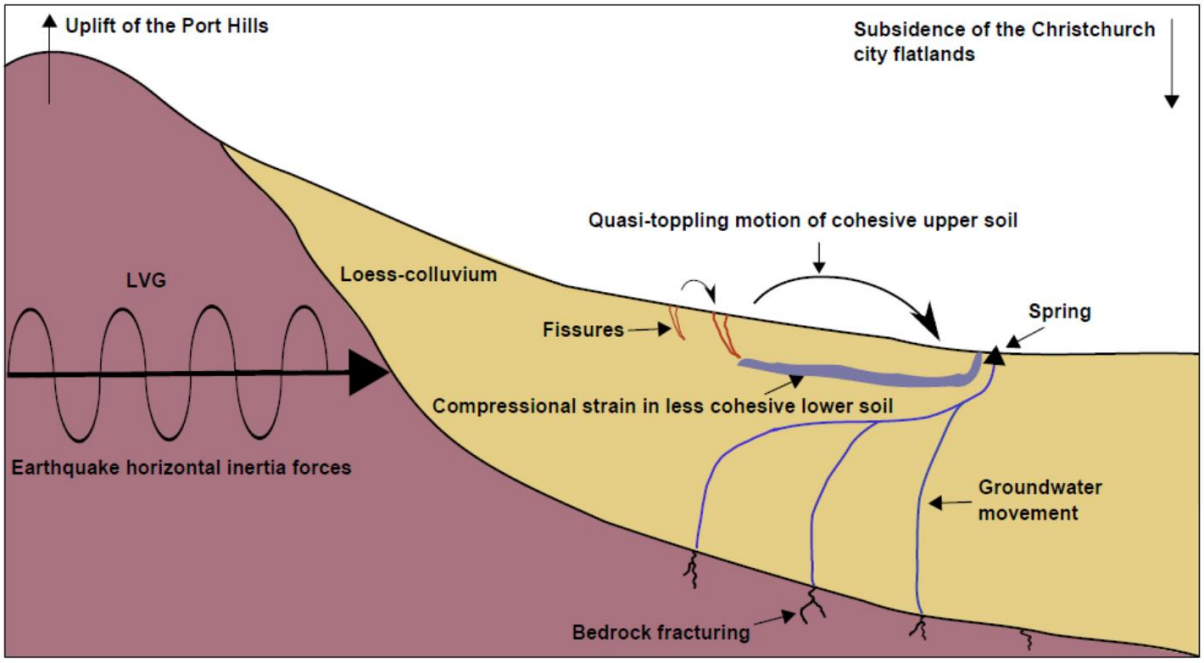

Figure 6.1: Preferred engineering geological model for the movement of the Ramahana Road fissure trace.

The reasons why the quasi-toppling movement is considered to be the most likely scenario are as follows:

- The fissure characteristics do not match typical mass movement features, and this indicates that the movement is not a typical form of landslide.
- The fissures are characterized by mostly horizontal displacement with minor vertical offset. There was no vertical offset observed in the mixed-colluvium layer that was intercepted by the fissure trace in the test pit.
- The multiple extensional features across the slope show that there is no single or principal headscarp.

- The quasi-toppling movement accurately fits the extensional and compressional features identified in this study and the geological model of the site area.
- The base of toppling can be viewed in the resistivity survey from the ground surface to ~8m and dissipating into the slope towards the extensional area as a high resistivity area.
- Springs have arisen in the compressional zone from the increased hydraulic head in the Banks Peninsula bedrock aquifer system at ~20m depth below the ground surface, and this indicates a connection to bedrock uplift.

6.4. Future Land Use along Ramahana Road

The vast majority of the fissures occurred during the 22nd of February 2011 Christchurch Earthquake. Little damage was observed following the original 4th of September 2010 Darfield Earthquake, or in any aftershocks with the exception of the Christchurch Earthquake. It is not thought that an earthquake less than M_W6.0 could produce enough intensity to cause fissuring in the loessial soils of the Port Hills. It is considered that extreme PGA (>0.5g) such as that recorded during the Christchurch Earthquake is a prerequisite to the development of the fissure traces, and as such they are only considered a possibility from a Port Hills Fault rupture. The Port Hills Fault has a recurrence interval of ~10,000 years (Villamor et al. 2011).

Whether the Alpine Fault could cause further fissuring in the loessial soils of the Port Hills is debatable: the magnitude could be high enough (~M_W6.0 in Christchurch city, estimated by Robinson & Davies, 2013), but the intensity of ground shaking and the peak ground accelerations would be much lower than those recorded in the Christchurch Earthquake. The seismic waves would also be of longer period and of different orientation, and there would be little effect on bedrock of the Port Hills.

Further research is needed to confirm the findings and suggested mechanisms in this thesis, but due to the large recurrence interval of the Port Hills Fault compared to the short general lifespan of a residential building, there is no reason why residential buildings and infrastructure should not be rebuilt within the fissure trace area. Any un-remediated fissure traces should be filled with a mixture of bentonite and SAP-20 gravel, as recommended by Christchurch City Council (2011), to stop infiltration of surface water prior to rebuild, but no accommodation for lateral displacement or settlement should need to be considered. Because

the fissure traces are not considered to be related to deep-seated slide movement, there is not a need for slope reinforcement or site abandonment.

It needs to be stressed that no construction should ever take place on loessial soils without a comprehensive understanding of the geotechnical model of the site. The mechanical behaviour of loessial soil is governed by its moisture content and clay content, and therefore the seasonal variations in the natural moisture content of the soil need to be understood for an accurate understanding of the geological model of the site. There are many papers and previous geotechnical investigations to draw from for future development on Port Hills loessial soils, and methods of erosion control are well documented.

6.5. Future Research

There are gaps in the current knowledge of exactly how the slope behaved in response to the cyclic shear stresses induced by the Christchurch Earthquake. To test the hypothesis and conclusions from this thesis it would be necessary to conduct further tests into the behaviour of loess-colluvium as distinct from primary loess. A summary of some of the potentially more useful tests are outlined below:

- Centrifuge Experiments: These experiments are useful when there is instability found in a slope, but the exact form of movement is not understood. Qualitative assessment can be carried out on the mechanisms and deformations involved in the movement, but quantitative assessments must be carried out subsequently using other tests. The inherent limitation of a centrifuge experiment is that the results are only as relevant as the accuracy of the model: the model must perfectly imitate the geometry of the slope and all geotechnical features within it. It is also costly and requires specialized equipment such as shake-tables. These are limitations that hindered the present research, but future research could use this test to good advantage, with adequate funding.

- Cyclic Triaxial Tests: These tests will be useful to test how the soil shear strength changes under cyclic loading. It would be beneficial to retrieve *in-situ* samples of loess-colluvium with varying natural moisture contents, clay contents, and plasticity indices to assess what affect each of these characteristics has on the shear strength of the soil under cyclic loading. Obtaining *in-situ* samples will be costly and difficult, and will require adequate funding.

- Dynamic Shear Tests: This would be a beneficial test to ascertain whether the loessial soil shear strength is diminished upon cyclic loading. It would be necessary to gain *in-situ* samples of loess-colluvium of varying natural moisture contents, clay contents, and plasticity indexes and test these under variable cyclic stress magnitudes.

- Test Pits: Test pits within the compressional zone would be beneficial to observe and test the compressional zone conditions to ≤3m depth. More test pits are also needed in the extensional zone to discover whether the fissure trace that was excavated for the purposes of this thesis was unique, or whether they all have similar features.

- Boreholes: The drilling of more boreholes in the extensional and compressional zone would be beneficial to gain more deep samples of loess-colluvium. Depths greater than 15m are not considered necessary unless bedrock profiles are required. Any CPT profile should be done with an adjacent borehole due to the inaccuracy of the soil behavioural type interpreted for loess-colluvium.

- Groundwater Assessment: Further information on the changes to the hydrogeology following the Christchurch Earthquake is required to determine how the springs in the compressional zone developed in the Hillsborough Valley and long-term dissipation of pore pressures.

References

Aoi S, Kunugi T, Fujiwara H 2008. Trampoline Effect in Extreme Ground Motion. Science 322: 727-730.

Ambraseys N, Srbulov M 1994. Earthquake induced displacements of slopes. Soil Dynamics and Earthquake Engineering 14: 59-71

ASTM D2487: 2011. Standard practice for classification of soils for engineering purposes (Unified Soil Classification System).

Bannister S, Gledhill K 2012. Evolution of the 2010-2012 Canterbury earthquake sequence. New Zealand Journal of Geology and Geophysics 55(3): 295-304.

Barr N, Zeldis J, Gongol C, Drummond L, Scheuer K 2012. Effects of the Canterbury earthquakes on Avon-Heathcote Estuary/Ihutai macroalgae. 36 p

Beavan J, Fielding E, Motagh M, Samsonov S, Donnelly N 2011. Fault Location and Slip Distribution of the 22 February 2011 MW 6.2 Christchurch, New Zealand, Earthquake from Geodetic Data. Seismological Research Letters 82(6): 789-799.

Beca Infrastructure Ltd 2011. Huntsbury No. 1 Reservoir - Geological Interpretative Report.

Been K, Jefferies M (2006) Soil liquefaction: a critical state approach. London: New York, Taylor & Francis.

Bell DH 1978. The engineering geology of Banks Peninsula loess deposits. Seminar on Slope Stability and Urban Development, University of Canterbury. 33pp.

Bell DH, Trangmar BB 1987. Regolith Materials and Erosion Processes on the Port Hills, Christchurch, New Zealand. Fifth International Conference and Field Workshop on Landslides. Pp. 93-105.

Bell DH, Namjou P, Sanders RA 1988. Springs as a potential groundwater resource on Banks Peninsula. Water Conference 1988.

Bell FG 1993. Engineering Geology. 2nd ed. Lanacre House, Jordan Hill, Oxford, Butterworth-Heinemann. 1-581 p.

Bell FG 1999. Earthquake Activity. Geological Hazards: Their assessment, avoidance and mitigation. 11 New Fetter Lane, London, E & FN Spon. Pp. 59-105.

Bjerrum L 1966. Progressive failure in slopes of overconsolidated plastic clay and clay shales. In: Hilf JW ed. The Third Terzaghi Lecture. Pp. 139-190.

Bradley BA, Cubrinovski M 2011. Near-source Strong Ground Motions Observed in the 22 February 2011 Christchurch Earthquake Seismological Research Letters 82(6): 853-865.

Brown LJ, Weeber JH 1992 Geology of the Christchurch Urban Area, 1:25000 geological map. Lower Hutt, Institute of Geological and Nuclear Sciences.

Brown LJ, Weeber JH 1994. Hydrogeological implications of geology at the boundary of Banks Peninsula volcanic rock aquifers and Canterbury Plains fluvial gravel aquifers. New Zealand Journal of Geology and Geophysics 37(2): 181-193.

Brown LJ, Beetham RD, Paterson BR, Weeber JH 1995. Geology of Christchurch, New Zealand. Environmental & Engineering Geoscience 4(4): 427-488.

Cox SC, Rutter HK, Sims A, Manga M, Weir JJ, Ezzy T, White PA, Horton TW, Scott D 2012. Hydrological effects of the MW 7.1 Darfield (Canterbury) earthquake, 4 September 2010, New Zealand. New Zealand Journal of Geologyand Geophysics 55(3): 16.

Cruden DM 1991. A simple definition of a landslide. Bulletin of the International Association of Engineering Geology 43: 27-29

Cruden DM, Varnes DJ 1996. Landslide Types and Processes. In: Turner KA, Schuster RL ed. Landslides Investigation and Mitigation. Washington, D.C., National Academy Press. Pp. 36-75.

Dellow GD, Massey CI, Davies TRH, Read SAL, Bruce ZRV, Van Dissen R, Barrell D, Jongens R, Heron D, Glassey P and others 2011. Rockfalls and landslides triggered by the February 2011 Christchurch (NZ) earthquake: the GeoNet response. In: Science G ed. Pp. 1.

Derbyshire E, Mellors TW 1986. Loess. In: Fookes PG, Vaughan PR ed. A Handbook of Engineering Geomorphology. New York, USA, Chapman and Hall. Pp. 258-269.

Di Stefano G, Ferro V, Mirabile S 2010. Comparison between grain-size analyses using laser diffraction and sedimentation methods. Biosystem Engineering 106: 205-215.

Dijkstra TA, Rogers CDF, Smalley IJ, Derbyshire E, Jin LY, Min MX 1994. The loess of north-central China: Geotechnical properties and their relation to slope stability. Engineering Geology 36: 153-171.

Eid HT 2010.Two- and three-dimensional analyses of translational slides in soils with nonlinear failure envelopes. Canadian Geotechnical Journal 47: 388-399.

English B 2011. Pre-election Economic and Fiscal Update 2011. 122 p.http://info.geonet.org.nz/display/home/Canterbury+Aftershocks#

Forsyth, P.J., Barrell, D.J.A., Jongens, R., 2008. Geology of the Christchurch Area, 1:250000 geological map 16: Lower Hutt, Institute of Geological & Nuclear Sciences.

Goldwater S 1990. Slope failure in loess a datailed investigation Allandale, Banks Peninsula. Unpublished Masters thesis, University of Canterbury, Unpublished. 159 p.

Grabowska-Olszewska B 1989. Skeletal microstructure of loesses - its significance for engineering-geological and geotechnical studies. Applied Clay Science 4: 327-336.

Green MJ 2015. Hydrogeological investigation of earthquake related springs in the Hillsborough Valley Christchurch, New Zealand. Unpublished Masters thesis, University of Canterbury, Unpublished. 109 p.

Griffiths E 1973. Loess of Banks Peninsula. New Zealand Journal of Geology and Geophysics 16(3): 657-675.

Hampton SJ 2010. Growth, Structure and Evolution of the Lyttelton Volcanic Complex, Banks Peninsula, New Zealand. Unpublished Doctoral thesis, University of Canterbury, Unpublished. 311 p.

Hancox G, Massey C, Perrin N 2011. Landslides and related ground damage caused by the MW 6.3 Christchurch earthquake of 22 February 2011. NZ Geomechanics News 81(15)

Harris SA 1983. Infilled Fissures in Loess, Banks Peninsula, New Zealand. Polarforschung 53(2): 49-58.

Higgins JD, Modeer VA 1996. Loess. In: Turner KA, Schuster RL ed. Landslides: Investigation and Mitigation. Washington, D. C., National Academy Press. Pp. 585-606.

Hovius N, Meunier P 2012. Earthquake ground motion and patterns of seismically induced landsliding. In: Clague JJ, Stead D ed. Landslides: types, mechanisms and modelling. Cambridge; New York, Cambridge University Press. Pp 24-36.

Hughes JT 2002. A detailed study of Banks Peninsula loess shear strength. Unpublished Masters thesis, University of Canterbury, Unpublished. 110 p.

Ives D 1972. Nature and Distribution of Loess in Canterbury, New Zealand. New Zealand Journal of Geology and Geophysics 16(3): 587-610.

Jefferies M, Been K 2006. Soil Liquefaction: A Critical State Approach. 2 Park Square, Milton Park, Abingdon, Oxon, Taylor & Francis. 479 p.

Kaiser A, Holden C, Beavan J, Beetham D, Benites R, Celentano A, Collet D, Cousins J, Cubrinovski M, Dellow G and others 2012. The Mw 6.2 Christchurch earthquake of February 2011: preliminary report. New Zealand Journal of Geology and Geophysics 55(1): 67-90.

Keefer DK 2002. Investigating landslides caused by earthquakes - a historical review. Surveys in Geophysics (23): 473-510.

Kingma JT 1974. The Geological Structure of New Zealand. Canada, John Wiley & Sons, Inc. 407 p.

Leopold M, Volkel J 2006. Colluvium: definition, differentiation, and possible suitability for reconstructing Holocene data. Quaternary International 162-163: 133-140.

Lucas Associates, historical maps of Christchurch, 1856 Black Map. Retrieved 20 August, 2015 from http://www.lucas-associates.co.nz/christchurch-banks-peninsula/historical-maps/

Lunne T, Robertson PK, Powell JJM 1997. Cone penetration testing in geotechnical practice. EF Spon/Blackie Academic, Routledge Publishers, London. 312 p.

Massey CI, Yetton MD, Carey J, Lukovic B, Litchfield N, Ries W, McVerry G 2013. Canterbury Earthquakes 2010/11 Port Hills Slope Stability: Stage 1 report on the findings from investigations into areas of significant ground damage (mass movements). 37 p.

McManus KJ, Cubrinovski M, Pender MJ, McVerry G, Sinclair T, Matuschka T, Simpson K, Clayton P, Jury R 2010. Geotechnical earthquake engineering practice: Module 1 - Guideline for the identification, assessment and mitigation of liquefaction hazards. 28 p.

Ministry of Business Innovation & Employment 2013. Guidance for building in toe slump areas of mass movement in the Port Hills (Class II and Class III). 16 p.

New Zealand Geotechnical Society 2005. Field description of soil and rock: guideline for the field classification and description of soil and rock for engineering purposes. 39pp.

New Zealand Geotechnical Society 2011. Guideline for hand held shear vane test. 10pp

New Zealand Standards 4402:1986 Methods of testing soils for civil engineering purposes.

NZPolice 2011. Christchurch earthquake: List of deceased. Retrieved 19/01/2015 2015, from http://www.police.govt.nz/major-events/previous-major-events/christchurch-earthquake/list-deceased

Obruchev VA 1945. Loess types and their origin. American Journal of Science 243: 256-262

Pecsi M 1990. Loess is not just the accumulation of dust. Quaternary International 7(8): 1-21

Pye K 1995. The Nature, Origin, and Accumulation of Loess. Quaternary Science Reviews 14: 653-667.

Quigley M, Van Dissen R, Litchfield N, Villamor P, Duffy B, Barrell D, Furlong K, Stahl T, Bilderback E, Noble D 2010. Surface rupture during the 2010 MW 7.1 Darfield (Canterbury) earthquake: Implications for fault rupture dynamics and seismic-hazard analysis. Geology 40(1): 55-58.

Raeside JD 1964. Loess Deposits of the South Island, and Soils Formed on them. New Zealand Journal of Geology and Geophysics 7(4): 811-838.

Rauch AF 1997. EPOLLS: An Emperical Method for Predicting Surface Displacements Due to Liquefaction-Induced Lateral Spreading in Earthquakes. Unpublished Dissertation thesis, Virginia Tech, Blacksburg, Virginia. 333 p.

Read SAL, Richards L 2007. Proceedings of the 1st Canada-US Rock Mechanics Symposium - Characteristics and classification of New Zealand greywackes. Rock Mechanics: Meeting Society's Challenges and Demands.

Rib HT, Liang T 1978. Recognition and identification. In: Schuster RL, Krizek RJ ed. Landslides Analysis and Control. Washington, D.C., National Academy of Sciences. Pp. 34-80.

Robertson PK 2009. CPT interpretation - a unified approach. Canadian Geotechnical Journal 46: 1-19

Robertson PK, Campanella RG, Gillespie D, Greig J 1986. Use of piezometer cone data. In-Situ'86, Use of In-situ testing in geotechnical engineering. GSP 6. ASCE, Reston, VA, Specialty Publication. Pp. 1263-1280

Robertson PK, Woeller DJ, Finn WDL 1992. Seismic cone penetration test for evaluating liquefaction potential under cyclic loading. Canadian Geotechnical Journal 29: 686-695

Robertson PK, Fear CE 1996. Estimating the undrained strength of sand: a theoretical framework: Reply. Canadian Geotechnical Journal 33(5): 847-848.

Robinson TR & Davies TRH 2013. Review Article: Potential geomorphic consequences of a future great (MW = 8.0+) Alpine Fault earthquake, South Island, New Zealand. Natural Hazards and Earth System Sciences 13: 2279-2299.

Rogers JD 2006. Subsurface exploration using the standard penetration test and the cone penetrometer test. Environmental and Engineering Geoscience 12(2): 161-179

Samuoelian A, Cousin I, Tabbagh A, Bruand A, Richard G 2005. Electrical resistivity survey in soil science: a review. Soil & Tillage Research 83: 173-193

Seed HB 1967. Landslides during earthquakes due to soil liquefaction. In: Hilf JW ed. The Fourth Terzaghi Lecture. Pp. 191-261.

Selby MJ 1976. Loess. New Zealand Journal of Geography 61: 1-18

Sewell, R.J., Weaver, S. D., and Reay, M. B., 1992. Geology of Banks Peninsula. Scale 1:100,000. Institute of Geological and Nuclear Sciences Map 3. Institute of Geological and Nuclear Sciences Ltd, Lower Hutt.

Shelley, D., 1987. Lyttelton-1 and Lyttelton-2, the 2 Centers of Lyttelton-Volcano. New Zealand Journal of Geology and Geophysics. 30, 159-168.

Sibson R, Ghisetti F, Ristau J 2011. Stress control of an evolving strike-slip fault system during the 2010-2011 Canterbury New Zealand, earthquake sequence. Seismological Research Letters 82: 824-832.

Skempton WA 1964. Long-term stability of clay slopes. Fourth Rankine Lecture. Geotechnique 14(2): 77-101

Sladen JA, D'Hollander RD, Krahn J 1985. The liquefaction of sands, a collapse surface approach. Canada Geotechnical Journal 22: 564-578

Sowers GF, Royster DL 1978. Chapter 4: Field Investigation. In: Schuster RL, Krizek RJ ed. Special Report 176: Landslides: Analysis and Control. Washington, D.C., TRB, National Research Council. Pp. 81-111.

Stephen-Brownie CJ 2012. Earthquake-Induced Ground Fissuring in Foot-Slope Positions of the Port Hills, Christchurch. Unpublished Masters thesis, University of Canterbury, Unpublished. 160 p.

Tan TK 1986. Fundamental properties of loess from Northwestern China. Engineering Geology 25: 103-122.

Terzaghi K 1950. Mechanisms of landslides, in application of geology to engineering practice, Berkey Vol. Geological Society of America. Pp 83-123

Varnes DJ 1978. Slope Movement Types and Processes. In: Schuster RL, Krizek RJ ed. Landslides Analysis and Control. Washington, D.C., National Academy of Sciences. Pp. 11-33.

Vick LM 2015. Evaluation of field data and 3D modelling for rockfall hazard assessment. Unpublished Doctoral thesis, University of Canterbury, Unpublished. 172 p.

Villamor P, Litchfield N, Hornblow S, Barrell D, Van Dissen R, Levick S 2011. Greendale Fault: investigation of surface rupture characteristics for fault avoidance zonation. GNS Science Consultancy Report. ECAN Report R11/25. 46p.

Wang L, Wang Y, Wang J, Li L, Yuan Z 2004. The liquefaction potential of loess in China and its prevention. 13th World Conference on Earthquake Engineering. Pp. 13.

Wieczorek GF 1996. Landslide triggering mechanisms. In: Turner KA, Schuster RL ed. Landslides Investigation and Mitigation. Washington, D.C., National Academy Press. Pp 76-90.

Wu TH 1996. Soil Strength Propoerties and Their Measurement. In: Turner KA, Schuster RL ed. Landslides Investigation and Mitigation. Washington, D. C. 1996, National Academy Press. Pp. 319-336.

Yetton MD 1992. Engineering geological and geotechnical factors affecting development on Banks Peninsula and surrounding areas In: Campbell JK ed. Geological Society of New Zealand and New Zealand Geophysical Society 1992 Joint Annual Conference. Pp. 103-136.

Zhungu Z 1980. Loess in China. GeoJournal. 4(6): 525-540.

Appendices

Appendix 1: Literature Review Extra Details

1.1. Christchurch City

The Ramahana Road fissure trace is situated in the suburb of Huntsbury within the city of Christchurch on the east coast of the South Island, New Zealand. Christchurch was primarily developed as a service centre for the requirements of the extensive primary industries working on the Canterbury Plains (at 8000 km^2 this is New Zealand's largest plain (Brown et al. 1995)). Today it is New Zealand's third largest city by population, partly due to the groundwater sourced from the greywacke gravel and sands of the Canterbury Plains aquifers, which are of excellent quality for residential, industrial, and agricultural use.

The growth of Christchurch has not been aided by the poor land on which it sits. In the past, before the extent of the earthquake hazard was recognized, there was much less thought given to the many geotechnical constraints of building within the area of the city. The main site of Christchurch is located on drained swamp land, inland from beach dune sand, estuaries, and lagoons. 90% of Christchurch lies within the former flood plains of the Waimakariri River, which has since been realigned and stop-banked (Brown et al. 1995). Two streams are still found flowing from springs in western Christchurch through the city towards the coast: the Avon and Heathcote, and these pose a moderate flood risk, as well as the risk of lateral spreading along their banks during an earthquake. Brown et al (1995) explain that the high ground water table, which increases towards the coast, as well as the relatively young and unconsolidated sediment, determines foundation constraints. Many of the houses located on the Christchurch flatlands are at risk of liquefaction and lateral spreading damage during an earthquake.

To the immediate south of the city there is the extinct volcanic complex known geographically as Banks Peninsula. A 2.6 km long tunnel passes through the most northerly located sequence of hills, known as the Port Hills, which links the city of Christchurch to the Port of Lyttelton in Lyttelton Harbour. Building on the Port Hills poses its own set of geotechnical constraints due to slope stability issues. Slope stability issues arise from the extensive discontinuities within the Banks Peninsula volcanics in the form of bedding planes and fracture sets (Brown et al. 1995). Historical coastal erosion has caused scouring of sheer cliff faces in the volcanic deposits bordering the suburbs of Sumner, Redcliffs, and Taylors

Mistake, and the residents who reside here face the hazards of rockfall and cliff collapse. Rockfall can also be an issue at any location where there is a volcanic outcrop located upslope of housing, particularly where rocks can be channelled into gullies leading towards infrastructure. Other slope stability issues are concerned with development on the loessial soils, which embrace the majority of surface soils on Banks Peninsula. The housing that has been built on top of loessial soils can be affected by soil erosion processes such as sheet, rill, and piping, and mass movement processes such as slide, flow, and complex.

1.2. Evolution of the Canterbury Plains

The Banks Peninsula volcanoes originally formed as an island off the coast of the former coastline of New Zealand, but the basin has subsequently been infilled with greywacke gravels and sands, which have joined the island to the mainland. According to Brown and Weeber (1994b) the basin has been within a process of subsidence since the Pleistocene; however the rate of sediment accumulation has outpaced the rate of subsidence, which has been occurring at a rate of 0.05 to -0.09 m/ka since the early Miocene (Herzer 1981 cited by Brown and Weeber 1994b). The substantial amounts of TT sediment that has been required to accommodate this accumulation were sourced from erosion of the uplifting Southern Alps, particularly during the glacial periods of the Pleistocene where the grinding power of glacial movement across mountain gullies eroded and transported vast quantities of sediment. The transport of this sediment from the foothills of the Southern Alps towards the Pacific Ocean was accommodated by movement of eastward-flowing meltwater streams and rivers, such as the Waimakariri and Rakaia Rivers (Brown et al. 1995). These streams formed large intermingled glacial outwash alluvial fans which over time formed the Canterbury Plains.

During the strong climatic variability of the Pleistocene, the cyclic growth and decay of continental ice sheets led to rising and falling sea levels. As aforementioned the glacial periods produced vast quantities of sediment that were successively deposited eastward towards the Pacific Ocean which would have been at a lower sea level during this period. In inter-glacial periods the sea level would have risen, causing the sea to cover the greywacke sediments that were deposited near the coast, leading to marine sands, silts, and muds being deposited over the greywacke sediment. The alternating depositional sequence has led to a series of confined aquifers, with the water being held in the coarser fluvial greywacke sediment, and confining by the finer marine sands, silts, and muds. The joining of Banks Peninsula to the Canterbury Plains diverted the predominantly southerly ocean swells, which

resulted in progradation of the coast north of Banks Peninsula and erosion of the coast to the south (Brown et al. 1995).

1.3. Loess Primary Classifications

The distinction between primary loess, which is of the original aeolian deposition; and secondary loess, which is primary loess that has undergone redepositional processes, or sufficient alteration/degradation *in situ* was originally emphasized by Obruchev (1945). Obruchev's 1945 report: *Loess Types and their Origin* would prove to become the basis behind modern loess sub-classification, as he also made the distinction between "cold" loess, which has a fluvio-glacial origin; and "warm" loess, which has a continental (desert) origin. "Cold" loess is associated with the major loess deposits of the world, such as the Loess Plateau, northern Argentina, and central USA, whilst "warm" loess is associated with more localised deposits such as in Israel, Iran, and the Sahara margins (Derbyshire & Mellors 1986).

In New Zealand's situation the deposits can be classified as "cold" loess, and of this, the primary loess can be further categorized into glacial loess and post-glacial loess. Following Ives (1972), the term glacial loess can embrace any loess deposit of Late Pleistocene age that ceased to accumulate around 10,000 years ago; and post-glacial loess can embrace any deposit of more recent age than this. Glacial loess in Canterbury can be identified on undulating to hilly land across the fringes of the Canterbury Plains, excluding at the coastal boundary, and the extent of mountain basins. Ives (1972) observes that the deepest deposits occur in South Canterbury rolling hill country and on Banks Peninsula, where their thickness is commonly in excess of 3 m; these deposits frequently show evidence of multiple phases of deposition by the occurrence of palaeosols. Post-glacial loess can be identified on fan and outwash surfaces of major rivers such as the Rakaia and Waimakariri. The material that makes up both deposits has been sourced from the greywacke of the Southern Alps and foothills; however the structure of the deposits is substantially different: glacial loess has a higher clay content, lower porosity, and a higher compaction than post-glacial loess; it also contains vertical cracks, a fragipan near the top of parent material in soils of over 2 m depth, and a coarse prismatic framework, whereas post-glacial loess is massive and contains only few vertical cracks (Ives 1972).

1.4. Geotechnical Properties of Banks Peninsula Loessial Soils

Parameter	Typical Range of Values	Source Reference
POROSITY	30 - 40%	Birrel & Packard (1953)
VOID RATIO	0.4 - 0.7	Birrel & Packard (1953) Miller (1971)
ATTERBERG LIMITS	LL 18 - 33 PL 17 - 22 (C layer) PI < 12	Alley (1966) Hughes (1985) Crampton (1985) Yetton (1986)
GRAIN SIZE	(Silt range > 0.002mm & < 0.06mm) Sand ≈ 10% Silt 65 - 80%, Clay 11 - 25%	Alley (1966) Hughes (1985) Crampton (1985) Yetton (1986)
DRY DENSITY	S layer average = 1.54t/m^3 (1.39 - 1.62t/m^3 range) C layer average = 1.64t/m^3 (1.51 - 1.88t/m^3 range) P layer average = 1.55t/m^3 (1.32 - 1.71t/m^3 range)	Evans (1977) Crampton (1985) Yetton (1986)
LINEAR SHRINKAGE	0 - 2% in lower S and P layers > 5% in C layer	Alley (1966) Yetton (1986)
PERMEABILITY	1.5 • 10^{-7} m/s (undisturbed) ≈1•10^{-7}m/s (In-situ test)	Birrel & Packard (1953) Sanders (1986)
INTERNAL ANGLE OF FRICTION	35 - 37° (Residual, Ring shear) 30° (Peak, Triaxial (total)) 30° (Peak, Triaxial (total)) 15 - 25° (Peak, Triaxial (effective))	Salt (1983) Mackwell (1986) McDowell (1989) Alley (1966)
COHESION	0 kPa (effective) 85 - 112kPa (apparent) 0 - 180 kPa (apparent)	Alley (1966) Macwell (1986) McDowell (1989)
COMPRESSION INDEX	Cc = 0.17 (1.7% vol. change dry to saturated)	Birrel & Packard (1953)
Ph	Acidic - 5(S layer) to 7(P layer)	Miller (1971)
SOLUBLE SALT CONCENTRATION	Incr. with depth, from 1meg/l to 60meg/l in P layer	Miller (1971)
EXCHANGEABLE SODIUM %	0.9 in S layer to41 deep in P layer	Hughes (1970)
SEISMIC VELOCITY	250 - 400m/s	Crampton (1985) Yetton (1986) McDowell (1989)
RESISTIVITY	Varying with depth from 90 ohm/m near surface to <10 ohm/m in P layer	Yetton (1986)
CONDUCTIVITY	From 1.0 •10^{-4} mho/cm to 14 •10^{-4} mho/cm with depth	Birrel & Packard (1953) Yetton (1986)

Figure 1.1: Geotechnical properties of Banks Peninsula loessial soils modified from Yetton (1990)

1.5. Construction Considerations in Loessial Soils

As aforementioned, the bearing capacity of loess is relatively high, in low moisture conditions. Under these conditions loess may support foundations with bearing pressures of 200-300 kN/m2, with no associated settlement (Derbyshire & Mellors 1986). It is prudent to note here that substantial consideration needs to be given to seasonal fluctuations in groundwater and moisture levels, before calculations of bearing capacity can be accurate. Loess can be remoulded and compacted at the surface to a few meters depth to achieve greater bearing capacity for heavier structures; however once again the groundwater level will need to be considered and drainage may be needed to achieve the desired bearing capacity in all seasons. Derbyshire and Mellors (1986) offer alternative options including the use of pile foundations to reach a greater depth, where the bearing capacity is greater; grouting the soil; excavating the loess and mixing with bentonite to make a slurry that is then compacted back in place; and preconsolidation, by way of flooding the loess, to induce settlement prior to construction (more relevant for collapsible loess).

Buried services induce an accelerated risk of piping around them. Water can form preferential pathways along the services, removing soil and forming cavities along the pipeline. This can remove support from the pipe, leading to cracks or failure of the pipe, in turn leading to exacerbated erosion from the additional water, and ultimately failure of the overlying soil. The design of buried services in loessial soils needs to incorporate filters or linings to minimise this risk (Derbyshire & Mellors 1986). Chemical stabilisation has also been used with great success in Banks Peninsula loessial soils by the mixing of loess with either hydrated lime (Ca(OH)2), quicklime (CaO), Portland cement, or orthophosphoric acid (H3PO4) and compacting at their optimum moisture content (Bell et al. 1986).

Construction on loessial soils on Banks Peninsula is also limited by the slope angle, moisture content, and climate variability. Yetton (1992) explains that endorsement of development on slopes at a greater angle than 25° shouldn’t be done without extreme caution due to the likelihood of a high intensity rainfall event, a major wet period, or a significant earthquake occurring within the lifespan of the building.

1.6. Historical Fissures in Banks Peninsula Loessial Soils

Because the fissures occurred following the Christchurch earthquake, it would be reasonable to assume that a previous Port Hills fault earthquake could have caused a similar behavioural

response in the loess-colluvium. In researching this it was found that there are multiple infilled fissure traces within a depositional sequence of primary loess' called the 'Summit Silt Loam'. The fissures occur within a primary loess facies known as 'Stony Bay Loess' and are infilled by the 'Te Oka Loess'. These fissure traces were investigated by Harris (1983) towards the goal of better understanding what caused the fissures and calibrating the palaeo climate at this time. It was concluded that these fissures were most likely caused by thermal contraction cracking and subsequent ice wedge formation; however in order for this to have occurred, the temperatures would have needed to be 16-18 degrees colder than the present day mean annual temperature (Harris 1983).

An alternative hypothesis might be that the fissure traces are the result of palaeo earthquake activity, and there are some similarities between the fissure traces formed after the Christchurch earthquake and those studied by Harris (1983); including the fact that they are open fissure traces and that they have low clay content within the fissured material. There are, however, many discrepancies, including their location: found on steeper, south facing slopes, and at a much greater distance from the Port Hills fault than in the fissures caused by the Christchurch earthquake; their size: they are much smaller features, being only up to 165 cm deep and usually 5-15 cm wide at the surface, but only up to 60 cm wide; their shape: they tend to be highly vertically orientated with little downslope curvature at the base; there are also many of them, and they are spaced quite closely together. See figure 1.2 for a photo of the palaeo fissures.

It must be concluded that these palaeo fissures are the result of a slightly different behavioural response than what caused the fissure traces during the Christchurch earthquake, but they could still have been triggered by a palaeo earthquake on a closer fault. Because these fissures are located within primary loess rather than loess-colluvium, perhaps the fissuring was along the inherent subvertical fractures, and this would explain their more vertical nature. It would be reasonable to assume that there have been fissures that formed from similar mechanisms to the ones that formed during the Christchurch earthquake in response to historical earthquakes from the Port Hills fault, but these have not been identified in previous studies.

There are two compelling reasons as to why similar palaeo fissures have not been identified. The first is because the fissures were infilled by the same material as the surrounding soil: the sequence is all loess-colluvium, and therefore the boundaries are not visible once they have

been infilled (this proved to be a problem when interpreting the fissure trace in the test pit). The second is that the fissures would also most likely be buried beneath subsequent depositional layers of loess-colluvium and therefore are unable to be seen at the ground surface.

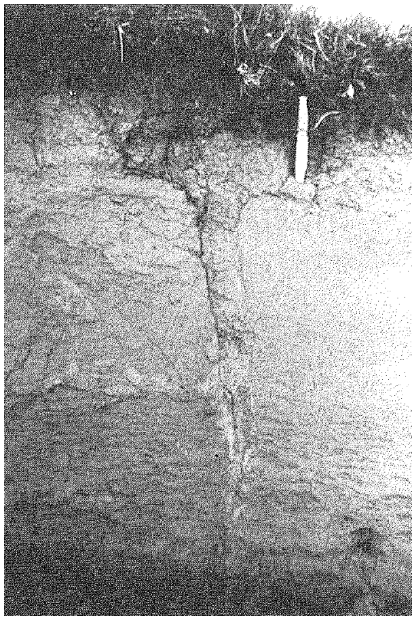

Figure 1.2: Infilled palaeo fissure in loess. After Harris (1983)

Appendix 2: Qualitative Methods: Subsurface Investigation Methods and Raw Data

2.1: Engineering Geological Mapping Photos

2.1.1: The cracked concrete pad in the extensional zone.

2.2.2: The main overgrown and in-filled, but undisturbed fissure trace.

2.2.3: The cracked concrete step in the compressional zone at the base of the slope.

2.2.4: The tilted garden retaining wall in the compressional zone adjacent to the cracked step.

2.2.5: Small ground crack running parallel to slope at the base of the slope.

2.2.6: 100 mm horizontal and 50 mm vertical offset in concrete path in the valley floor.

2.2: Test Pit

2.2.1. The condition and location of the fissure trace which was dug through by the digger at 17 Ramahana Road.

2.2.2: Test Pit Logs

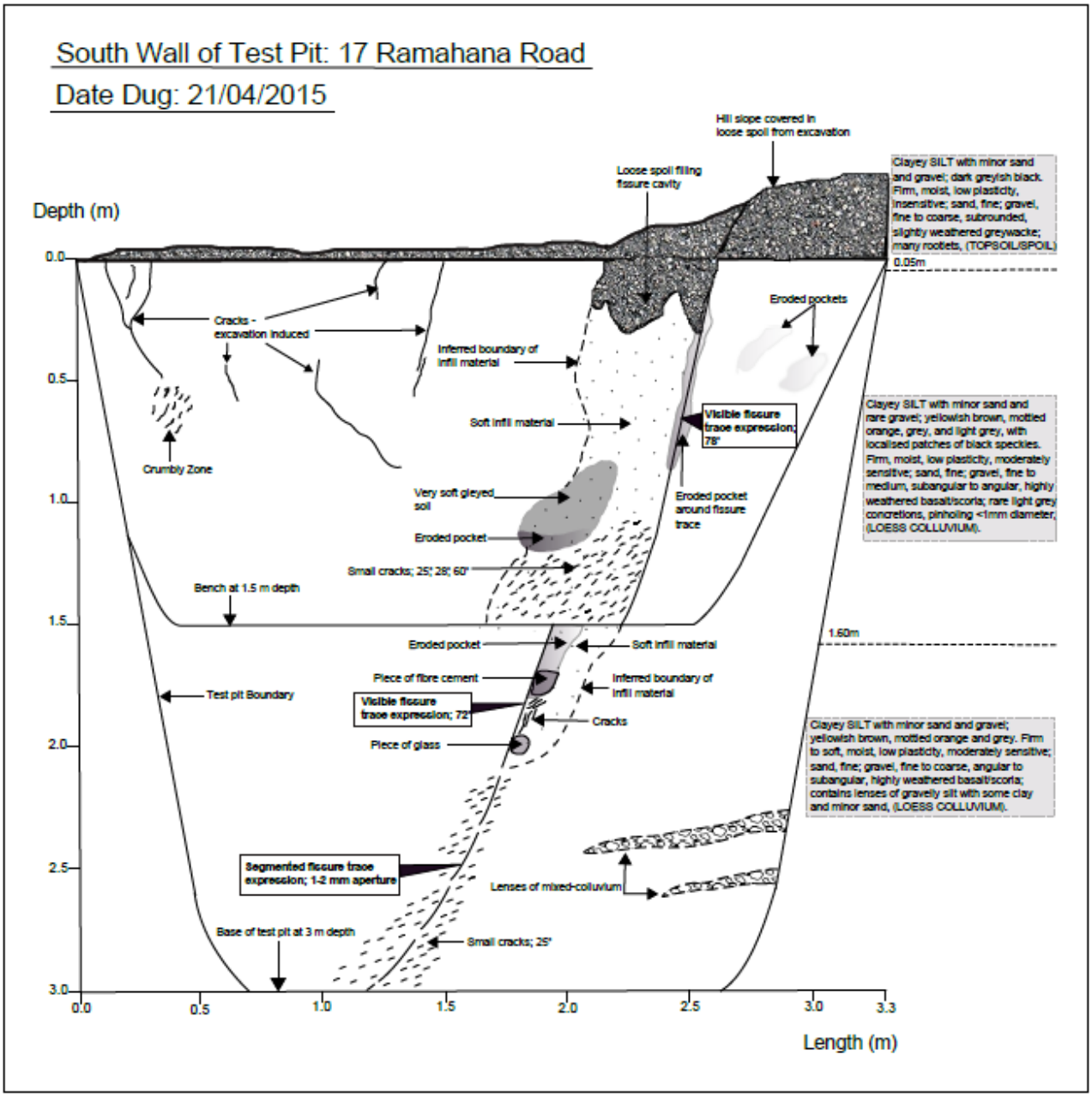

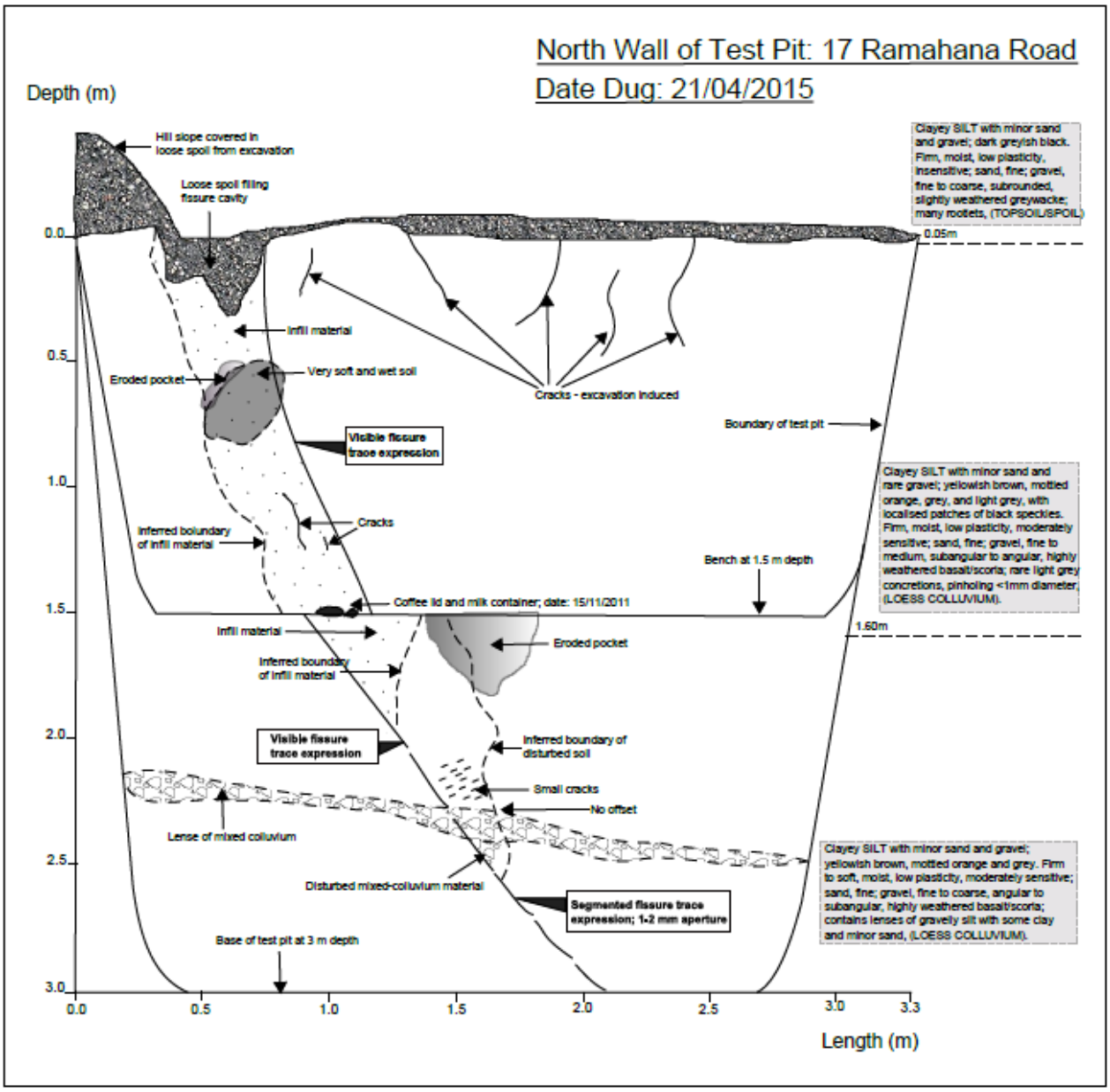
North Wall of Test Pit: 17 Ramahana Road
Date Dug: 21/04/2015
Depth (m)
Hill slope covered in loose spoil from excavation
Loose spoil filling fissure cavity
Clayey SILT with minor sand and gravel; dark greyish black. Firm, moist, low plasticity, insensitive; sand, fine; gravel, fine to coarse, subrounded, slightly weathered greywacke; many rootlets, (TOPSOIL/SPOIL)
0.05m
Infill material
Eroded pocket
Very soft and wet soil
Cracks - excavation induced
Visible fissure trace expression
Boundary of test pit
Clayey SILT with minor sand and rare gravel; yellowish brown, mottled orange, grey, and light grey, with localised patches of black speckles. Firm, moist, low plasticity, moderately sensitive; sand, fine; gravel, fine to medium, subangular to angular, highly weathered basalt/scoria; rare light grey concretions, pinholing <1mm diameter, (LOESS COLLUVIUM).
Inferred boundary of infill material
Cracks
Bench at 1.5 m depth
Coffee lid and milk container; date: 15/11/2011
1.60m
Infill material
Eroded pocket
Inferred boundary of infill material
Visible fissure trace expression
Inferred boundary of disturbed soil
Small cracks
No offset
Lense of mixed colluvium
Clayey SILT with minor sand and gravel; yellowish brown, mottled orange and grey. Firm to soft, moist, low plasticity, moderately sensitive; sand, fine; gravel, fine to coarse, angular to subangular, highly weathered basalt/scoria; contains lenses of gravelly silt with some clay and minor sand, (LOESS COLLUVIUM).
Disturbed mixed-colluvium material
Segmented fissure trace expression; 1-2 mm aperture
Base of test pit at 3 m depth
0.0
0.5
1.0
1.5
2.0
2.5
3.0
3.3
Length (m)

2.3: Hand Auger Logs

2.3.1. Hand Auger Logs in Extensional Zone at 17 Ramahana Road

BELL GEOCONSULTING LTD
HAND AUGER LOG

Hand Auger Number: HA2

Project: 17 Ramahana Road, Huntsbury	Date: 10/02/2015
BGL REF #:	Water level in hole:
Co-ordinates (NZTM) E: 1572176.00 N: 5176393.00	Orientation: Vertical
	Logged By: Chris White

WT	Samples	Depth (m)	Legend	STRATA DESCRIPTION - Subordinate Fraction, Major fraction, Minor Fraction, Colour, Structure, Strength, Moisture Condition, Grading, Bedding, Plasticity (NZ Geotechnical
		0.0		SILT with minor clay; light yellowish brown. Stiff, dry, low plasticity, (FILL).
		0.130		SILT with minor sand and trace gravel; dark greyish brown, Stiff, dry, low plasticity; sand, fine to coarse; gravel subrounded, slightly weathered greywacke; trace rootlets (TOPSOIL).
		0.265		SILT with some clay; light yellowish brown, slightly mottled orange and light grey. Stiff, dry, low plasticity, (LOESS COLLUVIUM)
				0.390 m becomes dark yellowish brown; firm
				0.470 m becomes moist, mottling becomes more pronounced
				Increasing moisture and decreasing consistency with depth
				1.550 m becomes soft, wet; mottling absent; trace sand and gravel present; sand, fine to coarse, gravel, fine sub-angular to angular, highly weathered to completely weathered basalt; dark orangish red.
				1.800 m gravel absent
				1.990 m Sand absent
				2.220m becomes slightly mottled orange and light grey; minor gravel present; gravel, fine, angular, highly weathered basalt; dark greyish purple.
				2.400m mottling absent
				2.640 to 2.700 m Coarse gravel clast; angular, completely weathered basalt; dark greyish purple; mottled orange and light grey around edges.
				2.7m gravel becomes completely weathered; mottled orange and light grey around edges.
		4.2		EOH 4.2 m

Comments:

Client:

BELL GEOCONSULTING LTD HAND AUGER LOG		Hand Auger Number:	HA3
Project:	17 Ramahana Road, Huntsbury	Date	10/02/2015
	BGL REF #:	Water level in hole	
Co-ordinates (NZTM)	E: 1572176.00	Orientation	Vertical
	N: 5176397.00	Logged By	Chris White

WT	Samples	Depth (m)	Legend	STRATA DESCRIPTION - Subordinate Fraction, Major fraction, Minor Fraction, Colour, Structure, Strength, Moisture Condition, Grading, Bedding, Plasticity (NZ Geotechnical
		0.0		SILT with minor clay and trace sand and gravel; light greyish brown. Stiff, dry, low plasticity; sand, fine to coarse; gravel, fine to medium, subrounded, slightly weathered greywacke. (FILL)
		0.270		SILT with some clay; light yellowish brown, slightly mottled orange and light grey. Stiff, dry, low plasticity. (LOESS (ALLUVIUM)
		0.770		0.770 - 0.880 Core loss
		0.880		becomes soft, moist.
		1.000		becomes wet; dark yellowish brown; mottling absent; trace sand and gravel; sand, fine to coarse; gravel, fine to medium, angular, highly weathered basalt; dark greyish purple; SILT liquifiable.
		1.2		Gravel, fine.
		2.590		Gravel and sand absent. Moisture content decreases.
		4.0		EOH 4.0m

Comments:

Core loss at 0.770 - 0.880 due to auger slipping; possibly because of forcing too much pressure onto auger in sudden soft, moist soil or possibly it indicates a tunnel gulley. The moisture content at 1m was higher than at any other auger hole.

Client:

BELL GEOCONSULTING LTD HAND AUGER LOG		Hand Auger Number:	HA4
Project:	17, Ramahana Road, Huntsbury BGL REF #:	Date	10/02/2015
		Water level in hole	
Co-ordinates (NZTM)	E: 1572180.00 N: 5176404.00	Orientation	Vertical
		Logged By	Chris White

WT	Samples	Depth (m)	Legend	STRATA DESCRIPTION - Subordinate Fraction, Major fraction, Minor Fraction, Colour, Structure, Strength, Moisture Condition, Grading, Bedding, Plasticity (NZ Geotechnical
		0.0		SILT with minor clay and trace sand and gravel; light yellowish brown. Stiff, dry, low plasticity; Sand, fine to coarse; gravel, fine to medium, rounded, slightly weathered greywacke; trace rootlets, (FILL)
		0.230		brick fragment
		0.370		SILT with some clay and trace fine sand; dark yellowish brown. Stiff, dry, low plasticity, (LOESS COLLUVIUM)
		0.750		becomes light yellowish brown.
		0.900		Slight mottled orange and light grey.
		1.000		becomes soft, moist, dark yellowish brown, mottled orange and light grey; trace sand absent.
		1.660		becomes wet.
		1.780		mottling less pronounced.
		2.000		mottling absent.
		2.950		becomes firm; trace gravel; fine, sub-angular, highly weathered basalt, dark greyish purple; less moisture.
		3.550		becomes soft, wet; gravel absent.
		4.0		EOH 4.0m

Comments:

0.370 - 0.750 Inferred to be an old topsoil layer due to darker colouring; however lack of rootlets to confirm.

Client:

BELL GEOCONSULTING LTD HAND AUGER LOG		Hand Auger Number:	HA5
Project:	17 Ramahana Road, Hunlsbury	Date	10/02/2015
	BGL REF #:	Water level in hole	
Co-ordinates (NZTM)	E: 1572183.00	Orientation	Vertical
	N: 5176394.00	Logged By	Chris White

WT	Samples	Depth (m)	Legend
		0.0	
		0.1	
		0.2	
		0.3	
		0.4	
		0.5	
		0.6	
		0.7	
		0.8	
		0.9	
		1.0	
		1.1	
		1.2	
		1.3	
		1.4	
		1.5	
		1.6	
		1.7	
		1.8	
		1.9	
		2.0	
		2.1	
		2.2	
		2.3	
		2.4	
		2.5	
		2.6	
		2.7	
		2.8	
		2.9	
		3.0	
		4.0	

STRATA DESCRIPTION - Subordinate Fraction, Major fraction, Minor Fraction, Colour, Structure, Strength, Moisture Condition, Grading, Bedding, Plasticity (NZ Geotechnical

SILT with some clay; light yellowish brown. Stiff, dry, low plasticity. (LOESS COLLUVIUM)

0.190 becomes dark yellowish brown

0.390 becomes slightly mottled orange and light grey

0.435 becomes firm, moist; trace gravel; fine, angular to sub-angular, highly weathered to completely weathered, dark greyish purple.

0.810 becomes mottled orange and light grey

1.100 becomes soft, wet

1.610 - 1.660 Coarse, angular, completely weathered basalt; dark greyish purple.

2.020 mottling absent; gravel, fine to medium, completely weathered.

2.460 gravel clasts absent

EOH 4.0m

Comments:

0 - 0.190 could be fill; however there is no sand or gravel as in other fills of this area.

Client:

BELL GEOCONSULTING LTD
HAND AUGER LOG

Hand Auger Number: HA6

Project:	17, Ramahana Road, Hurtbury	Date	10/02/2015
	BGL REF #:	Water level in hole	
Co-ordinates (NZTM)	E: 1572185.00	Orientation	Vertical
	N: 5176388.00	Logged By	Chris White

WT	Samples	Depth (m)	Legend
		0.0	
		0.1	
		0.2	
		0.3	
		0.4	
		0.5	
		0.6	
		0.7	
		0.8	
		0.9	
		1.0	
		1.1	
		1.2	
		1.3	
		1.4	
		1.5	
		1.6	
		1.7	
		1.8	
		1.9	
		2.0	
		2.1	
		2.2	
		2.3	
		2.4	
		2.5	
		2.6	
		2.7	
		2.8	
		2.9	
		3.0	
		4.0	

STRATA DESCRIPTION - Subordinate Fraction, Major fraction, Minor Fraction, Colour, Structure, Strength, Moisture Condition, Grading, Bedding, Plasticity (NZ Geotechnical

SILT with some clay and trace sand and gravel; light yellowish brown. Stiff, dry, low plasticity; sand, fine to coarse; gravel, fine to medium, angular, highly weathered andesite; light grey to grey; large feldspar phenocrysts, (LOESS (colluvium).

0.210 gravel and sand absent; mottled orange and light grey

0.530 becomes firm, moist; dark yellowish brown

0.900 becomes soft, wet; mottling less pronounced

1.120 mottling absent

EOH 4.0m

Comments:

The andesite observed in the top of the soil profile is thought to be introduced from prior gardening activities.

Client:

2.3.2: DCP Logs in Extensional Zone at 17 Ramahana Road

aurecon
www.aurecongroup.com

DYNAMIC CONE (SCALA) PENETROMETER TEST RECORD

SCALA PENETROMETER NO.
DCP1

PROJECT 17 Ramahana Road
Hunstsbury, Christchurch

PROJECT NO. 230981

CO-ORDINATES (NZTM 2000)
E 1572172.00
N 5176395.00

GROUND LEVEL N/A m RL

TESTED / SUPERVISED BY Kane Relihana
DATE 01/08/2012

CHECKED BY Richard Heritage
DATE 08/08/2012

Results

Depth (m)	Blows per 100 mm	Depth (m)	Blows per 100 mm
0.0	1	3.5	
	1		
	2		
	2		
0.5	2	4.0	
	1		
	1		
	0		
	1		
1.0	1	4.5	
	1		
	3		
	40		
1.5		5.0	
2.0			
2.5			
3.0			
3.5			

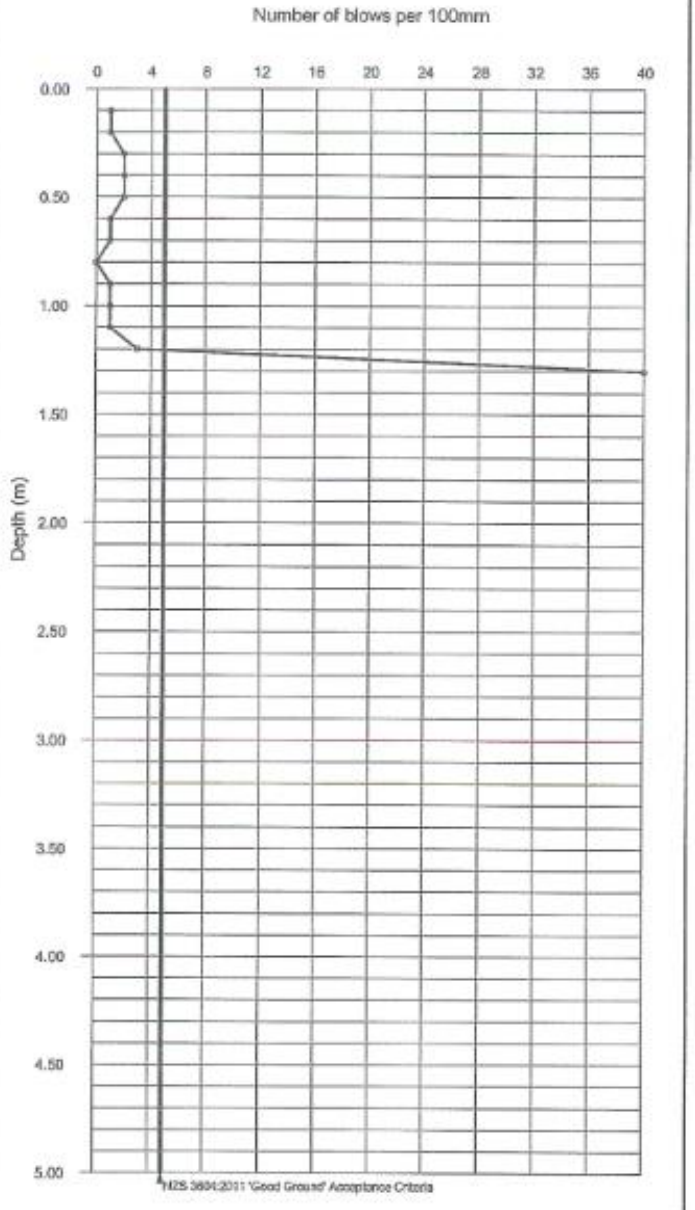

Remarks:
40 blows for 0mm in the last increment.

Refusal at 1.3m below ground level.

Coordinates from handheld GPS unit, accuracy of +/- 5m.

Aurecon, Unit 1, 150 Cavendish Road, Casebrook, Christchurch 8051. Tel: +64 3 379 0761 Fax: +64 3 379 8055 christchurch@aurecongroup.com

aurecon
www.aurecongroup.com

DYNAMIC CONE (SCALA) PENETROMETER TEST RECORD

SCALA PENETROMETER NO.
DCP2

PROJECT 17 Ramahana Road
Huntsbury, Christchurch

PROJECT NO. 230981

CO-ORDINATES (NZTM 2000)
E 1572176.00
N 5176303.00

GROUND LEVEL 18.00 m RL

TESTED / SUPERVISED BY Kane Reihana
DATE 01/08/2012

CHECKED BY Richard Heritage
DATE 08/08/2012

Results

Depth (m)	Blows per 100 mm
0.0	3
	5
	5
	5
0.5	7
	4
	3
	3
	2
1.0	2
	3
	5
	6
	6
1.5	7
	6
	4
	6
	5
2.0	4
	6
	9
	7
	9
2.5	7
	7
	6
	6
	5
3.0	5
	6
	12
	8
	12
3.5	11

Depth (m)	Blows per 100 mm
3.5	10
	9
	8
	6
4.0	6
4.5	
5.0	

Number of blows per 100mm

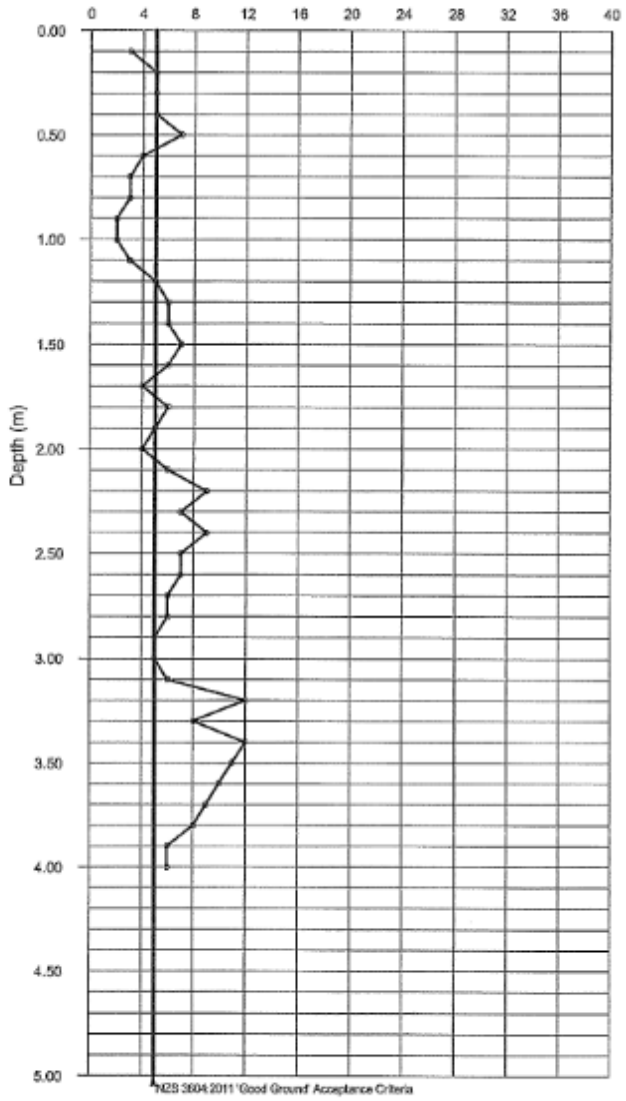

*NZS 3604:2011 'Good Ground' Acceptance Criteria

Remarks:
6 blows for 100mm in the last increment.

Target depth reached.

Coordinates from handheld GPS unit, accuracy of +/- 5m.

Aurecon, Unit 1, 150 Cavendish Road, Casebrook, Christchurch 8051. Tel: +64 3 375 0761 Fax: +64 3 375 8555 christchurch@aurecongroup.com

aurecon
www.aurecongroup.com

DYNAMIC CONE (SCALA) PENETROMETER TEST RECORD

SCALA PENETROMETER NO.
DCP3

PROJECT 17 Ramahana Road
Hunstbury, Christchurch

PROJECT NO. 230981

CO-ORDINATES (NZTM 2000)
E 1572176.00
N 5176397.00

GROUND LEVEL 20.00 m RL

TESTED / SUPERVISED BY Kane Relihana
DATE 01/08/2012

CHECKED BY Richard Heritage
DATE 06/08/2012

Results

Depth (m)	Blows per 100 mm
0.0	2
	6
	3
	3
0.5	4
	3
	3
	5
	4
1.0	3
	5
	4
	4
	5
1.5	4
	3
	3
	4
	3
2.0	3
	4
	4
	6
	6
2.5	7
	8
	6
	4
	6
3.0	4
	6
	7
	8
	11
3.5	8

Depth (m)	Blows per 100 mm
3.5	7
	6
	6
	6
4.0	6
4.5	
5.0	

Number of blows per 100mm

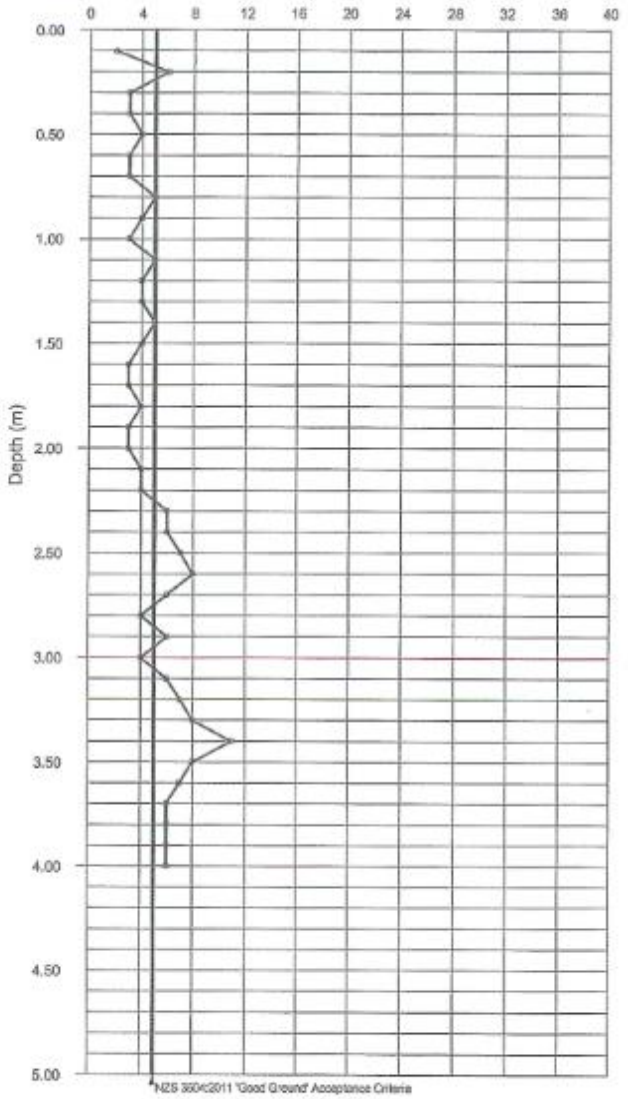

NZS 3604:2011 'Good Ground' Acceptance Criteria

Remarks:
6 blows for 100mm in the last increment.

Target depth reached.

Coordinates from handheld GPS unit, accuracy of +/- 5m.

Aurecon, Unit 1, 100 Carlton Mill Road, Casebrook, Christchurch 8051. Tel +64 3 375 0761 Fax +64 3 379 6955 christchurch@aurecongroup.com

aurecon
www.aurecongroup.com

DYNAMIC CONE (SCALA) PENETROMETER TEST RECORD

SCALA PENETROMETER NO.
DCP4

PROJECT 17 Ramahana Road
Huntsbury, Christchurch

PROJECT NO. 230961

CO-ORDINATES (NZTM 2000)
E 1572180.00
N 5176404.00

GROUND LEVEL 16.00 m RL

TESTED / SUPERVISED BY Kane Reihana
DATE 01/08/2012

CHECKED BY Richard Heritage
DATE 08/08/2012

Results

Depth (m)	Blows per 100 mm
0.0	1
	0
	1
	3
0.5	2
	2
	3
	5
	9
1.0	11
	11
	14
	10
	8
1.5	8
	6
	6
	7
	6
2.0	6
	9
	7
	7
	6
2.5	6
	4
	4
	5
	5
3.0	5
	5
	7
	6
	5
3.5	6

Depth (m)	Blows per 100 mm
3.5	6
	7
	11
	11
4.0	9
4.5	
5.0	

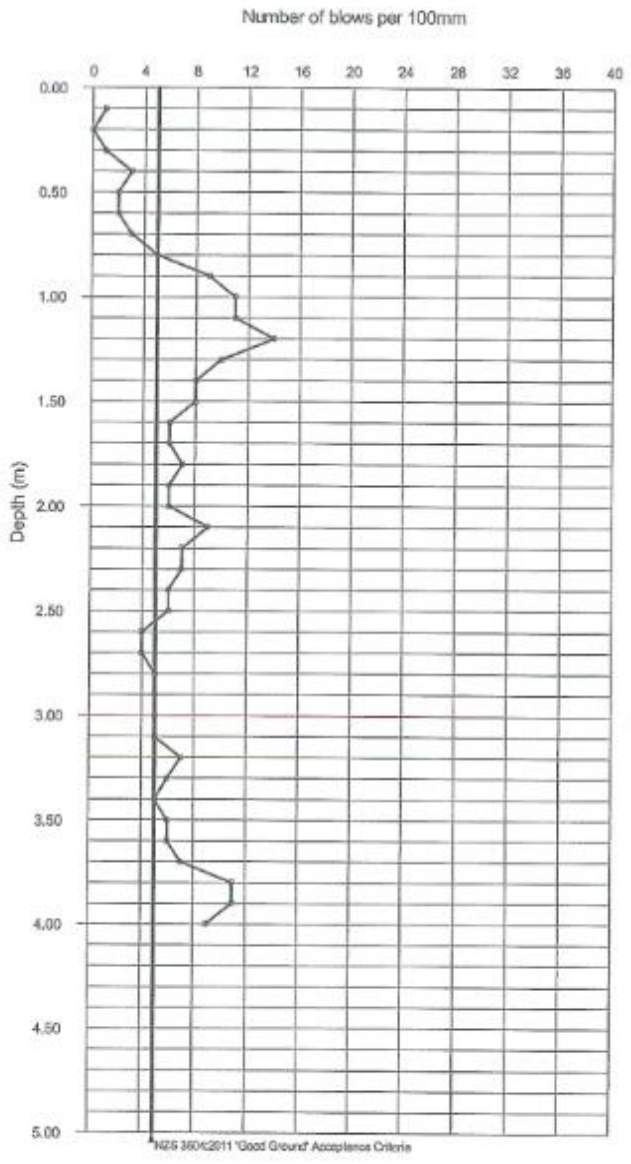

Remarks:
9 blows for 100mm in the last increment.

Target depth reached.

Coordinates from handheld GPS unit, accuracy of +/- 5m.

Aurecon, Unit 1, 150 Cavendish Road, Casebrook, Christchurch 8051. Tel: +64 3 375 0761 Fax: +64 3 379 6955 christchurch@aurecongroup.com

aurecon
www.aurecongroup.com

DYNAMIC CONE (SCALA) PENETROMETER TEST RECORD

SCALA PENETROMETER NO.
DCP5

PROJECT 17 Ramahana Road
Hunisbury, Christchurch

PROJECT NO. 230981

CO-ORDINATES (NZTM 2000)
E 1572183.00
N 5176394.00

GROUND LEVEL 20.00 m RL

TESTED / SUPERVISED BY Kane Reihana
DATE 01/08/2012

CHECKED BY Richard Heritage
DATE 08/08/2012

Results

Depth (m)	Blows per 100 mm	Depth (m)	Blows per 100 mm
0.0	1	3.5	8
	2		7
	2		8
	3		9
0.5	4	4.0	8
	5		
	3		
	3		
	2		
1.0	3	4.5	
	4		
	7		
	7		
	6		
1.5	6	5.0	
	6		
	7		
	8		
	8		
2.0	9		
	9		
	11		
	9		
	9		
2.5	8		
	11		
	11		
	11		
	12		
3.0	9		
	10		
	10		
	10		
	9		
3.5	8		

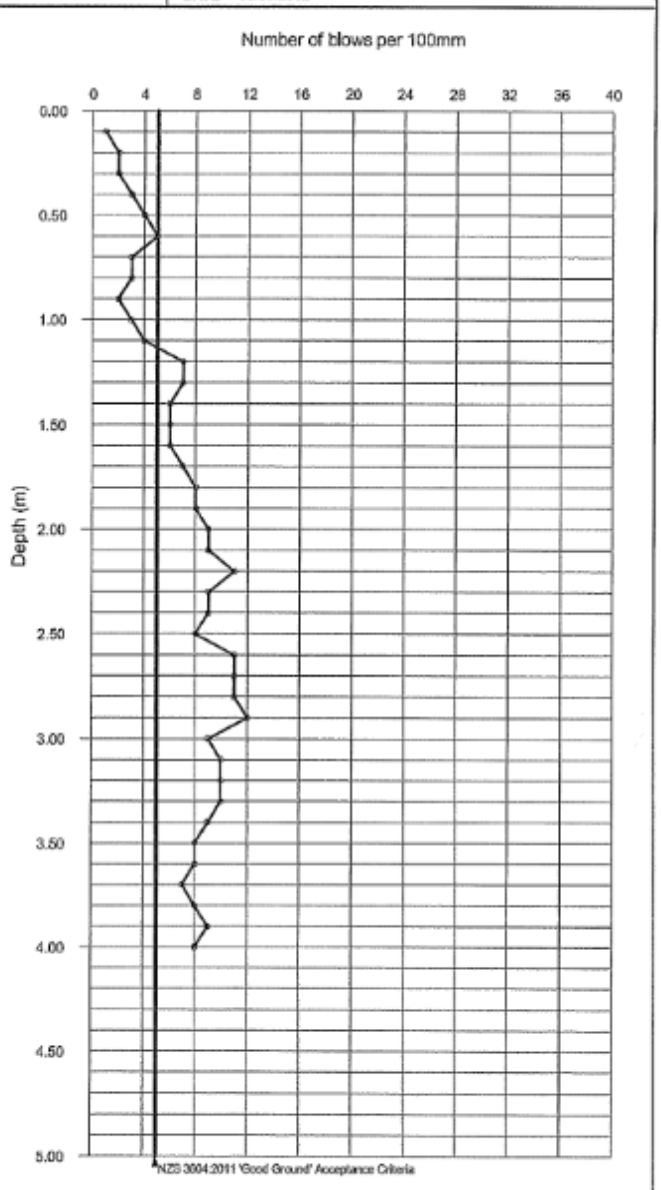

Remarks:
8 blows for 100mm in the last increment.

Target depth reached.

Coordinates from handheld GPS unit, accuracy of +/- 5m.

Aurecon, Unit 1, 193 Cavendish Road, Casebrook, Christchurch 8051. Tel: +64 3 375 0761 Fax: +64 3 379 6955 christchurch@aurecongroup.com

aurecon
www.aurecongroup.com

DYNAMIC CONE (SCALA) PENETROMETER TEST RECORD

SCALA PENETROMETER NO.
DCP6

PROJECT 17 Ramahana Road
Hunstsbury, Christchurch

PROJECT NO. 230981

CO-ORDINATES (NZTM 2000)
E 1572185.00
N 5176388.00

GROUND LEVEL 21.00 m RL

TESTED / SUPERVISED BY Kane Reihana
DATE 01/08/2012

CHECKED BY Richard Heritage
DATE 08/08/2012

Results

Depth (m)	Blows per 100 mm	Depth (m)	Blows per 100 mm
0.0	1	3.5	6
	2		10
	1		8
	3		10
0.5	7	4.0	9
	7		
	7		
	6		
	4		
1.0	4	4.5	
	4		
	4		
	5		
	5		
1.5	6	5.0	
	5		
	9		
	9		
	7		
2.0	5		
	6		
	7		
	7		
	6		
2.5	6		
	5		
	7		
	8		
	9		
3.0	7		
	8		
	10		
	10		
	8		
3.5	5		

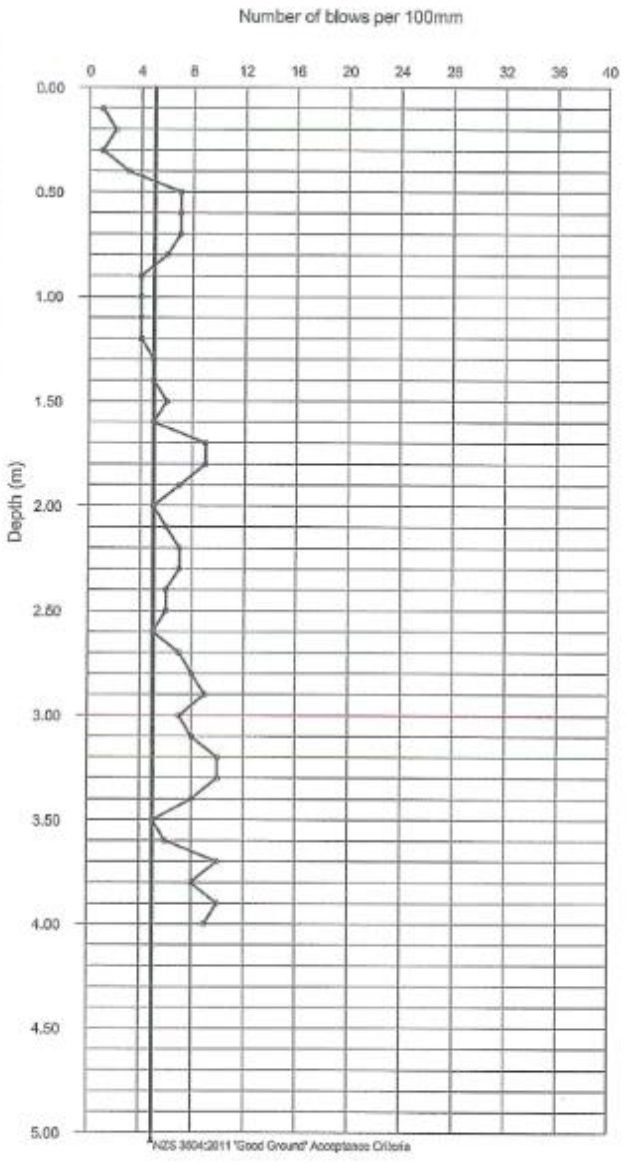

Remarks:
9 blows for 100mm in the last increment.

Target depth reached.

Coordinates from handheld GPS unit, accuracy of +/- 5m.

Aurecon, Unit 1, 150 Clarendon Road, Casebrook, Christchurch 8051. Tel +64 3 375 6761 Fax +64 3 379 6955 christchurch@aurecongroup.com

2.3.3: Hand Auger Logs in Compressional Zone

HA7 17 Ramahana Road

Sheet 1 of 1

Project: Fissure Traces in Loessial Soils	Easting: 394233.7
Location: Compressional zone	Northing: 802988.5
Date Drilled: 20/05/2015	Ground Level (RL): 15.00 m
Method: Hand Auger	Coord. Sys.: MPP CDD (Jan 2012)

RL (m CDD)	Depth (m)	Graphic Log	Soil/ Rock Description	Consistency
15.0	0.0		SILT with some clay and minor sand; dark blackish brown. Firm, moist, low plasticity; sand, fine; minor organics, (TOPSOIL).	
14.0	1.0		SILT with some clay and sand; yellowish brown, mottled orange and light grey; Firm, moist, slight to low plasticity; sand, fine, (LOESS COLLUVIUM).	M F
13.0	2.0		At 1.80 m becomes with minor sand; low plasticity.	
12.0	3.0		At 2.80 m becomes with some sand. At 2.90 m becomes greyish brown, mottled bluish grey and orange; soft; wet.	W S
11.0	4.0		At 3.80 m becomes slight plasticity. End of hole at 4.00 m.	

S1: 0.80-1.00
S2: 1.80-2.00
S3: 2.80-3.00
S4: 3.80-4.00

HA8 17 Ramahana Road

Sheet 1 of 1

Project: Fissure Traces in Loessial Soils	Easting: 394233.7
Location: Compressional zone	Northing: 802988.5
Date Drilled: 20/05/2015	Ground Level (RL): 15.00 m
Method: Hand Auger	Coord. Sys.: MPP CDD (Jan 2012)

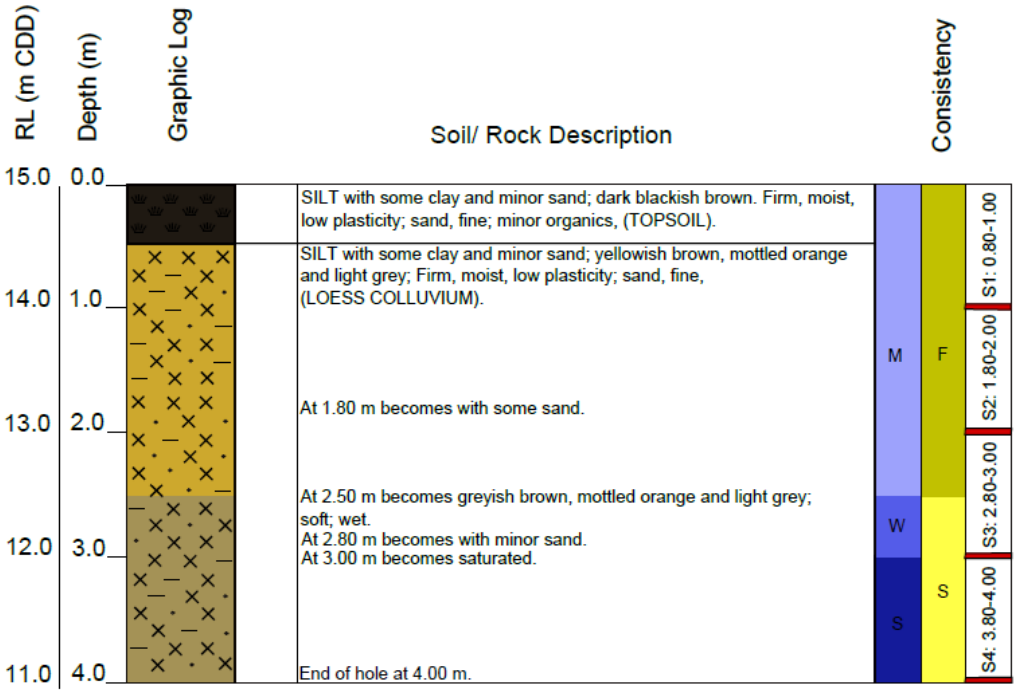

HA9 17 Ramahana Road

Sheet 1 of 1

Project: Fissure Traces in Loessial Soils	Easting: 394233.7
Location: Compressional zone	Northing: 802988.5
Date Drilled: 20/05/2015	Ground Level (RL): 15.00 m
Method: Hand Auger	Coord. Sys.: MPP CDD (Jan 2012)

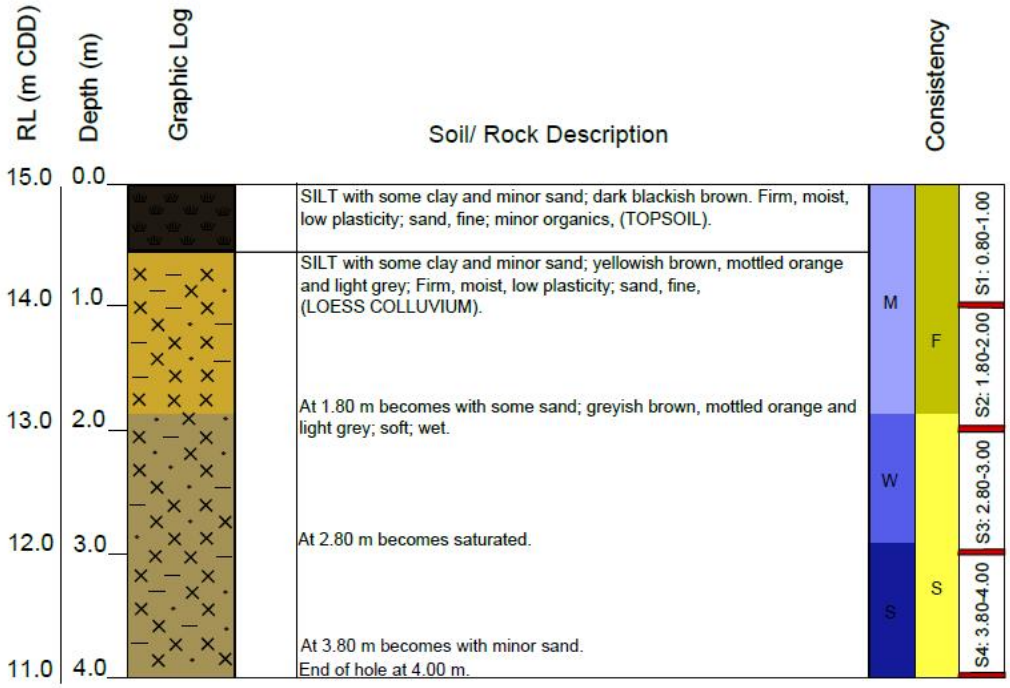

HA10 17 Ramahana Road

Project: Fissure Traces in Loessial Soils	Easting: 394233.7
Location: Compressional zone	Northing: 802988.5
Date Drilled: 20/05/2015	Ground Level (RL): 15.00 m
Method: Hand Auger	Coord. Sys.: MPP CDD (Jan 2012)

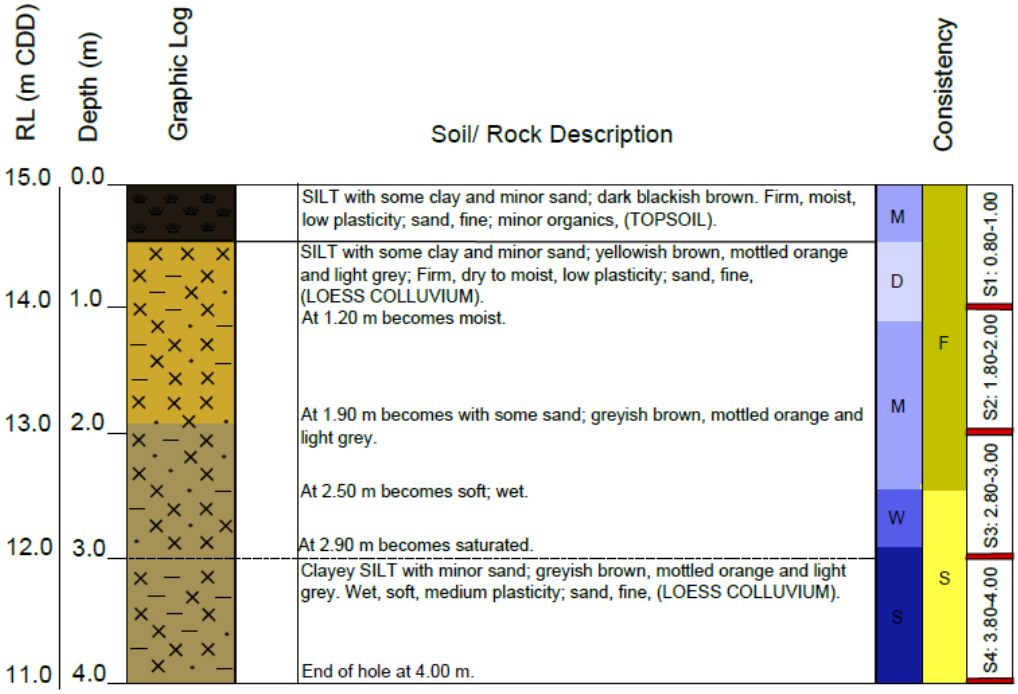

HA11 17 Ramahana Road

Project: Fissure Traces in Loessial Soils	Easting: 394233.7
Location: Compressional zone	Northing: 802988.5
Date Drilled: 20/05/2015	Ground Level (RL): 15.00 m
Method: Hand Auger	Coord. Sys.: MPP CDD (Jan 2012)

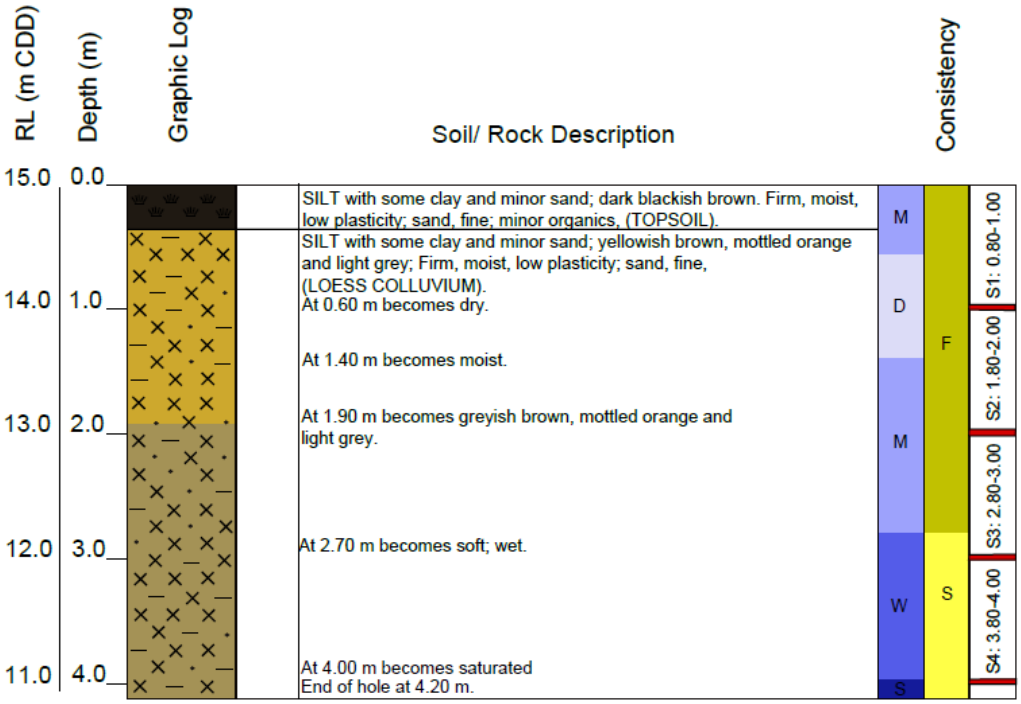

2.3.5: DCP Logs in Compressional Zone

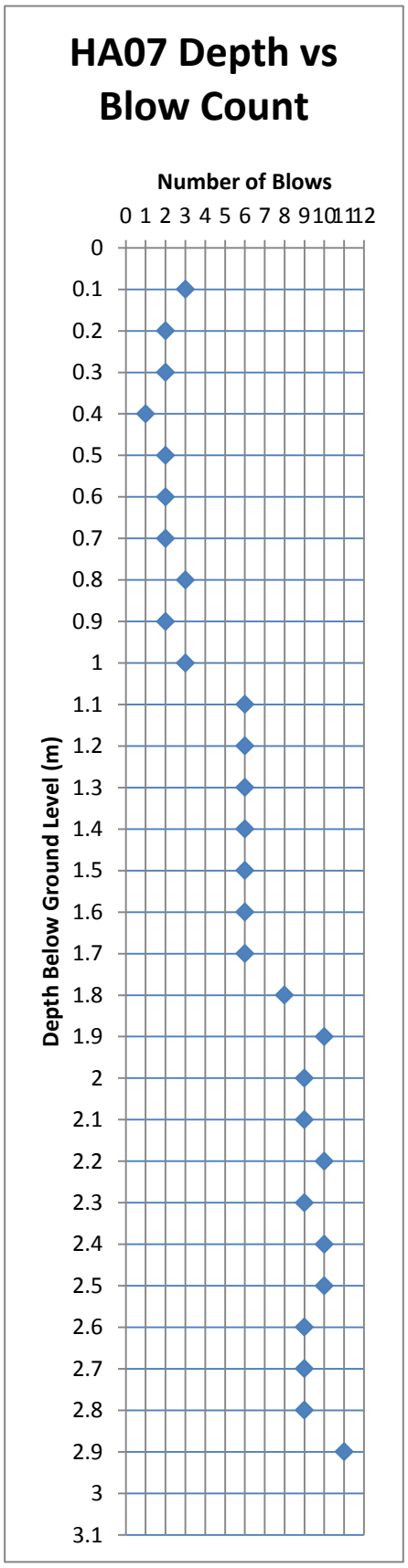

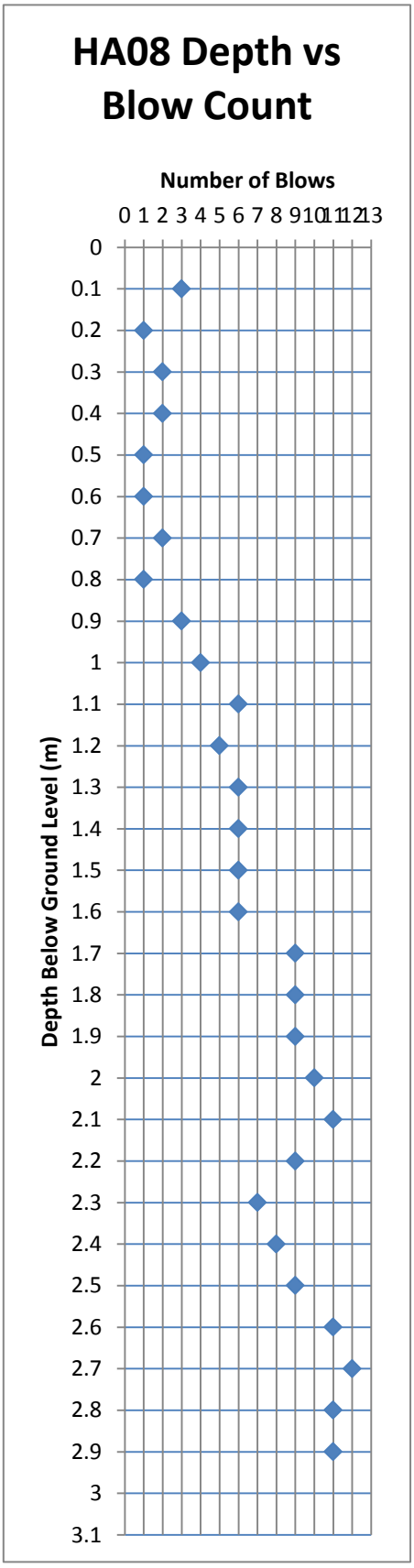

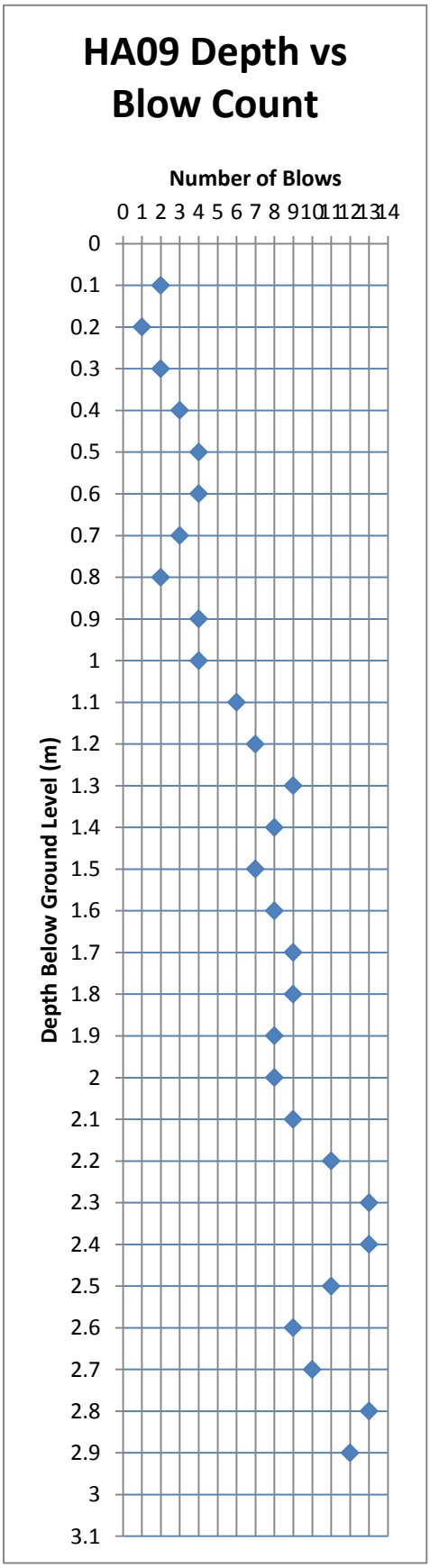
HA09 Depth vs Blow Count
Number of Blows
0 1 2 3 4 5 6 7 8 9 10 11 12 13 14
Depth Below Ground Level (m)
0
0.1
0.2
0.3
0.4
0.5
0.6
0.7
0.8
0.9
1
1.1
1.2
1.3
1.4
1.5
1.6
1.7
1.8
1.9
2
2.1
2.2
2.3
2.4
2.5
2.6
2.7
2.8
2.9
3
3.1

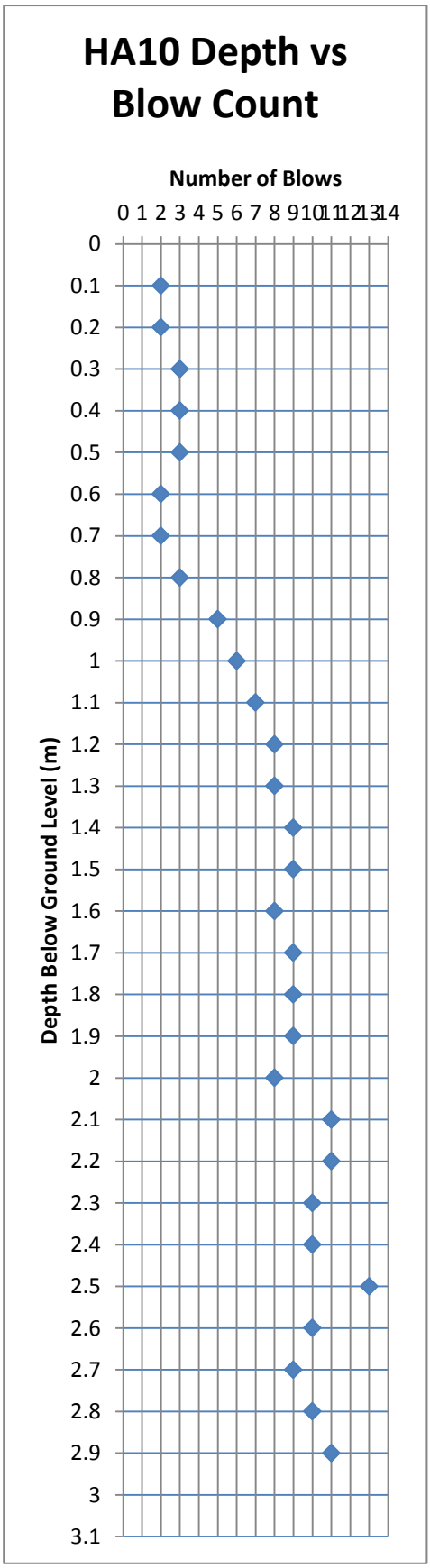
HA10 Depth vs Blow Count
Number of Blows
0 1 2 3 4 5 6 7 8 9 10 11 12 13 14
Depth Below Ground Level (m)
0
0.1
0.2
0.3
0.4
0.5
0.6
0.7
0.8
0.9
1
1.1
1.2
1.3
1.4
1.5
1.6
1.7
1.8
1.9
2
2.1
2.2
2.3
2.4
2.5
2.6
2.7
2.8
2.9
3
3.1

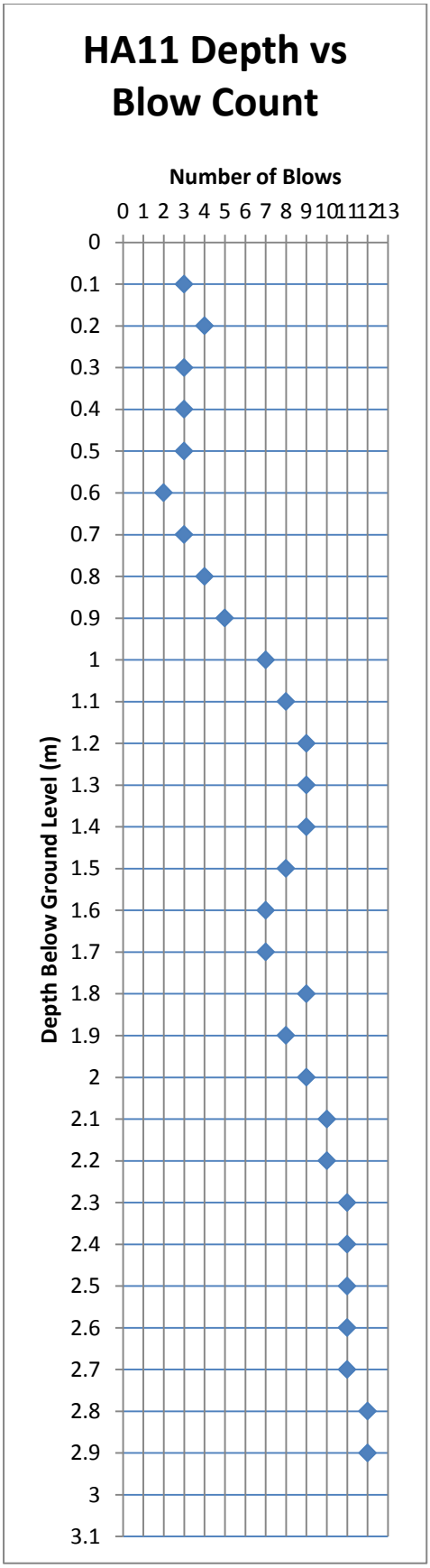
HA11 Depth vs Blow Count
Number of Blows
0 1 2 3 4 5 6 7 8 9 10 11 12 13
Depth Below Ground Level (m)
0
0.1
0.2
0.3
0.4
0.5
0.6
0.7
0.8
0.9
1
1.1
1.2
1.3
1.4
1.5
1.6
1.7
1.8
1.9
2
2.1
2.2
2.3
2.4
2.5
2.6
2.7
2.8
2.9
3
3.1

2.4: Geophysical Investigation Photos

2.4.1. Electrical resistivity line at 17 Ramahana Road.

2.4.2. Ground penetrating radar line at 17 Ramahana Road.

2.4.3. Seismic reflection line at 17 Ramahana Road.

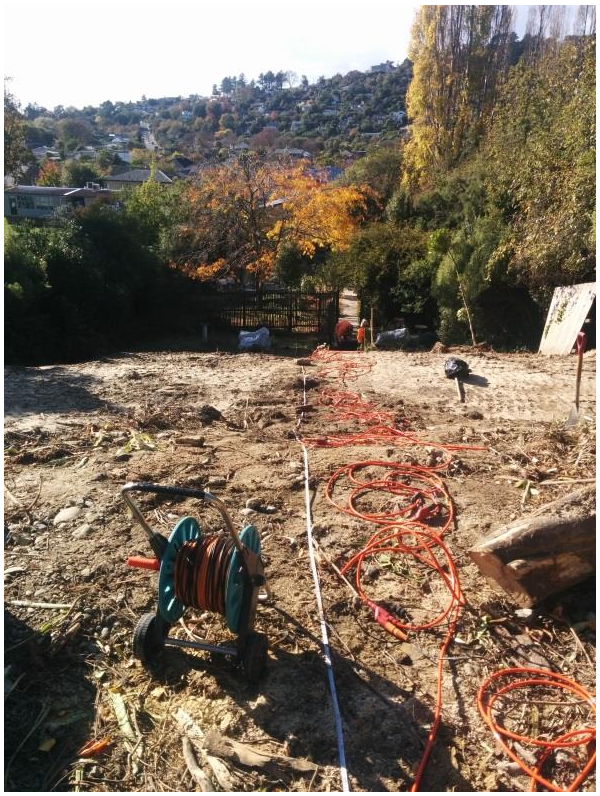

2.5: Seismic Reflection Survey Initial Models

Figure 2.1 is a model showing the coverage of the seismic waves from the ground surface into the soil profile and back to the geophones with no interpretation of the stratigraphy or topography.

Figure 2.2 is the initial model with the topography taken into account and no vertical exaggeration in the scale. The topography points were found using GPS locating at every geophone location. This model is useful to see how the initial data was received before it was interpreted by Southern Geophysical Ltd. In this model the velocity of the seismic waves generally increases with depth, however they then decrease at about 0 masl before increasing again until -20 masl where it decreases again.

The reasons for this can be seen in Figure 2.1 where the raypaths show that there is greater depth coverage within the middle of the survey line. At either end of the survey line the raypaths have less coverage, and therefore they do not penetrate to the depths where the density increases. This makes it appear that the density decreases underneath the density

maximum in the centre of the figure. The borehole logs from 17 Ramahana show that there is bedrock at 26.2 m below the ground surface and a very stiff gravely clay above this, so it is very unlikely that the density decreases at this point.

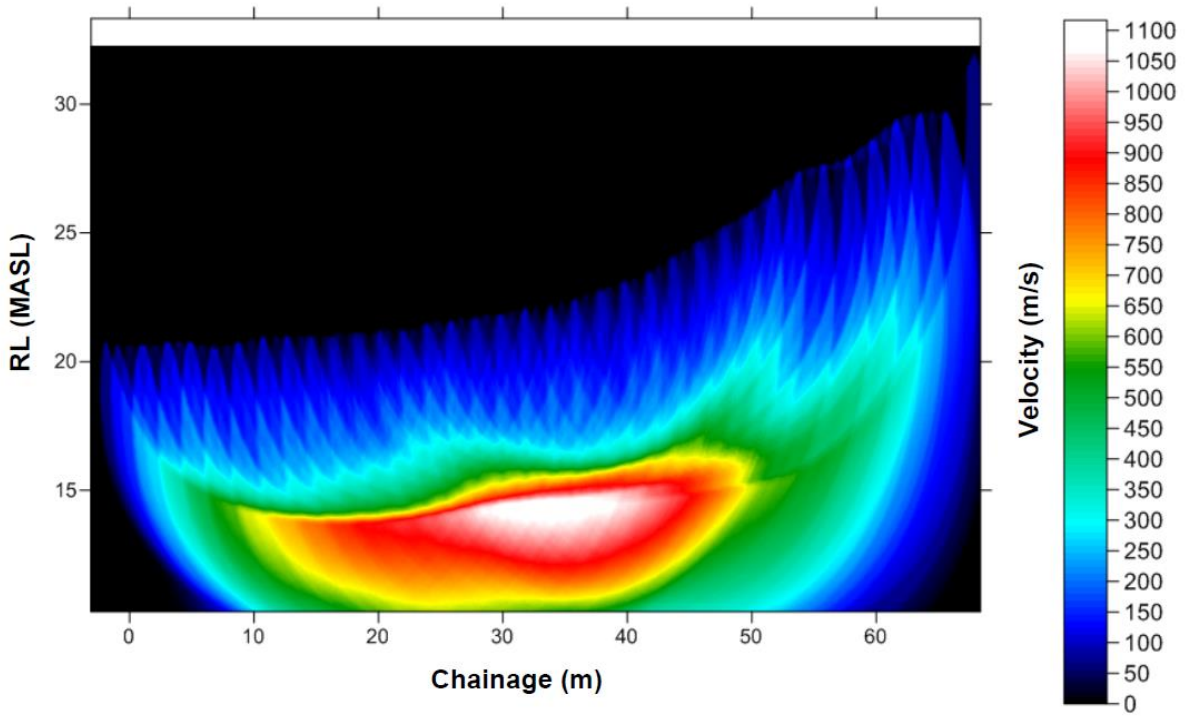

Figure 2.1: Model of the coverage of the seismic waves.

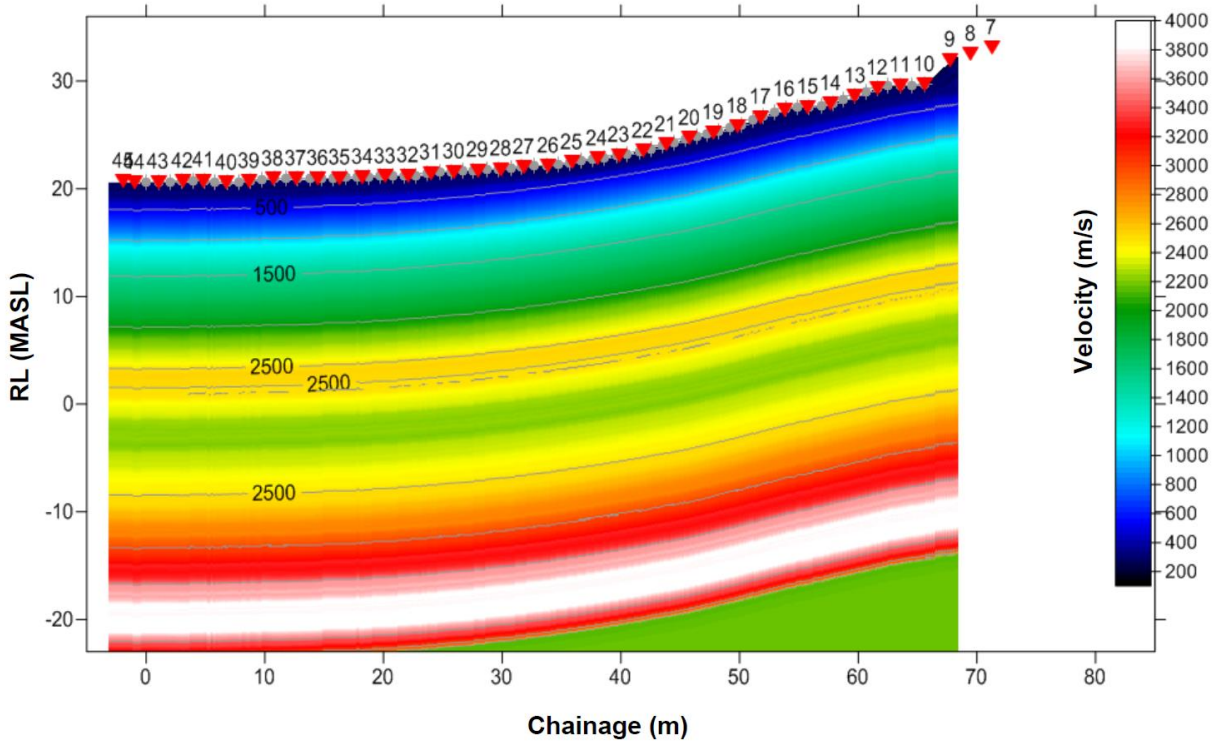

Figure 2.2: Initial model with topography and no vertical exaggeration. No assumptions or calculations have been made about the soil profile or raypaths.

2.6: CPT Log and Liquefaction Analysis

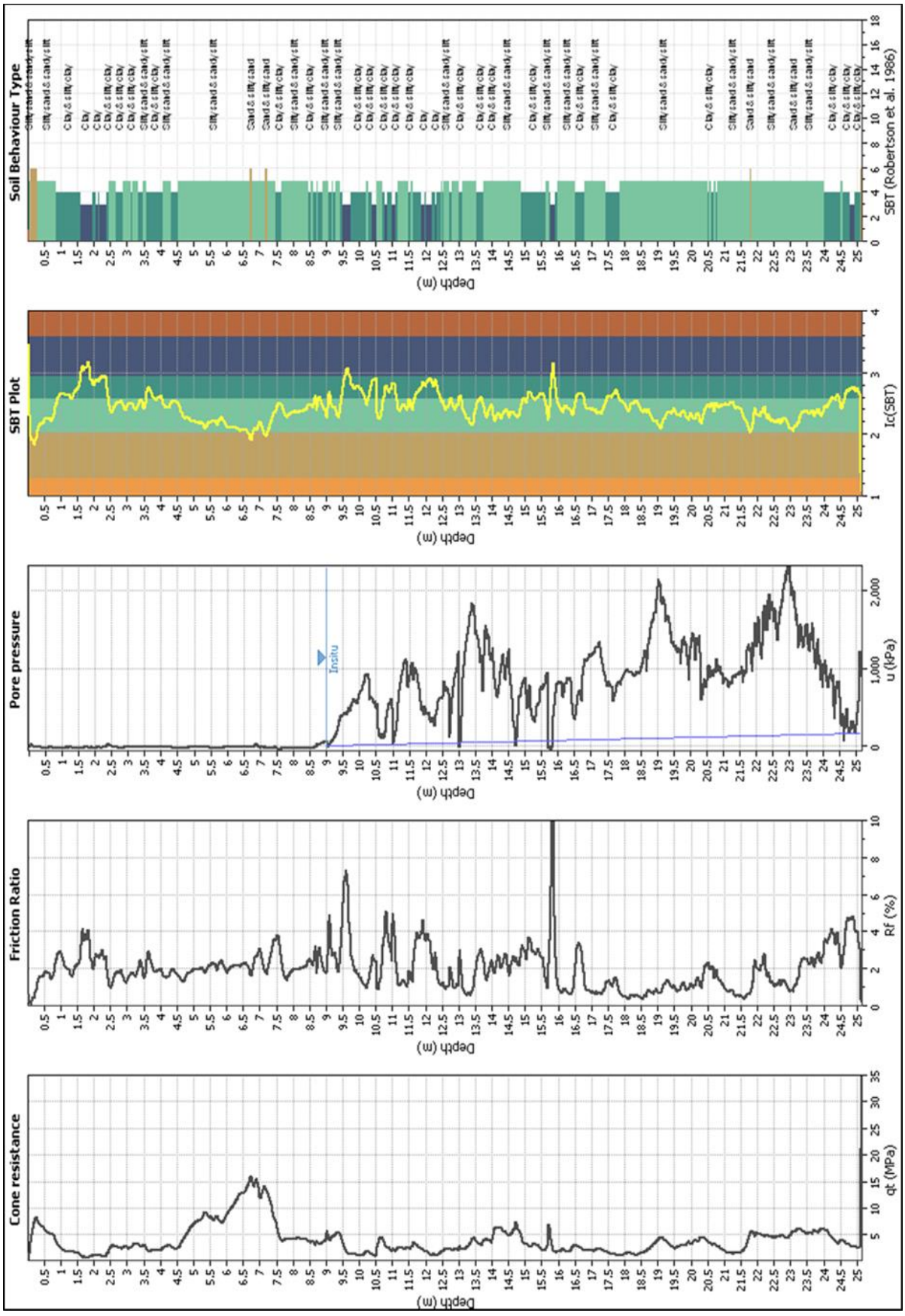

Figure #: CPT data results interpreted on CLiq: cone resistance, friction ratio, pore-pressure, SBT plot, and soil behavioural type, all with depth

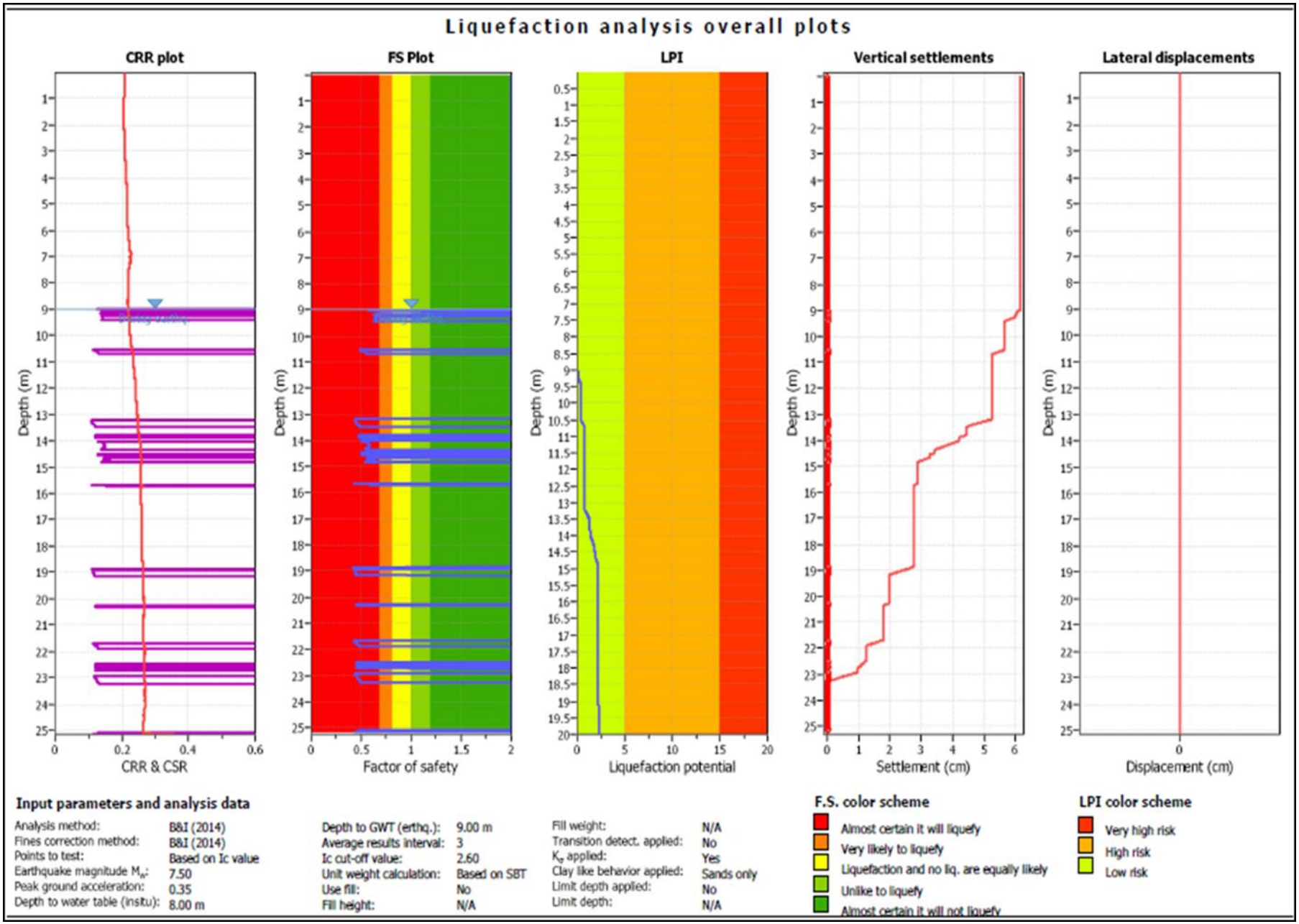

Figure #: Liquefaction analysis with depth: cyclic resistance ratio, factor of safety, liquefaction potential, settlement, and lateral displacement, all under ULS conditions

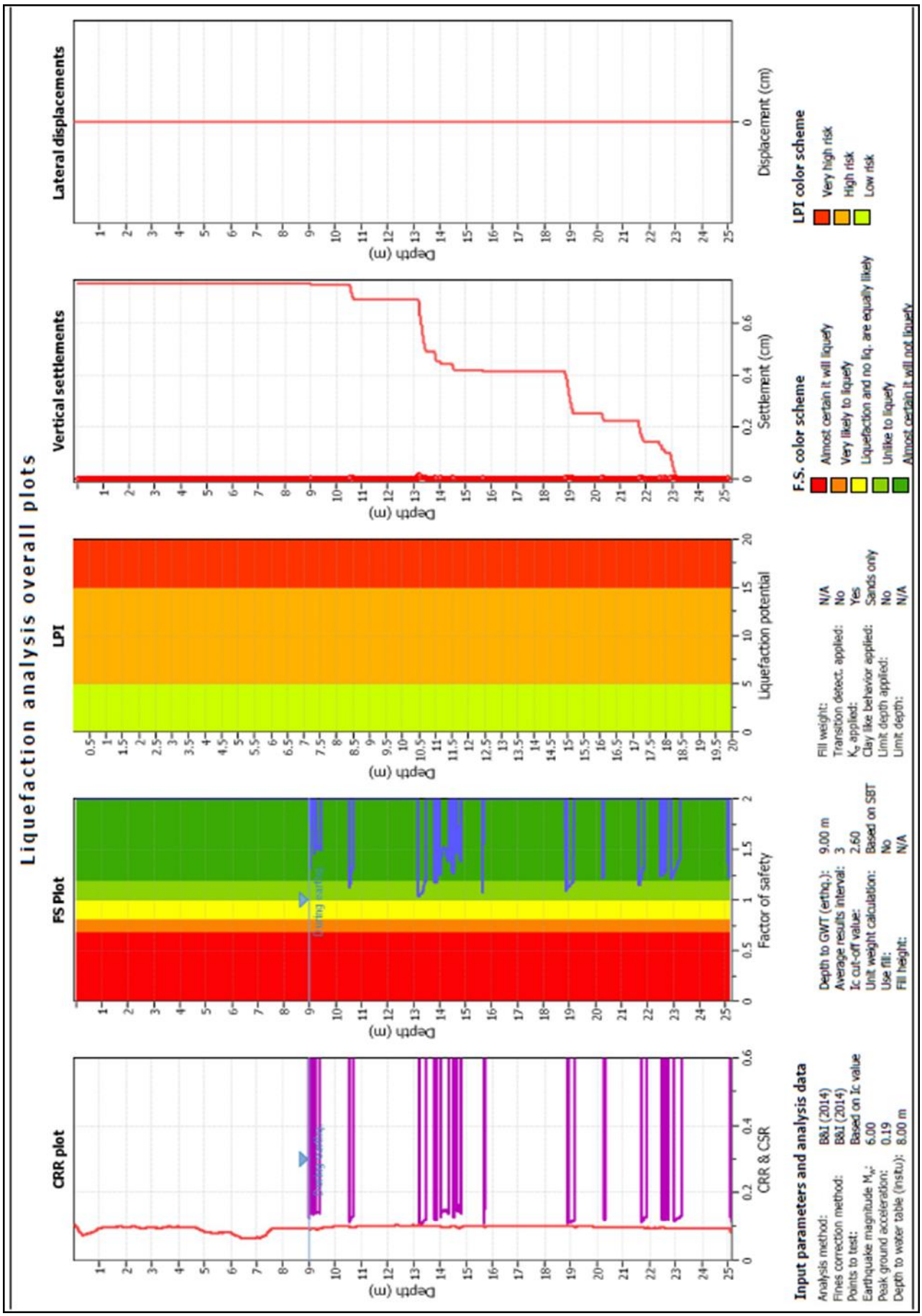

Figure #: Liquefaction analysis with depth: cyclic resistance ratio, factor of safety, liquefaction potential, settlement, and lateral displacement, all under SLS conditions

2.7: Pore Pressure Dissipation Tests Calculations

Using the equation defined by Robertson et al (1992) an estimate of the *in-situ* soil permeability can be calculated using the pore-water dissipation test. The equation for soil permeability is outlined below:

$$k_h = (c_h\ \Upsilon w)/M \quad (1)$$

Where k_h is the soil permeability, c_h is the coefficient of consolidation, Υw is the unit weight of water, and M is the 1-D constrained modulus. The coefficient of consolidation can be calculated using the equation defined by Robertson et al (1992), which is outlined below:

$$C_h = (0.0167)(10^{-4})10^{(1-\log t50)} \quad (2)$$

Where t50 is the time taken for 50% of the pore water pressure to dissipate, (this is for a cone of 10 cm2, but if the result must be increased by a factor of 1.5 if the cone has an area of $15cm^2$). The 1-D constrained modulus can be calculated using the equation also defined by Robertson et al (1992), outlined below:

$$M = \alpha m\ (qt - \Upsilon vo) \quad (3)$$

Where qt is the cone resistance, Υvo is the effective overburden stress, and αm is either the value of the normalized cone resistance if it is a value less than 14, or 14 if the normalized cone resistance is a value over 14. The unit weight of water on earth at 5° Celsius is 9.807 kN/m^3.

The method outlined above gives a relatively accurate estimation of soil permeability compared to other methods which use the Soil Behavioural Type (Ic) determined by the data from the CPT test and the equations defined by Robertson et al (1986). This alternative method to estimate of the soils permeability is done by using the equation defined by Lunne et al (1997), outlined below:

$$k\ (m/s) = 10^{(0.952 - 3.04\ Ic)} \quad (4)$$

Robertson explains that the equation defined by Lunne et al (1997) gives an approximate permeability (although it is usually within the right order of magnitude), whilst the equation by Robertson et al (1992), that incorporates pore water pressure dissipation tests, gives a much more accurate estimate.

9.00 m dissipation test.

$kh = (ch\ \Upsilon w)/m$

$ch = (0.01670)(10^{-4})10^{(1-logt50)}$

t50 = 4.7 minutes

$ch = (0.01670)(10^{-4})10^{(1-log4.7)} = 0.0000035531$ and $0.0000035531 \times 1.5 = 0.0000053297\ m^2/s$ = Ch

$m = \alpha m\ (qt - \Upsilon vo)$

Qt = 42.27 which is >14 so αm = 14

qt = 4.02 MPa = 4020 KPa

Υvo = 88.87 KPa

$m = 14(4020\text{-}88.87) = 55035.82\ KPa\ or\ kN/m^2$

$\Upsilon w = 9.807\ kN/m^3$

$kh = (0.0000053297\ m^2/s \times 9.807\ kN/m^3)/55035.82\ kN/m^2 = 0.0000000009497154\ m/s$

11.00 m dissipation test.

$ch = (0.01670)(10^{-4})10^{(1-log0.16666)} = 0.0001002004$ and $0.0001002004 \times 1.5 = 0.0001503006\ m^2/s$

$m = 14(2200\ KPa\text{-}105.35\ KPa) = 29325.1\ KPa\ or\ kN/m^2$

$kh = (0.0001503006\ m^2/s \times 9.807\ kN/m^3)/29325.1\ kN/m^2 = 0.000000050264039\ m/s$

13.00 m dissipation test.

Ch = $(0.01670)(10^{-4})10^{(1-\log 1.86666)}$ = 0.0000089464 and 0.0000089464 x 1.5 = <u>0.0000134196 m^2/s</u>

M = 14(2480KPa-120.97KPa) = <u>33026.42 Kpa or kN/m^2</u>

Kh = (0.0000134196 m^2/s x 9.807 kN/m^3)/33026.42 kN/m^2 = <u>0.0000000039848708 m/s</u>

2.8: Borehole Logs for 17 Ramahana Road

TONKIN & TAYLOR LTD

BOREHOLE LOG

BOREHOLE No: BH-RMH-01
Hole Location: 17 Ramahana Rd

SHEET 1 OF 4

PROJECT: Area Wide Land Assessment | LOCATION: Christchurch | JOB No: 52010.040

CO-ORDINATES 5176388 mN 1572170.3 mE | DRILL TYPE: Rotary | HOLE STARTED: 27/09/11

DRILL METHOD: OB/HQTT | HOLE FINISHED: 27/09/11

R.L. 20.50 m | DRILLED BY: DCN Drilling Ltd

DATUM NZTM | DRILL FLUID: Nil/Water | LOGGED BY: TIM | CHECKED: KJH

GEOLOGICAL | ENGINEERING DESCRIPTION

GEOLOGICAL UNIT, GENERIC NAME, ORIGIN, MINERAL COMPOSITION

FLUID LOSS | WATER | CORE RECOVERY (%) | METHOD | CASING | TESTS | SAMPLES | R.L. (m) | DEPTH (m) | GRAPHIC LOG | CLASSIFICATION SYMBOL | MOISTURE / WEATHERING CONDITION | STRENGTH/DENSITY CLASSIFICATION | SHEAR STRENGTH (kPa) | COMPRESSIVE STRENGTH (MPa) | DEFECT SPACING (mm)

SOIL DESCRIPTION
Soil type, minor components, plasticity or particle size, colour.

ROCK DESCRIPTION
Substance: Rock type, particle size, colour, minor components.
Defects: Type, inclination, thickness, roughness, filling.

TOPSOIL								20.5	0.0							TOPSOIL, brown, geosynthetic at base
FILL																FILL, gravel fill, dark grey, ~10mm dia.
								20.0	0.5							
								19.5	1.0							
								19.0	1.5							
								18.5	2.0							
								18.0	2.5							
LOESS COLLUVIUM		100	OPEN BARREL													CORE LOSS
		90	OB								ML	M	S			SILT, yellowish brown, soft, moist, non-plastic
								17.5	3.0							CORE LOSS
		93	OB								CL	M	F			CLAY, yellowish brown-orange mottled, firm, moist, low plasticity, trace weathered angular gravels
											ML	M	St			SILT, yellowish brown, stiff, moist, non to low plasticity, trace fine angular volcanic gravel, homogeneous
		100	HQTT					17.0	3.5							
		73	HQTT					16.5	4.0							CORE LOSS
											ML	M	St			SILT, as above
		100	HQTT					4.5								

Log Scale 1:25

TXT DATATEMPLATE.GDT David Leaker

TONKIN & TAYLOR LTD

BOREHOLE LOG

BOREHOLE No: BH-RMH-01
Hole Location: 17 Ramahana Rd

SHEET 2 OF 4

PROJECT: Area Wide Land Assessment | LOCATION: Christchurch | JOB No: 52010.040

CO-ORDINATES 5176388 mN, 1572170.3 mE | DRILL TYPE: Rotary | HOLE STARTED: 27/09/11

R.L. 20.50 m | DRILL METHOD: OB/HQTT | HOLE FINISHED: 27/09/11

DATUM NZTM | DRILL FLUID: Nil/Water | DRILLED BY: DCN Drilling Ltd

LOGGED BY: TIM CHECKED: KTH

GEOLOGICAL | ENGINEERING DESCRIPTION

GEOLOGICAL UNIT, GENERIC NAME, ORIGIN, MINERAL COMPOSITION

FLUID LOSS | WATER | CORE RECOVERY (%) | METHOD | CASING | TESTS | SAMPLES | DRILL (m) | DEPTH (m) | GRAPHIC LOG | CLASSIFICATION SYMBOL | MOISTURE CONDITION / WEATHERING | STRENGTH/DENSITY CLASSIFICATION | SHEAR STRENGTH (kPa) | COMPRESSIVE STRENGTH (MPa) | DEFECT SPACING (mm)

SOIL DESCRIPTION: Soil type, minor components, plasticity or particle size, colour.

ROCK DESCRIPTION: Substance: Rock type, particle size, colour, minor components. Defects: Type, inclination, thickness, roughness, filling.

GEOLOGICAL	DEPTH (m)	CORE RECOVERY (%)	METHOD	CLASSIFICATION SYMBOL	MOISTURE CONDITION	STRENGTH/DENSITY CLASSIFICATION	ENGINEERING DESCRIPTION
LOESS COLLUVIUM	5.0	64	HQTT	ML	M	F	CORE LOSS
	5.5						SILT, yellowish brown, firm, moist, non to low plasticity, trace fine angular gravel/coarse sand, volcanic derived gravel is weathered in places, homogeneous - no apparent structure
							CORE LOSS
	6.0	65	HQTT	ML	M	F	SILT, as above
	6.5						CORE LOSS
	7.0	80	HQTT	ML	M	F	SILT, as above
	7.5						CORE LOSS
	8.0	80	HQTT	ML	M	F	SILT, as above
	8.5						CORE LOSS
	9.0	70	HQTT	ML	M	F	SILT, as above
	9.5	100	HQTT		M	F	
	10						

T+T_DATATEMPLATE.GDT Build Unkno

Log Scale 1:25

BOREHOLE LOG 52010.040 BH-RMH-01 18/10/2011

TONKIN & TAYLOR LTD

BOREHOLE LOG

BOREHOLE No: BH-RMH-01
Hole Location: 17 Ramahana Rd

SHEET 3 OF 4

PROJECT: Area Wide Land Assessment | LOCATION: Christchurch | JOB No: 52010.040

CO-ORDINATES 5176388 mN, 1572170.3 mE | DRILL TYPE: Rotary | HOLE STARTED: 27/09/11

R.L. 20.50 m | DRILL METHOD: OB/HQTT | HOLE FINISHED: 27/09/11

DATUM NZTM | DRILL FLUID: Nil/Water | DRILLED BY: DCN Drilling Ltd | LOGGED BY: TIM | CHECKED: KSJH

GEOLOGICAL | ENGINEERING DESCRIPTION

GEOLOGICAL UNIT, GENERIC NAME, ORIGIN, MINERAL COMPOSITION	FLUID LOSS	WATER	CORE RECOVERY (%)	METHOD	CASING	TESTS	SAMPLES	DRILL (m)	DEPTH (m)	GRAPHIC LOG	CLASSIFICATION SYMBOL	MOISTURE CONDITION / WEATHERING	STRENGTH/DENSITY CLASSIFICATION	SHEAR STRENGTH (kPa)	COMPRESSIVE STRENGTH (MPa)	DEFECT SPACING (mm)	SOIL DESCRIPTION: Soil type, minor components, plasticity or particle size, colour. ROCK DESCRIPTION: Substance: Rock type, particle size, colour, minor components. Defects: Type, inclination, thickness, roughness, filling.
LOESS COLLUVIUM			100	HQTT				11.0	10.5		ML	M					SILT, as above
								10.0	10.5								CORE LOSS 10.5
			80	HQTT				9.5	11.0		ML	M	F				SILT, as above 11.0
								9.0	11.5		ML	M	S				SILT, median yellow brown, soft, moist, low plasticity, trace stiff nodules of silt 11.5
			30	HQTT				8.5	12.0								CORE LOSS 12.0
								8.0	12.5		ML	M	S				SILT, as above 12.5
			10	HQTT				7.5	13.0								CORE LOSS 13.0
								7.0	13.5		ML	M	VSt				SILT, yellowish brown, very stiff, moist, low plasticity, "blocky" texture with minor pin holding 13.5
			98	HQTT							ML	M	VSt				CORE LOSS 14.0
								6.5	14.0								SILT, as above Increase in "lumpy" texture, stiff silt nodules more apparent
			84	HQTT							ML	M	VSt				CORE LOSS 14.5
			70	HQTT				14.5	15		ML	M	VSt				SILT, as above

T+T_DATATEMPLATE.GDT David Lindsay

Log Scale 1:25

TONKIN & TAYLOR LTD

BOREHOLE LOG

BOREHOLE No: BH-RMH-01
Hole Location: 17 Ramahana Rd

SHEET 4 OF 4

PROJECT: Area Wide Land Assessment | LOCATION: Christchurch | JOB No: 52010.040

CO-ORDINATES: 5176388 mN, 1572170.3 mE
R.L.: 20.50 m
DATUM: NZTM

DRILL TYPE: Rotary
DRILL METHOD: OB/HQTT
DRILL FLUID: NB/Water

HOLE STARTED: 27/09/11
HOLE FINISHED: 27/09/11
DRILLED BY: DCN Drilling Ltd
LOGGED BY: TIM
CHECKED: KJH

GEOLOGICAL									ENGINEERING DESCRIPTION									
GEOLOGICAL UNIT, GENERIC NAME, ORIGIN, MINERAL COMPOSITION	FLUID LOSS	WATER	CORE RECOVERY (%)	METHOD	CASING	TESTS	SAMPLES	DRILL (m) / DEPTH (m)	GRAPHIC LOG	CLASSIFICATION SYMBOL	MOISTURE / WEATHERING CONDITION	STRENGTH/DENSITY CLASSIFICATION	SHEAR STRENGTH (kPa)	COMPRESSIVE STRENGTH (MPa)	DEFECT SPACING (mm)	SOIL DESCRIPTION: Soil type, minor components, plasticity or particle size, colour. ROCK DESCRIPTION: Substance: Rock type, particle size, colour, minor components. Defects: Type, inclination, thickness, roughness, filling.	
LOESS COLLUVIUM			50	HQTT				-5.0 15.5		ML	M	VS				CORE LOSS		
																SILT, yellowish brown, very stiff, moist, low plasticity		15.5
			15	HQTT				-4.5 16.0								CORE LOSS Driller notes soft easy drilling		16.0
								-4.0 16.5		ML	M	S				SILT, yellowish brown, stiff, moist, low plasticity		16.5
																END OF BOREHOLE AT 16.5m.		
								-3.5 17.0										17.0
								-3.0 17.5										17.5
								-2.5 18.0										18.0
								-2.0 18.5										18.5
								-1.5 19.0										19.0
								19.5										19.5
								20										

T+T DATATHIS.LATF.GDT Dec/Updated

Log Scale 1:25

TONKIN & TAYLOR LTD

BOREHOLE LOG

BOREHOLE No: BH-RMH-02
Hole Location: 17 Ramahana Rd

SHEET 1 OF 6

PROJECT: Area Wide Land Assessment | LOCATION: Christchurch | JOB No: 52010.040

CO-ORDINATES 5176392.3 mN, 1572185.1 mE | DRILL TYPE: Rotary | HOLE STARTED: 27/09/11

DRILL METHOD: OB/HQTT | HOLE FINISHED: 27/09/11

R.L. 15.50 m | DRILLED BY: DCN Drilling Ltd

DATUM NZTM | DRILL FLUID: NilWater | LOGGED BY: TIM/RH CHECKED: KJH

GEOLOGICAL										ENGINEERING DESCRIPTION						
GEOLOGICAL UNIT, GENERIC NAME, ORIGIN, MINERAL COMPOSITION	FLUID LOSS	WATER	CORE RECOVERY (%)	METHOD	CASING	TESTS	SAMPLES	RL (m) / DEPTH (m)	GRAPHIC LOG	CLASSIFICATION SYMBOL	MOISTURE / WEATHERING CONDITION	STRENGTH/DENSITY CLASSIFICATION	SHEAR STRENGTH (kPa)	COMPRESSIVE STRENGTH (MPa)	DEFECT SPACING (mm)	SOIL DESCRIPTION: Soil type, minor components, plasticity or particle size, colour. ROCK DESCRIPTION: Substance: Rock type, particle size, colour, minor components. Defects: Type, inclination, thickness, roughness, filling.
TOPSOIL								15.5								SILT, dark brown mottled orange, soft, moist, low plasticity, trace rootlets
LOESS COLLUVIUM			76	OPEN BARREL				15.0 0.5		CP	M	S				SILT, trace gravels, brown-slight orange mottling, firm, moist, non-plastic, pinholing; gravels fine, angular, volcanic 0.5
																CORE LOSS
			100	OPEN BARREL				14.5 1.0		ML	M	F				SILT, as above 1.0
										ML	M	F				SILT, with trace gravel, light yellow brown-mottled orange, firm, moist, low plasticity, pinholing; gravel is fine, angular, volcanic 1.5
			100	OB				13.5 2.0								2.0
			100	OB				13.0 2.5		GP	-	D				Sandy, coarse GRAVEL, dark brown/red, dense, gravels angular to sub-rounded clasts (volcanic), up to 40mm 2.5
			100	OB												CORE LOSS 3.0
			0	OB				12.5 3.0								
			100	OB						ML	M	F				SILT, minor sand and gravel, yellow brown, firm, moist, low plasticity; gravel sub-rounded to angular and volcanic derived, trace rootlets 3.5
								12.0 3.5								CORE LOSS 4.0
			73	OB				11.5 4.0		ML	M	F				SILT, as above 4.5
			100	OB				4.5								4.8 to 5.4m: With minor gravels, angular, volcanic, slight rootlets
								5								

T+T DATATEMPLATE.GDT David Lindley

Log Scale 1:25

TONKIN & TAYLOR LTD

BOREHOLE LOG

BOREHOLE No: BH-RMH-02
Hole Location: 17 Ramahana Rd

SHEET 2 OF 6

PROJECT: Area Wide Land Assessment | LOCATION: Christchurch | JOB No: 52010.040

CO-ORDINATES: 5176392.3 mN, 1572185.1 mE | DRILL TYPE: Rotary | HOLE STARTED: 27/09/11

DRILL METHOD: OB/HQTT | HOLE FINISHED: 27/09/11

R.L.: 15.50 m | DRILLED BY: DCN Drilling Ltd

DATUM: NZTM | DRILL FLUID: NilWater | LOGGED BY: TIM/RH | CHECKED: KSH

GEOLOGICAL | ENGINEERING DESCRIPTION

GEOLOGICAL UNIT, GENERIC NAME, ORIGIN, MINERAL COMPOSITION	FLUID LOSS	WATER	CORE RECOVERY (%)	METHOD	CASING	TESTS	SAMPLES	DRILL (m)	DEPTH (m)	GRAPHIC LOG	CLASSIFICATION SYMBOL	MOISTURE / WEATHERING CONDITION	STRENGTH/DENSITY CLASSIFICATION	BREAK STRENGTH (MPa)	COMPRESSIVE STRENGTH (MPa)	DEFECT SPACING (mm)	SOIL DESCRIPTION: Soil type, minor components, plasticity or particle size, colour. ROCK DESCRIPTION: Substance: Rock type, particle size, colour, minor components. Defects: Type, inclination, thickness, roughness, filling.
LOESS COLLUVIUM			100	OB				11.0			ML	M	F				SILT, as above
									5.0								CORE LOSS
			77	OB				10.0	5.5		ML	M	S				SILT, with minor sand, yellow brown, soft, moist, low plasticity, homogeneous
																	CORE LOSS
			29	HQTT				9.5	6.0								6.0
											ML	W	VS				SILT, yellow brown, very soft, wet, re-moulded in box, very low plasticity - liquifies easily under light finger tapping, some mottling, sand present 6.3
			77	HQTT				9.0	6.5		ML	W	S				CORE LOSS
											ML	M	F				SILT, yellow brown, soft, wet, low plasticity, liquifiable
																	SILT, with some gravel, yellow brown, firm, moist, low plasticity, fine volcanic angular gravel particles, pinholing 7.0
			38	HQTT				8.5	7.0								CORE LOSS
											ML	W	S				SILT, yellow brown, soft, wet, low plasticity, liquifiable, pinholing
								8.0	7.5								7.5
																	CORE LOSS
			0	HQTT				7.5	8.0								8.0
																	8.5
								7.0	8.5								CORE LOSS
																	9.0
			62	HQTT				6.5	9.0		ML	W	S				SILT, yellow brown with streaks of grey, soft, wet, low plasticity, liquifiable, blocky, homogeneous structure
																	9.5
								6.0	9.5								CORE LOSS
			76	HQTT					10		ML	W	F				

T:\T_DATA\TIMR\ATL.GDT David Leeles

Log Scale 1:25

TONKIN & TAYLOR LTD

BOREHOLE LOG

BOREHOLE No: BH-RMH-02
Hole Location: 17 Ramahana Rd

SHEET 3 OF 6

PROJECT: Area Wide Land Assessment | LOCATION: Christchurch | JOB No: 52010.040

CO-ORDINATES 5176392.3 mN, 1572185.1 mE
R.L. 15.50 m
DATUM NZTM

DRILL TYPE: Rotary
DRILL METHOD: OB/HQTT
DRILL FLUID: NB/Water

HOLE STARTED: 27/09/11
HOLE FINISHED: 27/09/11
DRILLED BY: DCN Drilling Ltd
LOGGED BY: TIM/RH CHECKED: KJH

GEOLOGICAL | ENGINEERING DESCRIPTION

GEOLOGICAL UNIT, GENERIC NAME, ORIGIN, MINERAL COMPOSITION	FLUID LOSS	WATER	CORE RECOVERY (%)	METHOD	CASING	TESTS	SAMPLES	RL (m) / DEPTH (m)	GRAPHIC LOG	CLASSIFICATION SYMBOL	MOISTURE CONDITION / WEATHERING	STRENGTH/DENSITY CLASSIFICATION	SHEAR STRENGTH (kPa)	COMPRESSIVE STRENGTH (kPa)	DEFECT SPACING (mm)	SOIL DESCRIPTION: Soil type, minor components, plasticity or particle size, colour. ROCK DESCRIPTION: Substance: Rock type, particle size, colour, minor components. Defects: Type, inclination, thickness, roughness, filling.
LOESS COLLUVIUM			76	HQTT				6.0 / 5.0 10.5		ML	W					SILT, yellow brown, firm, wet, low plasticity, homogeneous, liquifiable
										ML	M					SILT, as above
																SILT, dark yellow brown, firm, moist, low plasticity, homogeneous, bioturbated 10.1
																CORE LOSS
																CORE LOSS
			87	HQTT				4.5 11.0		ML	M	F				SILT, as above 11.0
								4.0 11.5		ML	M	F				SILT, light yellow brown, firm, moist, low plasticity, blocky, pinholing 11.5
																CORE LOSS
			75	HQTT				3.5 12.0		ML	M	F				SILT, as above 12.0
								3.0 12.5								12.5
			100	HQTT				2.5 13.0		ML	M	St				SILT, with trace gravel, light yellow brown, stiff, moist, low plasticity, pinholing, bioturbated, gravel mainly around 12.8m fine, angular, volcanic 13.0
			80	HQTT				2.0 13.5		ML	M	St				CORE LOSS
																SILT, with trace gravel, as above 13.5
			40	HQTT				1.5 14.0								CORE LOSS 14.0
								14.5		ML	M	St				SILT, with trace gravel, as above
											W					Grades wet 14.5
			50	HQ				15								CORE LOSS

T+T_DATATEMPLATE.GDT Daniel Liddon

Log Scale 1:25

TONKIN & TAYLOR LTD

BOREHOLE LOG

BOREHOLE No: BH-RMH-02
Hole Location: 17 Ramahana Rd

SHEET 4 OF 6

PROJECT: Area Wide Land Assessment | LOCATION: Christchurch | JOB No: 52010.040

CO-ORDINATES 5178392.3 mN, 1572185.1 mE | DRILL TYPE: Rotary | HOLE STARTED: 27/09/11 | HOLE FINISHED: 27/09/11

R.L. 15.50 m | DRILL METHOD: OB/HQTT | DRILLED BY: DCN Drilling Ltd

DATUM NZTM | DRILL FLUID: NB/Water | LOGGED BY: TIM/RH | CHECKED: VSBH

GEOLOGICAL											ENGINEERING DESCRIPTION
GEOLOGICAL UNIT, GENERIC NAME, ORIGIN, MINERAL COMPOSITION.	FLUID LOSS	WATER	CORE RECOVERY (%)	METHOD	CASING	TESTS	SAMPLES	R.L. (m) / DEPTH (m)	DRAWING LOG	CLASSIFICATION SYMBOL	MOISTURE / WEATHERING CONDITION	STRENGTH/DENSITY CLASSIFICATION	SHEAR STRENGTH (kPa)	COMPRESSIVE STRENGTH (MPa)	DEFECT SPACING (mm)	SOIL DESCRIPTION: Soil type, minor components, plasticity or particle size, colour. ROCK DESCRIPTION: Substance: Rock type, particle size, colour, minor components. Defects: Type, inclination, thickness, roughness, filling.
LOESS COLLUVIUM			50	HQTT				1.0								CORE LOSS
								0.0 15.5		ML	M	F				SILT, traces of medium sand, light yellow brown, firm, moist, low plasticity, homogeneous 15.5
																CORE LOSS 16.0
			63	HQTT				-0.5 16.0		ML	W	S				SILT, with some medium sand, yellow brown, stiff, wet, non-plastic, completely liquified
										ML	M	F				SILT, yellow brown, firm, moist, low plasticity 16.5
								-1.0 16.5		SM	M	-				Silty, medium SAND, yellow brown with orange and dark brown speckles, moist, non-plastic, some oxidation 17.0
			100	HQTT				-1.5 17.0		ML	M	-				SILT, with trace of sand, yellow brown with dark speckles, blocky, low plasticity; sand, medium
																CORE LOSS
			99	HQTT				-2.0 17.5		ML	M	-				SILT, with trace sand, as above 17.5
																CORE LOSS
			94	HQTT				-2.5 18.0		SM	M	MD				SAND, with some silt, yellowish brown with grey and orange speckles, medium dense, moist 18.0
										ML	M	F				SILT, with some sand, yellowish brown, firm, moist, low plasticity; sand, coarse 18.5
								-3.0 18.5								CORE LOSS
			59	HQTT				-3.5 19.0		ML	M	St				19.0 SILT, with trace of sand, yellowish brown, stiff, moist, low plasticity; sand, medium to coarse
								19.5								19.5
			100	HQTT				20		ML	M	St				SILT, with some sand and gravel, yellow brown, stiff, moist, low plasticity, blocky. Manganese oxide staining

T+T DATATEMPLATE.GDT Datrk Limited

Log Scale 1:25

TONKIN & TAYLOR LTD

BOREHOLE LOG

BOREHOLE No: BH-RMH-02
Hole Location: 17 Ramahana Rd

SHEET 5 OF 6

PROJECT: Area Wide Land Assessment | LOCATION: Christchurch | JOB No: 52010.040

CO-ORDINATES: 5176382.3 mN, 1572185.1 mE
R.L.: 15.50 m
DATUM: NZTM

DRILL TYPE: Rotary
DRILL METHOD: OB/HQTT
DRILL FLUID: Nil/Water

HOLE STARTED: 27/09/11
HOLE FINISHED: 27/09/11
DRILLED BY: DCN Drilling Ltd
LOGGED BY: TBM/RH CHECKED: KJH

GEOLOGICAL														ENGINEERING DESCRIPTION
GEOLOGICAL UNIT, GENERIC NAME, ORIGIN, MINERAL COMPOSITION	FLUID LOSS	WATER	CORE RECOVERY (%)	METHOD	CASING	TESTS	SAMPLES	R.L. (m) / DEPTH (m)	GRAPHIC LOG	CLASSIFICATION SYMBOL	MOISTURE CONDITION / WEATHERING	STRENGTH/DENSITY CLASSIFICATION	SHEAR STRENGTH (kPa)	COMPRESSIVE STRENGTH (MPa)	DEFECT SPACING (mm)	SOIL DESCRIPTION: Soil type, minor components, plasticity or particle size, colour. ROCK DESCRIPTION: Substance: Rock type, particle size, colour, minor components. Defects: Type, inclination, thickness, roughness, filling.
LOESS COLLUVIUM			100	HQTT				-4.0		ML	M	St				SILT, with some sand and gravel, brown yellow mottled dark brown, stiff, moist, low plasticity; sand, angular, coarse; gravels fine (volcanic derived), blocky structure, with Manganese oxide staining
								-5.0 20.5								20.5
																CORE LOSS
			80	HQTT				-5.5 21.0		ML	M	St				SILT, with some sand and gravel, as above
																21.0
								-6.0 21.5		SM	M	F				Silty, fine SAND, yellow brown, firm, moist, low plasticity (liquefied in core box during transport)
			100	HQTT				-6.5 22.0		CL	M	VSt				22.0 Sandy CLAY, with trace of gravel, red/brown, very stiff, moist, low plasticity; gravels of volcanic origin, pinholes, Manganese oxide staining
								-7.0 22.5								22.5
			95	HQTT						CL	M	VSt				CORE LOSS Sandy CLAY, with trace of gravel, as above
								-7.5 23.0								23.0
																23.5
			100	HQ				-8.0 23.5								Reddish colour increasing with depth
								-8.5 24.0								24.0
			100	HQTT				24.5								24.5
			100	HQ				25								

T+T_DATATEMPLATE.GDT Date/Time

Log Scale 1:25

TONKIN & TAYLOR LTD

BOREHOLE LOG

BOREHOLE No: BH-RMH-02
Hole Location: 17 Ramahana Rd

SHEET 6 OF 6

PROJECT: Area Wide Land Assessment | LOCATION: Christchurch | JOB No: 52010.040

CO-ORDINATES 5176392.3 mN, 1572185.1 mE
R.L. 15.50 m
DATUM NZTM

DRILL TYPE: Rotary
DRILL METHOD: OB/HQTT
DRILL FLUID: NB/Water

HOLE STARTED: 27/09/11
HOLE FINISHED: 27/09/11
DRILLED BY: DCN Drilling Ltd
LOGGED BY: TIM/RH CHECKED: K-J-H

GEOLOGICAL | ENGINEERING DESCRIPTION

GEOLOGICAL UNIT, GENERIC NAME, ORIGIN, MINERAL COMPOSITION	FLUID LOSS	WATER	CORE RECOVERY (%)	METHOD	CASING	TESTS	SAMPLES (DRILL PU)	DEPTH (m)	GRAPHIC LOG	CLASSIFICATION SYMBOL	WEATHERING / MOISTURE CONDITION	STRENGTH/DENSITY CLASSIFICATION	SHEAR STRENGTH (kPa)	COMPRESSIVE STRENGTH (MPa)	DEFECT SPACING (mm)	SOIL DESCRIPTION: Soil type, minor components, plasticity or particle size, colour. ROCK DESCRIPTION: Substance: Rock type, particle size, colour, minor components. Defects: Type, inclination, thickness, roughness, filling.
LOESS COLLUVIUM			100	HQTT				-9.0		CL	M	VSt				Sandy CLAY, with trace of gravel, reddish brown, very stiff, moist, low plasticity; sand, angular; gravel, fine, volcanic
								-10.0								25.5
								-10.5								CORE LOSS
			54	HQTT				-10.5								26.0
LYTTELTON VOLCANIC GROUP											HW	VWk				Highly weathered, reddish brown, coarse BASALT, very weak (recovered as gravel)
								-11.0								26.5
											SW	Ex/St				Slightly weathered, fine, grey BASALT, extremely strong
											SW	St				CORE LOSS
			93	HQTT				-11.5								Slightly weathered, fine, brownish red BASALT, strong
																27.0
			100	HQTT				-12.0								27.5
																28.0
			100	HQTT				-12.5								28.5
								-13.0								END OF BOREHOLE AT 28.7m.
								-13.5								Piezometer installed in base of hole. See PZ-RMH-2A for details. Inclinometer installed in borehole. See INC-RMH-02 for details. 29.0
								29.5								29.5
								30								

T+T DATATEMPLATE.GDT Dec6 Letter

Log Scale 1:25

TONKIN & TAYLOR LTD

BOREHOLE LOG

BOREHOLE No: BH-RMH-03
Hole Location: 17 Ramahana Rd

SHEET 1 OF 2

PROJECT: Area Wide Land Assessment		LOCATION: Christchurch	JOB No: 52010.040
CO-ORDINATES	5176402.5 mN 1572220.3 mE	DRILL TYPE: Rotary	HOLE STARTED: 27/09/11
		DRILL METHOD: OB/HQTT	HOLE FINISHED: 27/09/11
R.L.	9.20 m		DRILLED BY: DCN Drilling Ltd
DATUM	NZTM	DRILL FLUID: Water	LOGGED BY: RH CHECKED: KJH

GEOLOGICAL

GEOLOGICAL UNIT, GENERIC NAME, ORIGIN, MINERAL COMPOSITION

TOPSOIL

LOESS
COLLUVIUM

FLUID LOSS	WATER	CORE RECOVERY (%)	METHOD	CASING	TESTS	SAMPLES	R.L. (m)	DEPTH (m)
		100	OPEN BARREL				9.0	0.5
		100	OPEN BARREL				8.5	1.0
		74	OPEN BARREL				8.0	1.5
		100	OPEN BARREL				7.5	2.0
		71	OPEN BARREL				7.0	2.5
		84	OPEN BARREL				6.5	3.0
		91	OPEN BARREL				6.0	3.5
							5.5	4.0
							5.0	4.5
							4.5	5

ENGINEERING DESCRIPTION

GRAPHIC LOG	CLASSIFICATION SYMBOL	MOISTURE / WEATHERING CONDITION	STRENGTH/DENSITY CLASSIFICATION	SHEAR STRENGTH (kPa)	COMPRESSIVE STRENGTH (MPa)	DEFECT SPACING (mm)
	OL	M	S			
	ML	M	S			
	ML	M	S			
		M	S			
	ML	M	S			
	ML	M	S			

SOIL DESCRIPTION
Soil type, minor components, plasticity or particle size, colour.

ROCK DESCRIPTION
Substance: Rock type, particle size, colour, minor components.
Defects: Type, inclination, thickness, roughness, filling.

SILT, with some fine sand and medium gravels, organic, dark greyish brown, soft, moist, low plasticity; gravel is weathered

Colour change to dark brownish grey, no gravel or sand — 0.5

SILT, with some clay and sand, light yellowish brown with yellowish orange and light grey mottling, soft, moist, low plasticity, homogeneous, manganese staining

CORE LOSS — 1.0

SILT, with some clay and sand, as above — 1.5

Weathered gravel clast
Occasional rootlets found as low as 2.5m

Manganese staining dies out below 3m — 2.0

CORE LOSS — 2.5

Limit of manganese staining — 3.0

CORE LOSS

Limit of orange mottling
Core partially liquefied — 4.0

CORE LOSS

Limit of grey mottling — 4.5

Log Scale 1:25

T:\T_DATA\TEMPLATES.GDT David Liedtke

TONKIN & TAYLOR LTD

BOREHOLE LOG

BOREHOLE No: BH-RMH-03
Hole Location: 17 Ramahana Rd
SHEET 2 OF 2

PROJECT: Area Wide Land Assessment		LOCATION: Christchurch	JOB No: 52010.040
CO-ORDINATES	5176402.5 mN 1572220.3 mE	DRILL TYPE: Rotary	HOLE STARTED: 27/09/11
		DRILL METHOD: OB/HQTT	HOLE FINISHED: 27/09/11
R.L.	9.20 m		DRILLED BY: DCN Drilling Ltd
DATUM	NZTM	DRILL FLUID: Water	LOGGED BY: RH CHECKED: KJH

GEOLOGICAL													ENGINEERING DESCRIPTION							
GEOLOGICAL UNIT, GENERIC NAME, ORIGIN, MINERAL COMPOSITION	FLUID LOSS	WATER	CORE RECOVERY (%)	METHOD	CASING	TESTS	SAMPLES	R.L. (m)	DEPTH (m)	GRAPHIC LOG	CLASSIFICATION SYMBOL	MOISTURE CONDITION / WEATHERING	STRENGTH/DENSITY CLASSIFICATION	SHEAR STRENGTH (kPa)	COMPRESSIVE STRENGTH (MPa)	DEFECT SPACING (mm)	SOIL DESCRIPTION Soil type, minor components, plasticity or particle size, colour ROCK DESCRIPTION Substance: Rock type, particle size, colour, minor components. Defects: Type, inclination, thickness, roughness, filling.
LOESS COLLUVIUM			79	OB				4.0	5.5		ML	M	S				Grades to lightish grey brown
				OPEN BARREL				3.5									CORE LOSS
											ML	W	S				SILT, light greyish brown, soft, wet, low plasticity, homogeneous, angular firm coarse sand sized nodules of same material 5.5
								3.0	6.0								Gradual transition to lightish yellow brown 6.0
																	CORE LOSS
			87	OPEN BARREL				2.5	6.5		ML	W	S				SILT, as above Less firm coarse sand sized nodules 6.5
									7.0								Weathered, angular, fine gravel sized volcanics 7.0
								2.0	7.5								CORE LOSS
			75	OPEN BARREL				1.5			ML	W	S				SILT, as above 7.5
									8.0								8.0
								1.0	8.5		ML	W	S				SILT, light yellowish gray, soft, wet, low plasticity, with firm fine gravel sized nodules of silt 8.5
			100	OPEN BARREL				0.5	9.0		ML	M	F				SILT, light yellowish brown, firm, moist, low plasticity, homogeneous 9 to 9.1m: Fine gravel sized light yellowish white weathered concretions 9.0
								0.0				Sat	F				9.5
								-0.5	9.5								END OF BOREHOLE AT 10m.
									10								Piezometer installed in base of hole. See PZ-RMH-03 for details.

Log Scale 1:25

2.9: Engineering Geological Mapping Photos

2.9.1: Looking down at the boggy ground.

2.9.2: Ditch along path for surface water.

2.9.3: Very boggy ground where the spring is.

2.9.4: Close up of the boggy area.

2.9.5: Close up of where the spring is seeping water to the ground surface.

2.9.6: Ditch filled with stagnant water along the northern boundary of the park.

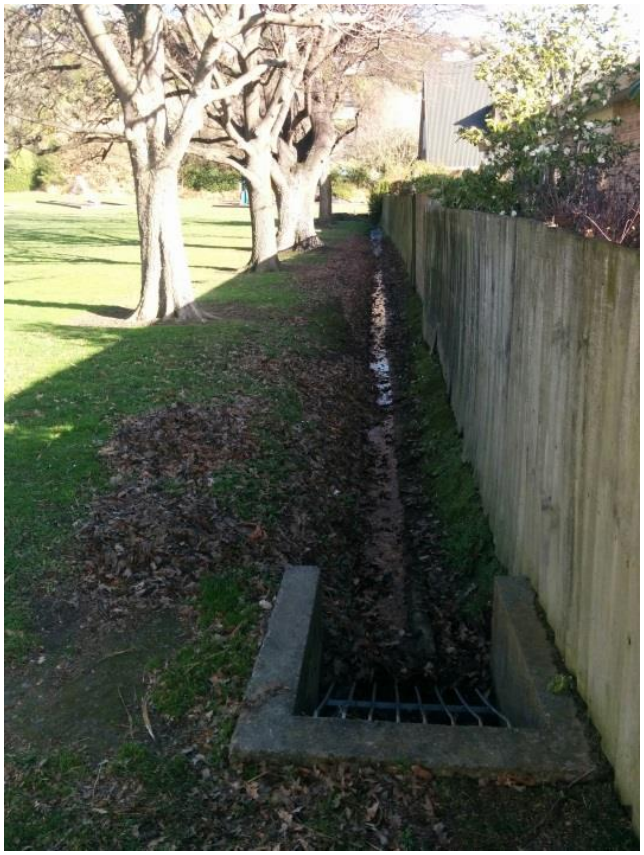

2.9.7: Ditch filled with stagnant water along eastern boundary of the park

2.9.8: Boggy ground in centre of park, looking west towards Ramahana Road.

2.9.9: Looking down at boggy ground in the centre of the park.

2.10: Re-logged Boreholes from Centaurus Park

BH1 Centaurus Park

Sheet 1 of 2

Project: Fissure Traces in Loessial Soils	Easting: 394233.7
Location: Ramahana Road, Huntsbury	Northing: 802988.5
Date Drilled: 28/11/2012	Coord. Sys.: MPP CDD (Jan 2012)
Method: Water Flush Rotary Sonic Drilling	Ground Level (RL): 15.00m
SPT:Automatic SPT hammer;91 % energy ratio	Logged by: C. S. White

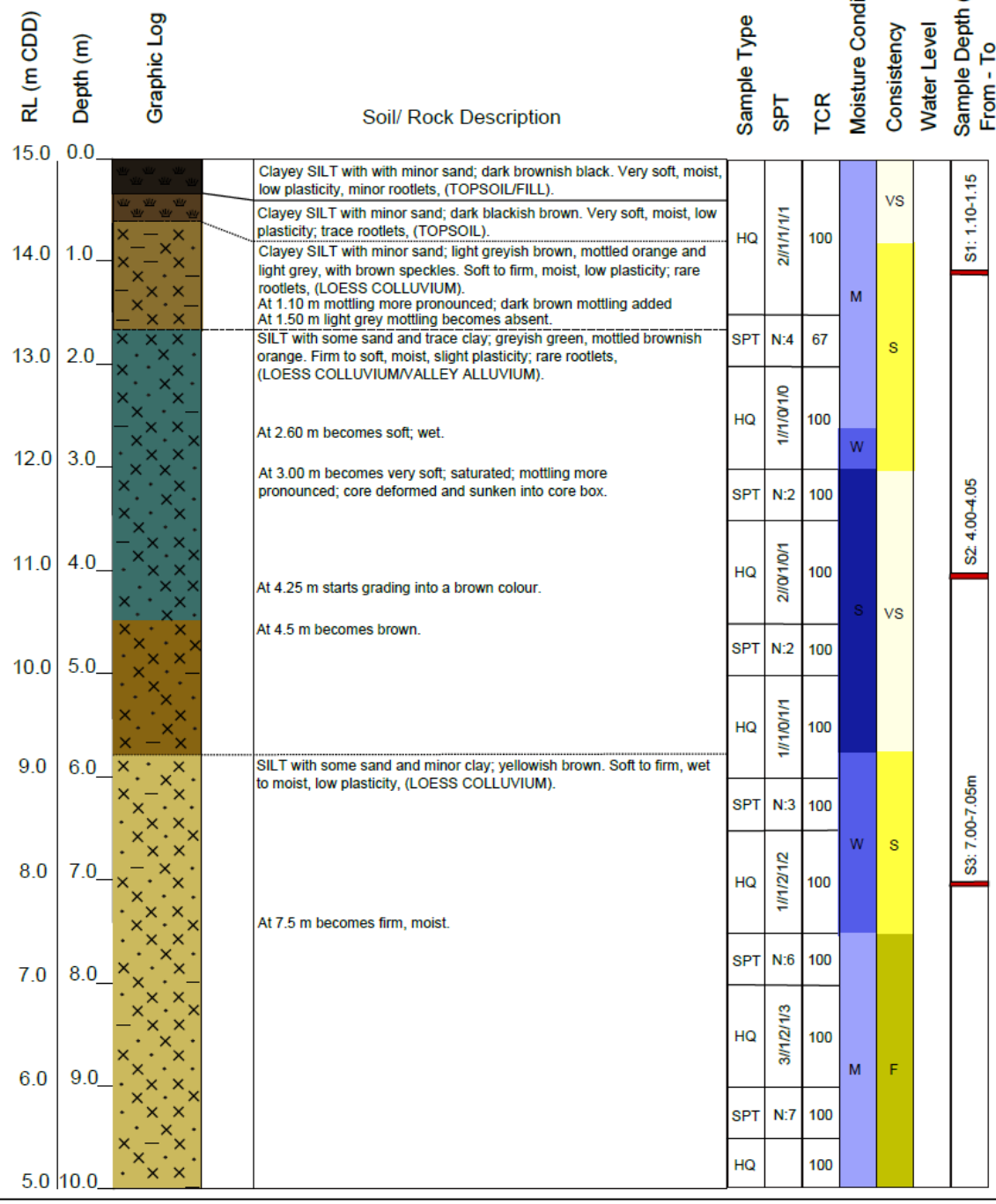

BH1 Centaurus Park

Sheet 2 of 2

Project: Fissure Traces in Loessial Soils	Easting: 394233.7
Location: Ramahana Road, Huntsbury	Northing: 802988.5
Date Drilled: 28/11/2012	Coord. Sys.: MPP CDD (Jan 2012)
Method: Water Flush Rotary Sonic Drilling	Ground Level (RL): 15.00m
SPT:Automatic SPT hammer;91 % energy ratio	Logged by: C. S. White

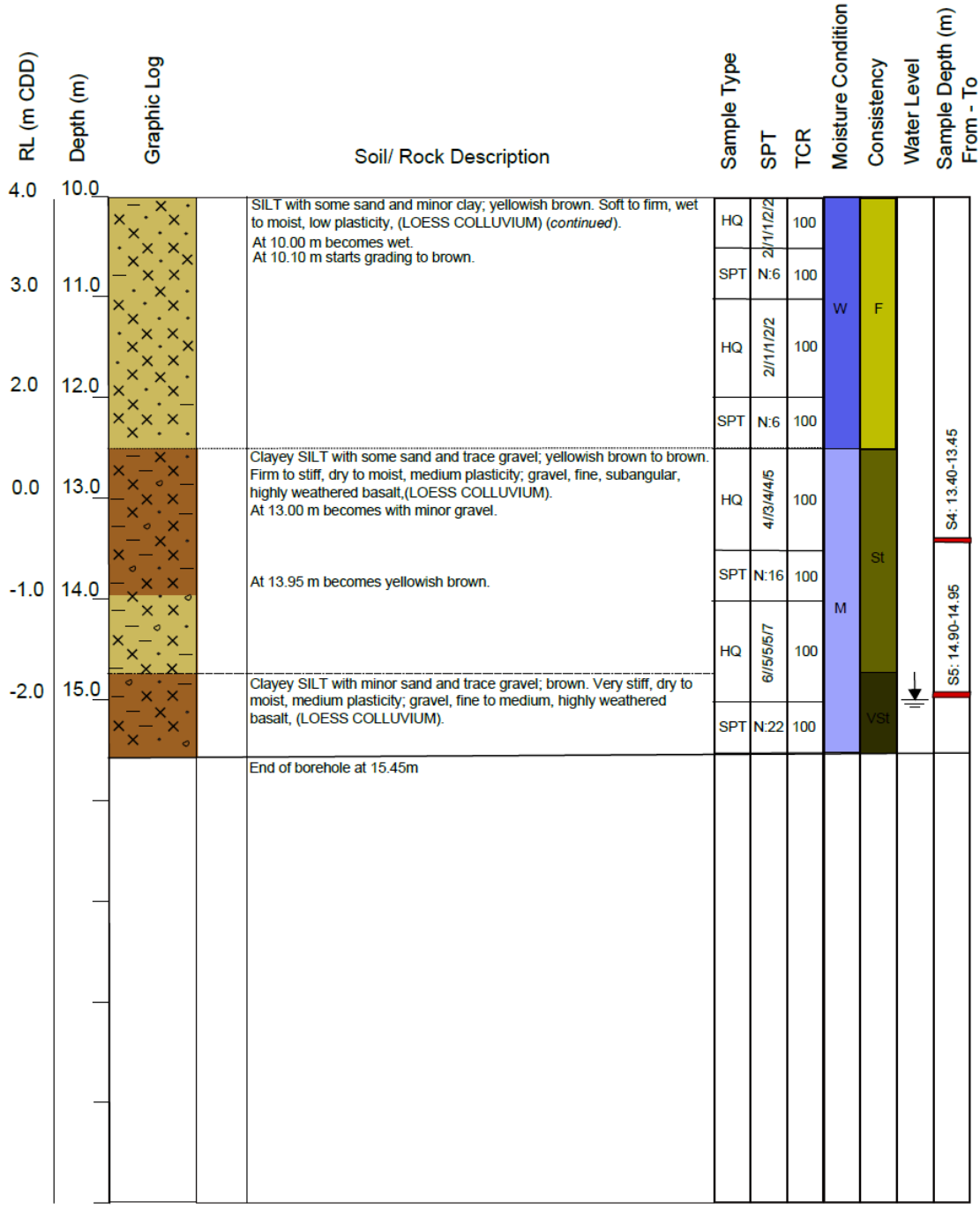

BH2 Centaurus Park

Sheet 1 of 2

Project: Fissure Traces in Loessial Soils	Easting: 394238.2 m
Location: Ramahana Road, Huntsbury	Northing: 802959.7 m
Date Drilled: 28/11/2012	Coord. Sys.: MPP CDD (Jan 2012)
Method: Water Flush Rotary Sonic Drilling	Ground Level (RL): 16.70m
SPT:Automatic SPT hammer;91 % energy ratio	Logged by: C. S. White

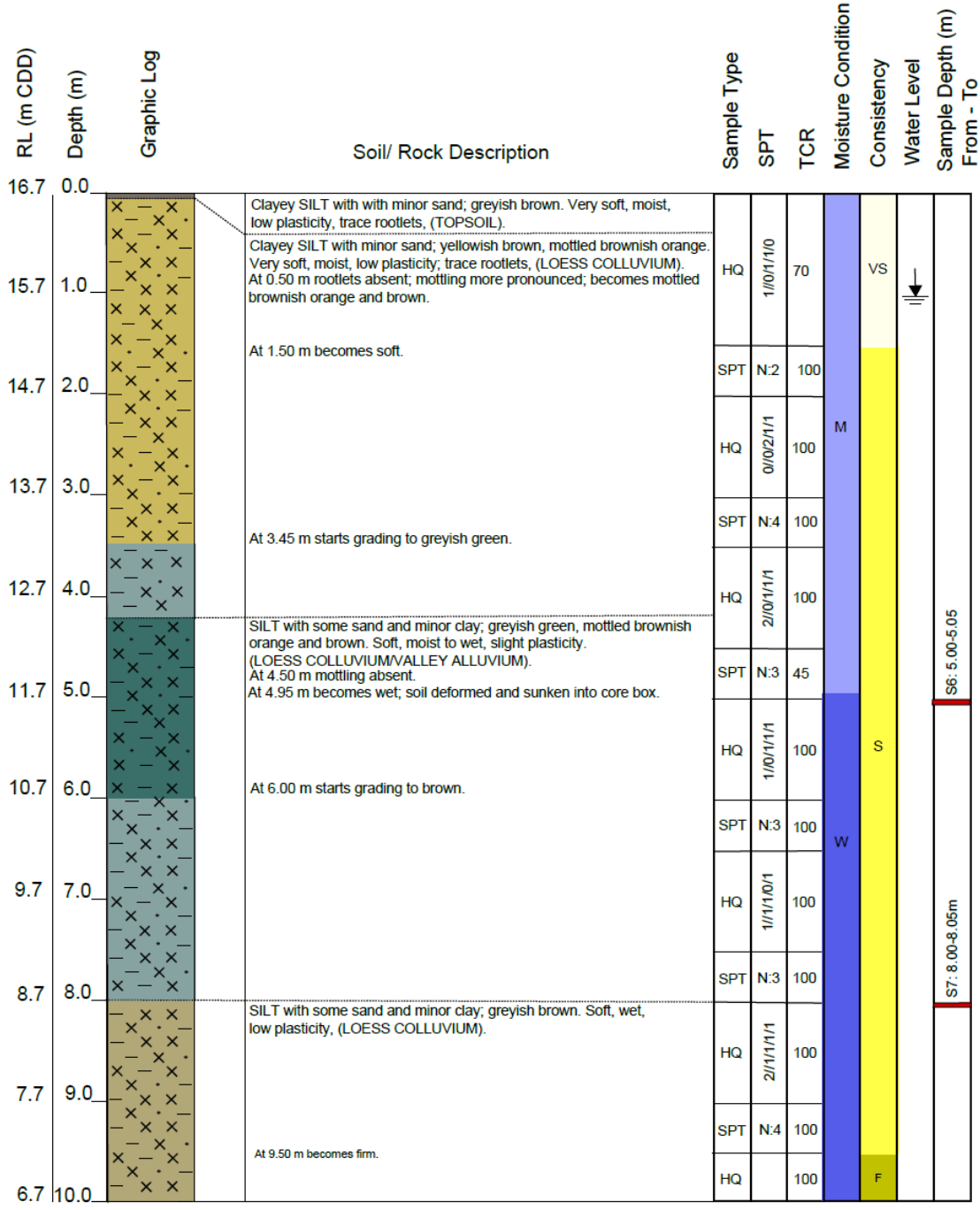

BH2 Centaurus Park

Sheet 2 of 2

Project: Fissure Traces in Loessial Soils	Easting: 394238.2 m
Location: Ramahana Road, Huntsbury	Northing: 802959.7 m
Date Drilled: 28/11/2012	Coord. Sys.: MPP CDD (Jan 2012
Method: Water Flush Rotary Sonic Drilling	Ground Level (RL): 16.70m
SPT:Automatic SPT hammer;91 % energy ratio	Logged by: C. S. White

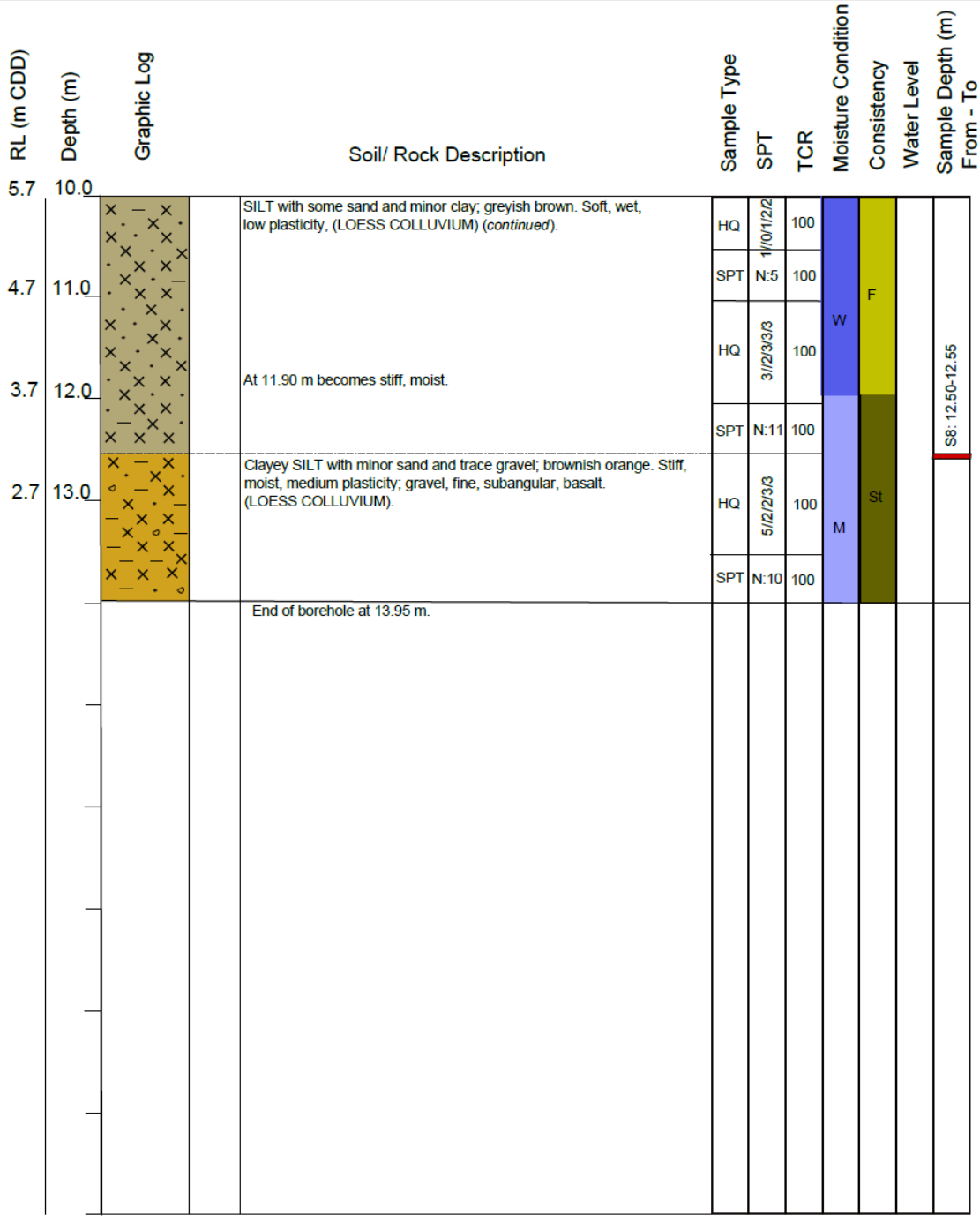

BH3 Centaurus Park

Sheet 1 of 3

Project: Fissure Traces in Loessial Soils	Easting: 394220.1 m
Location: Ramahana Road, Huntsbury	Northing: 802941.3 m
Date Drilled: 28/11/2012	Coord. Sys.: MPP CDD (Jan 2012)
Method: Water Flush Rotary Sonic Drilling	Ground Level (RL): 23.20m
SPT:Automatic SPT hammer;91 % energy ratio	Logged by: C. S. White

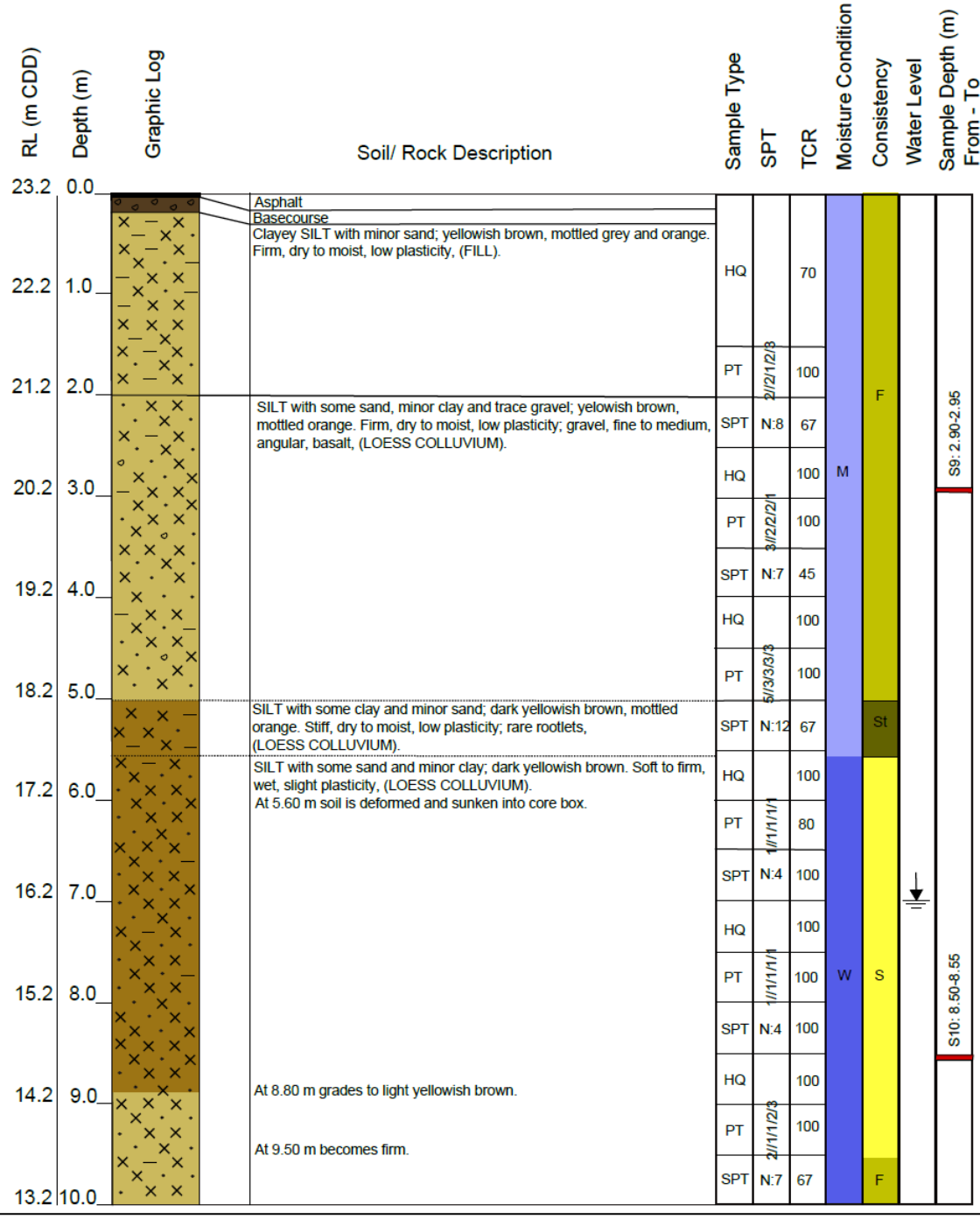

BH3 Centaurus Park

Project: Fissure Traces in Loessial Soils	Easting: 394220.1 m
Location: Ramahana Road, Huntsbury	Northing: 802941.3 m
Date Drilled: 28/11/2012	Coord. Sys.: MPP CDD (Jan 2012)
Method: Water Flush Rotary Sonic Drilling	Ground Level (RL): 23.20m
SPT:Automatic SPT hammer;91 % energy ratio	Logged by: C. S. White

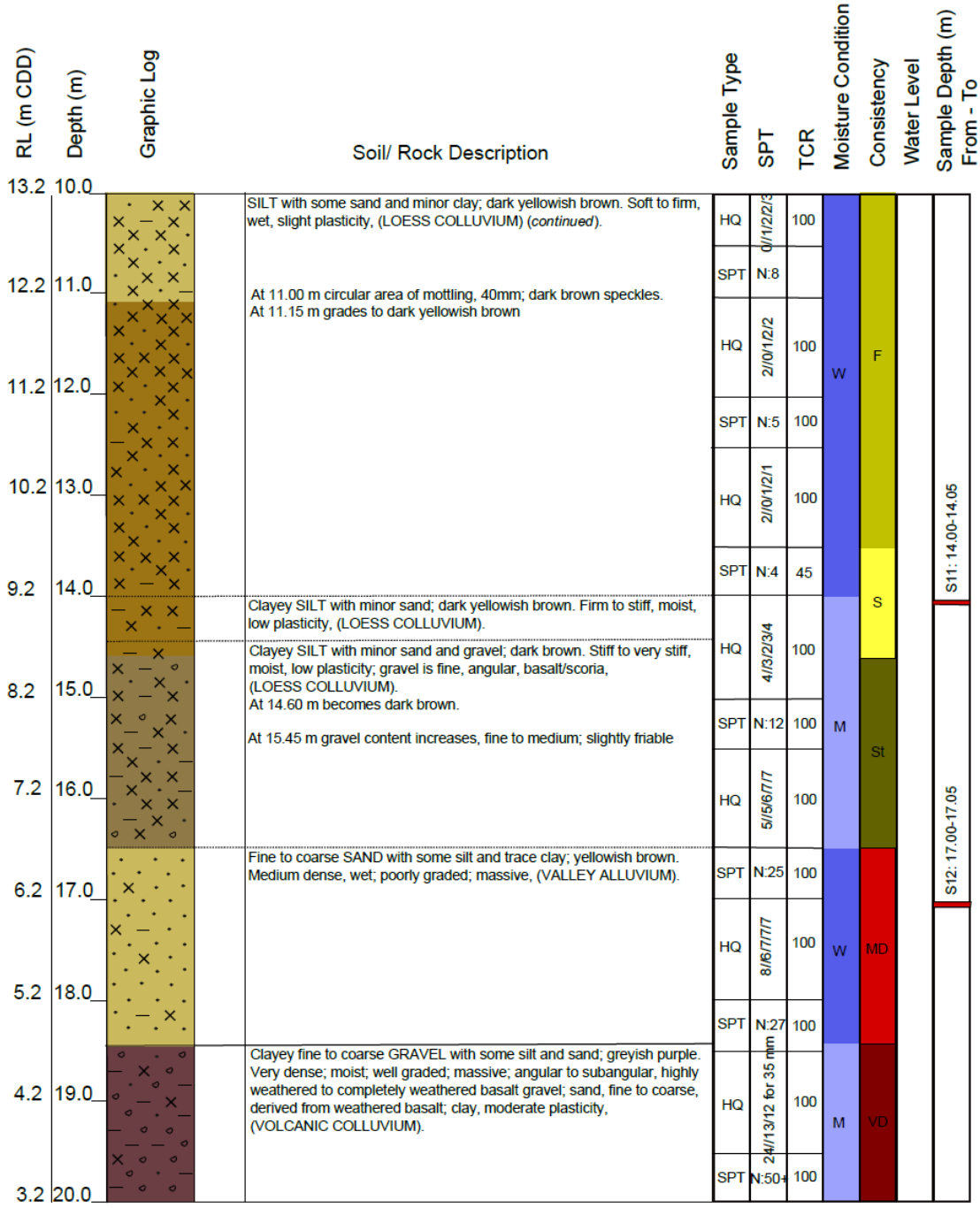

BH3 Centaurus Park

Sheet 3 of 3

Project: Fissure Traces in Loessial Soils	Easting: 394220.1 m
Location: Ramahana Road, Huntsbury	Northing: 802941.3 m
Date Drilled: 28/11/2012	Coord. Sys.: MPP CDD (Jan 2012)
Method: Water Flush Rotary Sonic Drilling	Ground Level (RL): 23.20m
SPT:Automatic SPT hammer;91 % energy ratio	Logged by: C. S. White

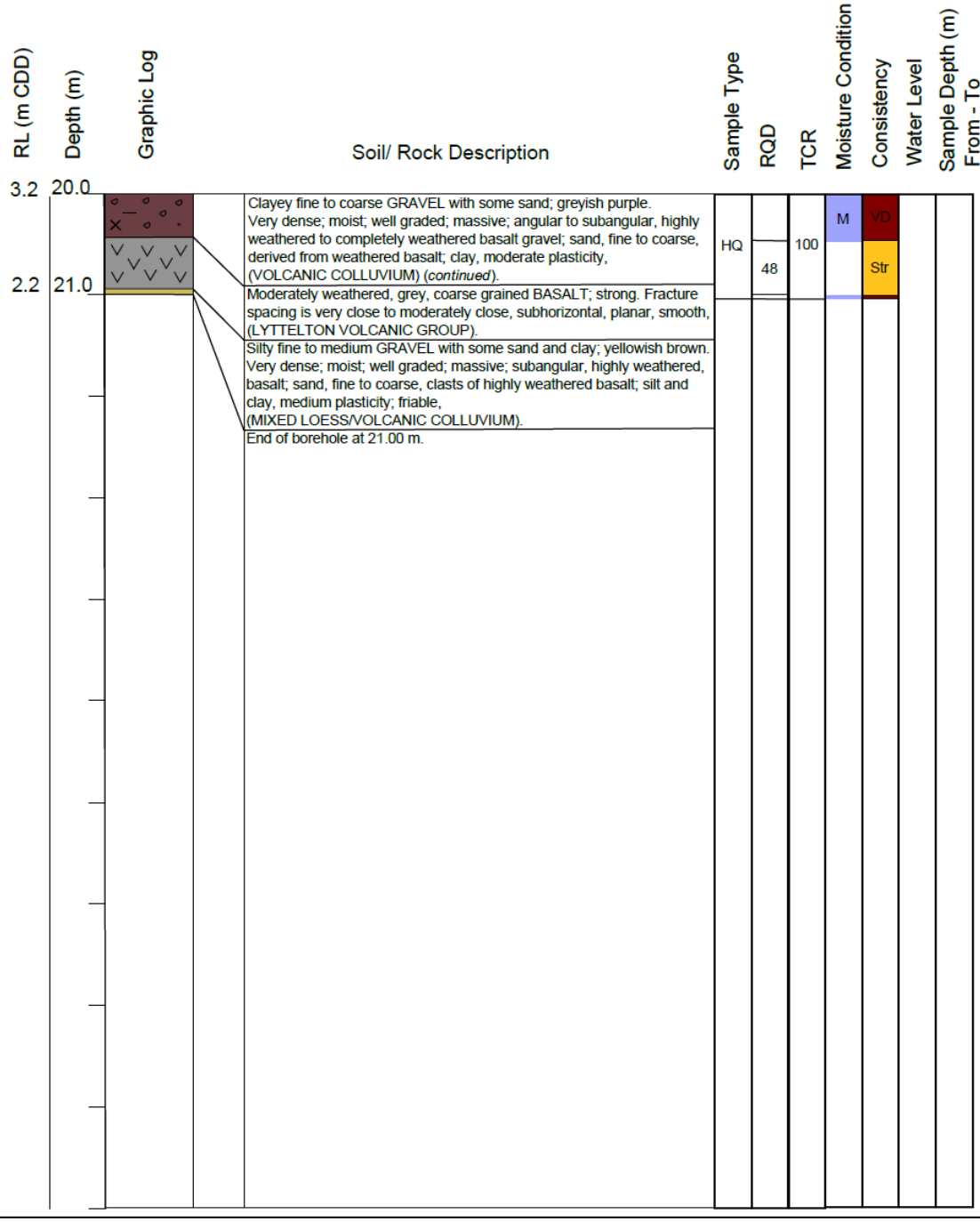

BH4 Centaurus Park

Project: Fissure Traces in Loessial Soils	Easting: 394220.5 m
Location: Ramahana Road, Huntsbury	Northing: 802963.8 m
Date Drilled: 04/12/2012	Coord. Sys.: MPP CDD (Jan 2012)
Method: Water Flush Rotary Sonic Drilling	Ground Level (RL): 25.08 m
SPT:Automatic SPT hammer;91 % energy ratio	Logged by: C. S. White

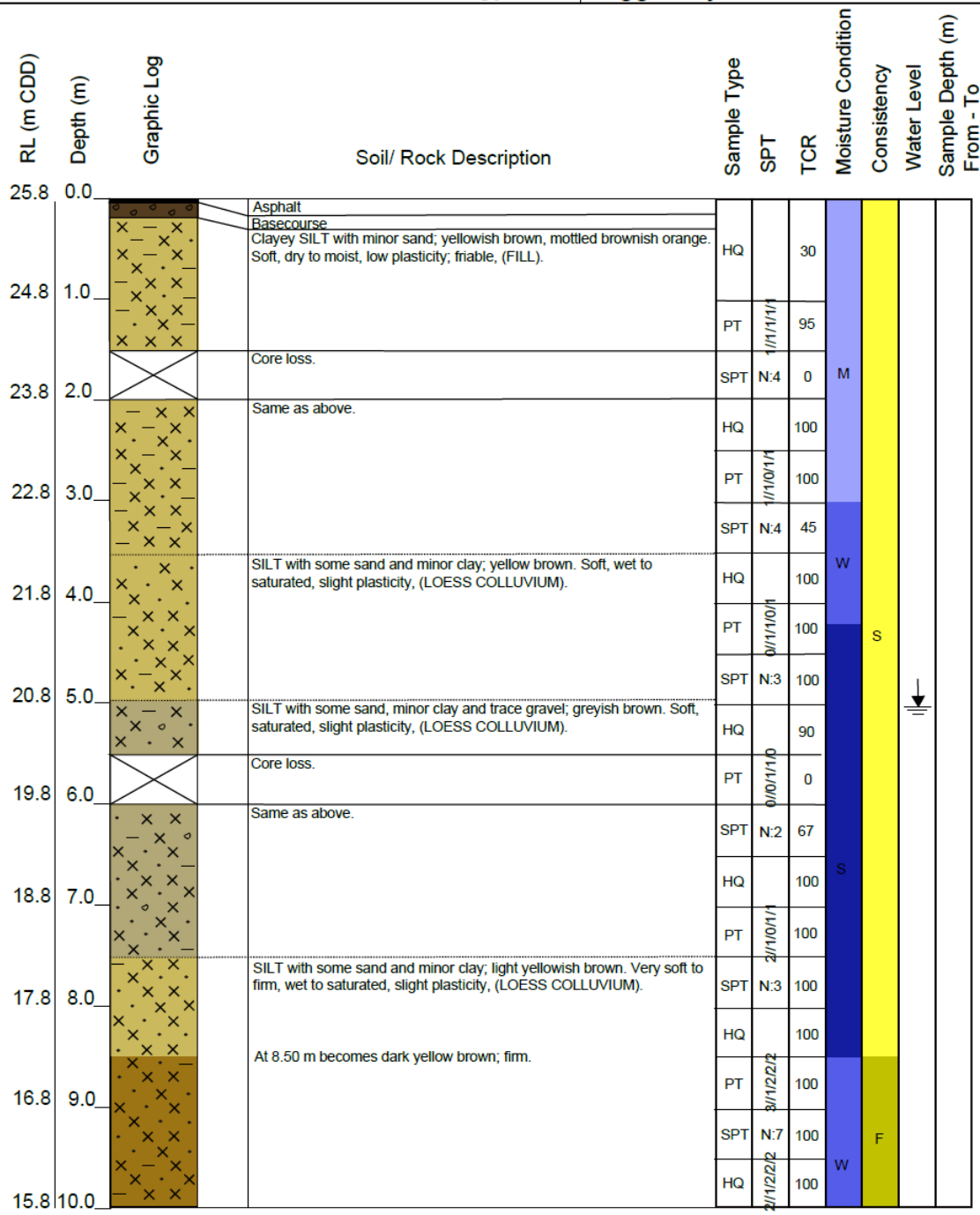

BH4 Centaurus Park

Project: Fissure Traces in Loessial Soils	Easting: 394220.5 m
Location: Ramahana Road, Huntsbury	Northing: 802963.38 m
Date Drilled: 04/12/2012	Coord. Sys.: MPP CDD (Jan 2012)
Method: Water Flush Rotary Sonic Drilling	Ground Level (RL): 25.08m
SPT:Automatic SPT hammer;91 % energy ratio	Logged by: C. S. White

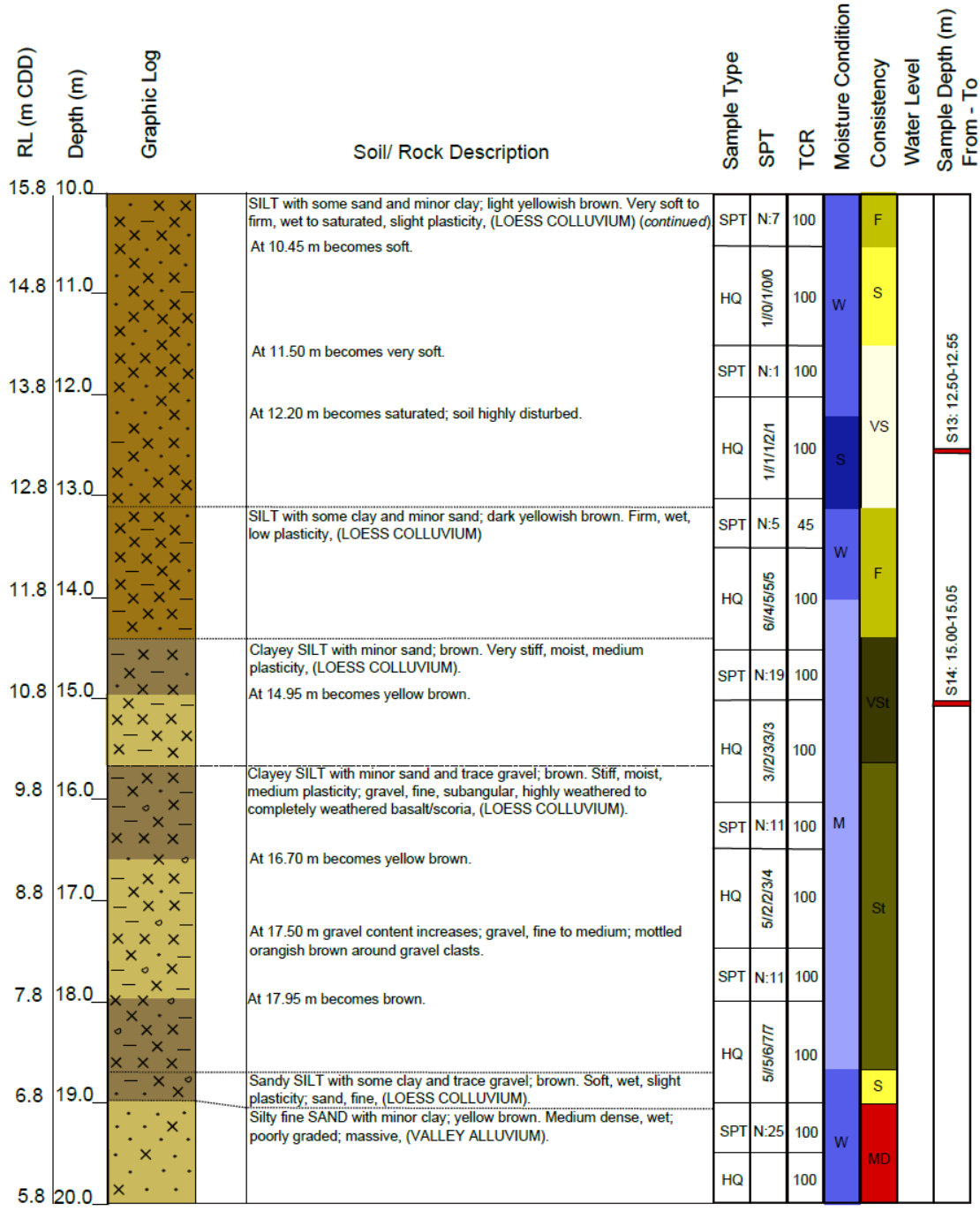

BH4 Centaurus Park

Sheet 3 of 3

Project: Fissure Traces in Loessial Soils	Easting: 394220.5 m
Location: Ramahana Road, Huntsbury	Northing: 802963.38 m
Date Drilled: 04/12/2012	Coord. Sys.: MPP CDD (Jan 2012)
Method: Water Flush Rotary Sonic Drilling	Ground Level (RL): 25.08m
SPT:Automatic SPT hammer;91 % energy ratio	Logged by: C. S. White

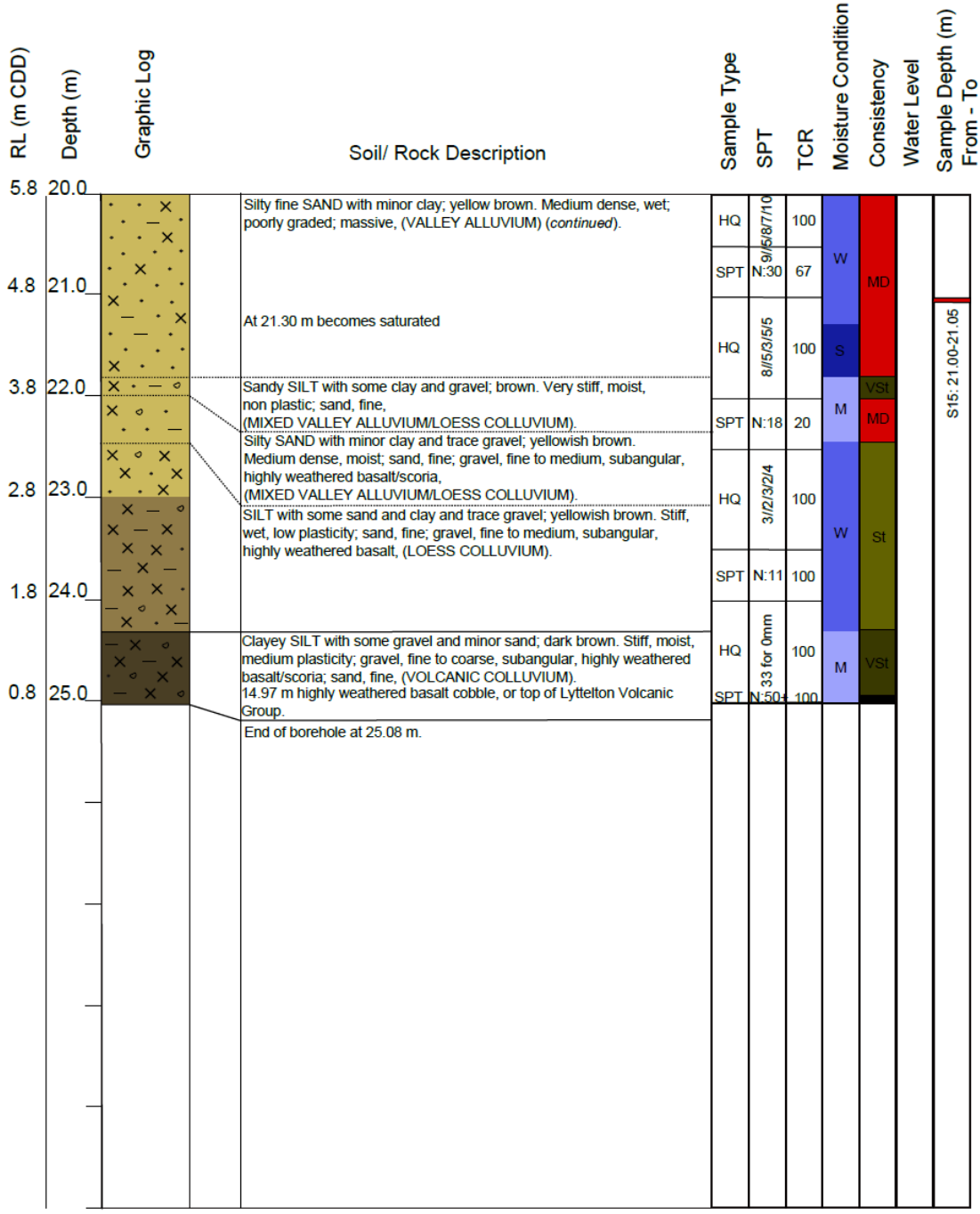

BH5 Centaurus Park

Sheet 1 of 3

Project: Fissure Traces in Loessial Soils	Easting: 394218.6 m
Location: Ramahana Road, Huntsbury	Northing: 802983.3 m
Date Drilled: 04/12/2012	Coord. Sys.: MPP CDD (Jan 2012)
Method: Water Flush Rotary Sonic Drilling	Ground Level (RL): 21.15 m
SPT:Automatic SPT hammer;91 % energy ratio	Logged by: C. S. White

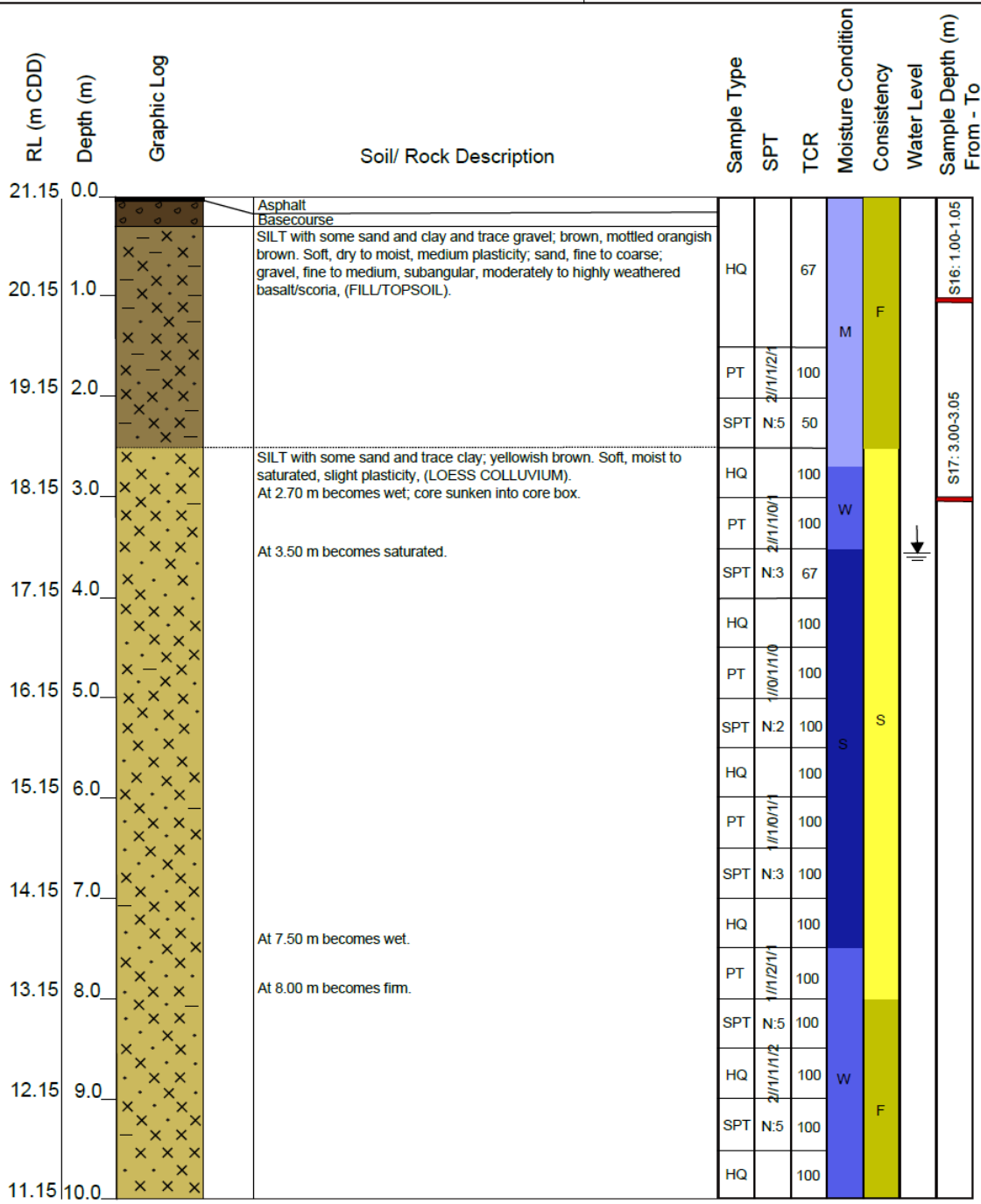

BH5 Centaurus Park

Project: Fissure Traces in Loessial Soils	Easting: 394218.6 m
Location: Ramahana Road, Huntsbury	Northing: 802983.3 m
Date Drilled: 04/12/2012	Coord. Sys.: MPP CDD (Jan 2012)
Method: Water Flush Rotary Sonic Drilling	Ground Level (RL): 21.15 m
SPT:Automatic SPT hammer;91 % energy ratio	Logged by: C. S. White

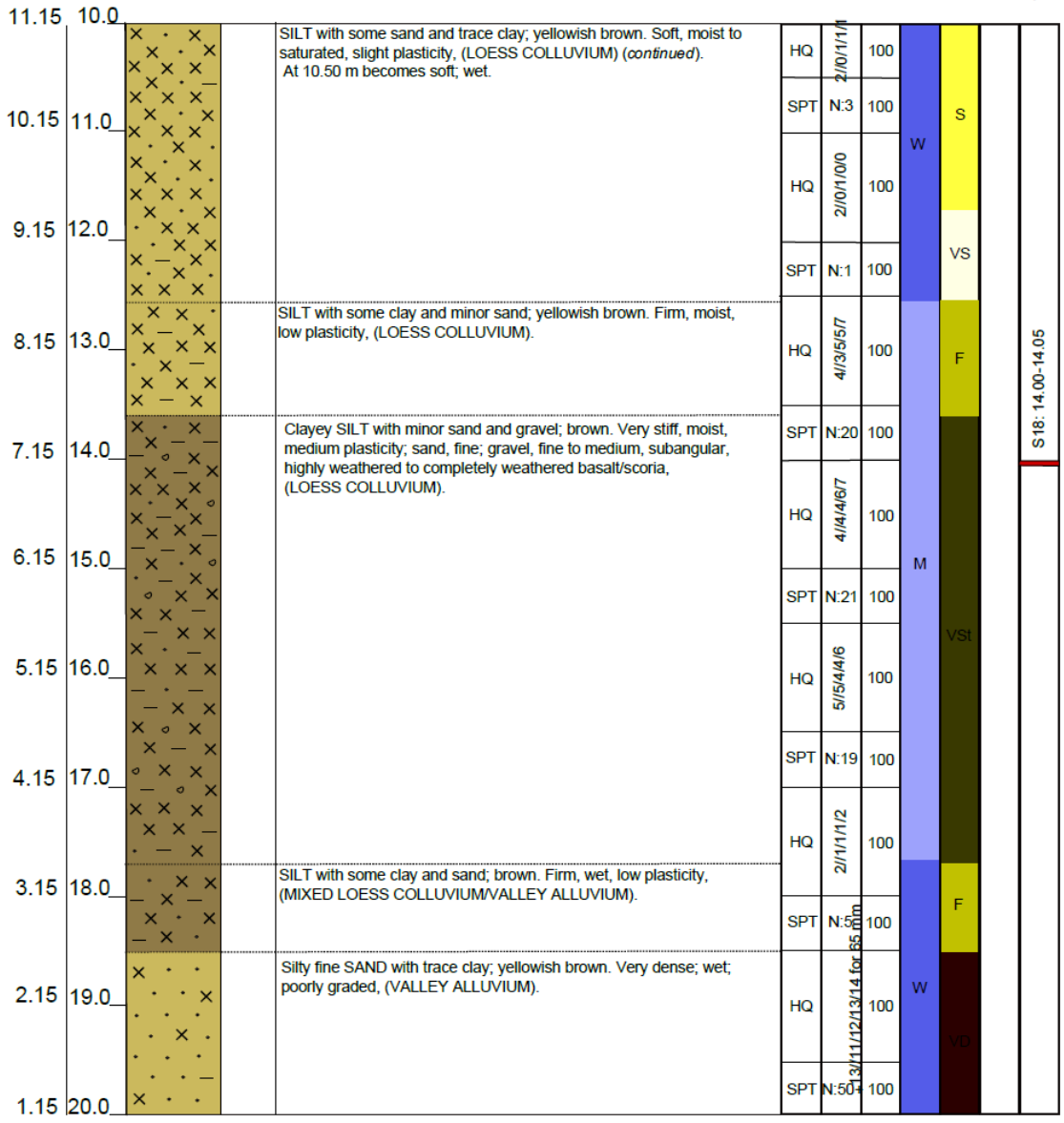

BH5 Centaurus Park

Project: Fissure Traces in Loessial Soils	Easting: 394218.6 m
Location: Ramahana Road, Huntsbury	Northing: 802983.3 m
Date Drilled: 04/12/2012	Coord. Sys.: MPP CDD (Jan 2012)
Method: Water Flush Rotary Sonic Drilling	Ground Level (RL): 21.15 m
SPT:Automatic SPT hammer;91 % energy ratio	Logged by: C. S. White

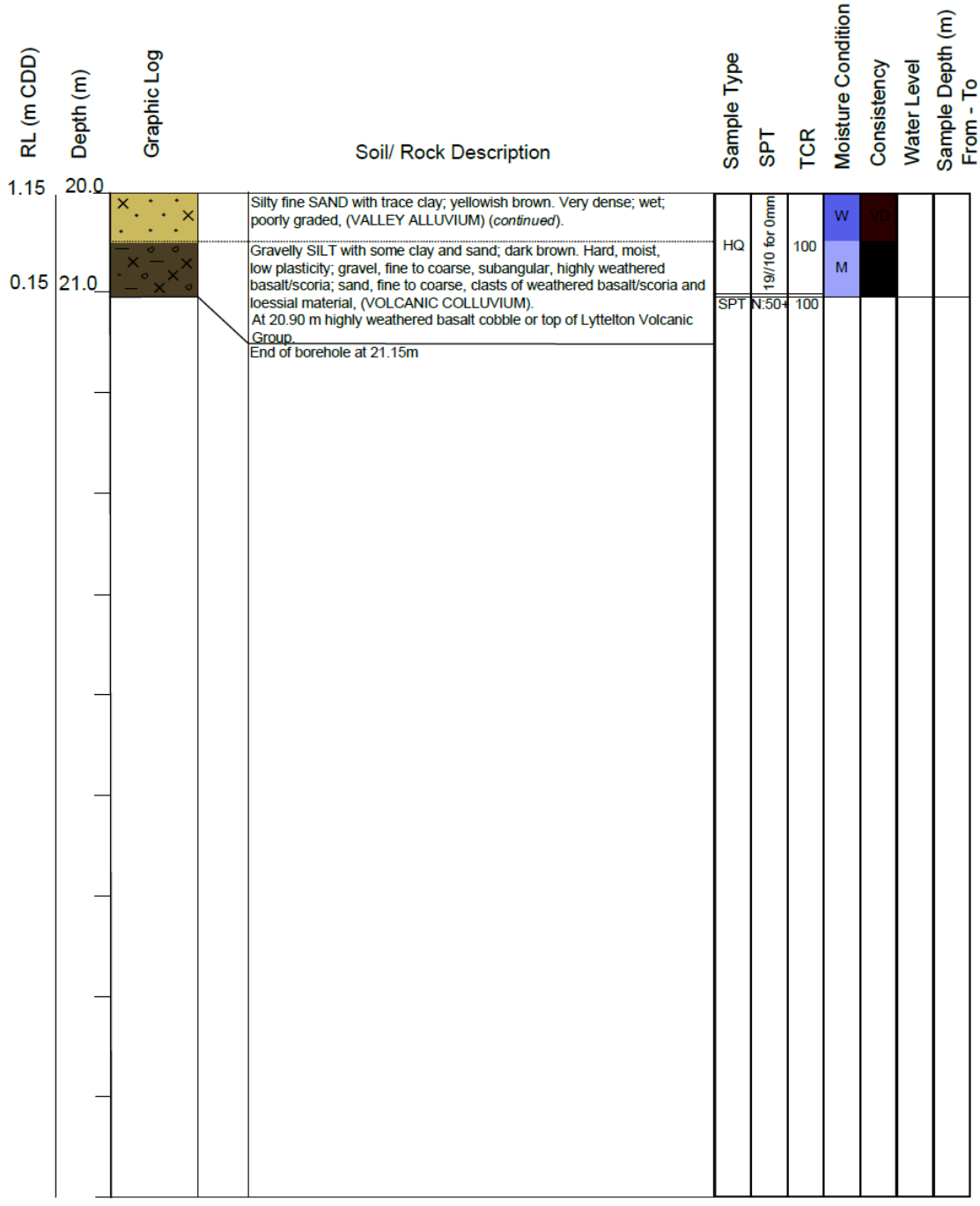

Appendix 3: Quantitative Assessment: Laboratory Investigation Methods and Raw Data

3.1: Classification Tests Data

Sample	Location	Sand	Silt	Clay	PL	LL	PI	MC
S1	BH1 1.10-1.15 m	9.2	70.7	20.1	17	28	11	17
S2	BH1 4.00-4.05 m	14.4	80.7	4.9	22	27	5	21
S3	BH1 7.00-7.05 m	13.2	78.8	8.0	19-18	22	3 to 4	16
S4	BH1 13.40-13.45 m	12.9	65.5	21.6	14-13	28	14 to 15	9
S5	BH1 14.90-14.95 m	11.5	64.5	24.0	14	27	13	10
S6	BH2 5.00-5.05 m	12.4	82	5.6	19	23	4	21
S7	BH2 8.00-8.05 m	15.3	75.9	8.8	19	26	7	18
S8	BH2 12.50-12.55 m	8.7	67.1	24.2	15	28	13	6
S9	BH3 2.90-2.95 m	16.5	75.9	7.6	17	25	8	8
S10	BH3 8.50-8.55 m	14.1	77.0	8.9	19	24	5	10
S11	BH3 14.00-14.05 m	11.6	70.1	18.3	18	25	7	18
S12	BH3 17.00-17.05 m	85.0	11.4	3.6	NA	NA	NA	20
S13	BH4 12.50-12.55 m	15.6	78.0	6.4	21-20	26	5 to 6	19
S14	BH4 15.00-15.05 m	10.4	69.4	20.2	15	28	13	9
S15	BH4 21.00-21.05 m	75.4	16.2	8.4	NA	NA	NA	20
S16	BH5 1.00-1.05 m	17.8	65.6	16.6	21-22	33	11 to 12	19
S17	BH5 3.00-3.05 m	14.6	81.3	4.1	21	25	4	23
S18	BH5 14.00-14.05 m	9.4	63.7	26.9	17	29	12	8
TPS1	TP 0.5 m	11.0	69.4	19.6	16	21	5	12
TPS2	TP 1.0 m	11.81	71.79	16.4	17-18	23	5 to 6	16
TPS3	TP 1.5 m	12.1	72.1	15.8	18	24	6	20
TPS4	TP 2.0 m	8.1	78.8	13.1	18	22	4	17
TPS5	TP 2.5 m	12.6	72.4	15.0	20-21	22	1 to 2	21
TPS6	TP 3.0 m	15.2	71.7	13.1	20	22	2	18
TPS7	TP gravel layer				NA	NA	NA	17
TPS8	TP nth wall pug	11.7	70.1	18.2	16	21	5	21
TPS9	TP sth wall pug	14.8	59.8	25.4	17-18	28	10 to 11	18
TPS10	TP infill 1.75 m nth wall	17.6	66.0	16.4	18	23	5	21
HA1:1	HA1 1 m	13.3	70.5	16.2	19	23	4	13
HA1:2	HA1 2 m	10.3	71.3	18.4	18	26	8	17
HA1:3	HA1 3 m	14.3	68.4	17.3	18	27	9	18
HA1:4	HA1 4 m	16.3	70.2	13.5	20	23	3	22
HA2:1	HA2 1 m	12.0	71.5	16.5	17-18	23	5 to 6	13
HA2:2	HA2 2 m	12.5	72.2	15.3	19	26	7	17
HA2:3	HA2 3 m	10.7	73.5	15.8	19	26	7	21
HA2:4	HA2 4 m	11.5	73	15.5	19	25	6	22
HA3:1	HA3 1 m	9.4	72.2	18.4	18	25	7	12
HA3:2	HA3 2 m	13.6	71.1	15.3	18-19	26	7 to 8	17
HA3:3	HA3 3 m	12.7	74.8	12.5	20	23	3	21
HA3:4	HA3 4 m	10.3	73.8	15.9	19	24	5	22
HA4:1	HA4 1 m	8.6	76.0	15.4	17	25	8	9
HA4:2	HA4 2 m	13.0	74.1	12.9	19	25	6	17
HA4:3	HA4 3 m	11.3	78.5	10.2	19	25	6	21
HA4:4	HA4 4 m	10.8	66.0	23.2	16	27	11	19
HA5:1	HA5 1 m	8.8	72.7	18.5	17	24	7	9
HA5:2	HA5 2 m	14.5	73.4	12.1	19	25	6	17
HA5:3	HA5 3 m	11.4	73.6	15.0	18	24	6	20
HA5:4	HA5 4 m	8.3	72.8	18.9	16	25	7	19

Table 3.1: Classification tests of soil samples taken from 17 Ramahana Road and Centaurus Park.

3.2: Sample Reconsolidation Method for Direct Shear Box Testing

The samples were reconsolidated by tamping using the Standard Procter test equipment within the shear-box test sample rings. The shear-box test sample rings were first placed into the mould followed by an amount of disturbed soil sample that had to be above the height of the shear-box test sample ring. The exact amount of the soil was judged for each individual sample on how much compaction was thought to be likely with the aim of getting the soil compacted to a height just above the edge of the sample ring.

25 blows from the hammer were then used to compact the soil directly into the shear-box test sample ring. If the blows from the hammer caused the soil to be compacted below the height of the sample ring then the soil was removed and disturbed before the method was repeated with a fresh sample of soil, alternatively if the soil was 5 mm above the height of the sample ring then the soil was also removed and disturbed before the method was repeated, due to the unlikelihood of the soil receiving adequate compaction within the ring. If the soil was above the sample ring but by less than 5 mm then the excess was cut off using a sharp knife and carefully deposited into the shear-box test machine for testing. These requirements were decided upon due to the need to keep the density of the sample as similar as possible.

The results of this method were satisfactory in the sense that a testable sample was created; however there was an unavoidable amount of variation in the density of the samples. The dry density of samples varied from 1658-1954 kg/m^3, with a median of 1738 kg/m^3 and an average of 1750 kg/m^3. This variation in density can be attributed to the variable moisture contents of the soils that were compacted, which would have allowed greater or lesser compaction depending on that individual soil's optimum moisture content for compaction; the individual soil's particle-size distribution; and human/testing induced error.

3.3: Direct Shear-Box Testing Data

Sample HA5:1 - 18.5 % clay, 9% MC						
Dry Unit Weight kg/m3	Applied Weight (kg)	P (Newtons)	τ (kPa)	σn (kPa)	C (kPa)	ϕ (°)
1758	20 kg	662	84	26	65	39
1709	50 kg	938	119	64		
1767	100 kg	1293	165	126		

Sample HA1:2 - 18.4 % clay, 17% MC						
Dry Unit Weight kg/m3	Applied Weight (kg)	P (Newtons)	τ (kPa)	σn (kPa)	C (kPa)	ϕ (°)
1664	20 kg	266	34	26	16	34
1731	50 kg	463	59	64		
1781	100 kg	801	102	126		
Sample HA5:4 - 18.9 % clay, 19% MC						
Dry Unit Weight kg/m3	Applied Weight (kg)	P (Newtons)	τ (kPa)	σn (kPa)	C (kPa)	ϕ (°)
1689	20 kg	171	22	26	5	34
1796	50 kg	374	48	64		
1775	100 kg	694	88	126		
Sample HA4:1 - 15.4 % clay, 9% MC						
Dry Unit Weight kg/m3	Applied Weight (kg)	P (Newtons)	τ (kPa)	σn (kPa)	C (kPa)	ϕ (°)
1759	20 kg	691	88	26	62	43
1788	50 kg	932	119	64		
1783	100 kg	1414	180	126		
Sample HA3:2 - 15.3 % clay, 17 % MC						
Dry Unit Weight kg/m3	Applied Weight (kg)	P (Newtons)	τ (kPa)	σn (kPa)	C (kPa)	ϕ (°)
1658	20	241	31	26	14	35
1663	50	476	61	64		
1710	100	796	101	126		
Sample HA2:4 - 15.5 % clay, 22 % MC						
Dry Unit Weight kg/m3	Applied Weight (kg)	P (Newtons)	τ (kPa)	σn (kPa)	C (kPa)	ϕ (°)
1666	20	201	26	26	4	38
1665	50	407	52	64		
1667	100	807	103	126		
Sample HA4:3 - 10.2 % clay, 10 % MC						

Dry Unit Weight kg/m3	Applied Weight (kg)	P (Newtons)	τ (kPa)	σn (kPa)	C (kPa)	ϕ (°)
1772	20 kg	456	58	26	37	41
1822	50 kg	752	96	64		
1860	100 kg	1145	146	126		
Sample HA4:3 - 10.2% clay, 16% MC						
Dry Unit Weight kg/m3	Applied Weight (kg)	P (Newtons)	τ (kPa)	σn (kPa)	C (kPa)	ϕ (°)
1741	20 kg	237	30	26	13	31
1800	50 kg	433	55	64		
1726	100 kg	830	106	126		
Sample HA4:3 - 10.2 % clay, 21% MC						
Dry Unit Weight kg/m3	Applied Weight (kg)	P (Newtons)	τ (kPa)	σn (kPa)	C (kPa)	ϕ (°)
1676	20 kg	200	25	26	2	38
1676	50 kg	376	48	64		
1675	100 kg	801	102	126		
Sample BH3 2.80-3.00 m - 7.6 % clay, 8 % MC						
Dry Unit Weight kg/m3	Applied Weight (kg)	P (Newtons)	τ (kPa)	σn (kPa)	C (kPa)	ϕ (°)
1909	20 kg	467	59	26	36	43
1949	50 kg	772	98	64		
1954	100 kg	1209	154	126		
Sample BH1 7.00-7.20 m - 8.0 % clay, 16 % MC						
Dry Unit Weight kg/m3	Applied Weight (kg)	P (Newtons)	τ (kPa)	σn (kPa)	C (kPa)	ϕ (°)
1684	20 kg	199	25	26	6	36
1724	50 kg	405	52	64		
1735	100 kg	763	97	126		
Sample BH2 5.00-5.20 m - 5.6 % clay, 21 % MC						
Dry Unit Weight kg/m3	Applied Weight (kg)	P	τ	σn	C	ϕ

		(Newtons)	(kPa)	(kPa)	(kPa)	(°)
1719	20 kg	202	26	26	5	37
1779	50 kg	52	52	64		
1779	100 kg	101	101	126		

Table 3.2: Direct shearbox strength test results on samples of varying clay contents and moisture

3.4: Slide Layered Models for 17 Ramahana Road

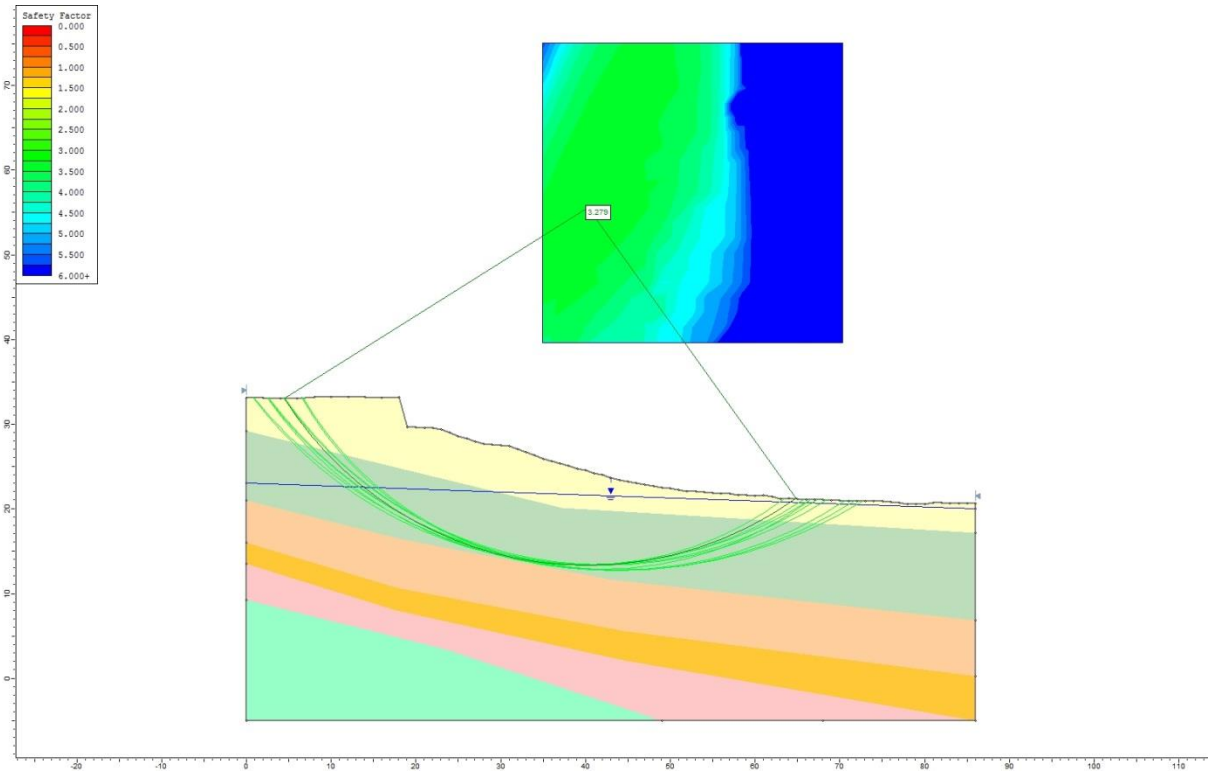

Figure 3.1: The 10 rotational slip surfaces with the lowest FOS in the layered model.

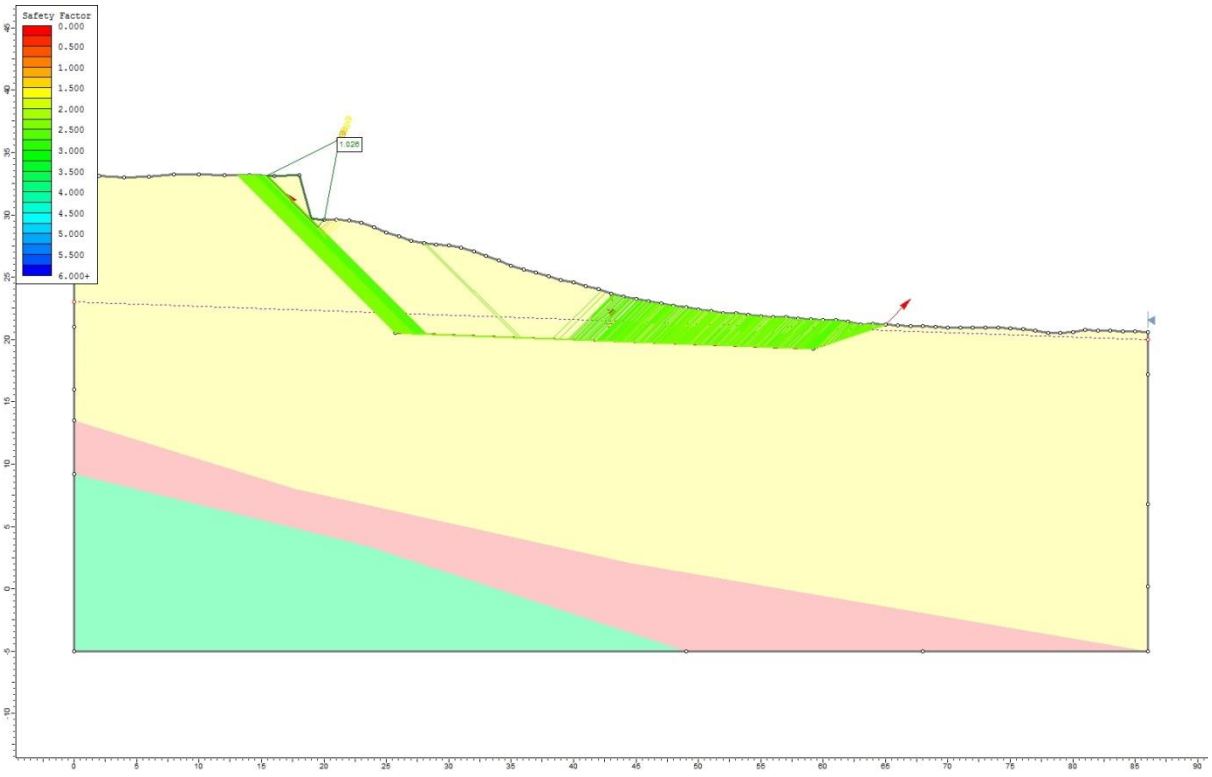

Figure 3.2: Translational slip surfaces with FOS <2.66 by Janbu method in the homogeneous model. The FOS has been filtered to <2.66 to find the lowest FOS failure surface that follows the fissure trace at 17 Ramahana Road.

Appendix 4: Detailed Mechanisms of Potential Movement Types

4.1: Slide Landslide Movement Type Mechanisms in an Earthquake

Hovius and Meunier (2012) explain that the triggering of a slide during an earthquake works in much of a similar way to the generation of the earthquake itself. An earthquake is triggered when two geologic blocks, separated by a fault or potential fault, are progressively displaced, leading to strain energy building around the fault zone. The earthquake is triggered when this strain exceeds the rock mass strength, and sudden failure occurs, which releases the stored energy. Likewise, a landslide is triggered when the shear stress builds along a shear surface or potential shear surface, and rupture occurs when the shear stress exceeds the shear strength of the material. According to Ambraseys & Srbulov (1994) the development of slides during an earthquake occurs in three consequent stages:

- Stage 1: gravity and seismic forces combine during the earthquake's relatively short duration, leading to instability in certain conditions. This occurs either through the generation of a failure surface, or through the activation of a pre-existing slip plane, and ultimately leads to a downslope displacement of the slope material. At this stage the displacements are generally small, unless the material's residual strength drops to very low values. The controlling factors in stage one displacement are: the magnitude and duration of the earthquake, the slope geometry, and the undrained strength of the material.
- Stage 2: further displacements will occur, immediately following the earthquake, if the residual undrained shear strength, on the failure surface, is a lesser value than what is required to resist displacement. The displaced material will accelerate downslope, accommodated by the outwards movement of the toe. At this stage the displacements can be large. The controlling factors in stage two displacements are: the velocity of motion, the undrained residual strength of the failure surface, and the resistance of the toe.
- Stage 3: Further displacement can in occur in stage three due to creep and consolidation of the displaced material. Large displacements are still possible at this stage if there are open cracks that lead into the failure surface, and these are subsequently infilled by surface waters.

Following the three stage concept introduced above, it can be reasoned that if the Ramahana Road fissure traces are the head scarps of earthquake-induced translational slide type movement, then the movement was limited to stage one displacement: the displacements were relatively small, and there was no associated larger movement immediately following the earthquake. There was no stage two development because once the earthquake ground motion had subsided the residual undrained shear strength of the loess-colluvium along the failure surface was high enough to resist further displacement. Stage three displacements of creep movement were observed, but these were only observed during other large earthquakes, so these could actually be deemed additional stage one displacements.

In the 1964, Fourth Rankine Lecture, Skempton reviewed the then current knowledge of residual shear strength, and progressive failures in overconsolidated clays. One of the most important conclusions of the lecture was that landslides in overconsolidated clays were brought on by a progressive development of a basal shear surface. Once sufficient time had passed for the development of a basal shear surface, then the slope stability was found to be only dependent upon the residual shear strength of the clay along this surface. The rate at which the basal shear surface developed varries according to the type of clay, and landslides that develop in stiffer clays can be delayed for centuries (Bjerrum 1966).

Bjerrum (1966) explains that progressive failures are only possible in situations where the shear stresses exceed the peak shear strength of the clay. For this to be achieved there needs to exist a discontinuity in the clay mass such as a steep slope face, an excavation at the slope toe, or simply a soft spot in the slope. If this is applied to the fissure traces, then the discontinuity would have to be liquefaction of the valley floor material or settlement of the peat in the valley floor, which would have resulted in a decrease of support at the toe of the slope. If the loss of support in the slope was sufficient then the shear stress would build-up in the adjacent upslope material, and decrease with distance up the slope. The progression of the failure surface upslope would have to be accommodated by local differential strain along the failure surface, and this strain must be enough to bring the clay to failure. In this way the stress is redistributed along the failure surface from the toe of the slope to a point further upslope where the peak strength of the clay is greater than the shear stress. The onset of strain must be followed by a rapid decrease in the shear strength of the clay so that the differential strain can be obtained upslope, and the stress redistributed upslope.

4.2: Lateral Spread Landslide Movement Type Mechanisms in an Earthquake

Liquefaction and its consequential compaction and associated settlement of the ground surface, commonly occurs in cohesionless soils (generally loosely packed sands and silts), during earthquakes (Bell 1999). During strong earthquakes the material loses all strength and behaves like a liquid, hence the term 'liquefaction'. Peck (1979) cited by Bell (1999a) describes how this occurs when the material densifies during an earthquake and does not have enough time to drain its water in response, leading to excessive pore water pressures, causing the soil to behave as a heavy fluid and loose effectively all of its shear strength. There has been considerable debate about what a concise definition of liquefaction should be. In acknowledgement of the controversy that surrounds the term liquefaction, Sladen et al. (1985) thought it was prudent to offer their definition of liquefaction:

> *'Liquefaction is a phenomenon wherein a mass of soil loses a large percentage of its shear resistance, when subjected to monotonic, cyclic, or shock loading, and flows in a manner resembling a liquid until the shear stresses acting on the mass are as low as the reduced shear resistance.'* (p. 564).

This is a relatively concise definition that refers to one particular type of liquefaction: flow liquefaction. There are, however, various behavioural responses in different soils, due to the build-up of pore water pressure during cyclic loading, that are all grouped under the classification of liquefaction, and do not follow the definition proposed by Sladen et al. (1985). Liquefaction can be thought of as a broad term; generally it is used to refer to the build-up of pore water pressure, and the corresponding loss of strength in saturated, cohesionless soils during cyclic loading.

Rauch (1997) suggested that 'liquefaction' be a term that can broadly describe the failure of saturated, cohesionless soils during earthquakes, but that the different behavioural responses in different soils are split into different classifications of liquefaction. Following the prior work of Robertson & Fear (1996), Rauch (1997) summarized the liquefaction classification system into two categories: flow liquefaction and cyclic softening.

Flow liquefaction occurs when a saturated, contractive soil flows under undrained conditions due to the static shear stress exceeding the residual strength, and this can be due to either monotonic or cyclic shear loading. This form of liquefaction fits with the definition given by

Sladen et al. (1985), and is what caused the sand boils and differential settlement on the Christchurch city flat lands.

Cyclic softening occurs when a saturated, dilative soil (under undrained monotonic shear) deforms due to the build-up of pore water pressure during cyclic shear loading. Dilative soils will soften in response to cyclic loading, but they will regain strength when cyclic loading ceases and monotonic loads resume, due to pore pressure reduction from dilation. Cyclic softening can be further classified into cyclic liquefaction and cyclic mobility: the former represents a condition where 0 effective stress can be achieved due to cyclic shear stresses exceeding the initial static shear stress, and the later represents a condition where cyclic shear stresses do not exceed the initial static shear stress. Large deformations can occur during cyclic liquefaction, whereas deformations are limited during cyclic mobility, because deformations can only occur during each cycle of shear stress.

Liquefaction generally occurs in soils with a particle size ranging from coarse silt to fine sand, but there have been many case studies of liquefaction occurring in non to low plasticity soils outside of this range around the world (McManus et al. 2010). Loess generally has a particle size range of 0.01 mm to 0.05 mm for > 50 % by weight (Bell & Trangmar 1987), which puts it within the possibility of liquefaction range for low coefficient of uniformity deposits and within the high possibility of liquefaction range for high coefficient of uniformity deposits in Figure 6.1. Other factors that increase the liquefaction susceptibility of a soil deposit are the particle cementation, soil framework, stress history, age, degree of saturation, water table level, plasticity index, dry density, and ground motion acceleration due to earthquake (Rauch 1997; Wang et al. 2004).

On a steep slope, liquefaction of a subsurface layer will lead to a catastrophic failure in the form of a flow slide. Rauch (1997) explains that a flow slide will develop in this instance because the shear resistance is less than the static driving shear stress, and this produces a contractive soil response. The static driving shear stress is higher in steeper slopes due to the higher confining pressure; conversely in a lateral spread displacement on gently sloping ground there is a lower static shear stress due to the lower confining pressure. When the shear resistance is greater than the static shear stress the soil can respond with dilative behaviour to cyclic loading. Under these conditions the soil will exhibit cyclic mobility, which can result in significant shear deformations, but limited when compared to that of a flow slide. After cyclic loading ends the soil will regain strength due to dilation under monotonic loading.

Figure 6.2 contrasts the contractive and dilative responses to cyclic stresses on steep slopes and flat slopes respectively.

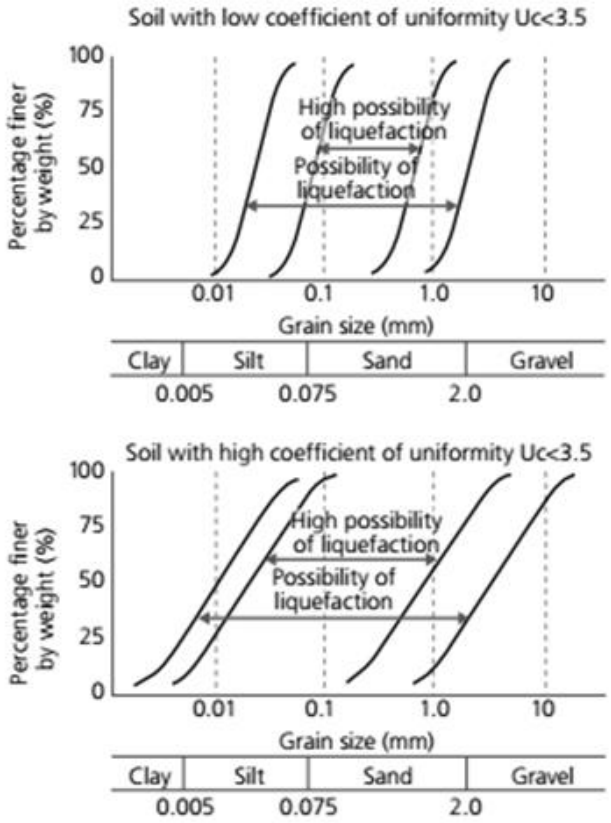

Figure 6.1. Grainsize distribution of liquefiable soils (Ministry of Transport, Japan, 1999 cited in NZGS, 2010)

The soil does not reach what is known as the steady-state condition during cyclic mobility, but it does during a liquefaction induced flow slide. The steady-state condition is when a soil is subjected to very large shear strains resulting in deformation at a constant volume or void ratio, constant effective stress, constant shear stress or resistance, and constant rate of shear strain (Rauch 1997). The soil's framework is reworked so that its particles are at a constant orientation; under these conditions the framework allows flow movement. The soil is in the steady-state flow condition until the deformations cease. Rauch (1997) explains that undrained or drained conditions during cyclic or monotonic loading can lead to the steady-state condition, depending on the soil conditions and magnitude of loading.

Wang et al (2004) were interested in the mechanisms behind the liquefaction of loess deposits in Lanzhou. They found that if the *in-situ* natural moisture content was greater than the plastic limit, then earthquake induced liquefaction of loess was possible. In laboratory liquefaction tests conducted by Wang et al (2004) it was found that liquefaction of loess has a

unique behaviour when compared to that of sands. Three subsequent stages were identified in the liquefaction process: the first stage was characterized by a rapid increase in pore water pressure with little corresponding increase in residual strain, the second stage involved a rapid increase in residual strain with little corresponding increase in pore water pressure, and in the third stage the residual strain continues to rapidly increase while the pore pressure remains stable. In interpretation of this Wang et al (2004) described how during the cyclic traixial test, the framework of the loess remained stable in the first stage, when cyclic loading increased the pore water pressure, but did not break down the loess framework. The pore water pressure ratio in this stage was lower than what is generally recorded in cyclic triaxial tests of sands. In the second stage the loess framework begins to breakdown which slows the pore water pressure increase; this breakdown is attributed to the water sensitivity and weak cementation of the loess framework. In the third stage the pore water pressure is at its maximum level so it remains stable, but the disintegration of the loess framework continues. Figure 6.3 portrays the results and interpretations of Wang et al. (2004).

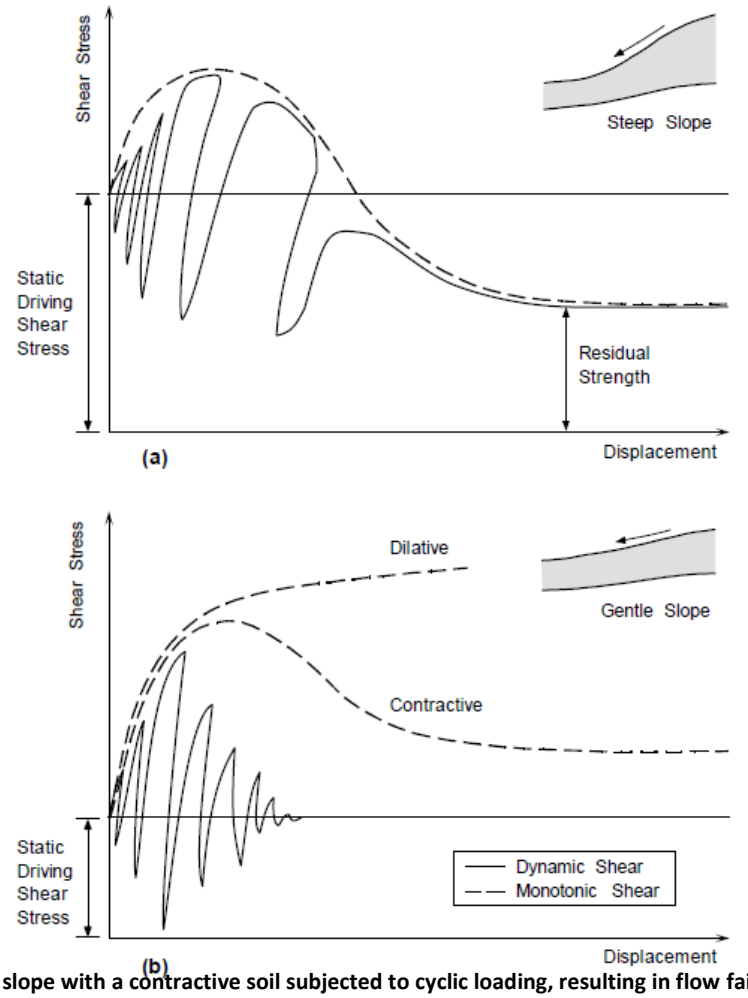

Figure 6.2: (a) A steep slope with a contractive soil subjected to cyclic loading, resulting in flow failure, (b) A gentle slope with a dilative and contractive soil subjected to cyclic loading resulting in limited deformation, after Ishihara (1994).

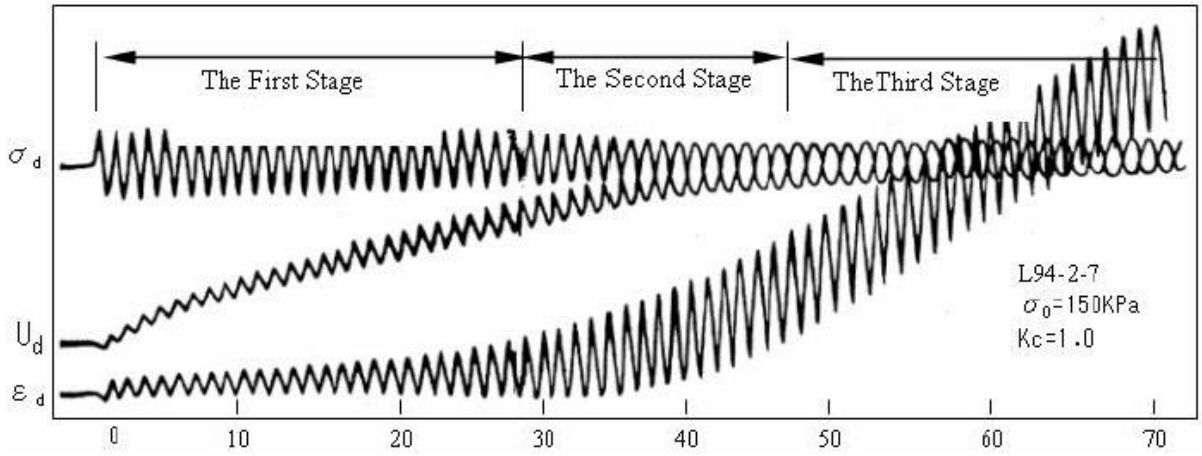

Figure 6.3: Stress, strain, and pore pressure responses over time for a sample of loess subjected to dynamic loading under undrained conditions in a dynamic triaxial test, after Wang et al. (2004).

It is prudent to note here once again that Chinese loess deposits vary quite considerably from New Zealand deposits, and a major difference in terms of liquefaction potential is that Chinese loess deposits contain larger pores and a higher salt content which both factor into liquefaction susceptibility: when the pore water pressure increases in Chinese deposits, the dissolvable salts dissolve or partly dissolve, which exacerbates the loss of microstructural strength in the loess and can cause the larger pores to collapse, this further exacerbates the pore pressure increase, which in turn exacerbates the loess framework's breakdown (Wang et al. 2004).

What is interesting about the liquefaction of loess is that liquefaction is meant to occur in cohessionless soils, but loess is a cohesive soil with most of its gradational size falling within the silt category. Banks Peninsula loess is known to generally have a plasticity index of <12%, and the Lanzhou loess deposits tested by Wang et al. (2004) have a plasticity index of 10-14. In section # it was noted that laboratory testing of loess with low clay contents, low densities, and high moisture contents have been found to have cohesion values of 0 on the Mohr Envelope. This suggests that while high clay content, high density, and low moisture content loess would be highly cohesive and therefore non-liquefiable; low clay content, low density, and high moisture content loess can have very low cohesion values, and would therefore be more susceptible to liquefaction.